



# Green all the way through!

The new Editorial Board for *Green Chemistry* met for the first time in March under the chairmanship of Colin Raston. We believe that the Board provides an excellent diversity of expertise and interest in keeping with the current scope and readership of the journal as well as providing a geographical mix that reflects the international nature of the journal. The research interests of the Board cover clean synthesis, alternative reaction media, life cycle assessment, innovative engineering and catalysis, with expertise covering all the traditional areas of chemistry, alongside chemical engineering, environmental strategy, legislation and industrial chemistry.

The first meeting of the new Board was constructive with numerous good ideas emerging. Most importantly, Colin expressed the sincere thanks on behalf of the current Boards and the RSC to all previous Board members for their hard work in making *Green Chemistry* the success that it is. The views of Advisory Board members who were not at the meeting, especially on matters relating to strategy, were carefully considered alongside the views of those present. While it was unanimously agreed that *Green Chemistry* is an international research journal, there was also strong support for the front section which, apart from being an information resource, could also be used to introduce new emerging subject areas and ones that are attracting increased attention in government, industry and education as well as in research. We identified a number of areas that fall into this category, including new greener products, genetically modified bacteria, alternative energy sources (as well as a better consideration of energy usage in green chemical processes), greener purification and separation technologies. As well as keeping readers up-to-date with activities in these areas we would also welcome associated review articles so that the readership can learn about these areas and understand their importance in the context of green chemistry.

*Green Chemistry* is the international journal on green chemistry, and as such it should help to show the way forward as well as reporting on how the scientific, industrial and educational communities are responding to current needs and perceptions. I am sensitive to the criticisms that so far green chemistry research has been too process-focussed and that we are not very good at evaluating the true 'greenness' of the improvement we report. We would like to encourage more articles (for both front and back sections) that consider raw materials (*e.g.* the use of renewable resources) and product fate and design (*e.g.* designing recyclability into the product).

We would also welcome more articles that consider green chemistry metrics. We need to build on the highly revealing but process-focussed E factors and atom economies to include a consideration of the environmental (as well as economic and societal) costs of obtaining the starting materials for a process and those associated with dealing with the product at the end of its life. We must also allow for the energy consumption throughout the product life cycle. These are challenging tasks

but I believe that the credibility of the green chemistry movement is at stake. We cannot afford to take any stage of the life cycle completely in isolation. A crop-based raw material might seem an attractive and certainly more sustainable alternative to one based on a petrochemical but its value is considerably diminished if we have to consume relatively large quantities of energy in its processing, for example. Similarly, a superficially green chemical process based on a reusable catalyst or a benign solvent may be 'blackened' by the use of an energy intensive reactor. We know all too well of the mistakes that have been made in the past over product design—chlorofluorocarbons for example—afford many excellent properties and advantages over alternatives but their damage to the environment has proven to be enormous. We are not infallible and we can only work within the constraints of our existing knowledge and our 'scientific good sense' but we can do better. I certainly do not want to stifle or unreasonably delay publications because the work does not consider full life cycle, but I do hope that an increasing number of our authors give reasonable consideration to them. We should strive to be not only green on the surface, but green all the way through!

#### *Award for Green Chemistry Board Member*

I am sure that everyone associated with *Green Chemistry* would want to join me in congratulating my Editorial Board colleague Martyn Poliakov on his election to a Fellowship of the Royal Society – a fitting tribute to many years of high-quality scientific research.



Martyn, who is Professor of Chemistry at the University of Nottingham, UK, is distinguished for his work on application of infrared spectroscopic techniques to the detection and characterisation of intermediates in organometallic chemistry; many of these significantly illuminate important catalytic processes. Based on this work he has pioneered the use of supercritical solvents for a wide range of applications:

the detection and isolation of previously inaccessible complexes; the study of photochemical and thermal reaction mechanisms; novel methods for heterogeneous catalysis as part of his contribution to green chemistry.

**James Clark**  
York  
May 2002

#### **US Presidential Green Chemistry Challenge Award Winners, 2002**

**Professor Eric J. Beckman** (University of Pittsburgh) – for Design of Non-Fluorous, Highly CO<sub>2</sub>-Soluble Materials  
**SC Fluids, Inc.** – for SCORR (Supercritical CO<sub>2</sub> Resist Remover)  
**Pfizer, Inc.** – for Green Chemistry in the Redesign of the Sertraline Process  
**Cargill Dow LLC** – for the NatureWorks™ PLA Process  
**Chemical Specialties Inc. (CSI)** – for ACQ Preserve®: The Environmentally Advanced Wood Preservative



# Supercritical fluids: a clean route to polymer synthesis and polymer processing

**Steve Howdle of the School of Chemistry at the University of Nottingham, UK, describes his pioneering research work on the use of supercritical fluids in polymer science and his other contributions to the field of green chemistry that led to his receiving the 2001 Jerwood Salters' Environment Award**

## Introduction

Dispersion polymerisation is an extremely important process both in the UK and worldwide for the synthesis of both commodity and speciality polymers based upon acrylate and methacrylate monomers. In 1995, J. M. DeSimone demonstrated that the conventional



Steve Howdle

dispersing solvent could be replaced by  $\text{scCO}_2$  and materials such as poly(methylmethacrylate) (PMMA) could be prepared effectively if the right stabiliser could be designed. In so doing, DeSimone demonstrated that a stabiliser based upon a poly (dihydrofluorooctylacrylate) (PFOA) was highly effective. This breakthrough triggered a flurry of activity in both industry and academia targeted at developing new stabilisers and expanding the potential uses of  $\text{scCO}_2$  for polymerisation. Much of the excitement arose because, in principle, the use of  $\text{scCO}_2$  (or dense phase  $\text{CO}_2$ ) could, at a

stroke, eliminate the need for the potentially toxic conventional solvents that are currently used in dispersion polymerisation. However, conventional dispersion polymerisation studies over many years have shown that the structure and quantity of the stabiliser required is very system dependent and is critical not only to achieving a successful polymerisation but also to its potential commercial viability. Thus the key to success in this field is the design of stabilisers that function effectively in  $\text{scCO}_2$ , lead to pure polymer product and are commercially viable.

The performance requirements for an active stabiliser are that it anchors to the growing particle of polymer, but at the same time, has sufficient interaction with the  $\text{scCO}_2$  solvent for a stable dispersion to form. This prevents flocculation and precipitation and allows the polymerisation process to continue successfully to completion. Thus, the stabilisers must contain both 'CO<sub>2</sub>-phobic' and 'CO<sub>2</sub>-philic' moieties. For example, the PFOA pioneered by DeSimone contains a CO<sub>2</sub>-phobic hydrocarbon backbone that associates with the growing PMMA chains and a series of fluorinated tails to provide the required solubility in  $\text{scCO}_2$  (Fig. 1).

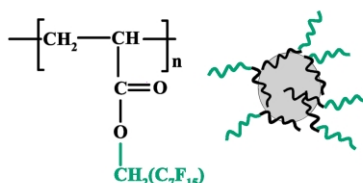


Fig. 1 Poly(1,1-dihydroperfluorooctyl acrylate) stabiliser (DeSimone *et al.*, *Science*, 1994, 265, 356).

Several other similar stabilisers have been developed by US and UK research teams (DeSimone, Beckman, Johnston,

Holmes) and the common theme is the presence of a CO<sub>2</sub>-philic fluorinated or siloxane based moiety and a hydrocarbon backbone. In all of these cases, effective stabilisation is observed at typical stabiliser loadings of *ca.* 5 wt% with respect to monomer. However, the stabilisers are not commercially available and they must be custom synthesised in most cases, by demanding synthetic methodologies that may not commercially viable in their own right. Furthermore, all of these stabilisers contain a hydrocarbon backbone from which hydrogen atoms may be abstracted during free radical polymerisation. The consequence of this is that a substantial portion of each stabiliser becomes covalently bonded into the PMMA product and the final polymer can seldom be regarded as 'pure'. Also, there is a substantial physical entrapment because the stabilisers are sufficiently large that entanglements within the product polymer trap them. Again from study on conventional dispersion polymerisation systems, such contamination has been shown to drastically effect the resultant polymer performance by introducing problems such as blooming, gloss reduction and interfacial delamination that should be avoided at all costs. Stabiliser incorporation is also a major drawback in the alternative approach of using siloxane macromonomers. This approach relies upon incorporation of a reactive stabiliser (macromonomer) (Fig. 2) into the backbone of the product PMMA, at levels

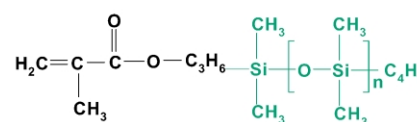


Fig. 2 PDMS macromonomer approach to stabilization of dispersion polymerization.



that can approach 3–5 wt% of the final polymer product.

### New strategies towards polymerisation in supercritical carbon dioxide

My research has been targeted at developing stabilisers that have the correct amphiphilic balance to be good stabilisers, but with none of the drawbacks described above. In order to do this we have developed a new stabiliser architecture based upon a single point anchoring mechanism. Here, a single 'polymer-philic' end group provides the method for anchoring the stabiliser to the growing polymer particle and a short oligomeric chain provides solubility and ensures the minimum chance of physical entrapment in the polymer product. Additionally the link was designed not to be a 'permanent' covalent bond but rather a 'reversible' interaction. This is *completely* different to all of the previously published examples of stabilisers which rely upon large polymeric molecules with many anchor groups and substantial potential for entrapment in the final polymer product. We chose a carboxylic acid terminated perfluoropolyether (Fig. 3) where the

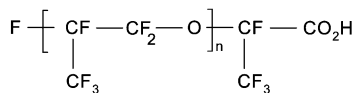


Fig. 3 Krytox 157 FSL – a commercially available carboxylic acid terminated perfluoropolyether ( $M_n$  2500 D,  $n \sim 14$ ).

interaction is through a hydrogen bond between the terminal acid functionality of the stabiliser and the ester grouping of MMA. Definitive proof of the hydrogen bonding interaction has been obtained through FTIR spectra of  $\text{scCO}_2$  solutions of MMA and the stabiliser. We believe that it is this same hydrogen bonding interaction that anchors the stabiliser to the growing polymer particles with the short perfluoropolyether (PFPE) tail (Fig. 3) providing the 'CO<sub>2</sub>-philicity' that is required to stabilise the dispersion.

This stabiliser is remarkably active. Only very low levels are required, and we have demonstrated stabilisation with as little as 0.001 wt% with respect to MMA monomer yielding 99+% yield of PMMA of controlled molecular weight. However, if control of the polymer morphology is also required, then the stabiliser levels need to be raised to 0.1% (Fig. 4); still an order of magnitude lower than the previously reported materials. In addition, the yield of polymer is almost

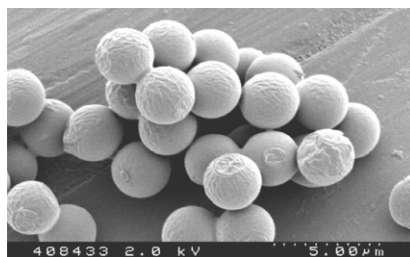


Fig. 4 SEM image showing spherical particles of PMMA produced in  $\text{scCO}_2$  using Krytox 157 FSL as the stabilizer.

quantitative and there are little or no residues of monomer in the final product. Additionally the structure of the stabiliser (Fig. 3) has been chosen because there are **no** C–H groups in the materials. Hence hydrogen abstraction and subsequent covalent bonding, the final method by which the stabiliser could be retained by the polymer, has been completely eliminated. From the resultant analysis of the polymer we have not yet been able to find any detectable residues of the stabilisers in the isolated polymer and we therefore conclude that:

- The hydrogen bonding mechanism is clearly reversible.
- The comparatively small molecular size of the stabilisers and the positioning of the anchor group ensures that they are not physically entrapped in the polymer product
- Covalent incorporation of the material has been removed by the elimination of C–H groups and hydrogen abstraction.

One of the key requirements of higher performance speciality dispersion polymerisation products is that the morphology of the polymer is suitable for commercial application. We have demonstrated that the single-point anchoring stabilisers do indeed provide excellent steric stabilisation and good morphology control for polymerisation of PMMA (Fig. 4).

Our work is now focussed upon copolymers. These are used in a very wide range of applications from adhesives, coatings and structural materials; through to food wrapping, cosmetic additives and medical implants. Some of the co-polymer compositions are extremely difficult to prepare in conventional solvent systems, but in collaboration with Dr D. J. Irvine at Uniqema, we are having some success in  $\text{scCO}_2$  using the single point anchoring stabilisers and producing materials in high yield, with good polymer quality. In all cases, the requirements for controlled,

residue free polymer products are paramount.

### Other green chemistry applications

This work on polymerisation stimulated my interest to explore the reversible plasticisation of polymers using  $\text{scCO}_2$ , and this has led to an entirely new supercritical mixing process for preparing novel biomaterials, drug delivery devices and scaffolds for tissue engineering developed in collaboration with Prof. K. M. Shakesheff.

The process relies upon the depression of glass transition temperature of polymers in the presence of  $\text{scCO}_2$  and then mixing of powdered bioactive material (e.g. drug, growth hormone) into the plasticised polymer. It is particularly applicable to polymers such as poly(lactic acid) and poly(lactide-co-glycolide) that are widely used for such biomedical applications (Fig. 5). Briefly, polymer

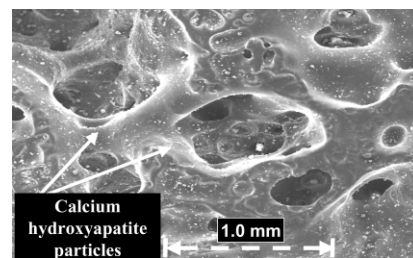


Fig. 5 SEM image of fracture surface of novel porous bone material prepared from PLA and calcium hydroxyapatite.

and the bioactive are placed inside a high-pressure autoclave and the polymer is plasticised by addition of  $\text{scCO}_2$ . The precise conditions of temperature and pressure required to achieve this state are determined by the composition of the polymer, but for the biodegradable polymers, PLA and PLGA, are at near ambient temperature (35 °C) and modest pressures (200 atm.) A highly efficient stirrer is then used to disperse the suspended bioactive particles throughout the swollen  $\text{scCO}_2$ /polymer mixture. The vessel is then depressurised to produce foamed bioactive composites with controlled porosity.

The great attraction of this technique is that no conventional solvents are required, and we have shown that for a very wide range of bioactives, there is **no loss of activity**. Thus we have prepared scaffolds for hepatocyte (liver cell) growth and porous structures targeted at regenerating bone *in vivo*. Preliminary results have shown great promise, and my first publication in the journal *Bone* has appeared very recently.





### Green chemistry in education

In the last few years I have sought to work to raise the profile of chemistry and science in schools and colleges, and in particular to encourage UCAS applications to scientific subjects. I present several lectures per year to schools and sixth-form colleges, and organise two days of 'A-level Chemistry' for 500 Sixth Formers and their teachers in the School of Chemistry. Along with other colleagues at Nottingham, 'Training days' for Sixth Formers in analytical/spectroscopic methods have also been developed, and National Science Week (SET Week) exhibitions at Nottingham have been visited by three hundred 5–11 year old children over three days for each of the last three years. The event helps the children to learn through "hands-on" demonstrations, about science and to discover what Universities do! I played a substantial role in designing and presenting 'hands-on' demonstrations of Green Chemistry at the 'Tomorrow's World Live' Event at Earls Court (June 1999), the Nottinghamshire County Show (1998), the Royal Society 'New Frontiers in Science' Exhibition and at SET 99 – held in the Houses of Parliament. The events were attended by a broad spectrum of society including schoolchildren, politicians, Royalty and Nobel Prize winners! Along with my colleagues M. Poliakoff and M. W. George, I will again be exhibiting

supercritical fluid research at the 2002 Royal Society Summer Exhibition in July.

To broaden the appeal of chemistry, I have led the team that has developed a new undergraduate course at Nottingham, *Green Chemistry and Process Engineering*. This course is the first of its kind in the world, and the first intake will arrive in October 2002. They will learn not only the application of the Twelve Principles of Green Chemistry, but also a unique blend of Chemistry and Chemical Engineering that will equip them to put these principles into practice. (<http://www.nottingham.ac.uk/chemistry/student-opportunities/undergraduate/greenchem.html>)

### Conclusion

The polymerisation processes described represent not only a replacement of conventional solvents with  $\text{scCO}_2$ , but introduce a step-change in the approach to stabilising free radical dispersion polymerisation processes. Although we have not conducted a full life cycle analysis, it is clear that the combination of zero residues, elimination of conventional solvent, and a facile route to high value, structurally complex copolymers will be beneficial. Moreover, the tantalising prospect of a single pot synthetic approach to such polymeric products will remove the need for the

costly purification stages that currently are required; providing environmental, economic and competitive advantages.

Our research is certainly not finished, and we anticipate new breakthroughs in the near future. If successful, these further developments will substantially enhance the applicability and environmental impact of our work.

### Selected references

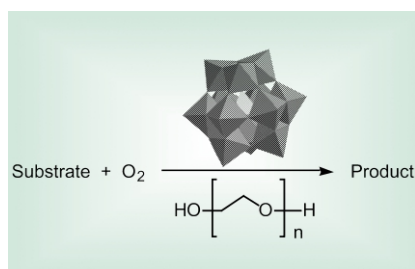
- Christian, P.; Howdle, S. M.; Irvine, D. J. *Macromolecules*, 2000, **33**, 237–239.  
 Christian, P.; Irvine, D. J.; Howdle, S. M. *et al.*; *Macromolecules*, 2000, **33**, 9222–9227.  
 Cooper, A. I., *J. Mater. Chem.*, 2000, **10**, 207–234.  
 Giles, M. R.; Hay, J. N.; Howdle, S. M. *Macromol. Rapid Commun.*, 2000, **21**, 1019–1023.  
 Giles, M. R.; Winder, R. J.; Hay, J. N.; Howdle, S. M. *Polymer*, 2000, **41**, 6723–6727.  
 Giles, M. R.; Griffiths, R. M. T.; Silva, M. M. C. G.; Howdle, S. M. *Macromolecules*, 2001, **34**, 20–25.  
 Howdle, S. M.; Watson, M.; Whitaker, M.; Shakesheff, K. M.; *et al.* *Chem. Commun.*, 2001, 109–110.  
 Johnston, K. P.; Harrison, K. L.; Clarke, M. J.; Howdle, S. M.; *et al.*; *Science*, 1996, **271**, 624–626.  
 Kendall, J. L.; Canelas, D. A.; Young, J. L.; DeSimone, J. M., *Chem. Rev.*, 1999, **99**, 543–563.  
 Lepilleur, C.; Beckman, E. J. *Macromolecules*, 1997 **30**, 745.  
 Oreffo, R. O. C.; Howdle, S. M.; Shakesheff, K. M. *et al.*, *Bone*, 2001, **29**, 523–531.  
 Yong, T.-M.; Holmes, A. B.; *et al.* *Chem. Commun.*, 1997, **18**, 1811.

## Highlights

### Duncan Macquarrie reviews highlights from the recent literature

#### Solvents

Alternative solvents are one of the hot topics in green chemistry. Among the desired properties sought are a lack of volatility, and ionic liquids have become very well researched. An alternative nonvolatile solvent class are polymers

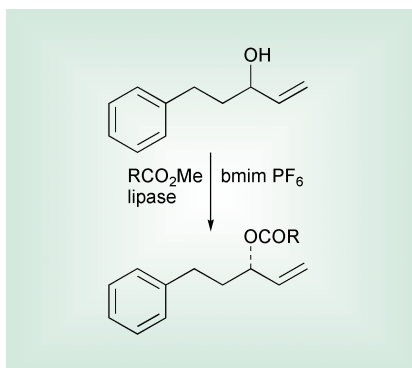


such as poly(ethylene glycol)s. Adina Haimov and Ronny Neumann of the Weizmann Institute in Rehovot, Israel, have now shown that PEGs are very well suited to the oxidation of alcohols to aldehydes with air using heteropolymetallates as oxidation catalysts (*Chem. Commun*, 2002, 876). Low molecular weight PEGs were found to give essentially complete oxidation to aldehyde. Oxidative dehydrogenation and sulfide oxidation were also shown to be possible, albeit with lower conversions and selectivities respectively.

#### Ionic liquids

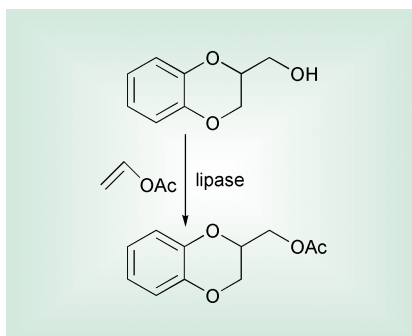
The use of enzymes in ionic liquids has recently been proven to be possible. One

drawback to lipase-based acylation systems is that the enzyme decreases in activity with time due to the build up of acetaldehyde by-products (acetaldehyde itself formed from the acyl donor). Toshiyuki Itoh and colleagues from Tottori University and Okayama University, Japan, have provided an elegant solution to this dilemma (*Chem. Lett.*, 2002, 154). They have used lipase in ionic liquids under reduced pressure to remove unwanted products from the system. This has meant that the vinyl acetate commonly used as acyl transfer agent could not be used, as it was too volatile. Methyl esters proved to be the solution, despite the adverse effects of methanol in conventional lipase systems.



The use of a high boiling ester allowed the transfer of the acyl group with evaporation of methanol being selectively achieved in the involatile solvent. Yields were reasonably good, and enantioselectivity was excellent.

An interesting study on the role of solvent and co-solvent in lipase-catalysed reactions in ionic liquids has been published by Manikrao Salunkhe and co-workers at the Institute of Science in Mumbai, India (*Tetrahedron Lett.*, 2002,



43, 2979). Hydrophilicity/phobicity is an important parameter with hydrophobic systems giving higher rates of reaction. They conclude that a good choice of ionic liquid can provide a very effective and convenient recyclable system for lipase-catalysed acylations.

### Hydroamination

Hydroamination is an addition reaction of an amine to a multiple bond. As such it is an inherently clean method for the formation of amines and imines. A team led by Thomas Müller at the Technical University of Munich, Germany, has

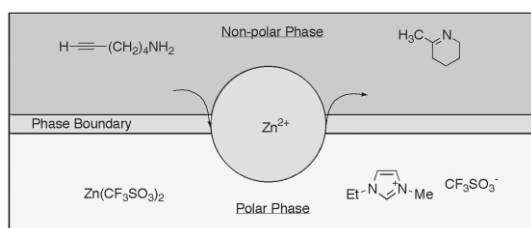
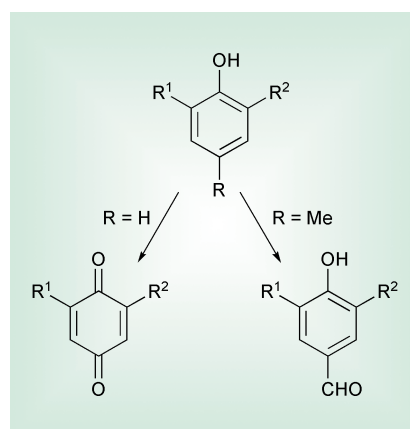


Fig. 1

developed a two-phase continuous system (Fig. 1) to carry out this reaction (*Chem. Commun.*, 2002, 906). They used a heptane solution of reactants and an ionic liquid, 1-ethyl-3-methylimidazolium trifluoromethane sulfonate, containing zinc triflate as catalyst. In this system, continuous conversion could be achieved using a continuous feed of heptane solution. Conversions were generally quantitative and a range of reactions (monomolecular and bimolecular) were demonstrated.

### Oxidation

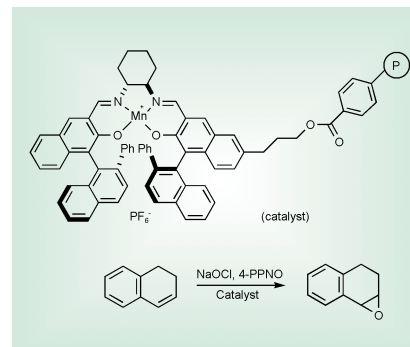
Oxidation using oxygen is an important route to functional molecules, and a group led by Ken Takaki at Hiroshima



University, Japan, has now shown that a polymer-supported Cu catalyst can oxidise phenols under relatively mild conditions (*Bull. Chem. Soc. Jpn.*, 2002, 75, 311). Two types of oxidation are possible, depending on the functionality at the C-4 position. If this is unsubstituted, then formation of benzoquinones is favoured, but if a methyl group is in the 4-position, then benzylic oxidation takes place to give high yields of the aldehyde, along with smaller amounts of some by-products.

### Heterogeneous asymmetric catalysts

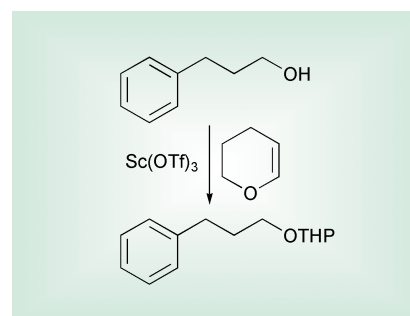
Highly efficient heterogeneous asymmetric catalysts are few and far between, despite the growing number of effective homogeneous complexes which



give excellent enantioselectivity. Keith Smith and Chia-Hui Liu of the University of Wales Swansea, UK, have published details of a Merrifield resin functionalised with an unsymmetrical salen ligand which functions as an efficient epoxidation catalyst (*Chem. Commun.*, 2002, 886). The catalyst, which has Mn as the active metal centre, has a loading of ca. 0.24 mmol g<sup>-1</sup> and catalyses the epoxidation of 1,2-dihydronaphthalene with an ee of 94%, identical to that obtained by model homogeneous equivalents. Reuse was also possible, with a very slight reduction in ee.

### Scandium triflate

Scandium triflate belongs to an intriguing class of water-tolerant Lewis acids, and as such is finding application in a range of reaction types, as a potential replacement for the water-intolerant, more conventional Lewis acids such as AlCl<sub>3</sub>. An example of its efficacy in the formation of tetrahydropyranyl ethers of alcohols has been published by Takeshi

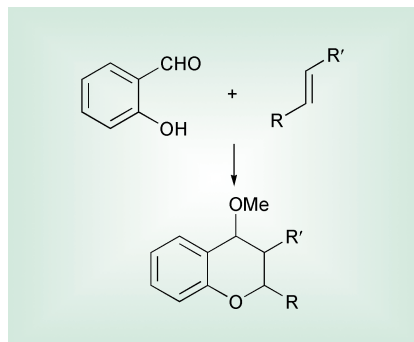


Oriyama and co-workers from Ibaraki University (*Bull. Chem. Soc. Jpn.*, 2002, 75, 367). They have found that a wide range of such ethers can be prepared at room temperature in ethyl acetate in essentially quantitative yields. Washing the product-containing solution with water followed by evaporation of the water layer allowed complete recovery of the catalyst, which could thus be reused.

Scandium triflate has also been shown to effect the synthesis of indenochromans



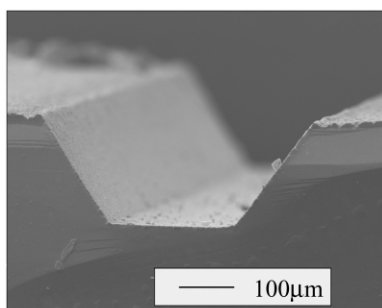
(*Tetrahedron Lett.*, 2002, **43**, 2999).  
Jhillu Yadav and colleagues from the  
Indian Institute of Chemical Technology



in Hyderabad, India, have shown that the scandium triflate catalyses the addition of *o*-hydroxybenzaldehydes to indene under mild conditions. The intermediate hydroxy compound is then trapped by methylation with (MeO)<sub>3</sub>CH to give the tetracyclic product in high yields. Simple alkenes also react smoothly to give benzopyrans.

### Catalytic microreactors

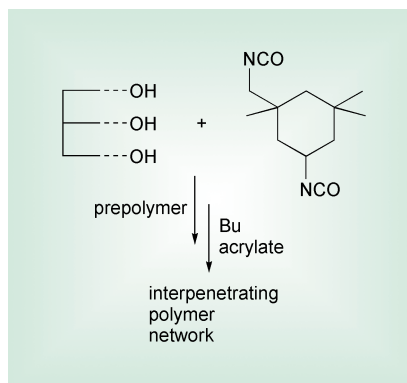
Catalytic microreactors have the potential for intensive and flexible processing. A team led by Asterios Gavriilidis at University College, London, UK, have published details of a microreactor coated with a thin film of TS-1 (*Chem.*



*Commun.*, 2002, 878). The zeolitic catalyst formed a film a few microns thick on the channels of the microreactor. The catalyst was shown to be effective for the epoxidation of 1-pentene. Using hydrogen peroxide, good yields were obtained, which were dependent on residence time, and reactor configuration.

### Polymer systems

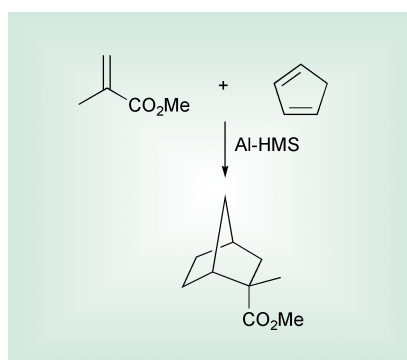
Interpenetrating polymer networks are an interesting class of polymers, where two polymers are physically enmeshed in one another, leading to a hybrid material with unique properties. One such system has been described by Vilas Athawale and Priti Pillay of the University of Mumbai, India (*Bull. Chem. Soc. Jpn.*, 2002, **75**,



369). What is particularly interesting about this polymer system is that it utilises as one of the two components, a polyurethane which is made from renewable resources. The polyurethane is produced from hydrogenated castor oil as the diol and isophorone diisocyanate. Mechanical and chemical properties are discussed, and the material shows some promising behaviour.

### Mesoporous silicas

Aluminium-containing mesoporous silicas have been known for about a decade, and have medium acidity. A group led by Makoto Onaka of the University of Tokyo has now shown that these materials are excellent catalysts for the

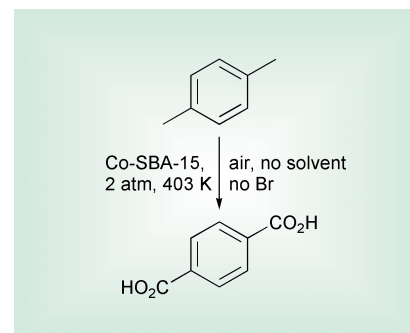


Diels-Alder reaction (*Chem. Lett.*, 2002, 166). Excellent yields were obtained for a range of substrate combinations, and in general the catalysts outperformed a series of alternative solid catalysts. Reuse of the catalyst was possible, although a slight decrease of activity was noted due to polymeric by-products on the catalyst surface, but such byproducts should be relatively easily removed by calcination.

### Terephthalic acid production

Milder conditions and less corrosive catalyst systems are very desirable goals in the production of terephthalic acid.

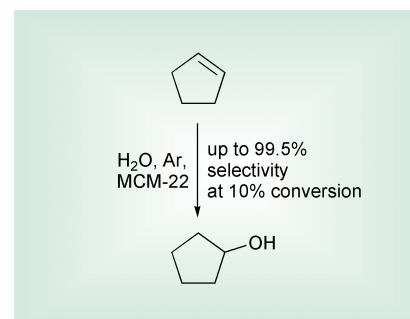
The current Co/Mn/Br catalyst system is the subject of many efforts aimed at replacing Br in particular, with a further important goal being the elimination of acetic acid solvent. A group led by Ki-Won Jun and Sang-Eon Park of the



Korea Institute of Chemical Technology have developed a promising Br-free silica SBA-15, functionalised with Co(III) species (*Chem. Lett.*, 2002, 212). This catalyst is bound to the support *via* carboxylate ligands, and the Co(III) state is stabilised by additional pyridine ligands. Under conditions of relatively low pressure, no solvent and at 130 °C this catalyst system was comparable to the existing commercial system, which also runs in acetic acid solvent.

### Hydration of alcohols

Hydration of alcohols is carried out using aqueous sulfuric acid. A cleaner alternative would be to use a solid acid to carry out this very useful conversion. Duangamol Nuntasri, Peng Wu and Takashi Tatsumi of Yokohama National University have now provided a highly active and selective catalyst which can hydrate cyclopentene effectively (*Chem.*



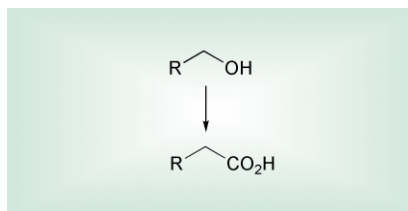
*Lett.*, 2002, **2**, 224). Their catalyst, MCM-22, was compared to various other potential catalysts, and was found to have better selectivity than the others. HZSM-5, a well-established zeolite, performed well, but MCM-22 maintains



high selectivity at higher conversion than HZSM-5.

### Avoiding separation steps

The development of consecutive reaction sequences without separations is one approach to minimising the waste generated during separation steps. The mild and selective oxidation of alcohols to acids using a combination of polymer-supported reagents has now been



demonstrated by Kusoke Yasuda and Steven Ley of the University of Cambridge, UK, (*J. Chem. Soc., Perkin 1*,

2002, 1024). The use of polymer-supported TEMPO, polymer-supported chlorite (from amberlyst IRA900 by ion exchange with  $\text{NaClO}_2$ ) and an immobilised dihydrogenphosphate buffer effected the oxidation of a range of alcohols under very mild conditions. The method is tolerant to a wide range of groups, including BOC, acetals, epoxides, and nitro groups, making it suitable for library generation.

# CRYSTAL Faraday Partnership on Green Chemical Technology

**The Faraday Partnership initiative in the UK is aimed at promoting improved interactions between industry and the science, engineering and technology base. Malcolm Wilkinson describes the 'CRYSTAL' Faraday partnership for Green Chemical Technology.**

### Mission and objectives



The CRYSTAL Faraday Partnership was established in May 2001 and officially launched by Lord Sainsbury, the Minister for Science and Technology in the UK Government on 23 October 2001.

Chaired by Dr Robin Paul the Partnership's mission is: *To be the lead organisation for the research, development and implementation of green technologies and practices in the UK chemical and allied industries.*

CRYSTAL's brief is to identify and match industry's technology needs with opportunities presented by academia's research output and thereby enhance business and environmental performance. In addition to promoting new and innovative research CRYSTAL will integrate and build on the activities of the existing consortia and network technology organisations (CANTO) significantly leveraging their impact.

CRYSTAL has six key objectives:

- Single point of contact for green chemical technology in the UK
- Transfer new, green technology and best practice into real application
- Identify core research priorities matching industry's needs with innovation in universities
- Stimulate new research or practical applications where they are needed
- Increase awareness of best practice for sustainable products and processes
- Train those involved for the culture change required

### Structure and operation

The Hub Partners are the Institution of Chemical Engineers, the Royal Society of Chemistry and the UK Chemical Industries Association. They are joined by 10 CANTO, 12 companies from all sectors of the industry and 18 university departments of chemistry and chemical engineering to form the network. These organisations direct CRYSTAL's activities through a Board of Management supported by the Research, Development and Technology Transfer (RD&TT) Steering Group and the Training, Education and Networking (TEN) Steering Group.

CRYSTAL operates from Rugby in the UK through a programme director and a network of technology translators whose job is to tackle the technical challenges on the ground. They have been active since January and have already held discussions with the majority of organisations in the network. These have resulted in an outline proposal to STI/MMI for development funding of a novel piece of equipment for VOC removal, a confidential workshop on ionic liquids and identification of a supply chain consortium for research into biodegradable packaging material.

CRYSTAL has also defined three priority areas of research focus for £1 million (*ca.* 1.5 million Euro) of earmarked EPSRC funding and has solicited 35 outline proposals which are currently being evaluated. In addition 7 Industrial CASE Awards have been allocated and one graduate student has commenced her research project.

### CRYSTAL and industry

CRYSTAL, like other Faraday Partnerships running in the UK, has the objective of transferring technology from the SET base to industry. We are trying to generate a pipeline of technologies coming to application, initially promoting the transfer of existing green chemical technologies (GCT) into industrial application; developing these where





necessary using targeted funding sources; and supporting longer term research which will under-pin the next generation of GCT.

All this of course requires an engaged and responsive industry but many see no benefit in applying GCT. As ICI's David Bott, Chair of the RD&TT, points out in his recent article in CRYSTAL Window, industry sees threats in the area rather than opportunities – upcoming legislation that changes the ground rules, large capital expenditure and public humiliation if we talk about our advances and get it wrong.

Because of this view, industry tends to approach GCT at two levels. At one level, the 'pragmatic' there are many simple changes to practices and processes that can yield small but important

improvements in environmental impact whilst improving business profitability. The challenge is finding out what is available and how to get the expertise to implement it. The other end of the scale is the approach of making large capital investment in disruptive technologies which change the normal means of doing things.

#### **Challenge for CRYSTAL**

CRYSTAL is encouraging activity at both these levels through its technology translators visiting companies and universities to put the right people in touch with one another, and at the second level trying to identify potential future areas of advance and investing in these. These are not just one-on-one relationships but will involve larger, often

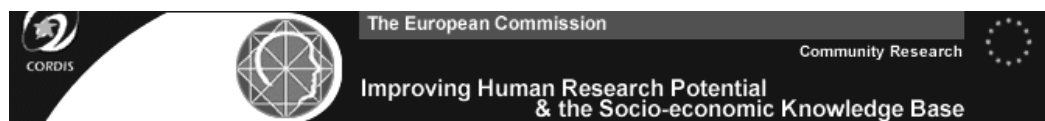
supply chain linked, collaborations. Starting in May and continuing in the Autumn CRYSTAL will be holding Research Workshops open to a wider community to identify these potential collaborative areas of activity.

In some ways CRYSTAL is a test for green chemistry; good science in itself is not sufficient, to have value in societal terms it has to be transformed into applied technology which additionally requires positive economic and social returns; the triple bottom line. It is both a daunting and exciting challenge in which with the help of its network partners CRYSTAL is determined to play its part.

*For more details about CRYSTAL Faraday, please contact Malcolm P Wilkinson on + 44 (0) 1788 434402 or by email: [mwilkinson@icheme.org.uk](mailto:mwilkinson@icheme.org.uk)*



Interuniversity Consortium  
"Chemistry for the Environment"



*Announcing the fifth edition of the:*

## **SUMMER SCHOOL ON GREEN CHEMISTRY**

*Venezia, Italy*

**September 08th – 14th, 2002**

*Admitted young scientists will receive full scholarships.*

*Deadline for applications is June 15th, 2002*

Contacts: Prof. Pietro Tundo (Director): [tundop@unive.it](mailto:tundop@unive.it)

Dr. Alvise Perosa: [alvise@unive.it](mailto:alvise@unive.it), [ssgc@unive.it](mailto:ssgc@unive.it)

Information and application: **<http://www.unive.it/inca>**





# The CHEMRAWN Action Plan

One of the key features of the IUPAC CHEMRAWN (Chemistry Research Applied to World Needs) meeting, is the development of a set of implementation recommendations. These are distributed widely within government, industry and academia to focus attention and funding on the specific issues raised. A significant

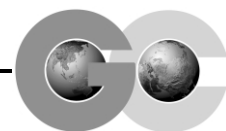
portion of the budget for the conference is reserved for the use of the Future Actions Committee. It is the job of the committee to work after the conference to facilitate the implementation of the ideas. Many of the recommendations from CHEMRAWN XIV (which took place at the University of Colorado Campus,

Boulder, CO, USA, from 9-13 June 2001) deal with education, R&D, industrial implementation and other issues associated with green chemistry and are already being worked on by GCI (USA), OECD, GCN(UK), JCII (Japan), Monash (Australia) and others.

The CHEMRAWN Action Plan is shown below:

CHEMRAWN XIV Recommended Actions	Ongoing Activities	Potential CHEMRAWN XIV Targets
National centers for green chemistry should be established or expanded and these centers should be linked to create an effective worldwide network.	<ul style="list-style-type: none"> <li>National centers in US, UK, Australia, Italy, Japan</li> <li>OECD recommendations and guidelines on establishing national programs (education and R&amp;D elements)</li> </ul>	<ul style="list-style-type: none"> <li>Support for international hub linking national centers into broader network.</li> <li>Support for local programs to make links to international hub</li> </ul>
Basic research funding in green chemistry needs to be significantly increased.	<ul style="list-style-type: none"> <li>EPA/GCI Industry R&amp;D program</li> </ul>	
Educational initiative funding in green chemistry focused on curriculum materials development, faculty training centers, fellowships, and recruitment and retention activities	<ul style="list-style-type: none"> <li>EPA, ACS, GCI, GCN doing educational materials development</li> <li>New Training Center at UO joins UMass-Boston 5/02</li> </ul>	<ul style="list-style-type: none"> <li>Support for additional training centers (~\$400 K each)</li> <li>Fund international distribution of ACS developed training and teaching labs</li> <li>CRYSTAL Faraday type fellowship support</li> </ul>
Increased incentives for the initial implementation of green chemistry technologies by industry to offset investment, policy and regulatory barriers that may exist.	<ul style="list-style-type: none"> <li>White House meeting between industry and Gov't. to discuss (2002).</li> <li>ACS support of tax break for dry-cleaning countered by DuPont opposition</li> <li>OECD, EU, Japanese discussion on green chemistry, especially with industry</li> </ul>	<ul style="list-style-type: none"> <li>Project to develop test case for tax incentive either in OECD country or developing country</li> </ul>
Green chemistry and next generation environmental technology market development project to build market position for commercial opportunities in international trade. International scientist exchange and research collaboration funding should be established	<ul style="list-style-type: none"> <li>GCI sponsored project w/ Zero Waste Alliance and US Dept. Commerce to educate Chinese business leaders</li> <li>Some GCI support for international attendance at Gordon Conf. (Oxford)</li> </ul>	<ul style="list-style-type: none"> <li>US DOC project funding available – match possible</li> <li>Funding of SE Asia training workshop in Thailand (May 02) DONE</li> <li>Additional regional Green Chemistry training programs (India, South America, Middle East)</li> <li>Co-sponsorship of green chemistry summer school attendance (EU or Pan-American)</li> </ul>
Informational outreach to educate industry, public, and environmental groups of the benefits of green chemistry adoption.	<ul style="list-style-type: none"> <li>OECD Sustainable Chemistry program</li> <li>EU Sixth Framework</li> <li>Numerous publications under development (texts, articles, case studies)</li> <li>GCI funding evaluation of metrics of green chemistry performance</li> <li>GCN, JCII, GCI planning major international (bi-annual) conferences on GC with initial focus on industry implementation</li> </ul>	<ul style="list-style-type: none"> <li>Fund distribution of metrics study to international business and government organizations</li> <li>Fund industry survey of impediments and incentives for green chemistry implementation</li> <li>Fund distribution of OECD recommendations on establishing national programs to developing country governments</li> <li>Fund specific attendees or sessions at international conferences</li> </ul>
OTHER		<ul style="list-style-type: none"> <li>CHEMRAWN XIV funded position to work on developments full or half-time (Clovis?)</li> </ul>

Further information can be obtained from Denny Hjeresen (Email: dlh@lanl.gov)



# An undergraduate teaching initiative to demonstrate the complexity and range of issues typically encountered in modern industrial chemistry

David Lennon,<sup>\*a</sup> Andrew A. Freer,<sup>a</sup> John M. Winfield,<sup>a</sup> Philip Landon<sup>a</sup> and Norman Reid<sup>b</sup>

<sup>a</sup> Department of Chemistry, Joseph Black Building, The University of Glasgow, Glasgow, UK G12 8QQ. E-mail: d.lennon@chem.gla.ac.uk

<sup>b</sup> Centre for Science Education, 22 Western Court, University of Glasgow, Glasgow, UK G12 8QQ

Received 12th March 2002

First published as an Advance Article on the web 27th May 2002

In 1997 the Chemistry Department at the University of Glasgow introduced a new initiative into its undergraduate teaching programme. Two exercises were developed that require the students to operate in small groups and to work through exercises that are representative of issues in contemporary industrial chemistry using a problem-based learning format. These modules, termed interactive teaching units, aim to demonstrate the number of factors, often disparate, that contribute to the implementation of successful and sustainable industrial chemical processes. The units are a vehicle for presenting applied chemistry, and also introduce the economic and environmental issues affecting an overall business area. Although these units do not specifically target the concepts of green chemistry, they do enhance student awareness of the principles that underpin the discipline. This report provides an overview of this initiative and briefly outlines the methodology adopted.

## 1. Introduction

In 1996 a review of the undergraduate teaching programme in chemistry at the University of Glasgow indicated a poor understanding amongst our first and second year undergraduate classes of the role of chemistry in society and how chemistry provides the materials required by a modern competitive economy. In particular, the students appeared to have little awareness of the role of the chemical industry. We wished to focus their attention with the following type of questions. Why is it there? Whom does it serve? Who drives the demand for its products? Worryingly, few of our students could produce reasonable and justified answers to these questions. In addition, it was recognised that chemistry was poorly represented in the media, with the majority of articles which featured chemistry tending to concentrate on negative environmental or hazardous issues. Against this background, we decided to consider ways of informing and stimulating our students to question certain aspects of this biased representation of the chemical industry. This report outlines how the Department of Chemistry decided to tackle this discrepancy and describes some of the material developed and introduced into our undergraduate teaching programme to communicate the 'chemical message'.

About this time, the Faculty of Medicine and the Institute of Biological and Life Sciences at the University of Glasgow had instigated a number of new courses based around Problem Based Learning.<sup>1</sup> Student evaluation showed these courses to be popular so it was decided to investigate the effectiveness and viability of this method for our initiative. Simultaneously, the Green Chemistry movement was emerging as a serious force in global chemistry.<sup>2-5</sup> Since green chemistry relates to sustainable processes, we intended this theme, along with the accompanying chemical, economic, legislative and environmental facts, to be the major issue in any material that we produced.

## 2. Aims

The following aims were identified: (1) To increase student awareness of the range of issues chemists typically encounter outside a university environment. (2) To emphasise the vocational nature of chemistry. (3) To develop new teaching units that will enhance student awareness of large-scale sustainable chemical processes. This aim is particularly relevant to the need for teaching material that illustrates the concepts of green chemistry. (4) To encourage student communication skills (small group interactions, oral presentations, written reports, *etc.*). (5) To introduce a new mode of teaching that offers diversification in the student learning experience.

### Green Context

**Chemistry undergraduate students are often thought to lack an appreciation of the role of chemistry in society and an awareness of the role of chemical industry. The increasing importance of explaining the value of chemistry in modern society and demonstrating how it can fit into a sustainable future makes it essential that we make our students more aware of these issues. This paper describes how one major Chemistry Department tackled this by developing new problem-solving, group-based exercises to communicate the 'chemical message.' The material is based on the topical and environmentally important issues of CFC replacement for refrigeration and the industrial scale manufacture of chlorine.**

JHC

### 3. Methodology and selection of material

We elected to adopt the problem based learning (PBL) approach successively implemented in other departments within the University of Glasgow.<sup>1</sup> We approached the University Teaching and Learning Service (TLS), who provided valuable advice on how to set about structuring such courses. Adopting the TLS format, which emphasises the importance of small groups, we chose to name our exercise Interactive Teaching Units (ITUs).

Several factors influenced the way the new materials were designed. For the kinds of aims in mind, educational research had indicated the nature of approach which was important.<sup>6–10</sup> There were many interactive teaching units already available for school chemistry,<sup>11–13</sup> as well as in biology at university level.<sup>1</sup> All used the process of interaction which has been described as internal mental interaction with new materials, ideas and concepts<sup>14</sup> and many involved high levels of interaction between students as they discussed and argued their way forward in solving a problem. Indeed, the solving of problems was a common feature of the units. In this, students usually worked in small groups to use their knowledge of chemistry (or whatever discipline was involved) to reach answers to problems which often had major social, environmental or economic implications.

The Interactive Teaching Unit has been described as a 'syllabus based, free-standing teaching resource which allows students to be involved in active learning by means of role play, decision taking and problem solving and seeks to simulate the kinds of experiences that they might face in the workplace or the wider world'.<sup>15</sup>

Overall, much of the material available was designed for schools, was dated or was too specific for our purposes. We required materials for the 1997–98 programme and the decision was taken to develop new materials rather than attempt to adapt other materials. Since then, some new materials have been developed elsewhere.<sup>16,17</sup> Our aim was that our materials should have an industrial dimension and demonstrate the importance of the chemical industry and chemists in contemporary society.

Although our intention was to feature large-scale industrial processes, initially we had no particular process in mind. After discussions within the Department of Chemistry's Industrial Liaison Committee, ICI Chemicals & Polymers Limited<sup>18</sup> supported our plans and Dr Neil Winterton (ICI Senior Research Associate, now at the University of Liverpool) agreed to help with validating any material we might produce. A major part of ICI Chemicals & Polymer Limited's business at that time was halogen-based and so we decided to concentrate on this area of industrial chemistry. Chlorine chemistry was ultimately selected as it involves high volumes of potentially hazardous materials that are used in a wide variety of products. Safe and economic processes for handling chlorine are at the heart of green chemistry.

The last major parameter that needed defining was which undergraduate class should we target? We decided to concentrate on our 2nd year class (approximately equivalent to a 1st year class in the English university system), as it is this year where the students formally elect which honours degree course they will follow. Our 2nd year class size comprises approximately 200 students, which would mean committing substantial staff resource to run any units and maintain small class sizes. Nevertheless, the initiative was endorsed by the Chemistry Department and the commitment acknowledged. Each ITU operates over 4 days allowing the class to be split up into groups of approximately 48. This is then further divided into 4 tutorial groups of 12 students. Each group is led by a tutor, who is a member of the academic staff. This arrangement is staff intensive but evaluation reveals the students benefit and appreciate the opportunity to interact in a relatively informal

manner, *i.e.* compared with lectures and practical classes, with faculty members.

After substantial investment in time and energy, two ITUs were produced. The first (ITU1), entitled 'The Age of Refrigeration', examines the issues associated with the replacement of chlorofluorocarbon (CFC) refrigerants. This unit aims to expose the students to relevant issues in chemistry, economics, environmental issues, politics and legislation that surround the topic. In order to illustrate the dynamic nature of the chemical industry, the issues are considered over a period of time, *viz.* 1970, 1987 and 1999. The second module (ITU2) is entitled 'Mercury, Membrane or Diaphragm' and examines the concept of producing chlorine, sodium hydroxide and hydrogen on an industrial scale. As such, it represents an exercise in applied electrochemistry. Comparable issues to those considered in ITU1 are examined but, in addition, emphasis is given to issues of safety, chemical engineering and concepts of scale. The specifics of both units are described individually in Section 4. The units were successfully trialed in 1997 and, after some tweaking, were formally introduced in to our undergraduate teaching programme in 1998.

Finally, it is worthwhile to comment on the expertise necessary to bring these units to a satisfactory standard. Firstly, the structuring, timing and composition of the units is crucial. TLS's experience in class dynamics was vital to maintain student interest and activity levels over the 3 h duration of which both exercises run. Secondly, in 1997 a large quantity of literature on the topics selected was not readily accessible in the public domain, with much of the wisdom retained within industry. This was particularly true in the case of the refrigerant unit (ITU1), although comprehensive review papers on this topic have just recently been published.<sup>19,20</sup> Acquisition of up to date data and validation of the whole exercise by experts in two very specific areas of chemistry were essential to produce units that were genuinely representative of the industrial scenario. Without the assistance of Dr Neil Winterton and his colleagues at ICI Chemicals & Polymers Ltd., the range of issues covered within the units would have been substantially restricted and, consequently, less relevant. Finally, it is noted that both the story about CFC replacements and chlorine production by electrolysis have their own dynamics and information current when the units were produced (1996–1998) can become obsolete very quickly. Nevertheless, the general principles remain valid and our students can learn and benefit from participation in such an exercise. The following section describes the Units as they currently stand. Future up-grades of the facts and figures will always be required.

## 4. Course content

### 4.1 ITU1. The age of refrigeration

This unit examines issues in the replacement of CFC refrigerants as viewed from different periods of time: 1970, 1987 and 1997. The unit starts by introducing the general concepts of refrigeration. Post-war, the market for refrigeration, and thereby refrigerants, has grown dramatically. Refrigeration is now a part of everyday modern life and represents a diverse market; ranging from relatively small scale domestic refrigerators and air conditioners to large scale industrial units.

Refrigeration is described using the classical thermodynamic approach,<sup>21</sup> which accounts for the transfer of heat from a cold compartment to hotter surroundings utilising the latent heat of vapourisation of a refrigerant. The refrigerant is moved about the system by means of a compressor. Fig. 1 schematically represents the general process. The refrigeration process can be described by eqn. (1):

$$w = m\Delta H_{\text{vap}} \left( \frac{T_h - T_c}{T_c} \right) \quad (1)$$

where  $w$  represents the work expended,  $m$  is the mass of refrigerant,  $\Delta H_{\text{vap}}$  is the enthalpy of vapourisation of the refrigerant,  $T_h$  is the temperature of the hot surroundings of the refrigerator and  $T_c$  is the temperature of the refrigerator cold compartment. The cyclic nature of the process is described and the pivotal requirement for condensation of the refrigerant from the vapour phase is emphasised.

**1970.** The students are then introduced to Table 1, which outlines some physical values of a range of potential refrigerants. The refrigerants selected are representative of the following subsets: chlorofluorocarbons, hydrochlorofluorocarbons, hydrofluorocarbons, inorganics and hydrocarbons. The students operating in groups of 12 are encouraged by their tutor to define and explain the importance of the enthalpy of vapourisation and to discuss the effects of hydrogen bonding on boiling points. This dataset also provides the opportunity to describe Trouton's Rule,<sup>22</sup> which rationalises comparable enthalpies of vapourisation as verification that the liquid  $\rightarrow$  gas transition is dominated by a large entropy factor.

Table 2 provides further information on the flammability, toxicity and relative cost of these possible refrigerants. In small working groups of four students, the concept of critical temperature ( $T_c$ ) and likely operational temperature ranges are considered. The critical temperature is the temperature above which a gas cannot be liquified by pressure alone. For temperatures in excess of  $T_c$ , there is no longer any distinction between liquid and vapour phases, *i.e.* only a (dense) gas phase exists. This parameter, specified for all candidate refrigerants in Table 1, excludes the use of  $\text{CO}_2$  as a potential refrigerant under conventional operating conditions because of its inability to be converted back to a liquid from a vapour as part of the refrigeration cycle. The students also need to realise that complete toxicological information for some compounds (*e.g.*  $\text{CF}_3\text{CH}_2\text{F}$ ) was not available in 1970.

Each student is then asked to decide which compounds should be selected as suitable refrigerants. Without exception, they select  $\text{CCl}_2\text{F}_2$  (a chlorofluorocarbon) as their first choice

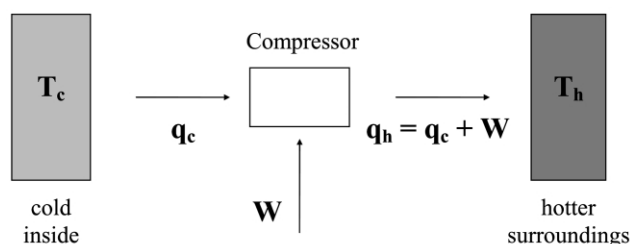


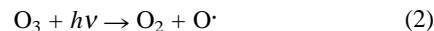
**Fig. 1** Schematic diagram of a refrigeration unit:  $T_c$  and  $T_h$ , respectively, represent the temperatures of the cold compartment and the surroundings;  $q_h$  is the heat passed to the surroundings, which is the sum of  $q_c$ , the heat taken from the cold compartment, and  $w$ , the amount of work involved. The figure is adapted from ref. 21.

**Table 1** Physical properties of a range of potential refrigerants

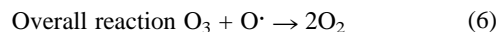
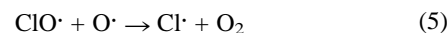
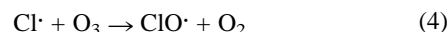
Refrigerant	Molecular weight	Enthalpy of vapourization, $\Delta H_{\text{vap}}/\text{kJ mol}^{-1}$	Bp/ $^{\circ}\text{C}$	Mp/ $^{\circ}\text{C}$	Critical temp./ $^{\circ}\text{C}$
$\text{CCl}_2\text{F}_2$	121	20.0	-29.8	-155.0	112
$\text{CHClF}_2$	86.5	20.2	-40.8	-160.0	96
$\text{CF}_3\text{CH}_2\text{F}$	102	22.1	-22.2	-108.0	101
$\text{NH}_3$	17	23.2	-33.4	-77.7	132
$\text{H}_2\text{O}$	18	40.4	100.0	0.0	374
$\text{C}_4\text{H}_{10}$ (isobutane)	58	21.0	-11.7	-159.7	135
$\text{CO}_2$	44	25.1	-78.5	-56.6	31

and  $\text{CHClF}_2$  (a hydrochlorofluorocarbon) as their second choice. This outcome is totally consistent with the refrigerants selected by industry from *ca.* 1944–1980.<sup>20</sup>

**1987.** The students are made aware of the pioneering paper by Rowland and Molina published in 1974<sup>23</sup> that suggested that chlorofluorocarbons (CFCs) are broken down by UV light in the stratosphere. In the upper atmosphere, ozone is normally in equilibrium with oxygen and oxygen radicals (eqn. (2)):



However CFCs can interact with stratospheric ozone by the following mechanism (eqns. (3)–(6)):<sup>24a,25</sup>



Hence, ozone is catalytically destroyed by chlorine atoms formed in the photolytic decomposition of CFCs. We acknowledge that this homogeneous mechanism is an oversimplification and a heterogeneous reaction is now the preferred mechanism,<sup>19,26</sup> but our 2nd year class have no experience of heterogeneous kinetics and the simpler scheme seems more appropriate for this level of study. The importance of UV absorption by ozone and the consequences for life processes are stressed.

Students are next informed about the Montreal Protocol<sup>19,20,27,28</sup> which aims to reduce ozone depleting chemicals (*e.g.* CFCs) in developing countries by 50% by the year 2000. Annual global CFC production figures are estimated at *ca.*  $1.11 \times 10^6$  tonnes, with sales of approximately £300 million per year. Thus CFC production represents a large and expanding market, for which replacement refrigerants or alternative refrigeration methodologies need to be found, quickly.

The gravity of the position is further heightened by informing the students about greenhouse gases and the topic of global warming.<sup>24b,29</sup> Table 3 quantifies the ozone depletion potential and the global warming potential of some candidate refrigerants.<sup>19,20</sup>

The alternatives to CFCs can be divided into four groups: (a) hydrofluorocarbons (HFCs), (b) hydrochlorofluorocarbons (HCFCs), (c) inorganic substances and (d) hydrocarbons. The tutor then divides up his group of 12 students into three sub-groups of four students who are asked to role play the positions of three distinct parties: (i) existing CFC manufacturers, (ii) manufacturers of refrigeration equipment and (iii) environmental monitoring and protection agencies. The tutor adopts the role of Government. The three sub-groups are supplied with a two page briefing document that represents the stance/perspective of that particular interest group. The groups are then asked to decide which replacement refrigerants should be adopted, for what reasons and to propose an implementation strategy. They make short oral presentations. An example of the



**Table 2** Assessment of the flammability, toxicity and relative cost of a range of potential refrigerants using information available in 1970

Refrigerant	Flammable?	Toxic? <sup>a</sup>	Relative cost (1970 values)
CCl <sub>2</sub> F <sub>2</sub>	No	+++++	Fairly cheap
CHClF <sub>2</sub>	No	+++++	Moderate
CF <sub>3</sub> CH <sub>2</sub> F	No	Unknown	Unknown
NH <sub>3</sub>	Yes <sup>c</sup>	+ <sup>d</sup>	Fairly cheap
H <sub>2</sub> O	No	+++++	Negligible
C <sub>4</sub> H <sub>10</sub> (isobutane)	Yes	+++ <sup>e</sup>	Expensive <sup>b</sup>
CO <sub>2</sub>	No	+++++	Negligible

<sup>a</sup> The greater the number of crosses, the lower the toxicity. <sup>b</sup> At the purity levels required. <sup>c</sup> Burns only in the presence of a supply of oxygen. <sup>d</sup> The powerful smell of ammonia makes poisoning unlikely. <sup>e</sup> Slight anaesthetic properties.

**Table 3** Ozone Depletion Potential (ODP) and Global Warming Potential (GWP) for a range of candidate refrigerants.<sup>19,20</sup> The ODP values are related to CCl<sub>3</sub>F (CFC-11), which is assigned a value of 1.0. The GWP values are relative to CO<sub>2</sub> over 100 years

Refrigerant	Ozone Depletion Potential (ODP)	Global Warming Potential (GWP)
CCl <sub>2</sub> F <sub>2</sub> (CFC-12)	1.0	8500
CHClF <sub>2</sub> (HCFC-22)	0.06	1700
CF <sub>3</sub> CH <sub>2</sub> (HFC-134a)	0.0	1300
NH <sub>3</sub>	0.0	Insignificant
C <sub>4</sub> H <sub>10</sub> (isobutane)	0.0	Insignificant

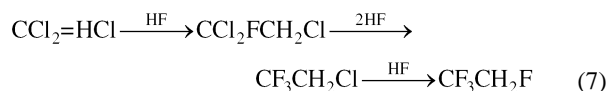
questions to be addressed by one of the groups, the CFC manufacturers, is presented below.

What would be the best replacement refrigerant? Who should pay for the changes? How much is your sub-group prepared to pay/contribute to the proposed changes? What assistance do you require from Governmental organisations to manage/support the proposed changes? Broadly identify the customers that you service and your financial base. Are there any alliances that you could consider forming?

The tutor, representing Government, then guides the tutorial group in a discussion where they try to agree an overall solution. A spokesperson is elected and their conclusions documented. The whole class of 48 students is then reunited and the outcomes from the four tutorial groups compared.

**1999.** The ITU terminates with a plenary session in which a lecturer summarizes the position from a contemporary perspective. The scientific significance of the topic is brought home to the students by the award of the 1995 Nobel prize in Chemistry to Rowland and Molina. They are up-dated on the levels of CFC production in Europe and America and the different political influences in these regions. Recent trends towards hydrocarbon refrigerants<sup>30</sup> are discussed but the hydrofluorocarbon CF<sub>3</sub>CH<sub>2</sub>F (HFC-134a) is identified as the major replacement for CFCs.<sup>19,20</sup> Industrial based organizations such as the Program for Alternative Fluorocarbon Toxicity Testing (PAFT) have published reliable data establishing the low toxicity of HFC-134a,<sup>20,31,32</sup> thereby giving it the green light for general usage.

Methods for the production of HFC-134a are considered, but the ICI route (eqn. (7)) is highlighted:<sup>20</sup>



The importance for a suitable catalyst in the final step, so that the process can operate at an acceptable rate, is emphasized. Viability of the process is ensured by extensive recycling of

organics and HF. ICI were awarded the MacRobert Engineering Award in 1993 in recognition of developing and commissioning an industrial process to manufacture HFC-134a. The class are made aware that successful achievement of such a substantial development project in only five years is exceptional and further emphasizes the highly competitive nature of the refrigerant manufacturing business.

The final topic to be considered is the concept of Total Equivalent Warming Impact (TEWI) applied to refrigeration and, in particular, the relative contribution of the actual refrigerant to global warming.<sup>33</sup> A domestic refrigerator is chosen as an example and the TEWI estimated. A *direct* contribution comes from the potential emission of (i) the refrigerant and (ii) the blowing agent for the foam insulation used in the construction of the refrigerator. Both of these materials can operate as greenhouse gases. However, more relevantly, there is a substantial *indirect* contribution to the TEWI that relates to the energy expenditure on operating a refrigerator continuously for approximately 10 years. Combustion of fossil fuels is still a major route for the generation of electricity. This process produces CO<sub>2</sub>, which is itself a potent greenhouse gas. The atmospheric half-life of CO<sub>2</sub> is approximately 500 years, so it is necessary to consider *at least* a 500 year time span to calculate a TEWI.<sup>33</sup> (We acknowledge that 100 year timespans are the accepted timescale under the Kyoto Protocol and are the standard used to calculate TEWI but we wished to illustrate the point that materials with long atmospheric lifetimes can have an effect over substantial timescales.) Fig. 2 illustrates the different contributions to the overall TEWI over this period.<sup>33</sup> The term radiative forcing is used as a measure of the extent of global warming.<sup>34</sup> Clearly, the indirect production of CO<sub>2</sub> is the major contributor to global warming. The use of HCFC-141b as a blowing agent for the refrigerator foam insulation makes the second largest contribution and, if HFC-134a is selected as the refrigerant, then this compound makes a negligible impact on the TEWI. Furthermore, in addition to the minimal magnitude of the effect of the actual refrigerant, it is noted that whereas the blowing agent and refrigerant are completely accounted for within 100 years, the CO<sub>2</sub> produced will continue to contribute to global warming for a further 400 years and beyond. Unfortunately, we cannot use

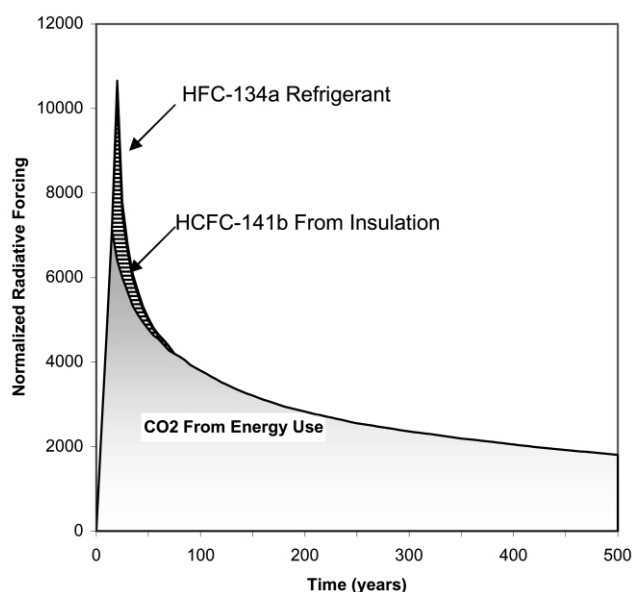


**Fig. 2** Radiative forcing of greenhouse gases (in kg of CO<sub>2</sub> equivalents) from a domestic refrigerator/freezer. The lower lightly shaded area represents the CO<sub>2</sub> contribution. The contribution from the foam blowing agent (HCFC-141b) is designated by the hatched lines. The negligible contribution from the refrigerant (HFC-134a) is signified by the thickness of the line that resides on top of the hatched and shaded areas. The figure is adapted from ref. 34.

all the amenities available to us at no cost to the environment. However, we can do our best to minimize their impact with an innovative chemical industry playing a vital role.

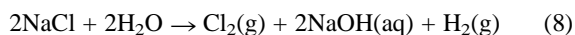
Collectively, this exercise aims to demonstrate the complexity that is common in modern industrial chemistry. Moreover, through example, it attempts to illustrate the fact that the successful implementation of new manufacturing procedures for an ever changing market place is a demanding task, in which chemists play an important and critical role.

In order to encourage active participation, the exercise is formally assessed and the students are asked to write a short essay on a topic related to the exercise. An example of a recent assignment is: 'The Minister for the Environment has been asked in the House of Commons to supply the Government's recommendation for which refrigerants should be used in the next decade. You are a scientific civil servant. Prepare a 1 page (ca. 500 word) briefing document for your Minister.' The essays are marked by the tutors and the ITU assessment comprises 5% of the overall course mark. Awarding a relatively high mark ensures that the students take the exercise seriously.

#### 4.2 ITU2. Mercury, membrane or diaphragm

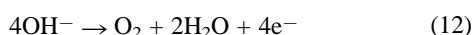
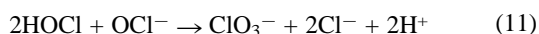
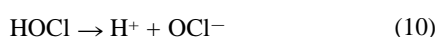
This ITU examines issues relevant to the chlor-alkali industry and concentrates on the industrial scale manufacture of chlorine, sodium chloride and hydrogen. An information pack on 'Green Chlorine', prepared by the Chemical Industry Education Centre at the University of York,<sup>35</sup> was available but this was targeted at 13–16 year olds and was deemed not to be suitable for our undergraduate classes.

The industrial process is carried out by electrolysis of rock salt and is governed by eqn (8).



Chlorine demand is traditionally the factor which governs the chlor-alkali industry.<sup>36,37</sup> However, sodium hydroxide also plays an important part. Demand dictates that the price of these commodities are rarely constant, causing substantial variations in the profitability of the overall process. For example, during the 1980s the lowest price for sodium hydroxide was \$40 per tonne and the highest price \$500 per tonne. And over a comparable period, wide variations in the chlorine price were also observed.<sup>38</sup> Given that chlorine and sodium hydroxide prices are rarely in phase,<sup>39</sup> it is a difficult task to manage the process in such a way that the overall business is economic.

Within tutorial groups comprising a maximum of 12 persons, the students participate in exercises that demonstrate the size of the markets and the market outlets for these products.<sup>36,37,39</sup> The students are generally unaware that, for example, the manufacture of PVC that is used in the guttering on their house/flat requires a source of chlorine, or that paper processing requires substantial quantities of sodium hydroxide. The class are reminded of the general concepts of electrolysis, then they are made aware of the problem with electrolysis applied to this particular chemical system. Specifically, because of the following reactions [eqns. (9–12)], the products must not be allowed to mix.<sup>36</sup>



Electrolysis in a simple one-pot vessel will lead to reaction of chlorine with sodium hydroxide to give unwanted sodium

hypochlorite ( $\text{NaClO}$ ), sodium chlorate ( $\text{NaClO}_3$ ) and oxygen as bi-products. In addition, the function of the cell design is also to keep hydrogen and chlorine gases separate because they can combine explosively.

The tutorial group is then split into three sub-groups which are asked to adopt the role of a process design team that considers the effectiveness of one of three types of electrochemical cell: a mercury cell, a membrane cell, or a diaphragm cell.<sup>36,37,39,40</sup> Each sub-group comprises four students. The sub-groups are provided with information on the respective cells in three stages. The introductory information is just sufficient for them to be able to work out how the cell might actually operate. The last batch of information effectively explains the complete operational characteristics of their particular cell. This format gives the participants experience of attempting to effect designs with limited information, a not untypical situation. Using the adage—'you don't fully understand something until you can explain it to others' the students interact in their sub-groups to give a presentation to the tutorial group as to how their cell operates. Fig. 3 shows an example of some of the introductory information pertaining to the mercury cell and Fig. 4 shows the completed diagram given to the sub-groups towards the end of the design session. The students are provided with Fig. 3 as an overhead projector acetate to assist them in their initial presentation.

Guided by the tutor, the three sub-groups discuss which electrochemical cell should be selected. They are provided with information on energy costs and typical purity levels associated with the three types of cell. The three sub-groups then debate amongst themselves the advantages/disadvantages of 'their' design and present the answers in another oral presentation. This unit therefore asks the students to consider issues in applied electrochemistry, with a process engineering perspective. The tutorial group elect a spokesperson who documents their conclusions.

In the plenary session the whole class of ca. 48 students is reunited. The tutorial group representatives summarize the conclusions from the four tutorial groups. The lead lecturer then uses slides and a video to show the students the mercury, diaphragm and membrane cells that operate at INEOS Chlor's plants at Runcorn and Lostock. The students get to appreciate the full scale of the operation and its associated power

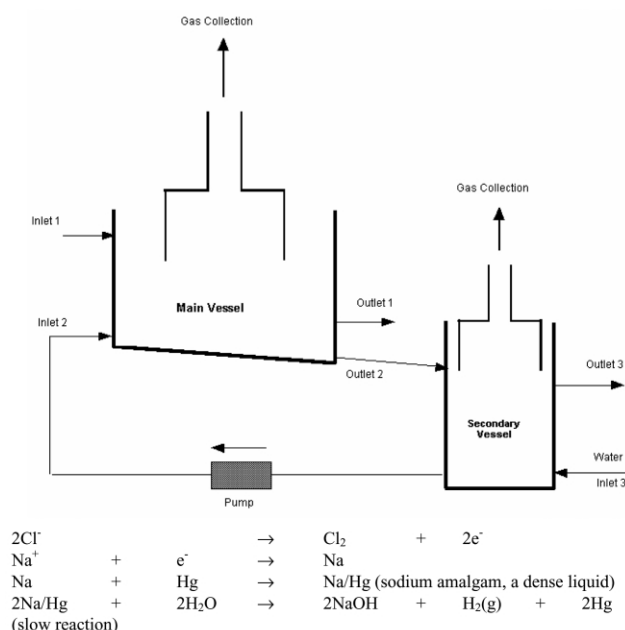
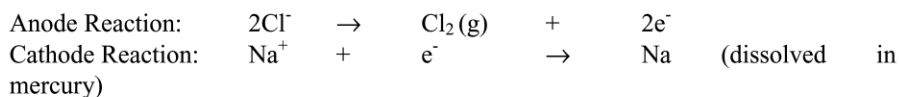
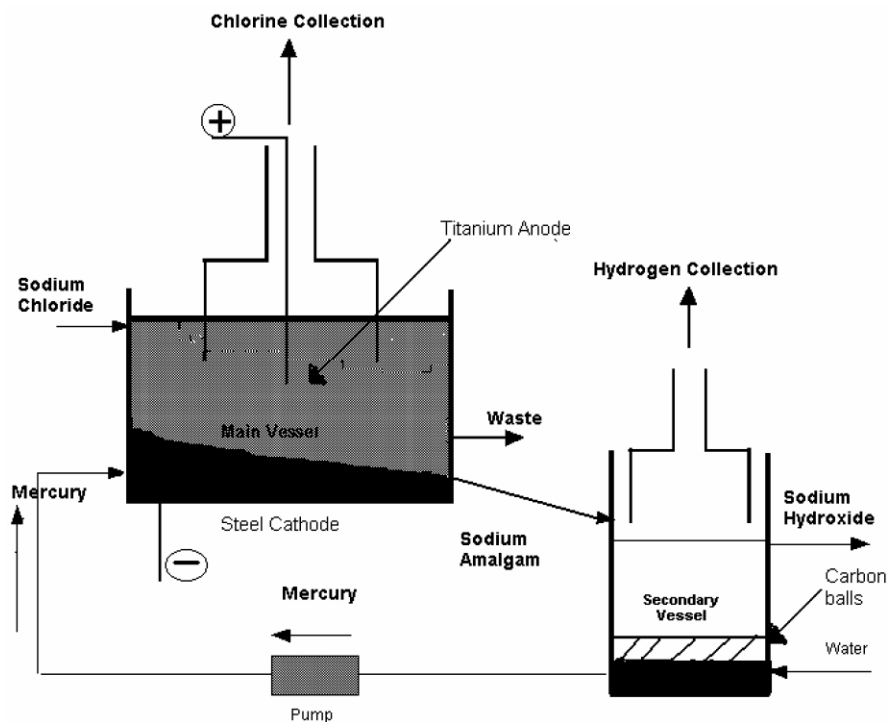


**Fig. 3** Initial schematic diagram of a mercury electrochemical cell given to assist the design team to understand how the equipment functions. They are also presented with the accompanying series of chemical equations, which they need to assign to the relevant parts of the apparatus.



In the secondary vessel, the following reaction occurs:

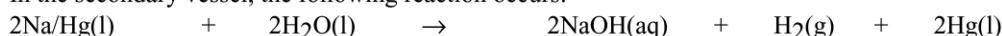


**Fig. 4** Completed schematic diagram of a mercury electrochemical cell presented to students at the end of the session when the design teams are asked to understand how their particular cells operate. They are also provided with the electrochemical equations.

requirements at this stage. The significance of environmental issues are shown to be increasingly important, by reference to incidents such as that which occurred in Minamata Bay, Japan in 1965 where mercury contamination led to severe health problems in the local population.<sup>36</sup> Geo-political and economic implications of such events are considered and discussed. The introduction of the coated titanium anode (aka dimensionally stable anode) in the 1970s is described and recognized as a major milestone in the chlor-alkali industry.<sup>36,37,41</sup> As with ITU1, coursework is assigned. Generally, this requires the students to explain how their specified cell operates and to compare their cell against the alternatives.

## 5. Student evaluation

At the end of each ITU session the students are asked to evaluate the course. Representative results from evaluation of ITU1 run

over the years 1998, 1999 and 2000 are shown in Table 4. Consistently high evaluations are received every year, which is felt justifies the considerable staff resource allocated to the running of these units. The ITU topics have a modest overlap to material the students are exposed to in lectures, which means that they have some connectivity to the topics being examined. They also seem to enjoy the applied aspect of the exercise that examines practical and associated elements of a complex dynamic. The significant 'no' response to the question, 'would you like to see more ITUs as part of your degree programme?' (Table 4) was unexpected and contrasted with the overall positive student response. However, further questioning revealed the origin of this negative response was the inherent reluctance of some of our students to make oral presentations to even quite small audiences. This is understandable but it is important that we continue to provide our students with the opportunity to develop their presentational skills. To further this aim, more opportunities for group presentations have recently

**Table 4** Examples of student evaluation results for ITU1 (The Age of Refrigeration). The sample relates to the response received from a total of 552 students spread over 12 sessions run in 1998 (4), 1999 (4) and 2000 (4). The specific response as a percentage of the full sample is presented in parentheses

	Very poor	Poor	Average	Good	Very good
1. Grade the overall effectiveness of the ITU to present the issues pertinent to the use of refrigerants.	1	2	42	354	155
	(0.2%)	(0.4%)	(7.5%)	(63.9%)	(28.0%)
2. Did you enjoy taking part in the exercise	Yes		No		
	521		31		
	(94.4%)		(5.6%)		
3. Would you like to see more ITUs as part of your degree performance?	Yes		No		
	415		133		
	(75.7%)		(24.3%)		

been introduced into the overall undergraduate teaching programme, and it is hoped that increased familiarity with the requirement to give modest oral presentations will minimize the trauma experienced by a proportion of the students.

## 6. Summary

The experience from introducing the two interactive teaching units into our 2nd year chemistry course at the University of Glasgow can be summarized by the following points.

The ITUs diversify the student learning experience and provide the opportunity for improvements in communication skills.

The ITUs provide an insight into industrial chemistry and the complexity of problems typically encountered in an industrial scenario.

The ITUs improve student understanding of the role of chemistry and the chemical industry in society.

The industrial support proved to be extremely valuable. Any exercise that attempts to present a perspective of activities outside the university environment will always benefit from feedback from experts on the field.

The Interactive Teaching Units (ITUs) are a stimulating medium to enhance student awareness of environmentally sustainable products and processes, *i.e.* green chemistry.

## Acknowledgements

The substantial assistance of ICI Chemicals & Polymers Limited (now INEOS Chlor Ltd. and INEOS Fluor Ltd.)<sup>18</sup> is gratefully acknowledged. Dr Neil Winterton (ICI, now at the University of Liverpool) coordinated the overall ICI contribution. Dr Dick Powell (ICI, now at the University of Manchester Institute of Science and Technology) and Mr Archie McCulloch (ICI, now at the University of Bristol) provided technical assistance relating to new refrigerants and Dr Mottram Couper (ICI, now at INEOS Chlor Ltd.) contributed to the electrochemistry module. INEOS Chlor Ltd. and INEOS Fluor Ltd. are thanked for also supporting this educational initiative. Dr Phil Landon acknowledges financial support from the Scottish Higher Education Funding Council. ICI are thanked for the provision of a Lectureship in Heterogeneous Catalysis (DL). The humour, wisdom and patience of past and present members of the ITU Tutorial Team (Dr John Carnduff, Dr John Dymond, Dr Adrian Laphorn, Dr David McComb, Dr Ken Muir, Dr Marie-Claire Parker, Dr David Procter, Dr David Rycroft and Dr Diane Stirling) are gratefully acknowledged. Without their persistence and strength these units would have died in the trial stage. Mrs Kirsty Letton (Teaching and Learning Service, University of Glasgow) assisted with the initial drafting of both units. Mrs Lesley Bell and Mr Bob Munro (Department of Chemistry) are thanked for careful preparation of the teaching material.

## References

- H. Clarkeburn, E. Beaumont, R. Downie and N. Reid, *J. Biol. Educ.*, 2000, **34**, 133.
- P. T. Anastas and J. C. Warner, *Green Chem., ACS Symp. Ser.*, 1996, **626**, 1.
- P. T. Anastas and T. C. Williamson, *Green Chemistry: Theory and Practice*, OUP, Oxford, 1998.
- R. A. Sheldon, *C. R. Acad. Sci. Ser. IIC*, 2000, **3**, 541.
- K. L. Mulholland, R. W. Sylvester and J. A. Dyer, *Environ Prog.*, 2000, **19**, 260.
- N. Reid, *Educ. Chem.*, 1976, **13**, 82–83.
- H. Johnstone and F. Percival, *Chem. Br.*, 1978, **14**, 507.
- N. Reid, in *Perspectives in Academic Gaming and Simulations*, Kogan Page, California, 1978, vol. 1 and 2, pp. 92–97.
- M. S. Byrne and A. H. Johnstone, *Educ. Chem.*, 1987, **24**, 75.
- M. S. Byrne and A. H. Johnstone, *Stud. Higher Educ.*, 1987, **12**, 325.
- N. Reid, in *Simulation and Games*, SAGE Publications Inc, CA, 1980, vol. 11, p. 107.
- A. H. Johnstone and N. Reid, *Chem. Ind. (London)*, 1979, **4**, 122.
- N. Reid, *Educ. Chem.*, 1980, **17**, 78.
- A. H. Johnstone and N. Reid, *Int. J. Sci. Educ.*, 1981, **3**, 205.
- N. Reid, *Educ. Chem.*, 1999, **36**, 23.
- T. Overton, *Univ. Chem. Educ.*, 1997, **1**, 28.
- The Titanium Dioxide Project*, Project Improve, Faculty of Science & The Environment, University of Hull, 1998.
- In January 2001 ICI Chemicals & Polymers Ltd. was divested into two separate organisations: INEOS Chlor Ltd. and INEOS Fluor Ltd. The former organisation operates chlorine-related processes and refrigerants are manufactured by the latter organisation.
- A. McCulloch, *J. Fluorine Chem.*, 1999, **100**, 163.
- R. L. Powell, in *Fluorine Chemistry at the Millenium, Fascinated by Fluorine*, ed. R. E. Banks, Elsevier, Amsterdam, 2000, p. 339.
- R. J. Dossat, *Principles of Refrigeration*, Wiley, Chichester, 1981.
- P. W. Atkins, *Physical Chemistry*, OUP, Oxford, 1990, p. 90.
- M. J. Molina and F. S. Rowland, *Nature*, 1974, **249**, 810.
- D. R. Raiswell, P. Brimblecombe, D. L. Dent and P. S. Liss, *Environmental Chemistry*, E. Arnold, London, 1980, (a) p. 124, (b) p. 38.
- P. Suppan, *Chemistry and Light*, Royal Society of Chemistry, London, 1994, p. 213.
- Stratospheric Ozone. 1990. Third Report of the UK Stratospheric Ozone Review Group, HMSO, London, 1990.
- Montreal Protocol on Substances that Deplete the Ozone Layer, *Alternative Fluorocarbons Environmental Acceptability Study*, Washington DC, 1995.
- WMO Global Ozone Research and Monitoring Project, Report No. 44, Geneva, 1999.
- The Green House Effect, Climatic Change, and Ecosystems*, ed. B. Bolin, B. R. Döös, J. Jäger and R. A. Warrick, Wiley, Chichester, 1989.
- A. Cavallini, *Int. J. Refrig.*, 1996, **19**, 485.
- HFC-134a Toxicology Summary, *Programme for Alternative Fluorocarbon Toxicity Testing*, Washington DC, 1995.
- Testing to Extremes, *Programme for Alternative Fluorocarbon Toxicity Testing*, Washington DC, 1997.
- Total Global Warming Impact, *Alternative Fluorocarbons Environmental Acceptability Study*, Washington DC, 1995.
- Contribution of Greenhouse Gases to Climate Forcing Relative to CO<sub>2</sub>, *Alternative Fluorocarbons Environmental Acceptability Study*, Washington DC, 1995.
- Green Chlorine, *Making Use of Science and Technology*, Chemical Industry Education Centre, University of York, 1996.
- S. F. Kelman, in *An Introduction to Industrial Chemistry*, ed. C. A. Heaton, Blackie, Glasgow, 1991, p. 284.
- L. C. Curlin, T. V. Bommaraju and C. B. Hansson, *Kirk-Othmer Encyclopedia of Chemical Technology*, 4th edn., 1991, vol. 1, p. 938.
- M. Beal, *Chem. Ind. (London)*, 1997, 434.
- K. H. Büchel, H.-H. Moretto and P. Woditsch, *Industrial Inorganic Chemistry*, Wiley-VCH, Weinheim, 2000, p. 146.
- C. Jackson and S. F. Kelham, *Chem. Ind. (London)*, 1984, 397.
- M. N. Mahmood, A. K. Turner, M. C. M. Man and P. O. Fogarty, *Chemistry and Industry*, 1984, 50.





# Cyclodextrins as inverse phase transfer catalysts for the biphasic catalytic hydrogenation of aldehydes: a green and easy alternative to conventional mass transfer promoters

Sébastien Tilloy, Hervé Bricout and Eric Monflier\*

Université d'Artois, Faculté des Sciences J. Perrin, Rue J. Souvraz, SP 18 - 62307 Lens Cedex, France. E-mail: monflier@univ-artois.fr

Received 17th September 2001

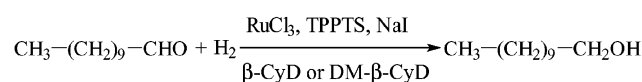
First published as an Advance Article on the web 13th February 2002

The ruthenium-catalyzed hydrogenation of water-insoluble aldehydes in an aqueous/organic two phase system has been investigated in the presence of cosolvents or cyclodextrins. At low content, *i.e.* a content that enables to recover quantitatively the catalytic system without loss of metal with a cosolvent,  $\beta$ -cyclodextrin and its dimethylated form appear to be more efficient than cosolvents for performing the reaction. The formation of inclusion complexes between cyclodextrin and various components of the reaction medium (aldehyde, alcohol, hydrocarbon of the organic phase) is discussed on the basis of mass spectrometry, NMR and catalytic experiments.

## Introduction

The main disadvantage of homogeneous catalysis *versus* heterogeneous catalysis is the difficulty to separate the products cleanly and easily of the expensive metal catalyst. Among the different approaches described in the literature to overcome this problem, catalysis in an aqueous/organic two-phase system with water soluble transition metal complexes is an economical and safe approach.<sup>1,2</sup> Indeed, aqueous biphasic catalysis allows quantitative recycling of the catalyst and decreases harmful emissions and costs associated with solvent recycling.<sup>2</sup> Furthermore, water presents many advantages such negligible price, non-toxicity and environmental safety. Numerous substrates such as olefins,<sup>3</sup>  $\alpha,\beta$ -unsaturated<sup>4</sup> or saturated aldehydes<sup>5</sup> and carbohydrates<sup>6</sup> have been hydrogenated under such conditions. The activities are satisfying for substrates which are slightly soluble in water. With insoluble compounds, the yields dramatically decrease due to mass-transport limitation between the two layers. To circumvent this problem, hydrogenation can be conducted in the presence of water soluble catalysts supported on silica (SAPC),<sup>7</sup> cosolvent,<sup>8</sup> surface active agents,<sup>9</sup> or colloidal metallic particles stabilized by surfactants.<sup>10</sup> Although SAPC and the approaches involving surface active agents give very good results in terms of activity and recovery, these systems are too sophisticated to be conveniently applied in an industrial context. Consequently, the use of cosolvent is generally the only alternative for the industrial chemist wishing to hydrogenate highly hydrophobic substrates in water.

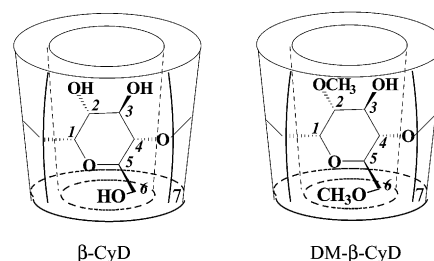
A promising development to promote the hydrogenation of water insoluble substrate in an aqueous/organic system is the use of cyclodextrins as inverse phase transfer agents. Indeed, we have reported that the hydrogenation rates of water insoluble aldehydes can be greatly increased by adding  $\beta$ -cyclodextrin or dimethyl- $\beta$ -cyclodextrin to an aqueous solution containing a ruthenium/TPPTS catalyst (TPPTS: trisulfonated triphenylphosphine sodium salt;  $[P(m-C_6H_4SO_3Na)_3]$ ) (Scheme 1).<sup>11</sup>



**Scheme 1** Ruthenium catalyzed hydrogenation of undecanal in the presence of  $\beta$ -cyclodextrin or dimethyl- $\beta$ -cyclodextrin.

Although we have shown in our preliminary communication that numerous chemically modified cyclodextrins can be used to enhance the mass transfer,  $\beta$ -cyclodextrin ( $\beta$ -CyD) and dimethyl- $\beta$ -cyclodextrin (DM- $\beta$ -CyD) are the most interesting cyclodextrins in the view of large scale applications (Scheme 2).

Indeed, these two compounds are non-toxic, cheap, biodegradable and are bulk industrial chemicals.<sup>12</sup> One of the fundamental characteristics of CyDs is the presence of a large hydrophobic cavity which can host a large variety of organic



**Scheme 2** Schematic representation of the shape of  $\beta$ -CyD and DM- $\beta$ -CyD. These compounds are cyclic oligosaccharides composed of seven glucose units linked by a  $\alpha$ -(1-4) glucosidic bond. The protons H-3 and H-5 are situated inside the host cavity, whereas protons H-1, H-2 and H-4 point outwards. In the case of DM- $\beta$ -CyD, about fourteen hydroxy groups out of twenty one have been methylated.<sup>13</sup>

## Green Context

**Biphasic reaction systems are one of the ways of solving the common problem of separating an inorganic (reagent, catalyst) from the organic (substrate, product) components. Traditional quenching for separation at the end of the reaction is one of the largest sources of waste in chemical processes. Here, cyclodextrin biphasic systems are studied and shown to be suitable, even for reactions of water-insoluble substrates, through the use of the cyclodextrins as inverse phase transfer catalysts. The methodology is successfully applied to the hydrogenation of aldehydes with good metal catalyst recovery.**

JHC

molecules.<sup>13</sup> This remarkable property is responsible for increase in the reaction rate in cyclodextrin biphasic systems. Indeed, we assume that CyDs enable an increase in the solubility in water of aldehydes by forming inclusion complexes with the aldehydes as schematically represented in Fig. 1.<sup>14</sup>

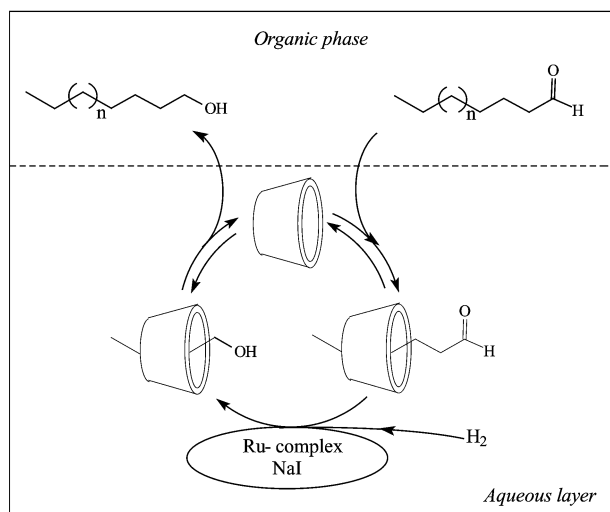


**Fig. 1** Cyclodextrin-like inverse phase transfer catalyst. The cyclodextrin is schematically represented by a truncated cone.

Interestingly, DM- $\beta$ -CyD was found in all cases to be more efficient than  $\beta$ -CyD in promoting the hydrogenation. The difference in reactivity between these two CyDs was attributed mainly to the higher affinity of DM- $\beta$ -CyD for aldehydes due to the higher hydrophobicity of its internal cavity. However, the association constants remain low and no poisoning of the CyDs can occur. This last point is very important because it enables use of catalytic amounts of CyDs.

Herein, we report that the  $\beta$ -cyclodextrin or its dimethylated form are mass transfer promoters which are more efficient than usual cosolvents for performing the hydrogenation of water insoluble aldehydes. We also give some evidences for the formation of inclusion complexes between the cyclodextrin and aldehyde or alcohol. The nature of the organic phase used in the hydrogenation process will also be discussed.

## Results and discussion

Hydrogenation of aldehydes to alcohols was first studied in the presence of different common cosolvents. The percentage by weight of cosolvent contained in the aqueous phase was fixed to 5%. Indeed, a higher amount of cosolvent prevents an efficient recovery of the catalytic system due to leaching of ruthenium metal in the organic layer. Typical results with undecanal as a model substrate are shown in Fig. 2. Results obtained under the

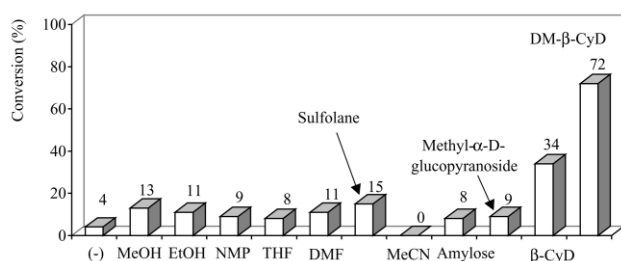


**Fig. 2** Conversion in undecanal after 30 min in the presence of various mass transfer promoters. *Experimental conditions:* mass transfer promoter: 0.8 g (5% by weight of the aqueous catalytic solution);  $\text{RuCl}_3$ : 0.1 mmol (21 mg); [undecanal]/[Ru]: 100; [TPPTS]/[Ru]: 6; [NaI]/[Ru]: 100; water: 14 mL; toluene: 8 mL;  $T = 80^\circ\text{C}$ ;  $P_{\text{H}_2} = 30$  atm.

same conditions with  $\beta$ -CyD and DM- $\beta$ -CyD are also presented in this figure.

As expected, the conversion is very low without a mass transfer promoter (<4%). Addition of 5% by weight of methanol (MeOH), ethanol (EtOH), tetrahydrofuran (THF), dimethylformamide (DMF), *N*-methylpyrrolidinone (NMP), sulfolane or acetonitrile (MeCN) in the aqueous phase leads to an increase in the conversion of undecanal by only a factor about 2–3. Although methyl- $\alpha$ -D-glucopyranoside and amylose (a linear polymer of D-glucose which possesses helical conformations with six glucose units per turn) have the same subunit as cyclodextrins, no outstanding enhancement of the conversion can be observed with these cosolvents, confirming that the presence of a hydrophobic cavity is required to increase the hydrogenation rate. At 5% by weight,  $\beta$ -CyD and DM- $\beta$ -CyD are undoubtedly more efficient than the common cosolvents. Indeed, the conversion is enhanced by a factor of 8 and 18 with  $\beta$ -CyD and DM- $\beta$ -CyD, respectively.

Interestingly, experiments conducted with a mixture of three aldehydes (nonanal, undecanal and tridecanal) using methanol,  $\beta$ -CyD or DM- $\beta$ -CyD as promoters show clearly that the cyclodextrins are more efficient than cosolvents for performing the hydrogenation of aldehydes containing a larger number of carbon atoms. Indeed, as shown in Fig. 3, whereas the ratio of the activity in the presence of promoter relative to the activity without mass transfer promoter decreases with the aldehyde chain length in the case of methanol, this ratio increases with the two cyclodextrins.

Thus, when the aldehyde chain length increases, the concentration of aldehyde/cyclodextrin complexes in water decreases probably less rapidly than the solubility of aldehyde in the methanolic aqueous solution.<sup>15</sup> Although the results are not presented here, it should be noted that a similar decrease in the ratio of activities has also been observed with other cosolvents.

In order to prove the inclusion phenomena which can explain why cyclodextrins are better promoters than cosolvents, mass spectrometry and NMR experiments have been conducted on aqueous solutions containing a mixture of cyclodextrin and undecanal or undecanol.

The existence of inclusion complexes was first studied by soft mass spectrometry methods such as electrospray ionization.<sup>16</sup> This method is employed to preserve the integrity of weak supramolecular associations in the gas phase. Fig. 4 shows the electrospray mass spectra of 1 : 1 mixtures of undecanol and  $\beta$ -CyD or DM- $\beta$ -CyD recorded in the positive mode at different orifice potentials.

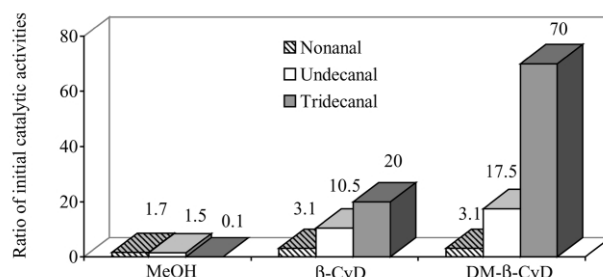


**Fig. 3** Effect of the nature of mass transfer promoter on the ratio of initial catalytic activities for three aldehydes (nonanal, undecanal, tridecanal). The ratio of initial catalytic activities is defined as the ratio between the initial catalytic activity in the presence of mass transfer promoter to the initial catalytic activity without mass transfer promoter. *Experimental conditions:* a mixture of nonanal (3 mmol), undecanal (3 mmol) and tridecanal (3 mmol) was added to 8 mL of toluene. Mass transfer promoter: 0.8 g (5% by weight);  $\text{RuCl}_3$ : 0.1 mmol (21 mg); [aldehydes]/[Ru]: 100; [TPPTS]/[Ru]: 6; [NaI]/[Ru]: 100; water: 14 mL;  $T = 80^\circ\text{C}$ ;  $P_{\text{H}_2} = 30$  atm; 15 min. The initial catalytic activity was defined as the number of mol of aldehyde converted per mol of Ru per hour calculated from the conversion after 15 min.

In both spectra (Fig. 4(a) and (b)), the peaks relating to  $\beta$ -CyD and DM- $\beta$ -CyD adducts are clearly detected, namely  $[\beta\text{-CyD} + \text{Na}]^+$  ( $m/z$  1157, Fig. 4(a)),  $[\beta\text{-CyD} + \text{K}]^+$  ( $m/z$  1173, Fig. 4(a)),  $[\text{DM-}\beta\text{-CyD} + \text{Na}]^+$  ( $m/z$  1335  $\pm$  14n, Fig. 4(b)). Besides peaks corresponding to the expected 1:1 inclusion complexes ( $[\beta\text{-CyD} + \text{undecanol} + \text{Na}]^+$ ,  $m/z$  1328.2, Fig. 4(a) and  $[\text{DM-}\beta\text{-CyD} + \text{undecanol} + \text{Na}]^+$ ,  $m/z$  1510.8, Fig. 4(b)), the mass spectra at a 10 V orifice potential exhibited peaks which were assigned to adducts of the ternary complexes formed by two CyD molecules and one undecanol molecule ( $[2\beta\text{-CyD} + \text{undecanol} + \text{Na} + \text{K}]^{2+}$ ,  $m/z$  1251.2, Fig. 4(a);  $[2\text{DM-}\beta\text{-CyD} + \text{undecanol} + \text{Na} + \text{K}]^{2+}$ ,  $m/z$  1408.5, Fig. 4(b)). The fact that higher voltages applied to orifice resulted in the fast disappearance of the peaks corresponding to 1:1 and 2:1 complexes indicates that these inclusion compounds are not very stable.

Similar mass spectrometry experiments with a 1:1 mixture of undecanal and cyclodextrins have unfortunately failed to characterise inclusion complexes. Indeed, we did not observe the peaks corresponding to undecanal/ $\beta$ -CyD or undecanal/DM- $\beta$ -CyD complexes but only the peaks from undecanoic acid/cyclodextrin complexes. This phenomenon is due to the oxidation of undecanal into undecanoic acid during the electron spray process or sample preparation that prevents direct observation of inclusion complexes.

As the direct observation of the inclusion complex is not possible by this technique, some NMR experiments were performed on an aqueous solution containing a 1:1 mixture of undecanal and  $\beta$ -CyD. Fig. 5 shows that the  $^1\text{H}$  NMR signals of the H-3 and H-5 protons of the  $\beta$ -CyD are mostly affected by the presence of undecanal.

This observation clearly evidences an inclusion process.<sup>17</sup> Indeed, when a guest molecule is inserted into the CyD cavity, the NMR frequencies of protons located inside the hydrophobic cavity of the  $\beta$ -CyD are altered. The inclusion of the aldehyde into the cavity of the cyclodextrin was confirmed by T-ROESY experiments which provides information about the interproton spatial proximities with a minimal contribution of scalar transfer.<sup>18</sup> Fig. 6 displays a partial plot of the T-ROESY spectrum of a 1:1 mixture of  $\beta$ -CyD/undecanal.

The strong cross-peaks between H-3 and H-5 of  $\beta$ -CyD and the methylene groups indicate that the alkyl chain is partially located inside the hydrophobic cavity. Similar results have been reported in the literature for nonanal/ $\beta$ -CyD inclusion complexes.<sup>19</sup> It is worth mentioning that the same comments can be made from the T-ROESY spectrum of a 1:1 mixture of undecanal and DM- $\beta$ -CyD, suggesting that the inclusion process of undecanal into DM- $\beta$ -CyD is similar to that described above for  $\beta$ -CyD. Finally, it should be pointed out that the  $^1\text{H}$  and  $^2\text{H}$  NMR spectra of 1:1 mixtures of undecanal

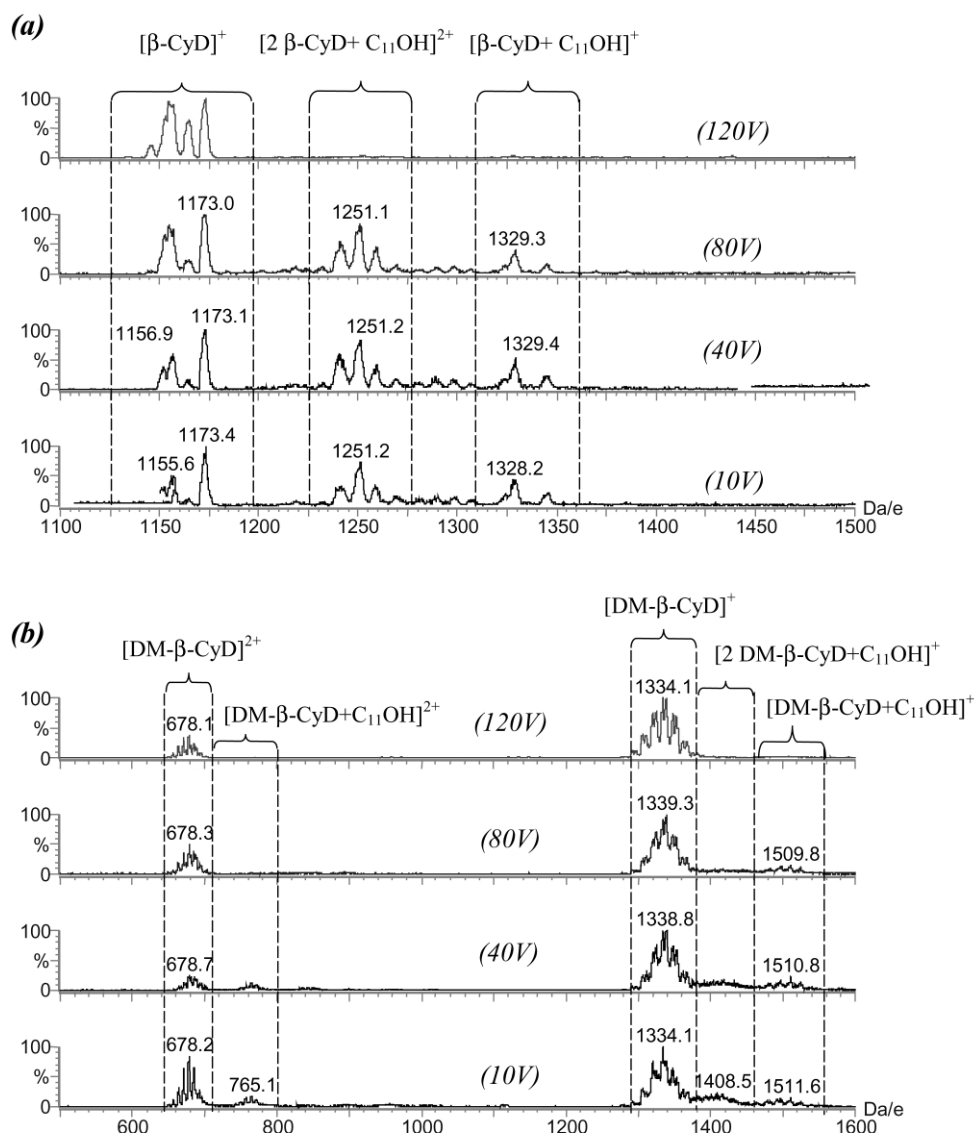
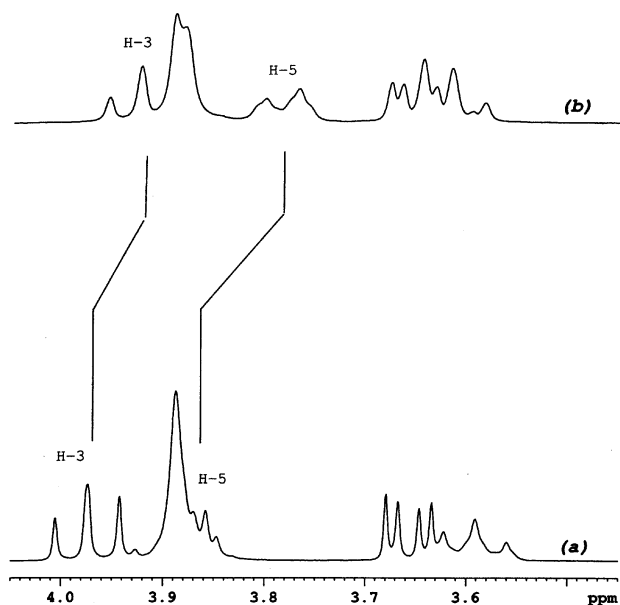
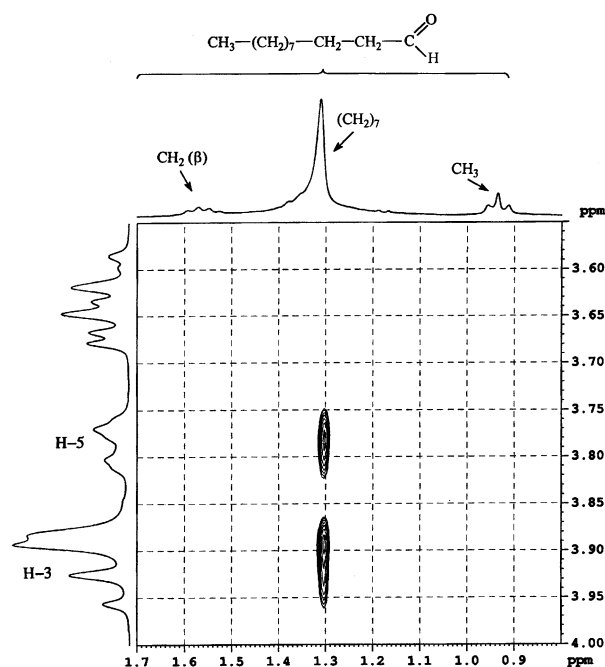


Fig. 4 Electrospray mass spectra of a 1:1 mixture of (a)  $\beta$ -CyD and (b) DM- $\beta$ -CyD with undecanol recorded in the positive mode at different orifice potentials.



**Fig. 5** Partial  $^1\text{H}$  NMR spectra of 10 mM  $\beta$ -CyD in the absence (a) and in the presence (b) of 10 mM undecanal ( $\text{D}_2\text{O}$ , 298 K, 300 MHz).



**Fig. 6** Partial contour plot of a T-ROESY experiment ( $\text{D}_2\text{O}$ , 298 K, 300 MHz) performed on a sample containing 10 mM of  $\beta$ -CyD and 10 mM of undecanal.

and  $\beta$ -CyD or DM- $\beta$ -CyD exhibited similar NMR signals that confirm the mass spectrometry experiments, *i.e.* formation of inclusion complexes between undecanal and  $\beta$ -CD or DM- $\beta$ -CD.

As the principle of our approach is based on molecular recognition processes between the water insoluble aldehyde and the cyclodextrin, the organic phase used to dissolve the aldehyde must be carefully chosen. Indeed, molecules of the organic phase can also be recognised by the cyclodextrins and, so, decrease the efficiency of the cyclodextrin. Thus, when the molecules of the organic phase are preferentially and strongly bound into the cyclodextrin cavity, poisoning of the system may even occur. In order to investigate this possibility, different organic phases have been tested. The initial catalytic activities obtained with these organic phases are presented in Fig. 7 and 8. The association constants<sup>20</sup> of hydrocarbons with  $\beta$ -CyD and the water solubilities of these compounds<sup>21</sup> are also indicated in the figures.

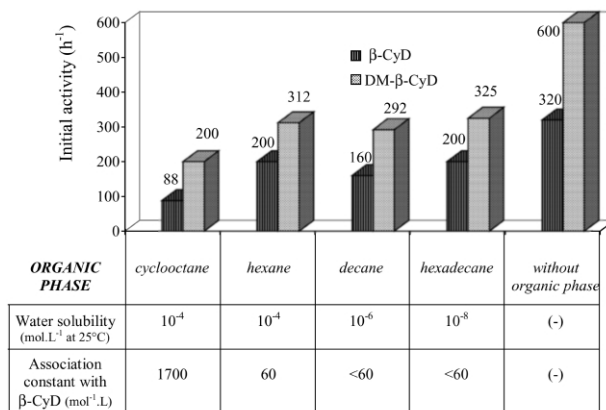


**Fig. 7** Effect of aliphatic hydrocarbons on initial catalytic activity. The water solubility and 1 : 1 association constant of hydrocarbons with  $\beta$ -CyD are shown below the histogram. *Experimental conditions:* [organic phase]: 8 mL; [cyclodextrin]: 0.8 g (5% by weight);  $\text{RuCl}_3$ : 0.1 mmol (21 mg); [undecanal]/[Ru]: 100; [TPPTS]/[Ru]: 6; [NaI]/[Ru]: 100; water: 14 mL;  $T = 80^\circ\text{C}$ ;  $P_{\text{H}_2} = 30$  atm; 15 min. The initial catalytic activity is defined as the number of mol of undecanal converted per mol of Ru per hour calculated from the conversion after 15 min.

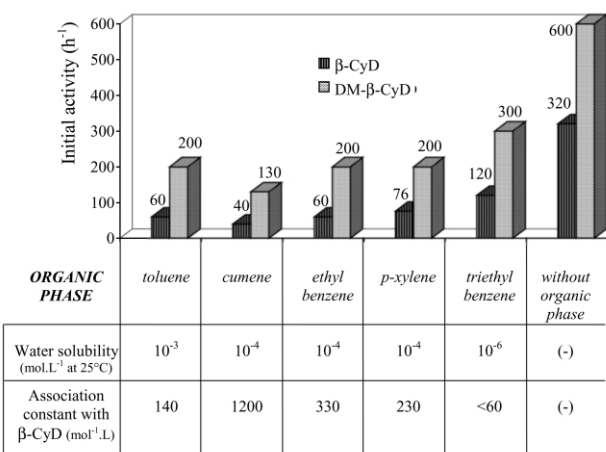


**Fig. 8** Effect of aromatic hydrocarbons on initial catalytic activity. The water solubility and the 1 : 1 association constant of hydrocarbons with  $\beta$ -CyD are mentioned below the histogram. *Experimental conditions:* see legend to Fig. 7.

From the data listed and catalytic results, four major comments can be made: (i) no aromatic or aliphatic hydrocarbon totally inhibited the reaction. (ii) at comparable solubility, the higher the association constant, the lower is the initial activity (compare results with cumene, ethylbenzene, *p*-xylene and the results with hexane and cyclooctane). (iii) When the association constant is very low (< 60), the nature of organic phase has no effect on the efficiency of the cyclodextrin. Indeed, the initial catalytic activities with hexane, decane, hexadecane or 1,3,5-triethylbenzene as organic phase were very similar. (iv) Best initial catalytic activity is obtained when the aldehyde is used pure without an organic phase.

These results indicate clearly that the complexing properties of the molecules of the organic phase can affect the catalytic activity. Thus, from a practical point of view, when an organic phase is absolutely necessary to dissolve the aldehyde *e.g.* for a solid aldehyde, its association constant should be as low as possible. When the aldehyde is a liquid the hydrogenation will be advantageously performed without an organic phase.

## Conclusion

We have demonstrated that the processes of molecular recognition between water-insoluble aldehydes and two commercially available cyclodextrins allow the hydrogenation of aldehydes to



be performed in a genuine two-phase system with activities which are in range desired for industrial catalytic processes (ca. 400–600 h<sup>-1</sup>). At low content, *i.e.* a content that enables quantitative recovery of the catalytic system without loss of metal with a cosolvent, the cyclodextrins appear to be more efficient than cosolvents. Finally, these results and our previous work<sup>22</sup> reinforce, so far, our idea that cyclodextrins should not be considered as exotic chemical products but rather as fundamental compounds for solving mass-transport limitation in biphasic catalysis.

## Experimental

### Material and apparatus

The chemically modified cyclodextrins were supplied by Roquette Frères (Lestrem, France) and Aldrich Chemical and were used as received without further purification. In particular, commercially available dimethyl- $\beta$ -cyclodextrin is a mixture of methylated- $\beta$ -cyclodextrins; about fourteen hydroxy groups of twenty one have been methylated. Ruthenium(III) chloride, sodium iodide and organic compounds were purchased from Strem Chemicals, Aldrich Chemical and Acros Organics in their highest purity and used without further purification. Trisodium tris(*m*-sulfonatophenyl)phosphine (TPPTS) was synthesized as reported by Gärtner *et al.*<sup>23</sup> The purity of the TPPTS was carefully controlled. In particular, <sup>31</sup>P solution NMR indicated that the product was a mixture of TPPTS (ca. 98%) and its oxide (ca. 2%). Hydrogen was used directly from the cylinder (>99.9% pure; Air Liquide). Distilled deionized water was used in all experiments. The water, solvents and liquid reagents were degassed by bubbling nitrogen for 15 min, or by two freeze–pump–thaw cycles before use. All manipulations were performed under nitrogen using standard Schlenk techniques.

Electrospray mass spectroscopy experiments were performed on a Micromass Quattro II. In order to obtain a concentration of about 20 pmol  $\mu\text{L}^{-1}$ , the sample was diluted in a mixture of ammonium acetate (0.06 mM), water and acetonitrile (50/50) and was introduced through the fused silica inlet capillary at a flow rate of 3 mL min<sup>-1</sup>. The ion spray needle potential and the orifice potential were set at 3100 V and 10–120 V, respectively. Positive ion detection mode was used and calibration was performed with polypropylene glycol.

<sup>1</sup>H NMR spectra were recorded at 300.13 MHz on a Bruker DRX 300 apparatus. The 2D T-ROESY experiments were run using the software supplied by Bruker. Mixing times for T-ROESY experiments were set at 100 ms. The data matrix for the T-ROESY was built up from 512 free induction decays, 1 K points each, resulting from the co-addition of 32 scans. The real resolution was 1.5 Hz/point in F2 and 6.0 Hz/point in the F1 dimension, respectively. They were transformed in the phase-sensitive mode after QSINE window processing.

### General procedure for hydrogenation of undecanal

RuCl<sub>3</sub> (0.1 mmol), TPPTS (0.6 mmol), NaI (10 mmol) and cyclodextrin or cosolvent (0.8 g) and water (14 g) were introduced under N<sub>2</sub> into a Schlenk tube. After dissolution of ruthenium, the aqueous solution was transferred to the organic phase composed of undecanal (10 mmol), solvent (8 mL) and undecane (1.5 mmol, GC internal standard). The resulting solution was charged under N<sub>2</sub> into a 50 mL stainless steel autoclave, then heated at 80 °C and pressurized with 30 atm of H<sub>2</sub>. The medium was stirred at 1000 rpm and the pressure was kept constant throughout the whole reaction by using a gas

reservoir along with a pressure regulator. The reaction was monitored by quantitative gas chromatographic analysis (CP Sil 5-CB, 25 m  $\times$  0.32 mm). Products were identified by comparison of retention time and spectral properties with authentic samples. It is noteworthy that at the end of the reaction, the biphasic system is easily separated by simple decantation and the aqueous catalytic layer can be reused. This system is recyclable at least five times without loss of activity.

## References

- For concepts developed for homogeneous catalyst recycling, see: aqueous biphasic catalysis: P. W. N. M. van Leeuwen, P. C. J. Kamer and J. N. H. Reek, *CATTECH*, 1999, **3**, 164; fluororous biphasic catalysis: B. Richter, A. L. Spek, G. Van Koten and B. J. Deelman, *J. Am. Chem. Soc.*, 2000, **122**, 3945; I. T. Horvath and J. Rabai, *Science*, 1994, **266**, 72; catalysis in molten salt: F. Favre, H. Olivier-Bourbigou, D. Commereuc and L. Saussine, *Chem. Commun.*, 2001, 1360; Y. Chauvin and H. Olivier-Bourbigou, *CHEMTECH*, 1995, **25**, 26; catalysis in supercritical conditions: P. G. Jessop, T. Ikariya and R. Noyori, *Chem. Rev.*, 1999, **99**, 475; R. J. Bonilla; B. R. James and P. G. Jessop, *Chem. Commun.*, 2000, 941; B. M. Bhanage, Y. Ikushima, M. Shirai and M. Arai, *Chem. Commun.*, 1999, 1277; catalysts on polymeric or silica supports: Q. H. Fan, C. Y. Ren, C. H. Yeung, W. H. Hu and A. S. C. Chan, *J. Am. Chem. Soc.*, 1999, **121**, 7407; L. Pu, *Chem. Eur. J.*, 1999, **5**, 2227; C. M. Crudden, D. Allen, M. D. Mikolouk and J. Sun, *Chem. Commun.*, 2001, 1154; membrane techniques: J. W. J. Knapen, A. W. Van der Made, J. C. de Wilde, P. W. N. M. van Leeuwen, P. Wijkens, D. M. Grove and G. Van Koten, *Nature*, 1994, **372**, 659; G. E. Oosterom, J. N. H. Reek, P. C. J. Kamer and P. W. N. M. Van Leeuwen, *Angew. Chem., Int. Ed.*, 2001, **40**, 1828.
- (a) *Aqueous Phase Organometallic Catalysis*, ed. B. Cornils and W. A. Herrmann, Wiley-VCH, Weinheim, 1998; (b) B. Cornils and E. G. Kuntz, *J. Organomet. Chem.*, 1995, **502**, 177; (c) B. Cornils and E. Wiebus, *CHEMTECH*, 1995, **25**, 33; (d) W. A. Herrmann and C. W. Kohlpaintner, *Angew. Chem., Int. Ed. Engl.*, 1993, **32**, 1524; (e) E. G. Kuntz, *CHEMTECH*, 1987, **17**, 570.
- (a) J. Bakos, R. Karaivanov, M. Laghmari and D. Sinou, *Organometallics*, 1994, **13**, 2951; (b) C. Larpent, R. Dabard and H. Patin, *Tetrahedron Lett.*, 1987, **28**, 2507; (c) A. Andriollo, A. Bolivar, F. A. Lopez and D. E. Paez, *Inorg. Chim. Acta*, 1995, **238**, 187.
- (a) J. M. Grosselin, C. Mercier, G. Allmang and F. Grass, *Organometallics*, 1991, **10**, 2126; (b) M. Hernandez and P. Kalck, *J. Mol. Catal.*, 1997, **116**, 131; (c) F. Joo and A. Benyei, *J. Organomet. Chem.*, 1989, **363**, C19; (d) A. Benyei and F. Joo, *J. Mol. Catal.*, 1990, **58**, 151.
- (a) E. Fache, F. Senocq, C. Santini and J. M. Basset, *J. Chem. Soc., Chem. Commun.*, 1990, 1776; (b) E. Fache, C. Santini, F. Senocq and J. M. Basset, *J. Mol. Catal.*, 1992, **72**, 337.
- S. Kolaric and V. Sunjic, *J. Mol. Catal.*, 1996, **110**, 189.
- E. Fache, C. Mercier, N. Pagnier, B. Despeyroux and P. Panster, *J. Mol. Catal.*, 1993, **79**, 117.
- (a) Y. Dror and J. Manassen, *J. Mol. Catal.*, 1977, **2**, 219; (b) R. Grzybek, *React. Kinet.-Catal. Lett.*, 1996, **58**, 315.
- (a) A. Kumar, G. Oehme, J. P. Roque, M. Schwarze and R. Selke, *Angew. Chem., Int. Ed. Engl.*, 1994, **33**, 2197; (b) H. Ding, B. E. Hanson and J. Bakos, *Angew. Chem., Int. Ed. Engl.*, 1995, **34**, 1645; (c) F. Robert, G. Oehme, I. Grassert and D. Sinou, *J. Mol. Catal.*, 2000, **156**, 127.
- (a) J. Schulz, A. Roucoux and H. Patin, *Chem. Commun.*, 1999, 535; (b) R. J. Bonilla, B. R. James and P. G. Jessop, *Chem. Commun.*, 2000, 941.
- E. Monflier, S. Tilloy, Y. Castanet and A. Mortreux, *Tetrahedron Lett.*, 1998, **39**, 2959.
- J. Szejtli, *Chem. Rev.*, 1998, **98**, 1743.
- G. Wenz, *Angew. Chem., Int. Ed. Engl.*, 1994, **33**, 803.
- This hypothesis is totally in agreement with the fact that the conversion increases with the  $\beta$ -CyD or DM- $\beta$ -CyD concentration. It should be noted that the increase in the activity in the presence of DM- $\beta$ -CyD cannot be attributed to a decrease in the interfacial tension due to surface active properties of the DM- $\beta$ -CyD.<sup>24</sup> Indeed, when DMCyD was added to an aqueous solution containing RuCl<sub>3</sub> (7.14 mmol l<sup>-1</sup>), TPPTS (42.84 mmol l<sup>-1</sup>) and NaI (0.714 mol l<sup>-1</sup>) (a representative mixture of the catalytic aqueous phase), the surface tension surprisingly increased. For example, the interfacial tension

value was equal to  $56 \text{ mN m}^{-1}$  at  $25 \text{ }^\circ\text{C}$  when the DM- $\beta$ -CyD concentration was fixed to  $50 \text{ mmol l}^{-1}$ , compared with  $40 \text{ mN m}^{-1}$  without DM- $\beta$ -CyD. At  $80 \text{ }^\circ\text{C}$ , the same phenomenon was observed. This increase in interfacial tension could be due to the formation of inclusion complexes between iodides and DM- $\beta$ -CyD.

- 15 K. Wakita, M. Yoshimoto, S. Miyamoto and H. Watanabe, *Chem. Pharm. Bull.*, 1986, **11**, 4663.
- 16 (a) A. Selva, E. Redenti, M. Zanol, P. Ventura and B. Casetta, *Org. Mass Spectrom.*, 1993, **28**, 983; (b) P. Cescutti, D. Garozzo and R. Rizzo, *Carbohydr. Res.*, 1996, **290**, 105.
- 17 (a) H. J. Schneider, F. Hacket and V. Rüdiger, *Chem. Rev.*, 1998, **98**, 1755; (b) F. Djedaïni, S. Z. Lin, B. Perly and D. Wouessidjewe, *J. Pharm. Sci.*, 1990, **79**, 643.
- 18 (a) T. L. Hwang and A. J. Shaka, *J. Am. Chem. Soc.*, 1992, **114**, 3157; (b) J. Lin, C. Creminon, B. Perly and F. Djedaïni-Pilard, *J. Chem. Soc., Perkin Trans. 2*, 1998, 2639.
- 19 A. Botsi, K. Yannakopoulou, B. Perly and E. Hadjoudis, *J. Org. Chem.*, 1995, **60**, 4017.
- 20 E. Fenyvesi, L. Szente, N. R. Russel and M. McNamara, in *Comprehensive Supramolecular Chemistry*, ed. J. L. Atwood, J. E. D. Davies, D. D. MacNicol and F. Vögtle, Pergamon, Oxford, 1996, **vol. 3**, p. 235.
- 21 P. Ruelle and U. W. Kesselring, *Chemosphere*, 1997, **34**, 275.
- 22 (a) R. Widehem, T. Lacroix, H. Bricout and E. Monflier, *Synlett*, 2000, **5**, 722; (b) S. Tilloy, F. Bertoux, A. Mortreux and E. Monflier, *Catal. Today*, 1999, **48**, 245; (c) E. Monflier, E. Blouet, Y. Barbaux and A. Mortreux, *Angew. Chem., Int. Ed. Engl.*, 1994, **33**, 2100.
- 23 R. Gärtner, B. Cornils, H. Springer and P. Lappe, (Ruhrchemie A. G.), *Ger. Pat.*, DE-B 3235030, 1982 (*Chem. Abstr.*, 1984, **101**, P55331t).
- 24 T. Mathivet, C. Méliet, Y. Castanet, A. Mortreux, L. Caron, S. Tilloy and E. Monflier, *J. Mol. Catal.*, 2001, **176**, 105.



# Substrate to catalyst dependent conversion of $\beta,\gamma$ -dihydroxyesters to butenolides and/or $\gamma$ -ketoesters: synthesis of heritol, heritonin and mintlactones

Subhash P. Chavan\* and Chitra A. Govande

Division of Organic Chemistry: Technology, National Chemical Laboratory, Pune 411 008, India. E-mail: spchaven@dalton.ncl.res.in

Received (in Cambridge, UK) 19th October 2001

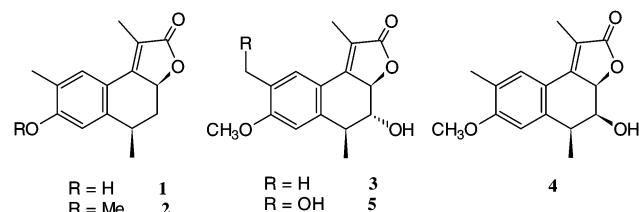
First published as an Advance Article on the web 11th February 2002

Conversion of  $\beta,\gamma$ -dihydroxyesters to butenolide and/or  $\gamma$ -ketoesters by solid acids and its application towards the synthesis of heritol, heritonin and mintlactones are described.

Synthetic and directed functional group transformations are of topical interest and are crucial and critical for the success of a synthetic sequence.

Butenolides are valuable synthetic intermediates<sup>1</sup> and key structural sub-units of a variety of natural products. Because of their unusual range of biological activity, there is a continuing need for the development of simple and versatile methods for their synthesis.

In continuation of our work in the synthesis of biologically active molecules *viz.* heritol **1**,<sup>2</sup> heritonin **2**,<sup>3</sup> heritanin **3**, vallapin **4**,<sup>3</sup> vallapianin **5**<sup>3</sup> and related compounds we have reported<sup>4,5</sup> novel methodologies for the synthesis of butenolides from the corresponding  $\beta,\gamma$ -unsaturated esters and acids.



$\gamma$ -ketoesters constitute key synthons in the synthesis of natural products including butenolides.<sup>6</sup> Additionally  $\beta$ -tetralones<sup>7</sup> in general and  $\alpha$ -substituted  $\beta$ -tetralones in particular are important in the synthesis of *cis*-fused bicyclic pyrrolidines and pyrrolidinones which are in turn intermediates in the total synthesis of U-93385, a serotonin-1A agonist.<sup>8</sup>

Heterogeneous catalysis is a fast progressing field in synthetic chemistry. We were interested in utilizing the obvious advantages of using solid acid catalysts in the synthesis of butenolides and  $\gamma$ -ketoesters.

An efficient entry to butenolides from  $\beta,\gamma$ -unsaturated esters *via* the corresponding diols involving an intramolecular transesterification and concomitant dehydration has been reported<sup>4</sup> by our group. It was reasoned that employing solid catalysts for this conversion could increase the efficiency of the reaction.

Various representative solid acid catalysts were screened for the intramolecular cyclization of the diols **6b** (prepared from  $\alpha$ -tetralone by Reformatsky reaction and dihydroxylation) to the corresponding butenolides. All the catalysts except the acidic ion-exchange resin Amberlyst-15 resulted in either no reaction or yielded the corresponding  $\gamma$ -ketoesters as the major or sole product (Table 1); treatment with Amberlyst-15 furnished the butenolide in 82% yield along with the ketoester as the minor product.

Hence Amberlyst-15 was chosen as the catalyst of choice for further studies. A marked difference in the ratio of the two

products was observed when the ratio of catalyst/substrate was changed. Use of excess catalyst/substrate ratio (2:1) resulted in the formation of the butenolide in good yields while when the reagent was used in catalytic amount (10% by weight), butenolide formation was suppressed and the ketoester was obtained as the major product. The formation of the ketoester as the possible intermediate step in butenolide formation was confirmed by separately treating it to the same conditions *viz.* 1:2 by weight of resin in refluxing toluene whereupon butenolide was obtained.

In order to demonstrate the generality of the methodology, the reaction was attempted on various substrates, all of which

**Table 1** Catalyst performance for intramolecular cyclization of diols **6b**

Entry	Catalyst	Substrate/ catalyst ratio	Reaction time/h	Yield (%) <b>7b</b>	Yield (%) <b>8b</b>
1	ZSM-5	1:1	1	None	31
2	ZSM-11	1:1	3	20	31
3	TS-2	1:1	1	None	47
4	Silica gel (60–120)	1:7	3	None	50
5	Amberlite IR-120	1:3	12	None	None
6	Amberlyst-15	1:2	0.5	82	12

## Green Context

The use of solid acid catalysts has been described for a range of processes, with significant success being achieved. Often though, these catalysts are used for very simple molecules, with less being done on more complex substrates. Here, the synthesis of three functionalised lactones is described using solid acid catalysts successfully. There are very interesting dependencies on the type of catalyst, with some being completely ineffective and some excellent, indicating that choice of catalyst is extremely important. *DJM*

**Table 2** Formation of butenolides (**7** and **8**) from diols **6** using Amberlyst-15

<i>n</i>	R <sup>1</sup>	R <sup>2</sup>	R <sup>3</sup>	R <sup>4</sup>	Yield (%) <b>7</b>	Yield (%) <b>8</b>
<b>a</b>	1	H	H	H	67	30
<b>b</b>	1	H	H	H	82	12
<b>c</b>	1	H	H	Et	69	21
<b>d</b>	1	H	H	<i>i</i> Pr	31	55
<b>e</b>	1	Me	H	Me	90	7
<b>f</b>	1	Me	OMe	Me	79	0
<b>g</b>	2	H	H	H	96	0
<b>h</b>	0	H	H	H	0	53

furnished the corresponding butenolides in good to excellent yields (Table 2).

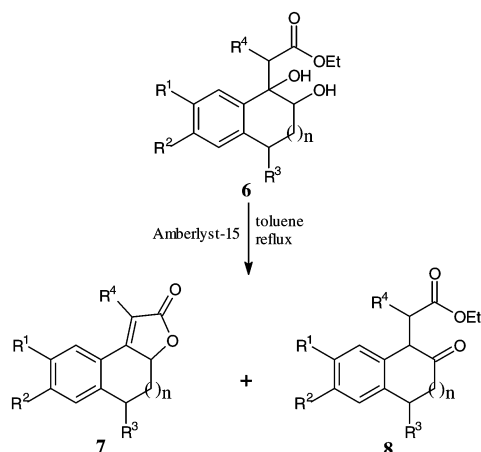
This methodology has been successfully employed for the synthesis of the natural product heritonin **2f** in good yield. Since the conversion of Heritonin to Heritol has already been reported<sup>9</sup> by us earlier, this constitutes a formal synthesis of heritol.

In order to study the effect of ring size on the outcome of the reaction, the conversion was also attempted on five- and seven-membered cyclic ketones. It is evident from Table 2 that seven-membered cyclic ketones furnished the butenolide **7g** in excellent yields while following the same protocol, 1-indanone furnished the  $\gamma$ -ketoester **8h** as the sole product.

Other cyclic ketones such as cyclohexanone and cyclopentanone gave the butenolide **11a** and the ketoester **10**, respectively, as the sole products (Scheme 1).

Following a similar set of reactions on 4-methyl cyclohexanone as described earlier the diol was obtained which upon cyclization using Amberlyst-15 resin yielded the butenolide **11b** in 75% yield as an inseparable mixture of mint- and isomint-lactone.

Points of interest in this methodology are the ring size having a profound effect on the outcome of the reaction and by changing the catalyst or the ratio of substrate/catalyst one can willfully access butenolide or ketoester according to need.

**Scheme 1**

## Experimental

### General procedure for the lactonization of diol **6**:

A mixture of the diol **6** (100 mg) and Amberlyst-15 (wet) ion exchange resin (200 mg, 1:2 by weight) was refluxed in distilled toluene (10 ml) and the reaction monitored by TLC. After completion of the reaction (0.5–1 h), the mixture was cooled and the used catalyst was filtered off and washed with ethyl acetate (10 ml). The organic washings were combined and the solvent evaporated under reduced pressure. The resulting residue was chromatographed over silica gel. The keto ester **8** was eluted out first with 5% ethyl acetate–light petroleum (bp 60–80 °C) followed by the butenolide **7** with 20% ethyl acetate–light petroleum.

### 6,7-Dihydronaphtho(1,2b)furan-2(5H)-one (**7a**)

Yield: 67%, mp 120 °C; IR (Nujol): 1760, 1640, 1620, 1480, 1440, 1360 cm<sup>-1</sup>

<sup>1</sup>H NMR (90 MHz):  $\delta$  1.8 (m, 1H), 2.6 (m, 1H), 3.0 (dd,  $J = 4, 10$  Hz, 2H), 5.1 (ddd,  $J = 2, 6, 12$  Hz, 1H), 6.1 (d,  $J = 2$  Hz, 1H), 7.2–7.6 (m, 4H).

<sup>13</sup>C NMR (CDCl<sub>3</sub>, 80 MHz):  $\delta$  172.75 (s), 165.58 (s), 137.51 (d), 131.00 (s), 128.72 (s), 126.69 (d), 126.54 (d), 126.39 (d), 108.00 (d), 79.47 (d), 29.55 (t), 27.00 (t).

Mass ( $m/z$ ): 186 (M<sup>+</sup>, 100), 157 (91), 129 (68), 115 (40), 102 (8%).

### Ethyl 2-(3,4-dihydro-2(1H)-naphthalenone)acetate (**8a**)

Yield: 30%; IR (neat): 1730, 1460, 1370, 1220 cm<sup>-1</sup>

<sup>1</sup>H NMR (80 MHz):  $\delta$  1.30 (t,  $J = 7$  Hz, 3H), 2.40–2.80 (m, 2H), 3.05 (d,  $J = 6$  Hz, 2H), 3.10–3.20 (m, 2H), 3.80 (t,  $J = 6$  Hz, 1H), 4.10 (q,  $J = 7$  Hz, 2H), 7.10 (s, 4H).

<sup>13</sup>C NMR (50 MHz):  $\delta$  14.4 (q), 28.4 (t), 33.4 (t), 37.5 (t), 49.0 (d), 61.0 (t), 125.8 (d), 127.2 (d), 127.3 (d), 128.0 (d), 135.7 (s), 137.6 (s), 172.2 (s), 210.1 (s).

Mass ( $m/z$ ): 233 ((M + 1)<sup>+</sup>, 13), 232 (M<sup>+</sup>, 25), 187 (43), 186 (100), 185 (24), 184 (19), 169 (9), 158 (66), 157 (56), 155 (17), 144 (33), 130 (44), 129 (47), 128 (39), 127 (30), 117 (26), 116 (28), 115 (56), 91 (9%).

## Acknowledgements

C. A. G. thanks CSIR, New Delhi for award of fellowship. Funding under the Young Scientist Award Scheme is gratefully acknowledged.

## References

- For excellent reviews on the synthesis of butenolides please, see: (a) Y. S. Rao, *Chem. Rev.*, 1976, **76**, 625; (b) D. W. Knight, *Contemp. Org. Synth.*, 1994, **1**, 287.
- D. H. Miles, D.-S. Lho, A. A. de La Cruz, E. D. Gomez, J. A. Weeks and J. A. Atwood, *J. Org. Chem.*, 1987, **52**, 2930.
- D. H. Miles, V. Chittawong, D.-S. Lho, A.-M. Payne, A. A. de La Cruz, E. D. Gomez, J. A. Weeks and J. L. Atwood, *J. Nat. Prod.*, 1991, **54**, 286.
- S. P. Chavan, P. K. Zubaidha and N. R. Ayyangar, *Tetrahedron Lett.*, 1992, **33**, 4605.
- S. P. Chavan, P. K. Zubaidha, C. A. Govande and Y. T. Subba Rao, *J. Chem. Soc., Chem. Commun.*, 1994, 1101.
- G. Stork, J. E. Davies and A. Meisels, *J. Am. Chem. Soc.*, 1959, **81**, 5516.
- D. C. Pryde, S. S. Henry and A. I. Meyers, *Tetrahedron Lett.*, 1996, 3243.
- M. D. Ennis, R. L. Hoffman, N. B. Ghazal, D. W. Old and P. A. Mooney, *J. Org. Chem.*, 1996, **61**, 5813.
- P. K. Zubaidha, S. P. Chavan, U. S. Racherla and N. R. Ayyangar, *Tetrahedron*, 1992, **47**, 5759.





# Microwave-assisted reactions: Part 2† One-pot synthesis of pyrimido[1,2-*a*]pyrimidines

Fawi M. Abd El Latif,<sup>a</sup> Magda A. Barsy,<sup>a</sup> Amal Mmohamed Aref<sup>a</sup> and Kamal Usef Sadek<sup>\*b</sup>

<sup>a</sup> Chemistry Department, Faculty of Science, South Valley University, Aswan, A. R, Egypt

<sup>b</sup> Chemistry Department, Faculty of Science, Minia University, 61519 Mina, A. R, Egypt.

E-mail: rumenia@enstinet.EG.net

Received 22nd November 2001

First published as an Advance Article on the web 8th February 2002

A simple route for the synthesis of pyrimido[1,2-*a*]pyrimidines by condensation of 2-aminopyrimidine **1**, aromatic aldehydes **2** and active methylene reagents **3** under microwave irradiation is reported.

## Introduction

The importance of pyrimido[1,2-*a*]pyrimidines is well recognized by synthetic as well as biological chemists.<sup>2,3</sup> The development of pyrimido[1,2-*a*]pyrimidines as having hypoglycemic and platelet aggregation-inhibitory activities,<sup>4</sup> as potential hosts in the enantioselective recognition of oxo anions in polytopic abiotic receptors,<sup>5</sup> anchor modules for oxo anionic functions of molecular guest species complexed by polytopic artificial receptors,<sup>6</sup> and as efficient insecticides, acaricides and nematocides,<sup>7</sup> have prompted us to investigate an efficient route for the synthesis of this ring system.

A previous synthesis for pyrimido[1,2-*a*]pyrimidines reported by Echavarren *et al.*<sup>8</sup> involved a nine-step procedure from L-asparagine with a total yield of 5.1%. However, this overall yield was improved by Kurzmeier and Schmidtehen<sup>5</sup> to 20%. Most of the other syntheses are either multi-stage routes<sup>9</sup> or give only poor to moderate yields.<sup>10</sup>

In recent years, microwave-induced rate acceleration technology has become a powerful tool in organic synthesis<sup>11–14</sup> in view of the mild, clean, convenient, enhanced selectivity, spontaneity of the reaction process in comparison to the conventional solution phase reactions and the associated ease of manipulation. It is of note that this technique offers an environmentally friendly process of organic synthesis.

## Results and discussion

In connection with our interest in the synthesis and biological evaluation of condensed azines,<sup>15,16</sup> we now report a novel and efficient route for the synthesis of pyrimido[1,2-*a*]pyrimidine derivatives under microwave irradiation. Simple addition of an equimolar mixture of 2-aminopyrimidine **1**, benzaldehyde **2a** and malononitrile **3a** under microwave irradiation and in the presence of piperidine as a catalyst gave either the 2-aminopyrimidino[1,2-*a*]pyrimidine **8a** or the 4-amino isomer **6a** (Scheme 1). Structure **6a** was considered more likely based on analytical and chemical data. <sup>1</sup>H NMR spectra revealed a singlet at δ 8.4 that integrated for two protons. This was assigned to an amino function at C-4. The downfield shift of this amino function could be explained by the anisotropic effect of the ring nitrogen. It is difficult to rationalize this amino function if the reaction product was **8a**. Moreover, pyrimidopyrimidine **6a** was con-

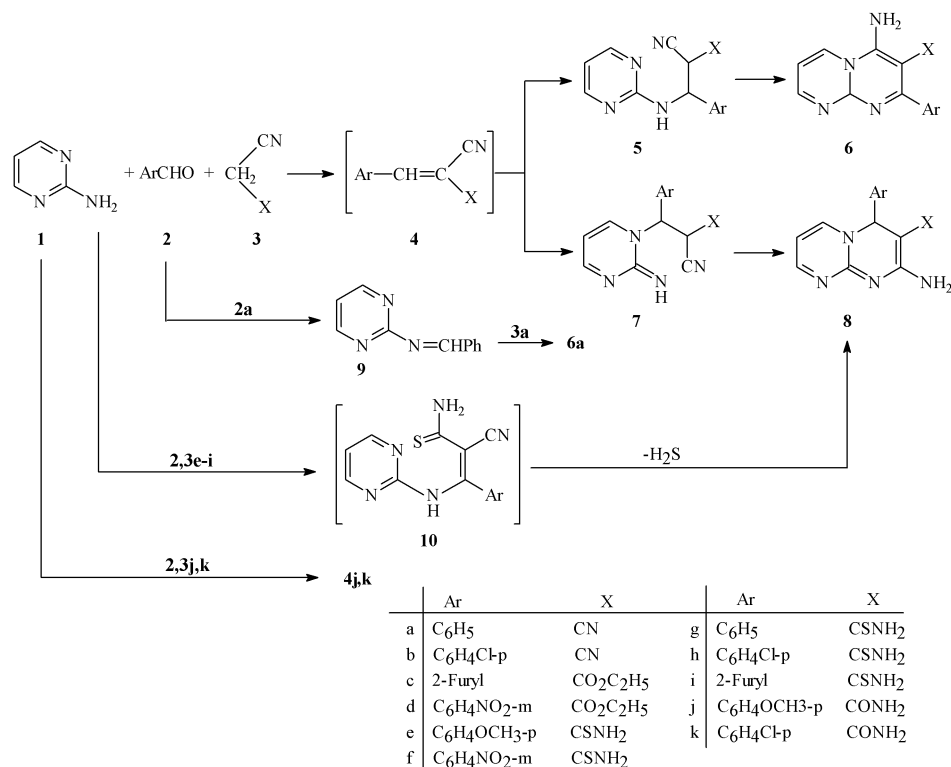
firmed chemically by its synthesis *via* another route by the reaction of 2-aminopyrimidine **1** with benzaldehyde **2a** to afford Schiff base **9** which was then treated with malononitrile **3a** in dioxane in the presence of a catalytic amount of piperidine. Similarly, microwave irradiation of 2-aminopyrimidine **1** with aldehydes **2b–d** and active methylenes **3b–d** afforded **6b–d**, respectively. The structure assigned for these reaction products were established from analytical and spectral data (see Experimental section). Two possible routes for the formation of **6a–d** are postulated. The first route involves the condensation of aldehyde with the active methylene reagent to afford the corresponding β-arylacrylonitrile derivative (**4**) followed by addition of the exocyclic amino function of 2-aminopyrimidine **1** to the activated double bond system in **4** to form Michael adduct **5** which undergoes intramolecular cyclization to give **6**; alternatively, addition of the ring nitrogen to **4** to form Michael adduct **7** will lead to the formation of **8**. The second route is the condensation of aldehyde **2** with 2-aminopyrimidine **1** to afford the corresponding Schiff base **9** followed by the addition of the active methylene moiety to form **6**. We believe that the first pathway is the predominant one through monitoring the reaction mixture. Thus, after microwave irradiation of a mixture of 2-aminopyrimidine **1**, benzaldehyde **2a** and malononitrile **3a** for 30 s and at 650 W, the corresponding β-arylacrylonitrile derivative **4** could be detected by TLC.

In contrast, the reaction of 2-aminopyrimidine **1** with aldehyde **2g** and cyanothioacetamide **3g** gave a completely different product than **6a**. Structure **8a** was assigned for this reaction product based on analytical and spectral data. Thus, the IR spectrum of the reaction product revealed both amino and cyano functions at ν 3250 and 2200 cm<sup>-1</sup>. <sup>1</sup>H NMR revealed a band at δ 4.64 that integrated for one proton. This was assigned to CH-4. It is difficult to rationalize this signal if the reaction product was **6a**. This product was assumed to be formed *via*

## Green Context

Reducing the number of steps in organic synthesis can be a very effective way of achieving many green chemistry reductions (of materials consumed, auxiliaries used, energy input and waste produced). Thus one-pot reactions involving several substrates have considerable appeal. Here the reactions of multiple substrates to important biologically active compounds are achieved with a small amount of catalyst *via* microwave activation. JHC

† Part 1: ref. 1.



Scheme 1

intermediacy of **10** and subsequent cyclisation *via* H<sub>2</sub>S elimination. Similarly, 2-aminopyrimidine **1** reacted with aldehydes **2e–i** and active methylenes **3e–i** to afford **8e–i**, respectively. In contrast, attempts at condensation of 2-aminopyrimidine **1** with aldehydes **2j, k** and active methylenes **3j, k** resulted in the formation of  $\beta$ -arylacrylonitriles **4j, k**. This was established based on spectral and chemical data and *via* synthesis through condensation of aldehydes **2j, k** with active methylenes **3j, k** under the same reaction conditions (see Experimental section).

## Conclusion

In conclusion we have shown that both the amino function and ring nitrogen in 2-aminopyrimidine are active sites of nucleophilic attack on  $\alpha, \beta$ -unsaturated nitriles. Accordingly, alternative structures should always be considered and strong arguments should be introduced when assigning structures to the products of these reactions. The difference in behaviour of **2,3j, k** can be rationalised in terms of the relative activities of the ylidic bond and the transition states leading to the end products. It is assumed that the Michael adduct formed from the reaction of **2,3j, k** with **1** is in equilibrium with its constituents and its cyclisation *via* water elimination is thermodynamically unfavourable.

## Experimental

All melting points are uncorrected. IR spectra were recorded in KBr with Shimadzu 470 spectrophotometer. <sup>1</sup>H NMR spectra were recorded on a Varian EM-390 400 MHz spectrometer in [<sup>2</sup>H<sub>6</sub>]DMSO as solvent and TMS as internal standard, chemical shifts are reported in  $\delta$  units (ppm). Mass spectra were measured on a JOEL JMS 600 at 70 eV. Microanalytical data were obtained from the microanalytical Data Unit at Cairo University.

## General procedure for the reaction of 2-aminopyrimidine **1**, aromatic aldehyde **2** and active methylene reagents **3**

A mixture of 2-aminopyrimidine **1** (0.951 g, 0.01 mmol), (0.01 mmol) of aromatic aldehyde **2a–k** and (0.01 mmol) active methylene reagents **3a–k** in the presence of a catalytic amount of piperidine was irradiated in microwave oven for 3 min at 650 W. After cooling to room temperature, the solid product formed was collected by filtration, dried and recrystallized from ethanol.

## 4-Amino-2-phenylpyrimido[1,2-*a*]pyrimidine-3-carbonitrile **6a**

Yield: 2.11 g (85%); mp 250 °C. IR (KBr)  $\nu_{\text{max}}$ : 3340 (NH<sub>2</sub>), 2200 (CN), 1580 cm<sup>-1</sup> (C=N). MS (EI, 70 eV):  $m/z$  250 (M + 1, 20%). <sup>1</sup>H NMR (DMSO),  $\delta_{\text{H}}$  8.4 (s, 2H, NH<sub>2</sub>), 7.2–7.8 (m, 9H, arom-H). C<sub>14</sub>H<sub>11</sub>N<sub>5</sub> (249.27): calc. C 67.45, H 4.44, N 28.09; found C 67.44, H 4.50, N 28.2%.

## Procedure for the preparation of compound **6a**; another route:

A mixture of 2-aminopyrimidine **1** (0.95 g, 0.01 mmol) and aromatic aldehyde **2a** afforded Schiff base **9** which was treated with active methylene reagent **3a** in dioxane in the presence of a catalytic amount of piperidine under reflux for 5 h. After cooling to room temperature the solid product formed was collected by filtration, dried and recrystallized from ethanol. The reaction product was found to be identical with compound **6a**, (mixed mp and IR).

## 4-Amino-2-(4-chlorophenyl)pyrimido[1,2-*a*]pyrimidine-3-carbonitrile **6b**

Yield: 2.35 g (83%); mp 240 °C. IR (KBr)  $\nu_{\text{max}}$ : 3350 (NH<sub>2</sub>), 2200 (CN), 1550 cm<sup>-1</sup> (C=N). MS (EI, 70 eV):  $m/z$  284 (M<sup>+</sup>,

7%).  $^1\text{H}$  NMR (DMSO),  $\delta_{\text{H}}$  7.32–7.63 (m, 8H, arom-H).  $\text{C}_{14}\text{H}_{10}\text{N}_5\text{Cl}$  (283.72): calc. C 59.26, H 3.55, N 24.68, Cl 12.49; found C 59.32, H 3.49, N 24.66, Cl 12.44%.

#### 4-Amino-2-(2-furyl)pyrimido[1,2-*a*]-pyrimidine-3-carboxylate **6c**

Yield: 2.31 g (81%); mp 230 °C. IR (KBr)  $\nu_{\text{max}}$ : 3400 ( $\text{NH}_2$ ), 1700 (ester CO), 1580  $\text{cm}^{-1}$  (C=N). Insoluble in commonly used  $^1\text{H}$  NMR solvents.  $\text{C}_{14}\text{H}_{14}\text{N}_4\text{O}_3$  (286.29): calc. C 58.73, H 4.92, N 19.57; found C 58.74, H 4.50, N 19.66%.

#### 4-Amino-2-(3-nitrophenyl)pyrimido[1,2-*a*]-pyrimidine-3-carboxylate **6d**

Yield: 2.86 g (84%); mp 135 °C. IR (KBr)  $\nu_{\text{max}}$ : 3400 ( $\text{NH}_2$ ), 1710 (ester CO), 1600  $\text{cm}^{-1}$  (C=N). MS (EI, 70 eV):  $m/z$  342 ( $M + 1$ , 32%).  $^1\text{H}$  NMR (DMSO),  $\delta_{\text{H}}$  8.9 (s, 1H, arom-H), 7.6–8.4 (m, 7H, arom-H), 4.3 (q, 2H,  $\text{CH}_2$ ), 1.13 (t, 3H,  $\text{CH}_3$ ).  $\text{C}_{16}\text{H}_{15}\text{N}_5\text{O}_4$  (341.33): calc. C 56.30, H 4.42, N 20.51; found C 56.33, H 4.44, N 20.66%.

#### 2-Amino-4-(4-methoxyphenyl)pyrimido[1,2-*a*]-pyrimidine-3-carbonitrile **8e**

Yield: 2.29 g (82%); mp 150 °C. IR (KBr)  $\nu_{\text{max}}$ : 3340 ( $\text{NH}_2$ ), 2200 (CN), 1570  $\text{cm}^{-1}$  (C=N). MS (EI, 70 eV):  $m/z$  280 ( $M + 1$ , 5%).  $^1\text{H}$  NMR (DMSO),  $\delta_{\text{H}}$  8.4 (s, 2H,  $\text{NH}_2$ ), 7.2–7.66 (m, 7H, arom-H), 4.54 (s, 1H, CH-4).  $\text{C}_{15}\text{H}_{13}\text{N}_5\text{O}$  (279.30): calc. C 64.50, H 4.69, N 25.07; found C 64.55, H 4.72, N 25.11%.

#### 2-Amino-4-(3-nitrophenyl)pyrimido[1,2-*a*]-pyrimidine-3-carbonitrile **8f**

Yield: 2.44 g (83%); mp 165 °C. IR (KBr)  $\nu_{\text{max}}$ : 3330 ( $\text{NH}_2$ ), 2200 (CN), 1610  $\text{cm}^{-1}$  (C=N). MS (EI, 70 eV):  $m/z$  295 ( $M + 1$ , 35%). Insoluble in commonly used  $^1\text{H}$  NMR solvents.  $\text{C}_{14}\text{H}_{10}\text{N}_6\text{O}_2$  (294.27): calc. C 57.14, H 3.42, N 28.55; found C 57.22, H 3.45, N 28.65%.

#### 2-Amino-4-phenylpyrimido[1,2-*a*]-pyrimidine-3-carbonitrile **8g**

Yield: 2.11 g (85%); mp 155 °C. IR (KBr)  $\nu_{\text{max}}$ : 3340 ( $\text{NH}_2$ ), 2200 (CN), 1610  $\text{cm}^{-1}$  (C=N). MS (EI, 70 eV):  $m/z$  250 ( $M + 1$ , 25%).  $^1\text{H}$  NMR (DMSO),  $\delta_{\text{H}}$  8.4 (s, 2H,  $\text{NH}_2$ ), 7.92–7.66 (m,

8H, arom-H), 4.6 (s, 1H, CH-4).  $\text{C}_{14}\text{H}_{11}\text{N}_5$  (249.27): calc. C 67.45, H 4.44, N 28.09; found C 67.52, H 4.45, N 28.22%.

#### 2-Amino-4-(4-chlorophenyl)pyrimido[1,2-*a*]-pyrimidine-3-carbonitrile **8h**

Yield: 2.26 g (80%); mp 170 °C. IR (KBr)  $\nu_{\text{max}}$ : 3340 ( $\text{NH}_2$ ), 2200 (CN), 1610  $\text{cm}^{-1}$  (C=N). MS (EI, 70 eV):  $m/z$  284 ( $M + 1$ , 7%). Insoluble in commonly used  $^1\text{H}$  NMR solvents.  $\text{C}_{14}\text{H}_{10}\text{N}_5\text{Cl}$  (283.72): calc. C 59.26, H 3.55, N 24.68; found C 59.33, H 3.52, N 24.67%.

#### 2-Amino-4-(2-furyl)pyrimido[1,2-*a*]-pyrimidine-3-carbonitrile **8i**

Yield: 1.96 g (82%); mp > 300 °C. IR (KBr)  $\nu_{\text{max}}$ : 3320 ( $\text{NH}_2$ ), 2200 (CN), 1560  $\text{cm}^{-1}$  (C=N). MS (EI, 70 eV):  $m/z$  240 ( $M^+$ , 26%). Insoluble in commonly used  $^1\text{H}$  NMR solvents.  $\text{C}_{12}\text{H}_9\text{N}_5\text{O}$  (239.23): calc. C 60.24, H 3.79, N 29.27; found C 60.35, H 3.82, N 29.33%.

Compounds **4j**, **k** were found to be identical with authentic samples (mixed mp and IR spectra).

## References

- 1 R. Mekeimer, R. M. Shaker, K. U. Sadek and H. H. Otto, *Heterocycl. Commun.*, 1997, **3**, 217.
- 2 A. Gleich and F. P. Schmidtehen, *Chem. Ber.*, 1990, **123**, 907.
- 3 F. Esser, *Synthesis*, 1987, 460.
- 4 F. Ishikawa, T. Imano and Y. Abiko, *Jpn. Kokai Tokyo Koho*, 1978, **78–79**, 890; *Chem. Abstr.*, 1979, **90**, 23133t.
- 5 H. kurzmeier and F. P. Schmidtehen, *J. Org. Chem.*, 1990, **55**, 3749.
- 6 A. Kosasayama and F. Ishikawa, *Chem. Pharm. Bull.*, 1979, **72**, 1596.
- 7 F. Maurer, I. Hammann and B. Homeyer, *Ger. Offen.*, 1978, **2**, 703–712; *Chem. Abstr.*, 1978, **89**, 180155g.
- 8 A. Echavarren, A. Galan, J. M. Lehn and J. de Mendoza, *J. Am. Chem. Soc.*, 1989, **111**, 4994.
- 9 D. Schmidt, *Chem. Ber.*, 1980, **113**, 2175.
- 10 J. Clark and M. Michael, *J. Chem. Soc., Perkin Trans. 1*, 1977, **16**, 1855.
- 11 A. Kamal, B. S. N. Reddy and G. S. K. Reddy, *Synlett*, 1999, **8**, 1251.
- 12 S. Caddick, *Tetrahedron*, 1995, **51**, 10403.
- 13 A. K. Bose, M. Jayaraman, A. Okawa, S. S. Barie, E. W. Robb and M. S. Manhas, *Tetrahedron Lett.*, 1996, **37**, 6989.
- 14 A. K. Chakraborti and G. Kaur, *Tetrahedron*, 1999, **55**, 13265.
- 15 K. U. Sadek and M. H. Elnagdi, *Synthesis*, 1988, **6**, 483.
- 16 K. U. Sadek, K. Abouhadid and A. H. Elghandour, *Liebigs Ann. Chem.*, 1989, 501.



# Sensitivity analysis of the 2-methylpyridine *N*-oxidation kinetic model

Maria Papadaki,\* Richard James Emery, Eduard Serra, Rosa Nomen and Julia Sempere

Chemical Engineering Department, School of Process, Environmental and Materials Engineering, The University of Leeds, Leeds, UK LS2 9JT. E-mail: m.papadaki@leeds.ac.uk

Received 16th October 2001

First published as an Advance Article on the web 22nd February 2002

A sensitivity analysis of a previously developed global kinetic model, of the *N*-oxidation of 2-methylpyridine, involving seven kinetic and equilibrium constants, has been performed. It has been identified how individual constants influence the power evolution profile. The conditions, which ensure measurements sensitive to all constants, are outlined. A readily applicable, simple methodology has been developed to achieve accurate evaluation of the kinetic constants involved.

## 1. Introduction

As the safety and the environmental impact of industrial processes are becoming of increasing importance, the legislation controlling the industry becomes more rigorous and demanding. It is necessary now, more than ever, to target the design of safer and more efficient processes. Regarding safety issues, multipurpose batch or semi-batch reactors, which are extensively used in the agrochemical, fine-chemicals and pharmaceutical industry, where a variety of reactions are performed and relatively simple control is implemented, are more prone to a reaction runaway.

An industrial batch or semi-batch exothermic reaction runaway could occur due to a number of reasons, a common one being a cooling failure. In the latter, the reactor is considered to act adiabatically, thus, increasing the reactor temperature. As the temperature increases, reaction rates increase until all reactants are consumed. If a sufficiently high temperature is reached, thermally autocatalytic decomposition reactions initiate resulting in a further, more rapid increase in temperature. Often non-condensable gases are evolved causing elevated pressures and a potential explosion. More often than not, such explosions result in toxic material release in the atmosphere.

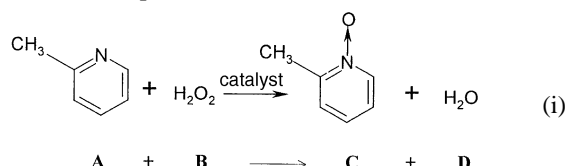
In similar occasions, questions to ask are, which temperature is critical, when it will be reached and how long after that time undesirable events will initiate. The answers to those questions define if, when and what action needs to be taken. The potential temperature rise is, in most cases, accurately determined following simple measurements. However, adequately accurate quantification of time-related quantities is feasible only when kinetic expressions, based on a sufficient understanding of the process chemistry and good quality thermodynamic data of the system, are available. It is also desirable, for these kinetic expressions to be simple and theoretically sound, while ensuring reliable runaway predictions in order to be of practical use. Except for their importance in developing safer processes, reliable kinetics can be readily used in process optimisation and the minimisation of material and energy waste.

Although the importance of reliable kinetics in industrial reactions cannot be disputed, there are practical aspects, which cannot be disregarded. Firstly, it is very difficult for the mechanism of a complex reaction to be revealed. Secondly, complicated kinetic expressions inevitably involve numerous constants, the evaluation of which is a cumbersome and, quite often, impossible task.

This article, which is product of an on-going research project on the *N*-oxidation of alkyipyridines, involves a sensitivity analysis of the kinetic constants of a moderately complex global kinetic model of the catalytic *N*-oxidation of 2-methylpyridine using hydrogen peroxide. This model was obtained using heat-flow reaction calorimetry measurements, which were proven to be an ideal tool for this type of reactions.<sup>1</sup> The target of the present work was to identify the conditions at which each individual kinetic constant is sensitive in, so as to enable their accurate calculation, following appropriately designed experiments. Such conditions have been identified.

### 1.1 The reaction system

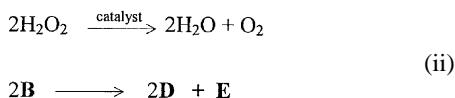
The desired reaction, eqn (i), shown below, is accompanied by the unwanted decomposition reaction (ii):



### Green Context

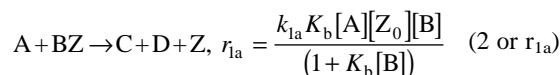
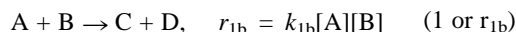
The safe running of a typical batch chemical reaction as routinely carried out by speciality and pharmaceutical chemical companies can be a matter of concern. Reaction runaway can occur for a number of reasons such as a cooling failure. We need to determine the conditions at which undesirable events will initiate and this requires accurate quantification of the process including sound kinetic expressions and good quality thermodynamic data. Reliable kinetics can also be used in process optimisation and minimisation of material and energy usage, thus satisfying many of the essential criteria for greening chemical processes. Here this approach is illustrated by a sensitivity analysis of the kinetic model for the *N*-oxidation of 2-methylpyridine—a reaction for which the use of a kinetic model to achieve process optimisation has previously been claimed. *JHC*



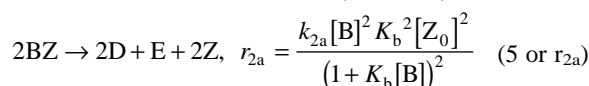
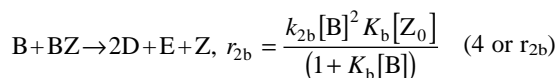
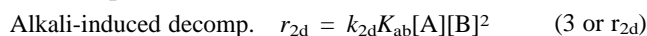


In this presentation, the nomenclature used by Sempere *et al.*<sup>2</sup> has been employed. It is cited here, together with the kinetic model equations, for the reader's convenience. The letters A, B, C, D and E correspond to 2-methylpyridine, hydrogen peroxide, 2-methylpyridine *N*-oxide, water and oxygen, respectively. Square brackets indicate concentration and  $Z_0$  stands for the initial moles of catalyst sites.

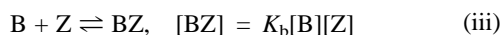
### *N*-oxidation



### Decomposition



The kinetic model assumes a very fast equilibrium, (iii), between catalyst and hydrogen peroxide for the formation of an intermediate, BZ. This intermediate then reacts with 2-methylpyridine (reactions  $r_{1a}$ ) but also contributes in the undesired decomposition reaction (reactions  $r_{2a}$ ,  $r_{2b}$ ).



with

$$[\text{Z}] = [\text{Z}_0]/(1 + K_b[\text{B}]) \quad (6)$$

where Z, is the number of moles of free catalyst sites in the reactor. The model also assumes, following a completely empirical approach, that the calculated concentration of the available to react hydrogen peroxide, the so-called  $[\text{B}_{\text{active}}]$ , is lower than the calculated hydrogen peroxide concentration,  $[\text{B}_{\text{apparent}}]$ , owing to the presence of 2-methylpyridine. The two concentrations are related via the following relation:

$$[\text{B}_{\text{active}}] = \frac{[\text{B}_{\text{apparent}}]}{1 + K_{ab}[\text{A}]} \quad (7)$$

This kinetic model was extracted from the experimentally obtained total power evolution (that is, the power produced by reactions (i) and (ii)), and the oxygen flow measurement. Its derivation was based exclusively on isothermal reaction calorimetry measurements, which were performed according to the methodology followed in the actual industrial process.

## 1.2 The measurement methodology

As mentioned before, the macroscopic reactions under the experimental conditions are (i) the *N*-oxidation of 2-methylpyridine for the formation of the 2-methylpyridine *N*-oxide and (ii) the catalytic decomposition of hydrogen peroxide producing gaseous oxygen. The total power generation was measured using heat-flow calorimetry. The produced oxygen was measured by means of a sensitive mass flow-meter. The oxygen flow measurement was then used to evaluate the extent and the power generated by the decomposition reaction as a function of time. The power produced by the *N*-oxidation reaction alone was subsequently evaluated from their difference. Calorimetric measurements were used for the calculation of the concentrations of each reactant as explained by Sempere *et al.*<sup>2</sup> The

concentration profiles were verified *via* analytical and IR concentration measurements as explained by Rodriguez-Miranda.<sup>1</sup> As explained in the same work, calorimetric concentration evaluation resulted in a smoother concentration profile of low scatter.

The sensitivity analysis and the methodology developed for the evaluation of the kinetic constants, presented in this article, is based on simulated power evolution profiles, using the values of constants presented by Sempere *et al.*<sup>2</sup> The impact of experimental error on the accuracy of the constants is considered elsewhere.<sup>3</sup>

## 1.3 The objectives of this study

The aforementioned kinetic model involves seven kinetic and equilibrium constants which need to be evaluated using, occasionally, relatively noisy data. The study performed by Sempere *et al.*<sup>2</sup> targeted the development of global reaction kinetics of industrial reactions, using calorimetric measurements, obtained by routine industrial tests. Experiments performed following the same experimental procedure but at different conditions, in a different reactor,<sup>4</sup> in principle corroborated the model of Sempere *et al.*<sup>2</sup>, although the second study<sup>4</sup> produced different values for two of the constants. Nevertheless, this was expected, as industrial processes are not performed at conditions sensitive enough to allow an accurate constant evaluation. However, it was rendered necessary to investigate the sensitivity of the kinetic model to changes of the parameters involved. One of the long-term objectives of this research is to identify the impact of the experimental error on the accuracy of the constants and on subsequent runaway predictions and then, to facilitate the selection of experiments and methodologies, which render the experimental error minimal. The first step of this study, the work presented here, resulted in identifying the range of conditions under which the kinetic model parameters can be reliably evaluated.

More specifically *via* the current study: it has been identified, how each of the two power generation curves is affected when the values of individual kinetic/equilibrium constants are varying.

A methodology, which allows accurate evaluation of constants, has been developed.

Experiments, which allow minimal error in the evaluation of all constants, in view of the existing level of noise in the measurement, have been designed.

## 2. Methodology

1. A simulation program was developed in EXCEL and VISUAL BASIC. The equations presented by Sempere *et al.*<sup>2</sup> together with the reported parameter values were employed in the program to calculate the power generation produced by reactions (i) and (ii).

2. The values of the kinetic constants were then changed, one at a time, so as to identify the range of each curve directly and distinctly influenced by this change.

3. A simple practical methodology was subsequently developed on how to accurately evaluate each constant. Preliminary validation tests of this methodology were also performed. An alternative, more sophisticated and complex methodology, not presented here is also being developed.<sup>3</sup>

### 2.1 Evaluation of the impact of the changed constant-values on the power generation profile

Fig. 1 shows the contribution of each reaction to the total power. The graph was produced by the simulation program employing

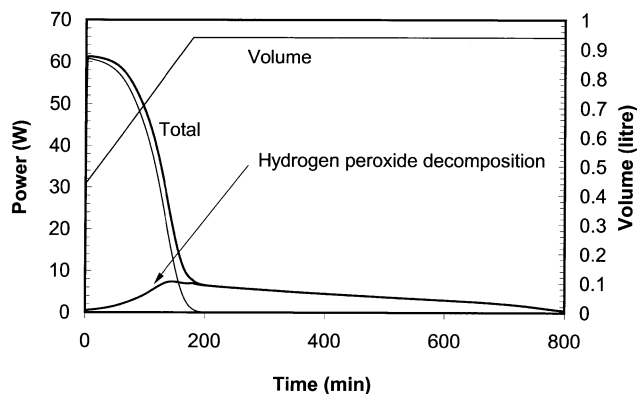


**Fig. 1** Simulated data for the semi-batch, 2-methylpyridine *N*-oxidation using the conditions, kinetic equations and the original constant values given by Sempere *et al.*<sup>2</sup>

the conditions and constants reported by Sempere *et al.*,<sup>2</sup> for an 1 litre reactor. Changing the value of all parameters, one at a time, usually by a factor of 10, 4, 2, 0.5, 0.01 and 0.05, a number of simulations were produced. Every run resulted in the power generation curves of all reaction paths as a function of time. Those simulations revealed the areas sensitive to each constant. Selected results are presented in Figs. 2–10. All figures show the two curves that can be obtained from a measurement, *i.e.* the total power and the power due to hydrogen peroxide decomposition. The figures also show a third curve, which corresponds to their difference (*N*-oxidation power). The change in the volume of the system is also shown, to highlight the progress of dosing. It was found that:  $K_b$  affects strongly and uniquely the gradient of the slope at the end of the decomposition reaction (Fig. 2). The larger the value of  $K_b$ , the steeper the curve. It also affects slightly the completion time. Larger  $K_b$  values correspond to shorter completion time as a comparison of Figs. 1 and 2 shows. It can also be seen that the  $K_b$  value affects slightly the *N*-oxidation reaction rate too, but the measurable effect is negligible.

When  $K_{ab}$  is large, the amount of hydrogen peroxide that decomposes increases dramatically (Fig. 3). Thus, reaction reaches completion earlier. At low values of  $K_{ab}$ , little changes. For the *N*-oxidation reaction presently under consideration,  $K_{ab}$  alone, can not be accurately evaluated.

Large values of  $k_{1a}$  result in both reactions (*N*-oxidation and decomposition) being controlled by dosing (Fig. 4). Small values of  $k_{1a}$  favour the parallel competitive reaction, namely the hydrogen peroxide decomposition thus, reducing the total time-to-completion. (Fig. 5). The value of  $k_{1a}$  affects strongly the initial part of the *N*-oxidation reaction.

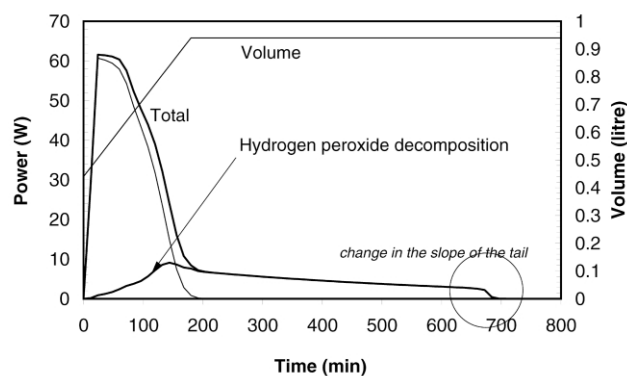


**Fig. 2** Simulated data for the semi-batch, 2-methylpyridine *N*-oxidation using the kinetic equations.<sup>2</sup>  $K_b = 10K_{b, \text{original}}$ . The remaining constant values are as in ref. 2. The circle indicates the area of the curve predominantly affected by the change in the value of the respective constant.

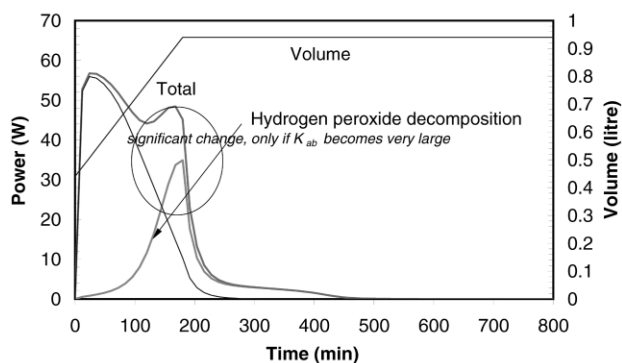


**Fig. 3** Simulated data for the semi-batch, 2-methylpyridine *N*-oxidation using the kinetic equations.<sup>2</sup>  $K_{ab} = 16K_{ab, \text{original}}$ . The remaining constant values are as in ref. 2. The circle indicates the area of the curve predominantly affected by the change in the value of the respective constant.

$k_{1b}$  affects the final part of the power produced by the *N*-oxidation. Comparison of Figs. 6 and 7 shows that low  $k_{1b}$  values result in high decomposition rates near the end of dosing (higher hydrogen peroxide accumulation) in contrast with low  $k_{1a}$  values (Fig. 5), which facilitate decomposition throughout the dosing period. High  $k_{1b}$  values result in a fast *N*-oxidation near the end of dosing rather than in the beginning (Fig. 8). It has also been noticed, that the influence of  $k_{1a}$  and  $k_{1b}$  is distinct on power profiles obtained using different amounts of catalyst.

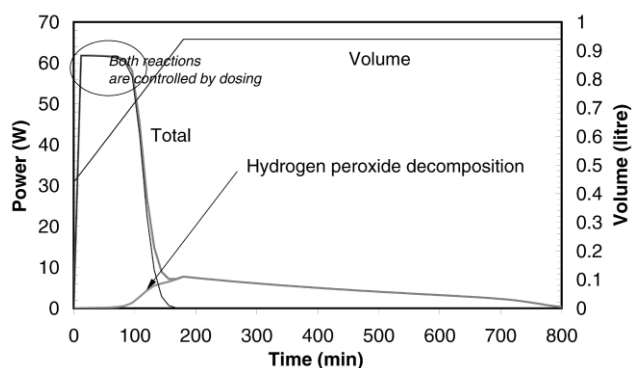


**Fig. 4** Simulated data for the semi-batch, 2-methylpyridine *N*-oxidation using the kinetic equations.<sup>2</sup>  $k_{1a} = 4(k_{1a, \text{original}})$ . The remaining constant values are as in ref. 2. The circle indicates the area of the curve predominantly affected by the change in the value of the respective constant.

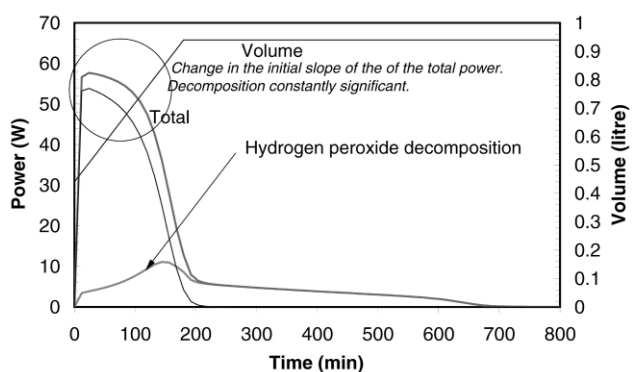


**Fig. 5** Simulated data for the semi-batch, 2-methylpyridine *N*-oxidation using the kinetic equations.<sup>2</sup>  $k_{1a} = 0.25(k_{1a, \text{original}})$ . The remaining constant values are as in ref. 2. The circle indicates the area of the curve(s) predominantly affected by the change in the value of the respective constant.

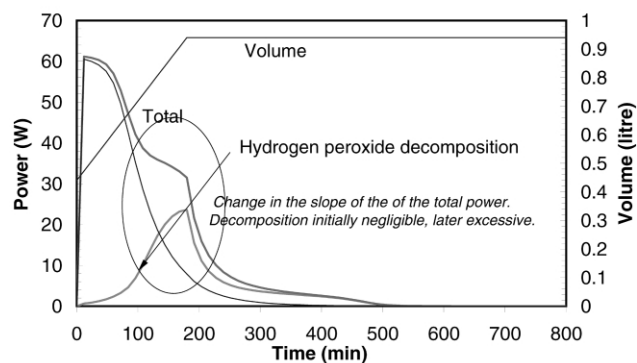


**Fig. 6** Simulated data for the semi-batch, 2-methylpyridine *N*-oxidation using the kinetic equations.<sup>2</sup>  $k_{1b} = 0.0625k_{1b \text{ original}}$ . The remaining constant values are as in ref. 2. The circle indicates the area of the curve(s) predominantly affected by the change in the value of the respective constant.

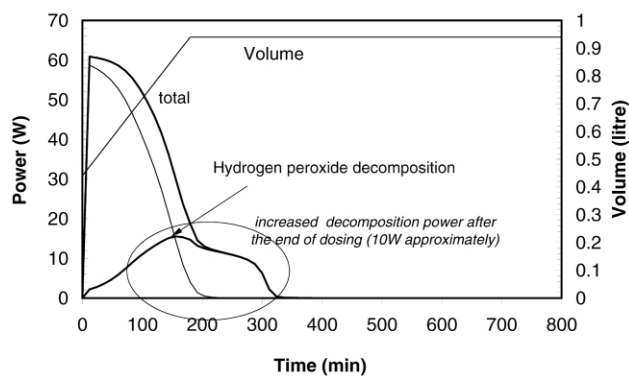


**Fig. 9** Simulated data for the semi-batch, 2-methylpyridine *N*-oxidation using the kinetic equations.<sup>2</sup>  $k_{2a} = 4k_{2a \text{ original}}$ . The remaining constant values are as in ref. 2. The circle indicates the area of the curve(s) predominantly affected by the change in the value of the respective constant.

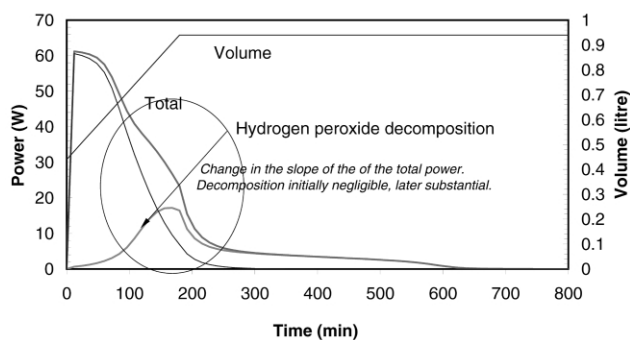


**Fig. 7** Simulated data for the semi-batch, 2-methylpyridine *N*-oxidation using the kinetic equations.<sup>2</sup>  $k_{1b} = 0.25k_{1b \text{ original}}$ . The remaining constant values are as in ref. 2. The circle indicates the area of the curve(s) predominantly affected by the change in the value of the respective constant.

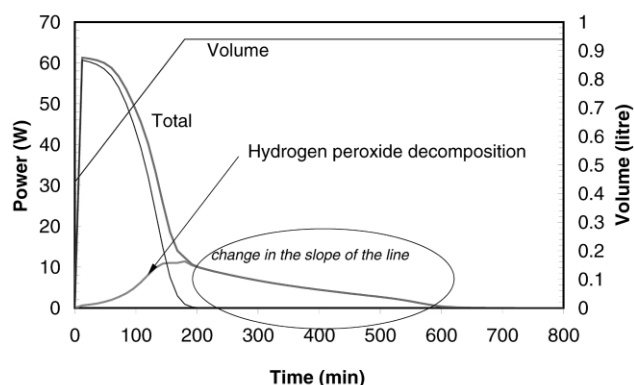


**Fig. 10** Simulated data for the semi-batch, 2-methylpyridine *N*-oxidation in a 1 litre reactor, using the kinetic equations.<sup>2</sup>  $k_{2b} = 2k_{2b \text{ original}}$ . The remaining constant values are as in ref. 2. The circle indicates the area of the curve(s) predominantly affected by the change in the value of the respective constant.

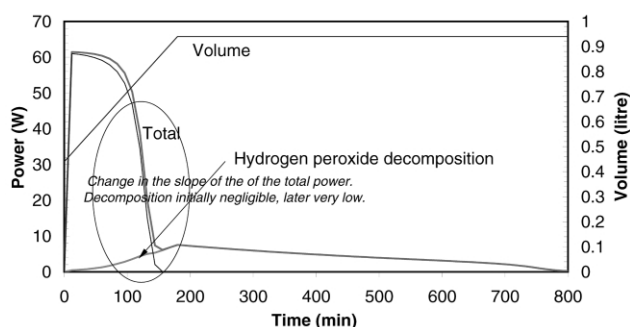


**Fig. 8** Simulated data for the semi-batch, 2-methylpyridine *N*-oxidation using the kinetic equations.<sup>2</sup>  $k_{1b} = 4k_{1b \text{ original}}$ . The remaining constant values are as in ref. 2. The circle indicates the area of the curve(s) predominantly affected by the change in the value of the respective constant.

$k_{2a}$  affects the power after the end of the *N*-oxidation and its value can be uniquely linked with the power produced when the respective reaction changes order (Fig. 9).

$k_{2b}$  is related to the gradient of the total power curve after dosing (Fig. 10).

$k_{2d}$  has a similar effect to that of  $K_{ab}$ , thus it is impossible to discriminate them. The product  $K_{ab}k_{2d}$  can though be accurately evaluated.

In conclusion, measurements should satisfy the following important conditions, in order to achieve accurate evaluation of each constant, including the group  $k_{2d}K_{ab}$ : (a) high power generation when only the decomposition takes place (evaluation of  $K_b$ ,  $k_{2a}$ ,  $k_{2b}$ ); (b) slow *N*-oxidation (evaluation of  $k_{1a}$ ,  $k_{1b}$ ).

### 3. Evaluation of constants

#### 3.1 Example of an ideal experiment

The present work has linked the rates of the two competitive reactions (i) and (ii) with the sensitivity of the individual model parameters. Fast or slow reaction rates can be achieved by changing temperature, amount of catalyst and reactant concentrations. So, for example, the use of a relatively high quantity of catalyst in the measurement provokes a high hydrogen peroxide decomposition rate (reaction (ii)). This will result in a better evaluation of  $k_{2a}$ ,  $k_{2b}$  and  $K_b$ . Simultaneously the alkali-induced decomposition is suppressed. It is explained later that the accuracy of  $k_{1a}$  and  $k_{1b}$  depends indirectly on the extent of the alkali-induced decomposition. The use of a low 2-methylpyridine concentration and of a lower than the nominal hydrogen peroxide strength allows for a slower *N*-oxidation. This will improve the sensitivity with regard to  $k_{1a}$  and  $k_{1b}$ . The simulated reaction profile presented in Fig. 11 was obtained using the values of constants presented by Sempere *et al.*<sup>2</sup> at 85 °C, but concentrations of reactants and catalyst were different than the nominal. The power evolution curves of Fig. 11 were used in the development of a simple methodology for an accurate evaluation of the kinetic model parameters. This methodology was subsequently followed for the calculation of all constants employed in the simulation, the accuracy of which was then assessed. Similar experiments were designed for measurements at higher temperatures. The methodology for the evaluation of the model parameters, using the profile of Fig. 11 is presented next.

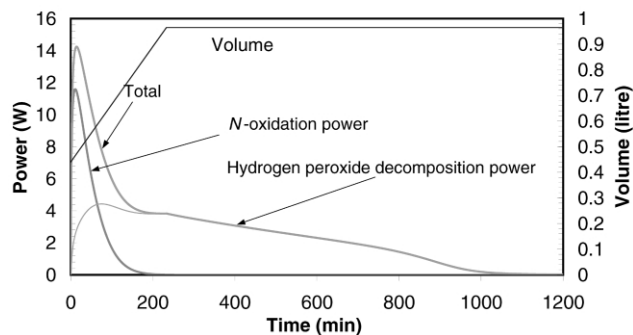


**Fig. 11** Simulated data for a 1 litre semi-batch reaction, performed under conditions, which will allow accurate evaluation of kinetic constants. Kinetic equations and kinetic constant values provided in ref. 2 have been used for the simulation.

### 3.2 Evaluation of $k_{2a}$ , $k_{2b}$ and $K_b$

Shortly after the end of dosing, the *N*-oxidation reaction is completed. Thus, only the decomposition reaction takes place following two catalytic paths with respective reaction rates,  $r_{2a}$ ,  $r_{2b}$ .

Eqns. (4) and (5) are typical examples of rates, which can change apparent order. The power generation profile of the decomposition reaction indicates a change of reaction order at around 800 min (Fig. 11). After all 2-methylpyridine is consumed the reaction rate, calculated as the total power of reaction,  $\dot{Q}_{tot}$ , divided by the volume of the system,  $V$  and by the heat of decomposition ( $-\Delta H_{dec}$ ) can be expressed as:

$$\frac{\dot{Q}_{tot}}{V(-\Delta H_{dec})} = r_{2b} + r_{2a} = \frac{k_{2b}[B]^2 K_b [Z_0]}{(1 + K_b[B])} + \frac{k_{2a}[B]^2 K_b^2 [Z_0]^2}{(1 + K_b[B])^2} \quad (8)$$

When  $K_b[B] \gg 1$ ,  $1 + K_b[B] \cong K_b[B]$  thus (8) reduces to (9)

$$(r_{2b} + r_{2a}) \cong k_{2b}([B][Z_0]) + k_{2a}([Z_0]^2) \quad (9)$$

Rate constants  $k_{2a}$ ,  $k_{2b}$  can be evaluated from eqn. (9) using linear regression.

After the evaluation of  $k_{2a}$  and  $k_{2b}$  using eqn. (9), relation (8) can be re-arranged to a quadratic equation with  $K_b$ , as the only unknown. Rate data for its solution are obtained from the area where  $K_b[B] \ll 1$ , and after the *N*-oxidation is completed.

The accuracy of constants  $k_{2a}$  and  $k_{2b}$  obtained via the aforementioned linear regression depends on the value of  $K_b$ . For moderately large values of  $K_b$ , the error in the value of  $k_{2b}$  is less than 1%, but worse than 10% for  $k_{2a}$ . The value of  $K_b$  obtained via the solution of relation (7), however, is insensitive to a 10% error associated with the value of  $k_{2a}$ . Thus, the values of  $k_{2a}$  and  $k_{2b}$  can be re-evaluated by division of the constants obtained via the linear regression by the quantities  $\{K_b[B]/(1 + K_b[B])\}^2$  and  $\{K_b[B]/(1 + K_b[B])\}$ , respectively. The resulting values of  $k_{2a}$  and  $k_{2b}$ , have an accuracy better than 2 and 0.2% respectively. Experiments using different amounts of catalyst can be used to improve further the accuracy of the value of  $k_{2a}$ , after an accurate evaluation of  $k_{2b}$  has been achieved.

### 3.3 Evaluation of $k_{2d}K_{ab}$

The rate of reaction (3) can be calculated by subtracting the rates of reactions (4) and (5) from the total decomposition rate. The accurate evaluation of  $k_{2d}$  and  $K_{ab}$  individually, appears problematic. The product  $k_{2d}K_{ab}$  however, can be evaluated via linear regression. Experimental evidence<sup>4</sup> suggests that more investigation is necessary for this empirically approximated reaction path (3). Nevertheless, the value of  $k_{2d}K_{ab}$  is required for the calculation of the so-called active hydrogen peroxide

(free hydrogen peroxide available for reaction), and the subsequent evaluation of  $k_{1a}$ ,  $k_{1b}$ . These values can be obtained via relation (10),

$$\frac{1}{r_{2d}} [B_{apparent}]^2 = \frac{1}{k_{2d}K_{ab}} \frac{1}{[A]} + \frac{1}{k_{2d}} \quad (10)$$

Following this method, the accuracy of the individual constants  $k_{2d}$  and  $K_{ab}$  is relatively poor. However, the accuracy of the value of the group  $k_{2d}K_{ab}$  is better than 1%. This was deemed satisfactory as it allows an adequately accurate calculation of the concentration of active (instead of apparent) hydrogen peroxide, which is essential for subsequent calculations. (As mentioned before, the accurate evaluation of each one of these constants is not of crucial importance, as this particular path is empirical and has insignificant contribution at high catalyst concentrations. This value is required only for the calculation of  $[B_{active}]$ , which is subsequently used in the evaluation of  $k_{1a}$  and  $k_{1b}$ ).

### 3.4 Evaluation of $k_{1b}$ and $k_{1a}$

The power generated by the *N*-oxidation,  $\dot{Q}_{N-Ox}$ , is calculated by subtracting the power of decomposition from the total power produced. From this, the sum of reaction rates (1) and (2) reduces to the following linear equation.

$$r_{1a} + r_{1b} = \frac{k_{1a}K_b[A][Z_0][B]}{(1 + K_b[B])} + k_{1b}[A][B]$$

$$\dot{Q}_{N-Ox} = [A][B] \left( k_{1a} \frac{K_b[Z_0]}{(1 + K_b[B])} + k_{1b} \right) \Delta H_{N-Ox} V \quad (11)$$

$$\left( \frac{\dot{Q}_{N-Ox}}{[A][B]\Delta H_{N-Ox}V} \right) = k_{1a} \left( \frac{K_b[Z_0]}{(1 + K_b[B])} \right) + k_{1b}$$

where  $\Delta H_{N-Ox}$ , is the enthalpy of the *N*-oxidation reaction, (i). The value  $K_b$  has already been calculated. The equation can therefore be solved using linear regression to provide the values of  $k_{1a}$  and  $k_{1b}$ . These can be calculated from this relation with a better than 1% accuracy.

### 3.5 Method validation: results of constant evaluation

The aforementioned simple methodology was subsequently used on the simulated data of Fig. 11 to evaluate the kinetic constants. Using the pure simulated data, all constants were evaluated with accuracy better than 2%. The influence of noise on the concentrations obtained from these data was also assessed. Experimental verification of the methodology is currently under way.

It is worth mentioning here that the accurate evaluation of  $k_{1a}$  and  $k_{1b}$  depends on the concentration of the so-called active hydrogen peroxide. Its calculation depends upon the value of the group of constants  $k_{2d}K_{ab}$ . The obtained value of this group of constants, following the presented methodology is better than 1%. The accurate evaluation of the individual constants however, has not been achieved in the present work. Nevertheless, the experiments performed by Sempere *et al.*,<sup>1</sup> provided a completely empirical rate for the alkali-induced decomposition of hydrogen peroxide and the experiments presented by and Papadaki *et al.*,<sup>4</sup> show that this rate expression is applicable to a limited range of conditions and that further investigation is necessary. Consequently, the accurate evaluation of the in-



dividual constants involved in the respective reaction rate was deemed, at present, superfluous.

## Discussion

Following the anterior analysis, we found that the margin of error in the measurements taken by Sempere *et al.*<sup>2</sup> and by Papadaki *et al.*,<sup>4</sup> in the measurements performed according to the industrial recipe, was large enough to justify the discrepancies in the results, except for the alkali-induced decomposition path. For this reaction path, as mentioned earlier, more research is rendered necessary.

Inspection of the equations used for the calculation of constants suggests that the accuracy of  $k_{2a}$  and  $k_{2b}$  depend on how well the slope and the intersection of straight line, eqn. (8), can be defined. In other words, they can be accurate, only if the power generation profile after the end of the *N*-oxidation, is high and steep enough. Similarly, the value of  $K_b$  depends strongly upon the same factors.

The values of  $k_{1a}$  and  $k_{1b}$  can be accurately evaluated only if the *N*-oxidation is slow enough to allow collection of sufficient data regarding the initial and the final part of the *N*-oxidation.

The catalytic *N*-oxidation path is predominantly faster than the non-catalytic one at significant catalyst concentrations, thus, the accurate evaluation of  $k_{1b}$  is difficult at high catalyst concentrations. At low catalyst concentrations its evaluation is possible but the power evolved after the *N*-oxidation is completed is not as high as in the case of high catalyst concentrations. The same stands for the accuracy of  $k_{2a}$  and  $k_{2b}$ .

Low catalyst concentrations, also favour the so called alkali-induced decomposition.

All the aforementioned formulae, use the concentration of active hydrogen peroxide. It is thus necessary to ensure its sufficiently accurate evaluation. As reported earlier, its calorimetric evaluation was proven to give the best results. Moreover, the higher the concentration the lower the error.

Similarly, the accuracy of the concentration of 2-methylpyridine will affect the accuracy of the obtained values of  $k_{1a}$  and  $k_{1b}$ . Table 1 shows the error in their evaluation if a random noise of 10% is introduced in the concentration of both 2-methylpyridine and hydrogen peroxide.

$k_{1a}$  and  $k_{1b}$  can be accurately evaluated following an accurate evaluation of  $K_b$  and of the group  $k_{2d}K_{ab}$ . Table 1 shows the impact that a 10% error in  $K_b$  has on their values. It can be seen on the same table, that a substantial error in  $K_{ab}k_{2d}$  group (an increment by a factor of 5), has hardly any effect on the obtained values. The group  $k_{2d}K_{ab}$  can be accurately evaluated in spite of the fact that the values of the two individual constants cannot be determined accurately. However, the accuracy of  $k_{2d}K_{ab}$  implicitly depends on  $K_b$ ,  $k_{2a}$  and  $k_{2b}$ , as the rate of this reaction is calculated via subtraction.

$k_{2a}$ ,  $k_{2b}$  and  $K_b$  can be accurately evaluated if appropriate conditions are selected.

The accuracy of the results of the first iteration for the calculation of  $k_{2a}$ ,  $k_{2b}$  is independent of the error in  $K_b$ , although it depends on its absolute value. As can be seen on Table 1, at higher  $K_b$  values, first iteration values of  $k_{2a}$  and  $k_{2b}$  have less error. The accuracy of  $k_{2a}$ ,  $k_{2b}$  obtained from the second iteration, is not strongly dependent on the accuracy of  $K_b$  neither on its absolute value. For high or moderately high values of  $K_b$ ,

**Table 1** Results obtained from the presented constant evaluation method

	$k_{2a}/1$ mol <sup>-1</sup> s <sup>-1</sup>	Error (%)	$k_{2b}/1$ mol <sup>-1</sup> s <sup>-1</sup>	Error (%)	$K_b/1$ mol <sup>-1</sup>	Error (%)	$K_{ab}k_{2d}/1^2$ mol <sup>-2</sup> s <sup>-1</sup>	Error (%)	$k_{1a}/1$ mol <sup>-1</sup> s <sup>-1</sup>	Error (%)	$k_{1b}/1$ mol <sup>-1</sup> s <sup>-1</sup>	Er- ror(%)
<b>Original values</b>	<b>1.560</b>		<b>2.79 × 10<sup>-3</sup></b>		<b>19.835</b>		<b>3.092 × 10<sup>-4</sup></b>		<b>5.208 × 10<sup>-2</sup></b>		<b>2.96 × 10<sup>-4</sup></b>	
<b><i>N</i>-oxidation</b>												
[H <sub>2</sub> O <sub>2</sub> ] <sub>active</sub>	N/A		N/A		N/A		3.0921 × 10 <sup>-4</sup>	0.00	5.208 × 10 <sup>-2</sup>	0.00	2.96 × 10 <sup>-4</sup>	0.00
[H <sub>2</sub> O <sub>2</sub> ] <sub>apparent</sub>	N/A		N/A		N/A		3.0921 × 10 <sup>-4</sup>	0.00	4.652 × 10 <sup>-2</sup>	-10.7	3.106 × 10 <sup>-4</sup>	4.9
[H <sub>2</sub> O <sub>2</sub> ] <sub>active</sub> , $K_b = 1.1K_b$	N/A		N/A		N/A		N/A		5.03 × 10 <sup>-2</sup>	-3.4	3.03 × 10 <sup>-4</sup>	2.4
$K_{ab}k_{2d} = 5 \times$ original value	N/A		N/A		N/A		N/A		5.03 × 10 <sup>-2</sup>	0.00	3.03 × 10 <sup>-4</sup>	0.00
±10% scatter in concentrations of both A and B	N/A		N/A		N/A		3.097 × 10 <sup>-4</sup>	0.2	5.238 × 10 <sup>-2</sup>	0.6	2.949 × 10 <sup>-4</sup>	-0.4
<b>Hydrogen peroxide decomposition</b>												
No correction	1.308	-16.1	2.98 × 10 <sup>-3</sup>	6.81	N/A		N/A		N/A		N/A	
Correction with $K_b = 19.835$	1.536	-2.0	2.79 × 10 <sup>-3</sup>	0.00	N/A		N/A		N/A		N/A	
Using $K_b$ correction with a 10% error in $K_b$	1.547	-0.8	2.76 × 10 <sup>-3</sup>	-1.08	N/A		N/A		N/A		N/A	
±10% scatter in power evolution values	1.520		2.85 × 10 <sup>-3</sup>		N/A		N/A		N/A		N/A	
10% error in $k_{2a}$	N/A		N/A		18.490	-6.8	N/A		N/A		N/A	
10% error in $k_{2b}$	N/A		N/A		19.502	-1.7	N/A		N/A		N/A	
<b>Error analysis employing a <math>K_b</math> value equal to 100</b>												
<b><i>N</i>-oxidation</b>												
[H <sub>2</sub> O <sub>2</sub> ] <sub>active</sub>	N/A		N/A		N/A		N/A		5.208 × 10 <sup>-2</sup>	0.00	2.96 × 10 <sup>-4</sup>	0.00
[H <sub>2</sub> O <sub>2</sub> ] <sub>apparent</sub>	N/A		N/A		N/A		N/A		4.959 × 10 <sup>-2</sup>	-4.8	3.02 × 10 <sup>-4</sup>	2.0
10% scatter in concentrations of both A and B	N/A		N/A		N/A		3.097 × 10 <sup>-4</sup>	0.2	5.227 × 10 <sup>-2</sup>	0.4	2.941 × 10 <sup>-4</sup>	-0.6
<b>Hydrogen peroxide decomposition</b>												
No correction	1.472	-5.6	2.83 × 10 <sup>-3</sup>	1.4								
Correction	1.523	-2.4	2.78 × 10 <sup>-3</sup>	-0.4								

the error in the evaluation of  $k_{2a}$  and  $k_{2b}$  does not induce a significant error in the evaluation of  $K_b$ . The evaluation of  $k_{2a}$  and  $k_{2b}$  can be accurate if the two step calculation is considered. The accuracy of their values in the first iteration depends on the absolute value of  $K_b$ , as it can be seen from Table 1 where the cases of  $K_b = 20$  and  $K_b = 100$  were considered. It can also be seen from the same table that a significant error in the calculated value of  $K_b$  does not affect much the accuracy of the values of the constants, obtained from the second iteration.

It was initially considered to add random noise in the simulated data of the heat evolution in order to approximate real experimental data. Experimental data however, are always smoothed using appropriately selected functions. Smoothing of the simulated data would result in the initially employed curves. Thus, this approach was rejected and only the impact of random noise on the concentration was considered. However, a study currently under way examines the impact of specific experimental errors on the kinetic constant evaluation. (More specifically, as the power of reaction is used to obtain the calculation of the reactant concentration and the extent of each reaction, wrong UA values employed, or temporary non-isothermal reactor operation, will inevitably affect the concentration profiles). Table 1 presents the effect that 10% noise on the concentration has on the kinetic constant values.

## Appendix

### List of symbols

A	: free molecular 2-methylpyridine
B or B <sub>active</sub>	: free hydrogen peroxide available for reaction
[B <sub>apparent</sub> ]	: concentration of total hydrogen peroxide in molecular or associated form
BZ	: intermediate compound between hydrogen peroxide and catalyst
C	: 2-methylpyridine <i>N</i> -oxide
D	: water
E	: oxygen
K <sub>ab</sub>	: equilibrium constant of the formation of an unspecified type intermediate related to 2-methylpyridine and hydrogen peroxide
K <sub>b</sub>	: equilibrium constant of the formation of an

	intermediate between hydrogen peroxide and catalyst
$k_{1a}, k_{1b}$	: rate constants of the reactions (2) and (1), respectively
$k_{2a}, k_{2b}, k_{2d}$	: rate constants of the reactions (5), (4) and (3), respectively
$\dot{Q}_{tot}$	: rate of total power generation
$\dot{Q}_{N-Ox}$	: rate of power generation owing to the <i>N</i> -oxidation alone
$t$	: time
$V$	: volume of the reaction mixture (a function of time)
$Z$	: free catalyst sites
$Z_0$	: total catalyst sites
$\Delta H_{N-Ox}$	: enthalpy of the <i>N</i> -oxidation
$\Delta H_{dec}$	: enthalpy of the decomposition of hydrogen peroxide.
[ ]	: square brackets have been used to indicate concentration.
suffix <sub>original</sub>	indicates the values provided by Sempere <i>et al.</i> <sup>2</sup>

### Acknowledgements

The authors wish to acknowledge EPSRC for the financial support they have provided towards this research *via* the GR/R14095/01 research grant, titled as 'Development of General Kinetic Models & Prediction of Runaway Consequences of Industrial Reactions'.

### References

- 1 J. L. Rodriguez-Miranda, Diploma Thesis, IQS, Barcelona, Spain, 1997.
- 2 J. Sempere, R. Nomen, J. L. Rodriguez and M. Papadaki, *Chem. Eng. Process.*, 1998, **37**, 33.
- 3 M. Papadaki and R. Emery, *Sensitivity analysis of calorimetrically extracted kinetic models. Case study of a complex catalytic oxidation*, in preparation.
- 4 M. Papadaki, R. Emery, E. Serra, V. Stoikou, D. Mantzavinos, R. Nomen and J. Sempere, *Catalytic N-oxidation of 2-methylpyridine I: Kinetic studies using reaction calorimetry*, submitted to ISCRE 17, Hong-Kong, August 2002.



# Dispersion and reactivity of Mo/Nb<sub>2</sub>O<sub>5</sub> catalysts in the ammoxidation of toluene to benzonitrile

Komandur V. R. Chary,\* Kondakindi Rajender Reddy, Thallada Bhaskar and Guggilla Vidya Sagar

Catalysis Division, Indian Institute of Chemical Technology, Hyderabad- 500 007, India.  
E-mail: kvrchary@iict.ap.nic.in

Received 16th October 2001

First published as an Advance Article on the web 8th March 2002

A series of Mo/Nb<sub>2</sub>O<sub>5</sub> catalysts were prepared with Mo loadings ranging from 2.5–15 wt% of Mo and characterized by X-ray diffraction (XRD), pulse oxygen chemisorption, temperature-programmed desorption of ammonia. Dispersion of molybdena was determined by oxygen chemisorption at 623 K in a dynamic method. At low Mo loadings molybdenum oxide is found to be present in a highly dispersed state. XRD results show the presence of crystalline MoO<sub>3</sub> at higher Mo loadings (from 10 wt%). The dispersion of molybdena was found to decrease with increased Mo loading due to formation of MoO<sub>3</sub>. The catalytic properties were evaluated for the vapour phase ammoxidation of toluene to benzonitrile and are related to different characterization results.

## Introduction

Catalysts containing molybdenum oxide/sulfide as an active component have been extensively employed in the recent past for the partial oxidation of hydrocarbons, alcohols and also extensively used for hydroprocessing reactions in the petroleum industry.<sup>1–10</sup> The most commonly used supports are Al<sub>2</sub>O<sub>3</sub>, TiO<sub>2</sub> and SiO<sub>2</sub>. In the last decade niobium based materials have attracted considerable interest in various reactions. Niobia can be used as a support, promoter and as a unique solid acid. Smits *et al.*<sup>11</sup> emphasized the advantages of niobia as a catalyst support for vanadia. These include: (i) niobium is in the same region of the periodic table as vanadium or molybdenum and is expected to have similar properties. (ii) Niobium is much more difficult to reduce than vanadium or molybdenum (easy reduction often causes low selectivity in selective oxidation reactions). (iii) The addition of niobium oxide to a mixture of molybdenum and vanadium oxides improves the activity and selectivity for oxidation, ammoxidation and oxidative dehydrogenation reactions.<sup>11,12</sup> Huuhtanen *et al.*<sup>13</sup> reported a comparison of different supports, and niobia appears to be promising as far as selectivity in toluene oxidation was concerned. Matsuura *et al.*<sup>14</sup> reported that the catalytic activity during the ammoxidation of isobutane to methacrylonitrile was improved with Bi–Mo based composites supported on Nb<sub>2</sub>O<sub>5</sub> rather than on  $\gamma$ -Al<sub>2</sub>O<sub>3</sub> or SiO<sub>2</sub>. A fundamental problem in catalytic oxidation is the estimation of the number of active sites on the surface of oxide catalysts. Simple methods to titrate surface metal centers in oxides would greatly assist in understanding the effect of structure in oxidation reactions. The efficiency of supported molybdenum oxide catalysts mainly depends on the dispersion of the active phase, which in turn can be greatly influenced by the nature of supported oxide and the method of preparation of the catalysts. In this paper we report the characterization of niobia-supported molybdenum oxide catalysts by various techniques. The catalytic properties have been evaluated for the vapour phase ammoxidation to produce benzonitrile which is used as a precursor for resins and coatings. Benzonitrile is also used as an additive in fuels and fibers. Stobbelaar<sup>15</sup> reported the ammoxidation of toluene over supported metal oxide catalysts and concluded that MoO<sub>3</sub>/Al<sub>2</sub>O<sub>3</sub> catalysts are also of comparable importance with other vanadia supported catalysts. MoO<sub>3</sub>/

MgF<sub>2</sub> catalysts were also reported for the ammoxidation of toluene to benzonitrile.<sup>16</sup> The conversion of toluene to benzonitrile was found to be higher for Mo/Nb<sub>2</sub>O<sub>5</sub> catalysts than for Mo/TiO<sub>2</sub> catalysts.<sup>17</sup>

## Results and discussion

The X-ray diffraction patterns of calcined MoO<sub>3</sub>/Nb<sub>2</sub>O<sub>5</sub> catalysts are presented in Fig. 1. In all the samples XRD reflections due to low temperature niobia were observed at  $d = 3.95, 3.14, 2.45, 1.97$  and  $1.66 \text{ \AA}$  and the corresponding  $2\theta$  values are  $22.5, 28.4, 36.6, 46$  and  $55.3^\circ$ . At higher Mo loadings (above 7.5 wt% Mo, Fig. 1(d)) XRD reflections due to a crystalline MoO<sub>3</sub> phase (JCPDS no. 5-0508) are observed at  $d = 3.26 \text{ \AA}$  ( $2\theta = 27.3^\circ$ ) and  $3.81 \text{ \AA}$  ( $2\theta = 23.3^\circ$ ), in addition to the characteristic reflections of niobia. The reflections due to MoO<sub>3</sub> are shown as filled circles in Fig. 1. The intensity of these reflections increases with MoO<sub>3</sub> loading. However, at low Mo loadings the absence of crystalline MoO<sub>3</sub> reflections cannot be ruled out, as the crystallites might be less than  $40 \text{ \AA}$  in size, which is beyond the detection capacity of the XRD technique. XRD results also suggest that no mixed oxide is formed between MoO<sub>3</sub> and Nb<sub>2</sub>O<sub>5</sub>. Ko and Weissman<sup>18</sup> reported that, at low calcination temperature (773 K) Nb<sub>2</sub>O<sub>5</sub> samples are found to be X-ray amorphous. However, the samples calcined between 773–873 K show the TT-phase of Nb<sub>2</sub>O<sub>5</sub>, and the samples calcined between 873–973 K indicate the formation of the T-

## Green Context

The conversion of toluene to benzonitrile *via* ammoxidation is a direct and convenient functionalisation of a hydrocarbon feedstock. Recently molybdenum supported on niobia has been shown to be a highly selective catalyst, partly due to the limited redox chemistry of the support. This paper indicates that a careful analysis of the surface species can lead to improvements in catalytic efficiency, leading to a cleaner process. *DJM*

phase of  $\text{Nb}_2\text{O}_5$ . At 1073 K, the M-phase and at 1273 K and above the H-phase of  $\text{Nb}_2\text{O}_5$  is observed. In the present study, the samples were calcined at 773 K and our XRD results (Fig.

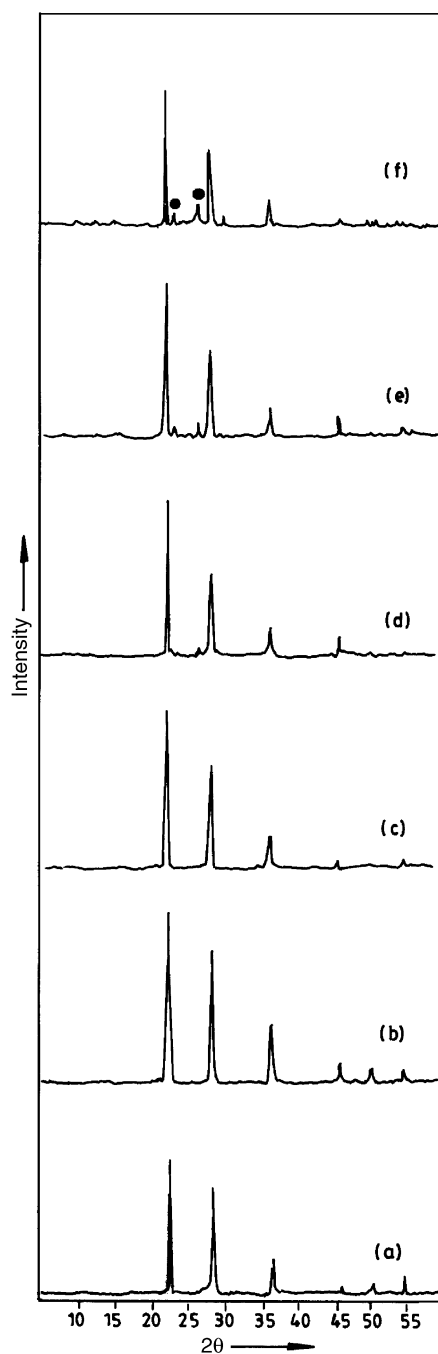


**Fig. 1** X-Ray diffractograms of various Mo/ $\text{Nb}_2\text{O}_5$  catalysts: (a) 2.5% Mo/ $\text{Nb}_2\text{O}_5$ , (b) 5.0% Mo/ $\text{Nb}_2\text{O}_5$ , (c) 7.5% Mo/ $\text{Nb}_2\text{O}_5$ , (d) 10% Mo/ $\text{Nb}_2\text{O}_5$ , (e) 12.5% Mo/ $\text{Nb}_2\text{O}_5$ , (f) 15% Mo/ $\text{Nb}_2\text{O}_5$ ; (●) reflections due to  $\text{MoO}_3$

1) also suggest the formation of the TT-phase of  $\text{Nb}_2\text{O}_5$ , which is in good agreement with the work of Ko and Weissman.<sup>18</sup> The  $d$  spacings of the TT- and T-phases of  $\text{Nb}_2\text{O}_5$  are similar, but the intensities differ. At  $d = 3.95 \text{ \AA}$  the relative intensities were found to be 100 and 84 for the TT- and T-phases, respectively, and at  $d = 3.14 \text{ \AA}$  the relative intensities were found to be 90 and 100. The intensities of  $d$ -spacings in the present XRD patterns (Fig. 1) suggest that only the TT-phase of  $\text{Nb}_2\text{O}_5$  is observed.

Fig. 2 shows oxygen uptake data for  $\text{Nb}_2\text{O}_5$ -supported samples measured at 623 K. The uptakes are plotted vs. the amount of molybdenum ( $\mu\text{mol g}^{-1}$ ) present in the samples. At low Mo loadings the oxygen uptakes approached the straight line corresponding to a stoichiometry of one oxygen atom per molybdenum atom and data are provided in Table 1. The oxygen chemisorption amounts obtained here represent irreversible uptakes by the samples, as indicated by the lack of a desorption tail at the end of each pulse and these amounts are doubled to obtain atomic oxygen uptake values. Previous studies,<sup>19,20</sup> used  $T_{\text{red}} = 773 \text{ K}$  and  $T_{\text{ads}} = 77 \text{ K}$ , followed by evacuation and readsorption at 195 K. These conditions were evaluated by Rodrigo *et al.*<sup>21</sup> who concluded that  $\text{O}_2$  chemisorption under these conditions does not provide a quantitative determination of Mo dispersion because a fraction of the reduced Mo is in the bulk. It has been shown that oxygen chemisorption sites are easily generated under very mild reduction conditions, such as those employed in this study.<sup>22</sup> The straight line in Fig. 2 corresponds to a 100% dispersion of the  $\text{MoO}_3$  with a stoichiometry of one oxygen atom per molybdenum atom. At low Mo loadings (<10 wt%) the adsorption behavior of the dispersion approached the straight line but was found to deviate from the straight line at higher Mo

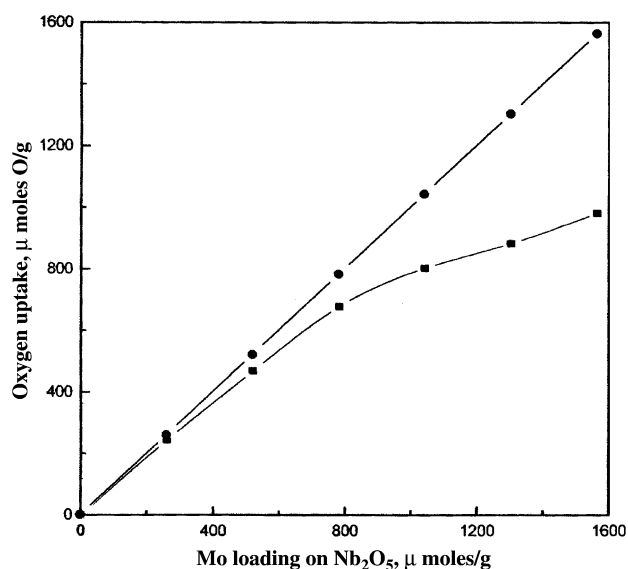


**Fig. 2** Oxygen uptake plotted as a function of molybdena loading on niobia.

**Table 1** Results of pulse oxygen chemisorption and temperature-programmed desorption of  $\text{NH}_3$

Sample	Mo loading on $\text{Nb}_2\text{O}_5$ (wt%)	Surface area/ $\text{m}^2 \text{ g}^{-1}$	$\text{O}_2$ uptake <sup>a</sup> / $\mu\text{mol g}^{-1}$	Dispersion <sup>b</sup> (O/Mo)	$T_1/\text{K}$	$\text{NH}_3$ uptake/ $\text{ml g}^{-1}$	$T_2/\text{K}$	$\text{NH}_3$ uptake/ $\text{ml g}^{-1}$
1	2.5	50	122.2	0.94	553	4.07	826	0.4
2	5.0	44	234.2	0.90	—	—	—	—
3	7.5	40	338.6	0.87	537	3.38	805	1.7
4	10.0	38	401.1	0.77	—	—	—	—
5	12.5	29	441.7	0.67	—	—	—	—
6	15.0	27	490.7	0.63	554	6.37	785	1.6

<sup>a</sup>  $T_{\text{ads}} = T_{\text{red}} = 623 \text{ K}$ . <sup>b</sup> Dispersion is defined as the fraction of Mo atoms at the surface assuming  $\text{O}_{\text{ads}} = \text{Mo}_{\text{surf}} = 1$



loadings. The decrease is due to formation of  $\text{MoO}_3$  crystallites at higher Mo loadings with monolayer coverage on niobia. Oxygen chemisorption on alumina-supported molybdena catalysts has been studied by Hall *et al.*<sup>23,24</sup> They employed a high reduction temperature of 773 K and adsorption temperatures between 77 and 195 K. They demonstrated that  $\text{O}_2$  chemisorption is site-specific and is correlated with the vacancy concentration of the reduced catalyst. Similarly, Seyedmonir and Howe<sup>25</sup> used reduction temperatures of 673 and 773 K on silica-supported samples containing polymolybdate species and molybdenum trioxide. They concluded that at 673 K reduction of polymolybdate occurred with the formation of  $\text{Mo}^{5+}$  species, while at 773 K reduction of  $\text{MoO}_3$  to  $\text{Mo}^{4+}$  species occurred. The group of Hall suggested that  $\text{O}_2$  chemisorption on  $\text{MoO}_3/\text{Al}_2\text{O}_3$  catalysts occurs on sites with at least two missing oxygen atoms while Fierro and Gamboro<sup>22</sup> suggest that on  $\text{MoO}_3/\text{SiO}_2$  adsorption occurs on  $\text{Mo}^{5+}$  sites.

The acidity values of  $\text{Mo}/\text{Nb}_2\text{O}_5$  catalysts determined by  $\text{NH}_3$ -TPD are given in Table 1. The acidity was found to lie in two regions and the corresponding peak maxima are also given in the Table 1. From  $\text{NH}_3$ -TPD measurements it is clear that the number of acid sites with moderate strength was found to increase with Mo loading on niobia. However, the  $\text{NH}_3$  uptake due to strong acid sites was found to be almost equal for 7.5 wt%  $\text{Mo}/\text{Nb}_2\text{O}_5$  and 15 wt%  $\text{Mo}/\text{Nb}_2\text{O}_5$  catalysts. This behaviour is in agreement with the catalytic activity beyond 7.5 wt% Mo loading, which did not change appreciably with increase of Mo loading on the niobia support. This clearly indicates that strong acid sites are responsible for toluene ammoxidation. The TPD results suggest that the strength of the acid sites plays a crucial role in determining the catalytic activity during ammoxidation of toluene, and the acidity of the catalysts is mainly due to the molybdena phase, since ammonia uptake increases with increase in molybdena loading.

Fig. 3 shows the results of ammoxidation of toluene over various  $\text{Mo}/\text{Nb}_2\text{O}_5$  catalysts at 673 K. The conversion and selectivity of the catalysts were found to increase with Mo loading up to a loading of 7.5 wt% whilst beyond this little difference was observed. Table 2 shows the activity of various supported molybdenum oxide catalysts in comparison to the present study. The activity results reported in Table 2 are the results from our laboratory. The conversion of toluene was found to be higher for  $\text{Mo}/\text{Nb}_2\text{O}_5$  catalysts compared to  $\text{Mo}/\text{TiO}_2$  catalysts and comparable to  $\text{Mo}/\text{ZrO}_2$  catalysts. The selectivity towards the formation of benzonitrile was found to

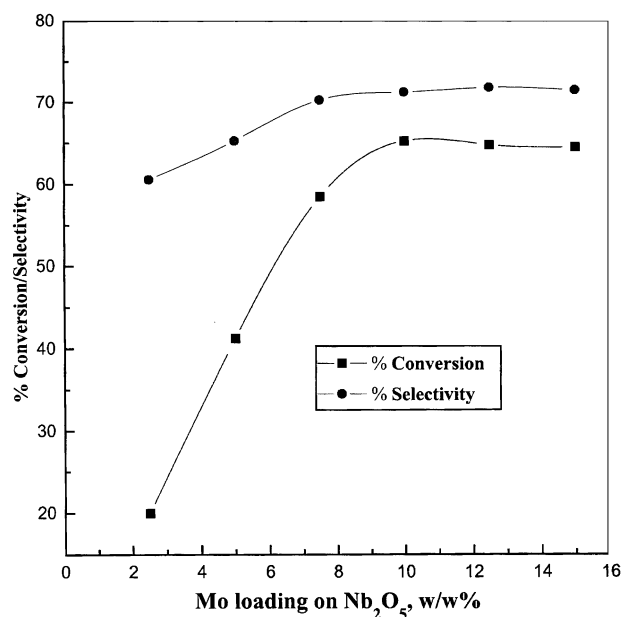


Fig. 3 Ammoxidation of toluene over various  $\text{Mo}/\text{Nb}_2\text{O}_5$  catalysts.

Table 2 Activity of various supported molybdenum oxide catalysts in the ammoxidation of toluene to benzonitrile

Catalyst	Conversion (%)	Selectivity (%)
10% $\text{Mo}/\text{Nb}_2\text{O}_5$	65.2	71.2
10% $\text{Mo}/\text{TiO}_2$ (Degussa, P-25) <sup>17</sup>	56.2	74.0
10% $\text{Mo}/\text{ZrO}_2$	64.0	68.4

be almost the same for all the catalysts. Further details about the preparation and characterization of these catalysts are reported elsewhere.<sup>17</sup>

To elucidate the relation between the ammoxidation activity of toluene and the dispersion of molybdena, a plot of turnover frequency (TOF) vs. Mo loading is shown in Fig. 4. The TOF was found to be almost constant ( $\approx 4 \times 10^{-3} \text{ s}^{-1}$ ) up to 7.5 wt% Mo and decreased at higher Mo loadings. Up to 7.5 wt% Mo loading, activity per site (constant TOF) is constant with an increase in the number of surface Mo sites. The decrease in TOF beyond 7.5 wt% Mo loading indicates the presence of different molybdena species such as  $\text{MoO}_3$  particles. The oxygen is chemisorbed on coordinatively unsaturated sites (CUS), which are located on a highly dispersed molybdenum phase, which is formed only at low molybdenum loadings and remain as a 'patchy monolayer' on the support surface. At higher molybdena loadings, a second phase is formed, in addition to the already existing monolayer, and this post monolayer phase does not appreciably chemisorb oxygen (Fig. 2). In the context of the above background, the correlation shown here indicates that the catalytic functionality of the dispersed molybdena phase supported on niobia, which is responsible for the ammoxidation of toluene to benzonitrile, is located on a patchy-monolayer phase and that this functionality can be titrated by the oxygen chemisorption method reported in this work.

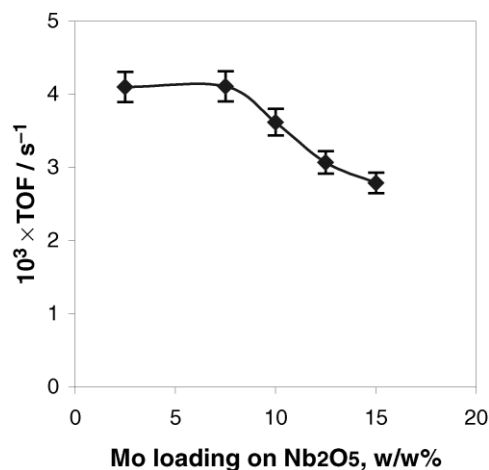


Fig. 4 The relation between turnover frequency and Mo loading on niobia.

## Experimental

A series of  $\text{MoO}_3$  catalysts with Mo loadings ranging from 2.5–15 wt% supported on  $\text{Nb}_2\text{O}_5$  (surface area  $55 \text{ m}^2 \text{ g}^{-1}$ ) was prepared by incipient wetting of the support using aqueous ammonium heptamolybdate solution at pH 8. The catalysts were subsequently dried at 383 K for 16 h and calcined in air at 773 K for 6 h. The niobium pentoxide hydrate (Niobia HY-340, CBMM, Brazil) was calcined in air at 773 K for 4 h to obtain  $\text{Nb}_2\text{O}_5$  before impregnation with ammonium heptamolybdate.

Oxygen chemisorption was measured by the dynamic method on AutoChem 2910 (Micromeritics, USA) instrument. Prior to

adsorption measurements, 0.5 g of the samples were prereduced in a flow hydrogen (50 ml min<sup>-1</sup>) at 623 K for 2 h and flushed in the pure He flow (purity 99.999%) for 1 h at the same temperature. Oxygen uptakes were determined by injecting pulses of oxygen from a calibrated on-line sampling valve onto a He stream passing over the reduced samples at 623 K. Adsorption was deemed to be complete after at least three successive peaks showed the same area. The surface areas of the catalysts (taking 0.162 nm<sup>2</sup> as the cross sectional area of an N<sub>2</sub> molecule) were determined by the BET method on an all-Pyrex glass high vacuum system which is capable of attaining a vacuum of 10<sup>-6</sup> Torr. X-Ray diffractograms were recorded on a Siemens D-5000 diffractometer using graphite-filtered Cu-K $\alpha$  radiation.

### Temperature-programmed desorption (TPD) of NH<sub>3</sub>

TPD experiments were also conducted on AutoChem 2910 instrument. In a typical experiment for TPD studies ca. 200 mg of an oven-dried sample (dried at 383 K for 16 h) was taken in a U shaped quartz cell. Prior to TPD studies the catalyst sample was pretreated by passing high purity helium (50 ml min<sup>-1</sup>) at 473 K for 2 h. After pretreatment, the sample was saturated by passing (75 ml min<sup>-1</sup>) 10% NH<sub>3</sub>-He at 353 K, and subsequently flushing at 378 K for 2 h to remove the physisorbed ammonia. TPD analysis was carried out from ambient temperature to 1073 K at a heating rate of 10 K min<sup>-1</sup>. The NH<sub>3</sub> uptake amounts were calculated using GRAMS/32 software.

A down-flow fixed bed reactor operating at atmospheric pressure and made of Pyrex glass was used to test the catalysts during the ammoxidation of toluene to benzonitrile. About 0.5 g of the catalyst diluted with an equal amount of quartz grains were charged into the reactor and were supported on a glass wool bed. Prior to introducing the reactant toluene with a syringe pump the catalyst was activated at 723 K for 2 h in an air flow (40 ml min<sup>-1</sup>). After activation the reactor was fed with toluene, ammonia and air, keeping the mol ratio of toluene:NH<sub>3</sub>:air at 1:14:30. The reaction products (mainly benzonitrile) were analyzed using an HP 6890 gas chromatograph equipped with FID using an OV-17 column. The only by-products formed were carbon oxides and analysis was carried out on a GC-MS HP 5973 instrument using a Porapak Q column.

### Conclusions

XRD results show the presence of crystalline MoO<sub>3</sub> at higher loadings (>7.5 wt%). The dispersion of molybdena (determined by pulse chemisorption) is directly related to the catalytic

activity. NH<sub>3</sub>-TPD results also directly relate to the results of ammoxidation of toluene.

### Acknowledgements

K. V. R. thanks the EMR division of Council of Scientific and Industrial Research (CSIR) for the grant under the Young Scientist Award Scheme, K. R. R. thanks the CSIR for a Senior Research Fellowship (SRF) and G. V. S. thanks the CSIR for a Junior Research Fellowship (JRF).

### References

- 1 F. E. Massoth, *Adv. Catal.*, 1978, **27**, 265.
- 2 P. Grange, *Catal. Rev-Sci Eng.*, 1980, **21**, 135.
- 3 H. Knozinger, in *Proc. 9th Int. Congress Catal., Calgary*, 1988; ed. M. Phillips and M. Ternan, The Chemical Institute of Canada, Ottawa, 1989, vol. 5, p. 20.
- 4 B. M. Reddy, K. V. R. Chary, V. S. Subrahmanyam and N. K. Nag, *J. Chem. Soc., Faraday Trans 1*, 1985, **81**, 1655.
- 5 K. Y. S. Ng and E. Gulari, *J. Catal.*, 1985, **95**, 33.
- 6 J. S. Chung, R. Miranda and C. O. Bennett, *J. Catal.*, 1988, **144**, 898.
- 7 C. Louis, J. M. Tatibouet and M. Che, *J. Catal.*, 1988, **109**, 354.
- 8 Y. C. Liu, G. L. Griffin, S. S. Chan and I. E. Wachs, *J. Catal.*, 1985, **94**, 108.
- 9 Y. Masuoka, M. Niwa and Y. Murakami, *J. Phys. Chem.*, 1990, **94**, 1477.
- 10 W. Zhang, A. Desikan and S. T. Oyama, *J. Phys. Chem.*, 1995, **99**, 14468.
- 11 R. H. H. Smits, K. Seshan, J. R. H. Ross, L. C. A. Van den Oetelaar, J. H. J. M. Helwegen, M. R. Anantharaman and H. H. Brongersma, *J. Catal.*, 1995, **157**, 584.
- 12 T. C. Watling, G. Deo, K. Seshan, I. E. Wachs and J. A. Lercher, *Catal. Today*, 1996, **28**, 139.
- 13 J. Huuhtanen and S. L. T. Andersson, *Appl. Catal. A: General*, 1993, **98**, 159.
- 14 I. Matsuura, H. Oda and K. Hoshida, *Catal. Today*, 1993, **16**, 547.
- 15 P. J. Stobbelaar, Ph.D. Thesis, University of Eindhoven, 2000.
- 16 J. Haber and M. Wojchechowska, *J. Catal.*, 1988, **110**, 23.
- 17 K. V. R. Chary, K. Rajender Reddy and Ch. Praveen Kumar, *Catal. Commun.*, 2001, **2**, 277.
- 18 E. I. Ko and J. G. Weissman, *Catal. Today*, 1990, **8**, 27.
- 19 A. Lopez Agudo, F. J. Gil-Ilambias, P. Reyes and J. L. G. Fierro, *Appl. Catal.*, 1981, **1**, 59.
- 20 B. M. Reddy, K. S. P. Rao and V. M. Mastikhin, *J. Catal.*, 1988, **115**, 556.
- 21 L. Rodrigo, K. Marcinkowska, A. Andot, P. C. Roberge, S. Kaliaguine, J. M. Stencel, L. E. Makowsky and J. R. Deihl, *J. Phys. Chem.*, 1986, **90**, 2690.
- 22 L. A. Gambaro and J. L. G. Fierro, *React. Kinet. Catal. Lett.*, 1981, **18**, 495.
- 23 W. K. Hall and W. S. Millman, *J. Catal.*, 1979, **59**, 311.
- 24 W. K. Hall and J. Vallyon, *J. Catal.*, 1983, **84**, 229.
- 25 S. R. Seyedmonir and R. F. Howe, *J. Catal.*, 1988, **110**, 216.



# Synthesis of 3-nitrophthalic acid by oxidation of 1-nitronaphthalene using $\gamma$ -alumina supported ceria(IV) as a catalyst

Taduri Rajiah,<sup>a</sup> Komandur V. R. Chary,<sup>\*a</sup> Kamaraju Sita Rama Rao,<sup>a</sup> Ramiseti Nageswara Rao<sup>b</sup> and Rajendra Prasad<sup>c</sup>

<sup>a</sup> Catalysis & Physical Chemistry Division, Institute of Chemical Sciences, Hyderabad-500007, India. E-mail: Kvrchary@iict.ap.nic.in

<sup>b</sup> Analytical Chemistry Division, Institute of Chemical Sciences, Hyderabad-500007, India

<sup>c</sup> Institute of Chemical Sciences, Devi Ahilya ViswaVidyalay, Takshasila Campus, Khandwa Road, Indore-452 001, India

Received 19th November 2001

First published as an Advance Article on the web 3rd April 2002

The synthesis of 3-nitrophthalic acid has been achieved by catalytic oxidation of 1-nitronaphthalene using  $\gamma$ -alumina supported ceria(IV) as a catalyst at 363 K in 80 mol% yield with 98% selectivity.

Oxidation of alkyl benzenes is one of the most important reactions for synthesis of fine chemicals.<sup>1,2</sup> There are several examples of oxidation of aromatic compounds in the literature including hypervalent chromium, manganese, vanadium and ruthenium mediated oxidations.<sup>3,4</sup> However these stoichiometric oxidants possess serious disadvantages in that they are expensive and/or toxic and produce equimolar amounts of deoxygenated wastes, which often makes isolation of the products difficult. Furthermore, inevitable by-products represent environmental pressures demanding the use of inexpensive oxidants, preferably under catalytic and energy saving conditions. Supported vanadium oxides have been extensively employed for the oxidation of naphthalene.<sup>5</sup>

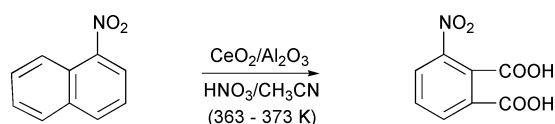
In recent years, the use of CeO<sub>2</sub>-based materials as heterogeneous catalysts has shown a rapid increase because of their ability to release and store oxygen.<sup>6</sup> The addition of ceria to a support such as  $\gamma$ -alumina and other transition metals such as Pt, Pd and Rh has been shown to enhance the effectiveness of its catalytic properties in the oxidation of CO and hydrocarbons.<sup>7</sup> In the exhaust gas treatment from automobiles, CeO<sub>2</sub> was found to be an active ingredient in the so-called three-way catalyst reported for the oxidation of isobutene.<sup>8</sup> However, a thorough search of literature has revealed that ceria has not so far been studied as a selective catalyst for the oxidation of naphthalene and its derivatives.

In recent years, there has been a great interest in the synthesis of aromatic dicarboxylic acids as versatile raw materials for high performance polymers and liquid crystalline materials.<sup>8</sup> 3-Nitrophthalic acid is one of the important dicarboxylic acid intermediates and is produced in industry by two different methods.<sup>9</sup> In the first, naphthalene is nitrated and the nitronaphthalene is oxidized to nitrophthalic acid, while in the second case phthalic acid is nitrated with fuming nitric acid in the presence of sulfuric acid at 373 K. These methods have several disadvantages such as poor yields as well as long and tedious processes. Therefore, there is a need for the development of mild and efficient processes for the synthesis of 3-nitrophthalic acid using environmental friendly technologies. Recently an improved process based on the liquid-phase oxidation of 1-nitronaphthalene in an acidic aqueous solution containing Ce(IV), Mn(II) or Co(III) was reported for synthesis of 3-nitrophthalic acid under mild experimental conditions.<sup>10</sup> However, it involves not only the treatment of huge quantities

of waste-water containing heavy metals as environmental pollutants but also electrolytic oxidation to regenerate the catalyst for recycling. In this paper we report a simple and efficient method for the synthesis of 3-nitrophthalic acid by the solid-phase oxidation of 1-nitronaphthalene in an acidic-aqueous solution employing  $\gamma$ -alumina supported ceria(IV) as a catalyst.

$\gamma$ -Al<sub>2</sub>O<sub>3</sub> (2 mm spheres, crushed and sieved to 18–25 BSS mesh obtained from M/S. ACC, India) having a BET surface area of 168 m<sup>2</sup> g<sup>-1</sup> was used as a support material. After calcination in air for 4 h at 773 K the support was impregnated with a requisite amount of (NH<sub>4</sub>)<sub>2</sub>[Ce(NO<sub>3</sub>)<sub>6</sub>] in aqueous solution with constant stirring for 2 h followed by drying/evaporating the excess water on a water bath. The dried catalyst was calcined in air at 723 K for 3 h to obtain the CeO<sub>2</sub>/ $\gamma$ -Al<sub>2</sub>O<sub>3</sub> catalyst. The BET surface areas of CeO<sub>2</sub> and CeO<sub>2</sub>/Al<sub>2</sub>O<sub>3</sub> were found to be 22.5 and 138 m<sup>2</sup> g<sup>-1</sup>, respectively.

In a typical procedure (Scheme 1), 1-nitronaphthalene (0.04 mol) dissolved in acetonitrile (5 ml) and dilute nitric acid (0.16 mol) were mixed well and 1 g of 5% CeO<sub>2</sub>/ $\gamma$ -Al<sub>2</sub>O<sub>3</sub> was added and the mixture stirred for 1 h at 363–373 K. After the reaction, the reaction mixture was cooled to room temperature and filtered. The filtrate was neutralized with Na<sub>2</sub>CO<sub>3</sub>/NaOH and



Scheme 1

## Green Context

Selective oxidation is one of the most challenging areas of chemistry, with a wide range of target processes. This paper describes the development of a supported ceria catalyst for the selective oxidation of a naphthalene to a phthalic acid derivative. High yields and excellent selectivity are found under very mild conditions with nitric acid as primary oxidant. The catalyst performs favourably compared to current processes.

DJM

**Table 1** Catalytic effect of CeO<sub>2</sub>/γ-Al<sub>2</sub>O<sub>3</sub> for production of 3-nitrophthalic acid from 1-nitronaphthalene

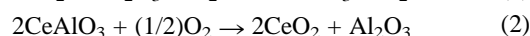
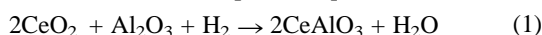
Catalyst	Type	Yield of 3-nitrophthalic acid (mol%)	Selectivity to 3-nitrophthalic acid (%)
CeO <sub>2</sub>	Heterogeneous (unsupported)	20.6	50
Ammonium ceric nitrate	Homogeneous	34.2	60
5% CeO <sub>2</sub> /γ-Al <sub>2</sub> O <sub>3</sub>	Heterogeneous	60.3	98

Conditions: 5% CeO<sub>2</sub>/γ-Al<sub>2</sub>O<sub>3</sub> (0.5 g), 30 ml acetonitrile, nitric acid and water, 2 g 1-nitronaphthalene, 363 K, 0.5 h.

washed with ethyl acetate and adjusted to a pH of 2.0 with HCl prior to extraction of the product with methanol. Product analysis in the reaction mixture prior to extraction was made by high performance liquid chromatography (HPLC) and analysis showed the purity of the product to be 95–98%. The main product was isolated from methanol by evaporation under reduced pressure and confirmed to be 3-nitrophthalic acid by comparison with an authentic sample (HPLC, IR, MS, <sup>1</sup>H NMR). The yield and selectivity of 3-nitrophthalic acid were calculated on the basis of the starting amount of 1-nitronaphthalene and the total amount of the product formed, respectively.

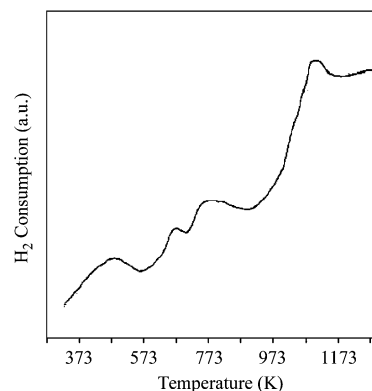
Table 1 exhibits the catalytic effect of CeO<sub>2</sub> for selective oxidation of 1-nitronaphthalene to 3-nitrophthalic acid under different conditions. The liquid-phase oxidation using ammonium ceric nitrate yielded 34 mol% of 3-nitrophthalic acid while with CeO<sub>2</sub> as a solid-phase catalyst the yield was found to be around 20 mol%. In the presence of CeO<sub>2</sub>/γ-Al<sub>2</sub>O<sub>3</sub> the yield of 3-nitrophthalic acid is 60 mol% with a selectivity of 98%. In the absence of CeO<sub>2</sub>, however the reaction does not proceed at all. These results indicate that the use of CeO<sub>2</sub> on a support of γ-Al<sub>2</sub>O<sub>3</sub> significantly enhanced not only the yield but also the selectivity of 3-nitrophthalic acid.

The yield of 3-nitrophthalic acid on CeO<sub>2</sub>/γ-Al<sub>2</sub>O<sub>3</sub> catalyst is nearly three times than that on bulk CeO<sub>2</sub> catalyst. The higher activity on this catalyst can be attributed to the presence of CeO<sub>2</sub> in higher dispersion state over γ-Al<sub>2</sub>O<sub>3</sub>. In other words, the number of active CeO<sub>2</sub> species responsible for the oxidation of 1-nitronaphthalene are higher in CeO<sub>2</sub>/γ-Al<sub>2</sub>O<sub>3</sub> catalyst than in the bulk CeO<sub>2</sub> catalyst. The active CeO<sub>2</sub> sites, which are reducible, are often called coordinatively unsaturated sites (CUS) of CeO<sub>2</sub>. These CUS of CeO<sub>2</sub> species can be titrated back with oxygen at low temperatures *via* a low temperature oxygen chemisorption (LTOC) technique. In CeO<sub>2</sub>/Al<sub>2</sub>O<sub>3</sub> catalysts, Miki *et al* have reported that 0.5 mol O<sub>2</sub> is sufficient to titrate 2 mol of reducible CeO<sub>2</sub> surface species [eqns. (1) and (2)].<sup>11</sup>



From the LTOC experiments, we found that each mole of CeO<sub>2</sub> in CeO<sub>2</sub>/Al<sub>2</sub>O<sub>3</sub> catalyst occupies  $142.3 \times 10^{-4}$  m<sup>2</sup>, whereas each mole of CeO<sub>2</sub> in bulk CeO<sub>2</sub> occupies  $5.6 \times 10^{-4}$  m<sup>2</sup>. Thus it is clear that the active surface area of CeO<sub>2</sub> in CeO<sub>2</sub>/Al<sub>2</sub>O<sub>3</sub> catalyst is ~25 times greater than that of bulk CeO<sub>2</sub>. From the active CeO<sub>x</sub> species titratable with O<sub>2</sub> (101.2 μmol of CeO<sub>x</sub>/g catalyst). It appears that approximately three overlayers of CeO<sub>x</sub> might have formed on the surface of Al<sub>2</sub>O<sub>3</sub>. Thus the high productivity of 3-nitrophthalic acid over CeO<sub>2</sub>/Al<sub>2</sub>O<sub>3</sub> catalyst can be attributed to the high active CeO<sub>2</sub> area of this catalyst.

In order to determine the reducible species present in the 5% CeO<sub>2</sub>/Al<sub>2</sub>O<sub>3</sub> catalyst, the catalyst sample has been characterized by temperature programmed reduction (TPR) using 5% H<sub>2</sub>/Ar flow with a temperature ramp of 10 K min<sup>-1</sup> from ambient to 1073 K. The TPR pattern (Fig. 1) indicates the presence of reducible species in five-temperature regions *viz.*, at *T*<sub>max</sub> of 473, 673, 773, 973 (as a shoulder) and at 1073 K. The low temperature signal is probably due to the reduction of adsorbed O<sub>2</sub> on Al<sub>2</sub>O<sub>3</sub>. The signals at 673 and 773 K may be due to the

**Fig. 1** Temperature-programmed reduction profile for 5 wt% CeO<sub>2</sub>/Al<sub>2</sub>O<sub>3</sub>**Table 2** Effect of the amount of 5% CeO<sub>2</sub>/γ-Al<sub>2</sub>O<sub>3</sub> on the yield and selectivity of 3-nitrophthalic acid

Amount of catalyst/g	Reaction time/h	Yield of 3-nitrophthalic acid (mol%)	Selectivity to 3-nitrophthalic acid (%)
0.50	1.0	54.2	97
0.75	1.0	86.3	98
1.00	0.5	75.9	96
1.00	1.0	85.4	98

reduction of surface O<sub>2</sub> associated with CeAlO<sub>3</sub>. Partial reduction of CeAlO<sub>3</sub> species to form non-stoichiometric CeO<sub>x</sub> (x is in the range 1.7–1.9) might have taken place at 973 K. The high temperature peak can be attributed to the formation of Ce<sub>2</sub>O<sub>3</sub>. These results are in agreement with the literature.<sup>12</sup> Table 2 shows the dependence of the yield of 3-nitrophthalic acid on the initial mole ratio of CeO<sub>2</sub>/γ-Al<sub>2</sub>O<sub>3</sub> catalyst to 1-nitronaphthalene. The yield increases with increasing amounts of CeO<sub>2</sub>/γ-Al<sub>2</sub>O<sub>3</sub> and has a maximal value (80 mol% with 100% selectivity) at a mol ratio 0.7.

In conclusion, selective oxidation has been achieved by the one-step reaction of 1-nitronaphthalene with 5% CeO<sub>2</sub>/γ-Al<sub>2</sub>O<sub>3</sub> catalyst in acetonitrile in presence of aqueous acid at 363 K producing 3-nitrophthalic acid in 80 mol% yield with 98% selectivity.

## References

- (a) R. C. Larock, *Comprehensive Organic Transformations*, VCH, New York, 1989, pp. 604 and 834; (b) M. Hudlicky, *Oxidation in Organic Chemistry*, ACS Monograph Ser. 186, American Chemical Society, Washington D.C., 1990, p. 114; (c) A. R. Karritzky, O. Mesh-Cihn, C. W. Rees, G. Pattenden and C. J. Moody, *Comprehensive Organic Functional group Transformations*, Elsevier Science, Oxford, vol. 3 and 5.
- (a) G. Franz and R. A. Sheldon, *Ullmann's Encyclopedia of Industrial Chemistry*, ed. B. Elvess, S. Hawkins and G. Schulz, VCH, Weinheim, 5th edn., 1991, vol. A18, p. 261; (b) *Kirk-Othmer Encyclopedia of Chemical Technology*, ed. J. L. Kroschwitz and M. Howe-Grant, Wiley, New York, 4th edn., 1991.



- 3 (a) I. F. Feisser and M. Fiesser, in *Reagents for Organic Synthesis*, Wiley, New York, 1967, vol. 1, pp. 142, 1059; (b) G. Cianelli and C. Cardillo, *Chromium Oxidations in Organic Chemistry*, Springer Verlag, New York, 1948, p. 118.
- 4 (a) E. J. Corey and J. W. Suggs, *Tetrahedron Lett.*, 1975, 2647; (b) G. Piancatelli, A. Scettri and M. D. Auria, *Synthesis*, 1982, 542; S. Chandrashekhar, M. Jakhi and S. Mohapatra, *Synth. Commun.*, 1996, **26**, 3a; (c) B. Ozgun and N. Degirmenbas, *Synth. Commun.*, 1996, **26**, 3601; (d) E. J. Corey and D. L. Boger, *Tetrahedron Lett.*, 1978, 2461; (e) E. J. Corey and S. Schmidt, *Tetrahedron Lett.*, 1979, 309; (f) F. S. Catritic and F. A. Luzzia, *Synthesis*, 1980, 691; (g) M. N. Bhattacharjee and M. K. Chaudhari, *Synthesis*, 1982, 588; (h) K. Balasubramaniam and V. Pratibha, *J. Chem.*, 1986, 326.
- 5 (a) D. J. Hucknall, *Selective Oxidation of Hydrocarbons*, Academic Press, 1974; (b) *Ullman's Encklopaedie der Technischem Chemie*, Verlag Chemie, Weinheim, 4th edn., 1979, vol. 17, p. 483.
- 6 (a) T. X. T. Sayle, S. C. Parker and C. R. A. Catlow, *J. Chem. Soc., Chem. Commun.*, 1992, 977; (b) A. Naydenov, R. Stoyanova and D. Mahand Jiev, *J. Mol. Catal.*, 1995, **98**, 9; (c) F. Zamar, A. Trovarelli, C-de Leitenvurg and G. Dalcetti, *J. Chem. Soc., Chem. Commun.*, 1995, 965; (d) S. Murata, K. Aika and J. Onishi, *Chem. Lett.*, 1990, 1067; (e) G. Wrobel, M. P. Sohler, A. D. Huysser, J. P. Bonnelle and J. P. Mazcq, *Appl. Catal. A*, 1993, **101**, 73.
- 7 (a) H. C. Yao and Y. Yu. Yao, *J. Catal.*, 1984, **86**, 254; (b) G. Sandez and J. L. Gazquez, *J. Catal.*, 1987, **104**, 120.
- 8 (a) C. De Leifenburg, A. Trovarelli, J. Llorca, F. Cavari and G. Bini, *Appl. Catal. A*, 1996, **139**, 161; (b) J. G. Nunan, H. J. Robota, M. J. Cohn and S. A. Bradly, *J. Catal.*, 1992, **133**, 309.
- 9 (a) H. Hirai, *Polym Adv. Technol.*, 1997, **8**, 666; (b) Y. Shivaishi, S. Tashira and N. Toshima, *Chem. Lett.*, 2000, 828.
- 10 (a) Miller, *Ann.*, 1881, **208**, 223; (b) Matheus, *J. Chem. Soc.*, 1914, **105**, 2476.
- 11 T. Miki, T. Ogawa, A. Ueno, S. Matsura and M. Sato, *Chem. Lett.*, 1998, 565.
- 12 J. Z. Shyu, W. H. Weber and H. S. Gandhi, *J. Phys. Chem.*, 1988, **92**, 4964.



# Environmentally friendly laboratory-scale remediation of PAH-contaminated soil by using pressurized hot water extraction coupled with pressurized hot water oxidation

Juhani Kronholm, Benjamin Desbands, Kari Hartonen\* and Marja-Liisa Riekkola\*

Laboratory of Analytical Chemistry, Department of Chemistry, PO Box 55, FIN-00014 University of Helsinki, Finland. E-mail: marja-liisa.riekkola@helsinki.fi

Received 22nd January 2002

First published as an Advance Article on the web 15th April 2002

Water is an alternative solvent and reaction medium to many conventional organic solvents. In pressurized hot water extraction (PHWE) and pressurized hot water oxidation (PHWO) the altered physico-chemical properties of heated and pressurized water are exploited for the treatment of wastes in solid and liquid states. On-line coupled PHWE and PHWO equipment was used to extract polyaromatic hydrocarbons (PAHs) from a soil sample and then to destruct them with potassium persulfate as oxidant. In PHWE experiments, study was made of the effects of flow direction and flow rate in the extraction vessel on the recovery of PAHs. Compared with Soxhlet extraction, PHWE gave better recoveries overall. In PHWE–PHWO, temperature, flow rate (reaction time) and oxidant concentration affected the conversion of the PAHs. It was important that temperature was high enough and reaction time long enough for effective oxidation. These parameters had thus to be chosen carefully for optimal results. Under optimized conditions almost 100% PAH conversions were obtained, and also a clear reduction in total organic carbon content of the effluent was evident. However, some organics remained in the effluent after the procedure, and a considerable amount of sulfate was released in water. Further treatment of the effluent is thus required as a final step.

## Introduction

Polyaromatic hydrocarbons (PAHs) have long time been a cause of concern because of their impact on human health and the environment. Some of these compounds, for example, benzo[*a*]anthracene, chrysene, dibenzo[*a,h*]anthracene, and benzo[*a*]pyrene, are highly toxic, carcinogenic and mutagenic.<sup>1,2</sup> The major sources of PAHs are combustion processes, particularly industrial processes, domestic heating, and traffic. Public concern about PAH residues in the environment has spurred the development of techniques for the treatment of polluted sites.

Pressurized hot water (PHW) is referred to as supercritical water (SCW) when temperature and pressure exceed the critical temperature and pressure of water ( $T_c = 374\text{ °C}$ ,  $P_c = 221\text{ bar}$ ). In the supercritical state, the density and solvent properties of water are closer to liquid than gas. Relative to its properties in liquid state, diffusivity is increased, while viscosity, hydrogen bonding between water molecules, and the dielectric constant are decreased.<sup>3–7</sup> For example, at 500 °C and 230 bar the dielectric constant is about 1.5, whereas at room temperature the value is close to 80. In extraction, the key parameter in interpreting solvent–solute interactions is the dielectric constant and this can be related to polarity. A high dielectric constant favors the solubility of high polarity compounds and a lower dielectric constant the solubility of low polarity compounds such as PAHs.<sup>8</sup> In the supercritical state, and to some extent under milder conditions, gases and organic compounds of low polarity are soluble in water, while inorganic compounds such as salts are insoluble.<sup>9–12</sup>

Water can be described as a ‘green’ solvent, because it is nontoxic, nonflammable and it poses no threat to the environment. It is also readily available and cheap. Technically, water is attractive because its properties change dramatically with temperature and pressure. Pressurized water at elevated temperature can be used in place of organic solvents and additives in both extraction and oxidation.

Pressurized hot water extraction (PHWE) can be successfully used in the treatment of contaminated soil and sediments. Both liquid water and steam ( $T = 200\text{–}300\text{ °C}$ ) have been applied in the extraction of organic compounds, including PAHs, polychlorinated biphenyls (PCBs), polychlorinated dibenzofurans (PCDFs), naphthalenes, and alkanes from solid sample matrices.<sup>13–16</sup> Good extraction efficiencies can be obtained at temperatures lower than the critical temperature of water, which is important in terms of cost. Also other extraction processes—for example, accelerated solvent extraction (ASE) and supercritical fluid extraction (SFE)—have been developed to reduce the amounts of organic solvents now being used. Supercritical carbon dioxide can be used in environmentally friendly SFE processes, but its polarity is low and organic modifier often must be added when analytes of a more polar nature are to be extracted.<sup>17</sup>

Supercritical water oxidation (SCWO) is an efficient technique for the treatment of wastewaters and sludges.<sup>18,19</sup> A considerable disadvantage, however, are the high temperatures needed in the process. It is economically favorable if the oxidation process can be carried out effectively under mild conditions. Wet air oxidation processes, the most familiar PHWO processes, typically rely on temperatures of 120–300 °C and pressures of 1–10 MPa.<sup>20</sup> Below the critical temperature of

## Green Context

The use of high temperature water for the extraction of organics from various matrices is an attractive option due to water being safe, cheap and a good solvent for organics at elevated temperatures. This paper couples the efficient extraction of polyaromatic hydrocarbons from soil using high temperature water with an improved total oxidation method, which forms an effective method for the decontamination of soils.

DJM

water, catalysts are often added to enhance oxidation by lowering the activation energy of the reaction. Transition metals have been found effective in the treatment of wastewaters, for example.<sup>21–23</sup> Water is highly corrosive at high temperatures and pressures, especially with some oxidant added, and materials incorporated in the equipment need to be resistant to corrosion. In this respect, Inconel 600 and 625 and Hastelloy 276 are better choices of material than ordinary stainless steel.<sup>24, 25</sup>

Oxygen and hydrogen peroxide are the most widely used oxidants in SCWO and PHWO. Although the efficiency of potassium persulfate has been demonstrated, it has rarely been used as oxidant in continuous flow type oxidation processes. It is nevertheless an attractive choice as oxidant because it is inexpensive and easy and safe to handle and the reaction is free of serious interferences. In earlier work<sup>26,27</sup> we oxidized phenolic compounds efficiently with potassium persulfate in a continuous flow reactor at temperatures clearly below the critical temperature of water. The oxidant starts to react effectively at about 100 °C, forming sulfate radicals, which react with organic compounds in a complex radical chain mechanism.<sup>28,29</sup> It needs to be added that some studies in this area have shown that persulfate oxidation of soil organic matter and dissolved organic matter is incomplete.<sup>30,31</sup> Related to this, it has been demonstrated that persulfate selectively oxidizes PAHs that are bioavailable in soils and sediments.<sup>32,33</sup> Poorly bioavailable PAHs, which are mainly sorbed to condensed organic matter, are desorbed slowly, whereas readily available PAHs, which are mainly sorbed to expanded organic matter, are desorbed rapidly.

There are only a few publications in the literature describing on-line coupled PHWE–PHWO and PHWE–SCWO processes. Misch *et al.*<sup>34</sup> coupled PHWE with electrochemical oxidation in supercritical water. Recently we applied PHWE–SCWO processes to the oxidation of PAHs with hydrogen peroxide as oxidant.<sup>35,36</sup> Good extraction and oxidation efficiencies were obtained in these studies, which encouraged us to continue experiments with potassium persulfate as oxidant. The primary aim of the present work was to apply on-line coupled PHWE–PHWO in the treatment of PAH-polluted soil with potassium persulfate as oxidant. A wide range of temperatures below the critical temperature of water was tested to determine the feasibility of using potassium persulfate.

## Materials and methods

### Solid matrix

Air-dried and homogenized soil (from the decommissioned coal gasification plant at Husarviken, Stockholm, Sweden) was employed as the solid sample. The soil was kindly supplied by Dr Bert van Bavel (Umeå University, Sweden). Table 1 gives the reference values for the PAHs in the soil (only one measurement for each compound), obtained at Umeå University by accelerated solvent extraction (ASE) and HRGC–LRMS analysis.

### Reagents

Distilled deionized water was used as solvent for extraction and potassium persulfate (E. Merck AG, Darmstadt, Germany, 98%) as oxidant with working concentration from 21.1 to 52.8 g l<sup>-1</sup>. 4,4'-Dibromooctafluorobiphenyl (Aldrich, Gillingham, UK, 99%) was employed as an internal standard (*c* = 2.0 mg ml<sup>-1</sup> in isoctane). Liquid–liquid extraction of the collected samples (effluent) was carried out with dichloromethane (Lab-Scan, Analytical Sciences, Dublin, Ireland, HPLC grade). A PAH standard mixture of 17 compounds (Z-014G-R, Accu-Standard, Inc., CT, USA, *c* = 2.0 mg ml<sup>-1</sup> in CH<sub>2</sub>Cl<sub>2</sub>/benzene 1:1, v:v) was used for identification and quantitation of the PAHs (Table 1). Soxhlet extraction was performed with toluene (Lab-Scan, Analytical Sciences, Dublin, Ireland, HPLC grade) as solvent.

### PHWE–PHWO Equipment

The equipment used in the studies is described in Fig. 1. Tubes (1/8 in. o.d., 1.5 mm i.d.) in the ovens (oven 1 for extraction: Carlo Erba Fractovap Mod. G1, Milan, Italy; oven 2 for oxidation: Carlo Erba Series 2350, Milan, Italy) and between them were made of Inconel 600 (Nickel alloy, Ni >72%, Cr 15.5%). The volume of the preheating tube in the oven 1 was 1.8 ml (*l* = 1.0 m) and that of the reaction tube for oxidation (in oven 2) was 16.3 ml (*l* = 9.2 m). The volume of the tube in oven 2 for temperature equilibrium before entering the T junction

**Table 1** Ions used for quantitation and identification of the PAHs, detection limits obtained with a PAH standard solution, and the amounts of the PAHs determined by ASE (for calculation of oxidant consumption)

No.	Compound	Quantitation ion ( <i>m/z</i> )	Qualifier ion ( <i>m/z</i> )	Detection limit/ng (S/N = 3)	Amount (µg g <sup>-1</sup> ) analyzed by ASE <sup>a</sup>
1	Naphthalene	128	102	0.85	6.5
2	Acenaphthylene	152	76	1.61	23
3	Acenaphthene	153	152	0.95	1.6
4	Fluorene	166	165	0.80	23
5 <sup>b</sup>	Phenanthrene	178	76	1.44	180
5 <sup>b</sup>	Anthracene	178	76	1.17	43
6	Fluoranthene	202	101	0.79	292
7	Pyrene	202	101	0.40	222
8 <sup>b</sup>	Benzo( <i>a</i> )anthracene	228	114	0.65	174
8 <sup>b</sup>	Chrysene	228	113	0.64	116
9 <sup>b</sup>	Benzo( <i>b</i> )fluoranthene	252	126	0.72	112
9 <sup>b</sup>	Benzo( <i>k</i> )fluoranthene	252	126	0.76	96
10	Benzo( <i>a</i> )pyrene	252	126	0.81	178
11	Indeno-1,2,3( <i>c,d</i> )-pyrene	276	138	1.70	88
12	Benzo( <i>g,h,i</i> )perylene	276	138	1.32	65

<sup>a</sup> Quantitative analysis of the PAHs in soil carried out at the University of Umeå (Sweden). Sample pre-treatment: homogenization and air-drying. ASE with hexane/acetone (1:1, v/v) at 150 °C and 14 MPa. Evaporation, clean-up through a silica column, elution with 25 ml hexane and 25 ml hexane/dichloromethane (3:2, v/v). Evaporation, and change of the solvent to toluene. Analysis: HRGC–LRMS (Fisons GC 8000/Fisons MD 800). <sup>b</sup> Compounds **5**, **8** and **9** were analyzed as one peak due to poor chromatographic resolution in the analysis of the soil sample

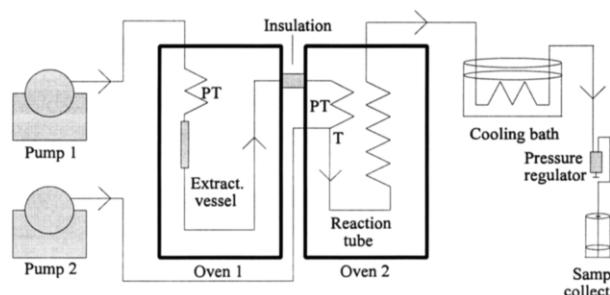


**Fig. 1** PHWE–SCWO equipment used in the study. The reaction tube was flushed from the T junction on except in the experiments for TOC. PT refers to preheating tube.

was 3.5 ml ( $l = 2.0$  m). The tube connecting the ovens was insulated. The oxidant was not preheated.

One high-pressure pump (pump 1: Jasco PU-980 HPLC pump, Tokyo, Japan) was employed to deliver water into the extraction vessel in oven 1. Two types of vessel (Fig. 2) were used (vessel 1:  $V = 2.2$  ml,  $100 \times 4.6$  mm i.d., Keystone Scientific, Inc., Bellefonte, PA, USA; vessel 2,  $V = 2.8$  ml,  $37 \times 10$  mm i.d., laboratory constructed, made of stainless steel). A second pump (pump 2: Jasco PU-1580 HPLC pump, Tokyo, Japan) was employed to deliver oxidant at the T junction in oven 2. An ice bath was used to cool the stream before it entered the pressure regulator (stainless steel, micrometering valve, Jasco). The capillary (1/16 in. o.d., 0.5 mm i.d.) leading from the pressure regulator to sample collection was made of ordinary stainless steel.

## Procedure

Four experiments were carried out under similar conditions. 0.5 g contaminated soil and  $\sim 2.5$  g (type 1 vessel) or  $\sim 3.0$  g (type 2 vessel) sea sand were weighed into the extraction vessel (see Fig. 2). PHWE procedures without a PHWO period were carried out to determine the effects of flow direction and flow velocity and the geometry (diameter) of the extraction vessel on the recoveries of the PAHs. The water flowing into the extraction vessel first entered the PAH contaminated area and only after this the sea sand area.

In PHWE–PHWO experiments, oven 2 was first heated to the selected temperature (100–360 °C) and the oxidant flow (pump 2:  $v = 1.0$  or  $4.0$  ml  $\text{min}^{-1}$ ) was started before pump 1 was launched to deliver water ( $v = 1.0$  ml  $\text{min}^{-1}$ ) to the extraction chamber. After this the temperature in oven 1 was adjusted to 300 °C for the extraction. In the PHWE procedures (without PHWO), water instead of oxidant was pumped (pump 2) to the T junction at 300 °C. The nominal extraction time was 20 min.

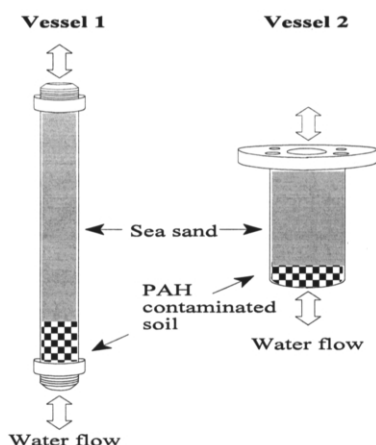


**Fig. 2** Extraction vessels and flow types used in the study.

The total time for the entire extraction was 18 min longer at 300 °C than the nominal extraction time at isothermal conditions, because it took time to heat oven 1 to the selected temperature. The concentration of potassium persulfate noted in the text and tables is the concentration of the oxidant in the pump, not the concentration in the reaction tube after mixing at the T junction.

The density and volume values under various conditions for the calculation of the reaction times in the oxidation tube were calculated by the NIST/ASME Steam Properties program (Formulation for General and Scientific Use, Standard Reference Database 10 Version 2.01., USA).

For sample collection for GC–MS analysis, the exit capillary was inserted in dichloromethane ( $V = 20$  ml) in a bottle. After every PHWE and PHWE–PHWO procedure the tube from the T junction to the sample collection was flushed with  $\sim 40$  ml of dichloromethane and the internal standard ( $V = 50$   $\mu\text{l}$ ) was added to the sample. The separated water sample was extracted with dichloromethane ( $4 \times 10.0$  ml), and the organic fractions were combined and concentrated to about 1.5 ml with gentle nitrogen evaporation for GC–MS analysis.

For comparison of the recoveries of PAHs, 20 h Soxhlet extraction (toluene as solvent) was applied for the soil sample. After the Soxhlet extraction, the internal standard ( $V = 50$   $\mu\text{l}$ ) was added and the sample was concentrated by rotavapor to about 10 ml; the final concentration step to about 1.5 ml for GC–MS analysis was carried out by gentle nitrogen evaporation.

## GC–MS Analysis

Compounds in the effluent were investigated with a Hewlett–Packard model 5890 gas chromatograph and a model 5989A quadrupole mass spectrometer (USA). All MS analyses were carried out in SCAN mode (50–500 amu) with electron impact ionization (EI, 70 V). The temperature of the GC–MS interface was 300 °C, that of the ion source 250 °C, and that of the analyzer 120 °C. Samples were injected ( $V_{\text{inj}} = 2.0$   $\mu\text{l}$ ) in on-column mode with a Hewlett–Packard 7636 autosampler. The analytical column was a 25.0-m HP-5 (Hewlett Packard, USA) of 0.2 mm i.d. and 0.11  $\mu\text{m}$  film thickness. A 2.0–3.0 m retention gap (BGB Analytik AG, Rothenfluh, Switzerland) of 0.53 mm i.d. with DPTMDS (1,2-diphenyl-1,1,3,3-tetramethyl-disilazane) deactivation was connected to the analytical column with a press-fit connector (BGB Analytik AG, Rothenfluh, Switzerland). The temperature program of the GC oven was 30 °C (2 min), heating 10 °C  $\text{min}^{-1}$ , 300 °C (10 min).

The ions used in quantification and identification of PAHs are presented in Table 1. Ions at  $m/z$  456 and 296 were selected for the internal standard, for quantitation and identification, respectively. Calibration was generated from the GC–MS runs of dilution series of the PAH standard solution. The software used in the computer connected to the GC–MS was a Hewlett–Packard ChemStation (G1034C version C 03.00). The software included a mass spectra library (Wiley) which was used in identifying the organic compounds. A library match  $>95$  (100 is the maximum) was considered as the minimum requirement for a positive identification. Other organics than PAHs were not fully quantified; only the ratios of the peak areas of the organics to the peak area of the internal standard were calculated. The concentration of the internal standard in the vial was about 67  $\mu\text{g ml}^{-1}$ .

## TOC Analysis

TOC analysis was carried out independently of the GC–MS studies. Four effluent samples were collected under each set of conditions. The tube leading on from the T junction was not flushed with dichloromethane because, with solvent added, the



analysis would have given erratic results. A Shimadzu TOC-5000 analyzer (USA) was employed to measure total organic carbon in the sample. Standard method SFS-EN 1484 was employed in the analysis. The samples were kept in an ultrasonic bath for *ca.* 10 min before the TOC analysis.

## Results and discussion

### PHWE Experiments

Destruction of PAHs in high-temperature ovens during PHWE was assumed to be negligible, though this is theoretically possible and could lead to losses in recovery. The geometry (diameter) of the extraction vessel (see Fig. 2) had a significant effect on the recoveries of the PAHs (Figs. 3 and 4). The vessel of smaller diameter (vessel 1,  $d = 4.6$  mm) gave better recoveries than the vessel of larger diameter (vessel 2,  $d = 10$  mm) probably because compounds near the walls were extracted more effectively in vessel 1 than vessel 2. Probably, too, the matrix was unable to move with the flow as easily in vessel 1 as in the vessel 2 and the extraction efficiency was thus enhanced. The sample matrix can also be considered as a stationary phase in a chromatographic column with internal diameter and length affecting the separation process.

In experiments with similar types of extraction vessels but with use of water in steam phase instead of liquid, Andersson *et al.*<sup>37</sup> did not observe marked differences in recoveries of PAHs due to the vessels. Evidently, in the steam phase, water is well distributed through the sample, whereas in the liquid phase it moves along channels and its ability to remove PAHs from the outer layers of the sand is decreased. Andersson *et al.* also

mixed the sample with the sand instead of applying different layers as we did, and this may have affected the recovery.

In the tests of the effect of flow direction (Figs. 3 and 4) recoveries were much better when flow came from the top of the vessel than from the bottom. Depending on the flow direction, there may be differences in the degree of flow channel formation inside the sample, affecting the recovery of the PAHs.

Two flow velocities were tested with extraction vessel 2 (Fig. 3). Recoveries of the PAHs were higher when the flow velocity was increased from 1.0 to 2.0 ml min<sup>-1</sup> (flow coming from the bottom). This shows that the extraction was solubility limited. Recoveries were higher still, however, with extraction vessel 1 and flow of 1.0 ml min<sup>-1</sup> from the bottom and highest of all with extraction vessel 1 and flow of 1.0 ml min<sup>-1</sup> from the top. Experiments with flow velocity of 2.0 ml min<sup>-1</sup> were not easy to carry out technically because of problems in adjusting the pressure and only one experiment with this was performed. Hawthorne *et al.*<sup>38</sup> also observed increase in the recovery of PAHs with increased flow velocity of water (0.1–1.1 ml min<sup>-1</sup>).

Compared with Soxhlet extraction and ASE, PHWE gave better overall recoveries for the PAHs, even for PAHs of high molecular mass (Fig. 4). About three times as high recovery of low molecular mass acenaphthylene was obtained with PHWE as with Soxhlet extraction. However, some of the variation in the recoveries of the PAHs, especially PAHs of low molecular mass, may be due to high volatility of the compounds.<sup>39</sup> We also note that only one experiment was carried out with ASE and it was not possible to estimate the repeatability of the method. In a comparison of PHWE, PLE (pressurized liquid extraction, similar to ASE), and Soxhlet extraction techniques, Hawthorne *et al.*<sup>40</sup> observed that the mean recoveries of PAHs of low and medium molecular mass were generally better with PHWE than with Soxhlet extraction, but the recoveries of PAHs of high molecular mass were closely similar or even better with Soxhlet extraction. Our Soxhlet extracts were much darker (color dark brown/black) and more turbid than PHW extracts (color orange). The same was observed by Hawthorne *et al.*<sup>40</sup>

Vessel 2 was selected for the PHWE–PHWO experiments because often there were leaks with vessel 1. Leaks were mainly due to old and worn parts that were difficult to tighten. Flow direction from top to bottom was chosen for the PHWE–PHWO studies in view of the better recoveries in PHWE.

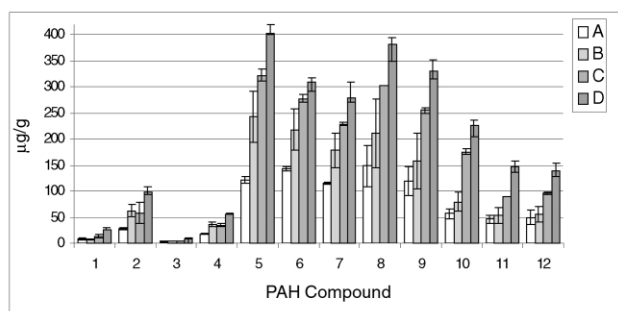


**Fig. 3** PHWE of PAHs (numbered according to Table 1) with different extraction vessels, flow velocities, and flow directions. RSDs shown as error bars ( $n = 4$ ). Extraction vessels are described in Fig. 2 and in the text. Explanation of symbols: A: Vessel 2, flow 1.0 ml min<sup>-1</sup> upwards. B: Vessel 2, flow 2.0 ml min<sup>-1</sup> upwards. C: Vessel 1, flow 1.0 ml min<sup>-1</sup> upwards. D: Vessel 1, flow 1.0 ml min<sup>-1</sup> downwards

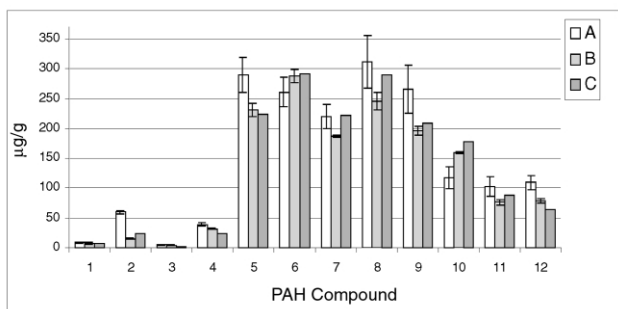


**Fig. 4** Comparison of PHWE, Soxhlet extraction, and ASE of PAHs (numbered according to Table 1). RSDs shown as error bars. Only one replicate was carried out with ASE and no RSD is given. Explanation of symbols: A: PHWE, vessel 2, flow 1.0 ml min<sup>-1</sup> downwards. This was used in PHWE–PHWO studies ( $n = 4$ ). B: Soxhlet extraction (20 h), toluene as solvent ( $n = 4$ ). C: ASE, method described below Table 1 ( $n = 1$ ).

### PHWE–PHWO Experiments

The average reaction time ( $t$ ) in the reaction tube in the PHWO process was defined as the ratio of the volume of the reaction tube ( $V$ ) to the volumetric pump flow ( $v$ ). The reaction times were 1.9–7.9 min depending on the temperature, pressure, and flow rate in the reaction tube (the length of the tube was constant in all experiments).

Calculations of the amount of potassium persulfate needed for oxidation of the PAHs were made on the basis of the stoichiometry of the oxidation reactions of the compounds. The equivalent amount of potassium persulfate (0.16 mmol) was calculated on the basis of the amounts of the PAHs determined by ASE (23 different PAHs were quantified and the total amount of the compounds was 1704  $\mu\text{g g}^{-1}$ ). Only 15 PAHs (total amount 1644  $\mu\text{g g}^{-1}$ ) were determined in the PHWE recovery and PHWE–PHWO conversion studies (Table 1). With all the PAHs in the 20.0 ml fraction considered to be extracted during the process, the equivalent concentration of potassium persulfate required would have been 7.82 mM. The lowest concentration used was 10 times this concentration (*i.e.* 78.2 mM = 21.11 g l<sup>-1</sup>). The soil sample typically also contained organic compounds other than PAHs. Although the amounts of these compounds were considered to be negligible

in the calculations of oxidant concentration for the needs of PAHs, oxidant was used in such great excess that the concentration could be assumed to be sufficient.

Conversion (removal efficiency) of the PAHs in the PHWE–PHWO procedure was calculated by comparing the amounts of the PAHs found in the PHWE–PHWO treated sample with those found in the PHWE sample treated at 300 °C and 20 min extraction time.

Tables 2 and 3 show the conversions of the PAHs under various PHWE–PHWO conditions. With oxidant concentration of 21.1 g l<sup>-1</sup>, 100 °C was clearly too low a temperature for efficient conversion of PAHs of high molecular mass even though the reaction time was the longest studied (Table 2). Like us, Cuypers *et al.*<sup>32</sup> have found that PAHs of high molecular mass (5–6 rings) are more resistant to persulfate oxidation ( $T = 70$  °C and oxidation time 3 h) than PAHs of lower molecular mass (1–2 or 3–4 rings). In our study, conversions of the PAHs of high molecular mass increased at 150 and 225 °C, but they were still well below 100%. The conversions of the PAHs of low and medium molecular mass often decreased when temperature was further raised up to 300 °C. This was probably due to the decreased reaction times at higher temperatures. It has also been reported that the decomposition of persulfate is increased at higher temperature and the success or failure of the oxidation process depends on whether the organic material can be oxidized before persulfate decomposition.<sup>41</sup>

An increase in conversions was achieved at 300 °C by increasing the oxidant concentration from 21.1 to 52.8 g l<sup>-1</sup>

(Table 2). Oxidant concentration could not be increased further in the pump because potassium persulfate was not soluble in water at higher concentrations (room temperature). To increase oxidant concentration in the reaction tube and thus the conversion efficiency, oxidant flow was increased from 1.0 to 4.0 ml min<sup>-1</sup> (Table 3). On the other hand, increase of the total flow in the reaction tube from 2.0 to 5.0 ml min<sup>-1</sup> decreased the reaction time, with opposite effect on the conversion of the PAHs. No marked difference in conversions of PAHs of different size was observed with flow of 4.0 ml min<sup>-1</sup> and oxidant concentration of 52.8 g l<sup>-1</sup> at 300 and 360 °C. The conversions were most efficient at 300 °C, where no PAHs were detected. The RSDs for some conversions were quite large, especially those presented in Table 3 and related to conversions below 90%. This poor repeatability under certain conditions must be considered when interpreting the results.

Other compounds found in the soil after PHWE and PHWE–PHWO are presented in Table 4. Since 1[3H]-isobenzofuranone and 9H-xanthen-9-one were not found in PHWE, they probably were reaction intermediates formed during oxidation. Relative those found in PHWE, the amounts of benzoic acid and 9,10-anthracenedione were clearly increased after the oxidation step. It is worth noting that none of the compounds listed in Table 4 were detected by PHWE–PHWO with 1.0 ml min<sup>-1</sup> oxidant flow at 100 or 150 °C nor with 4.0 ml min<sup>-1</sup> oxidant flow at 100, 150, 225 or 300 °C. The higher concentrations of some compounds in PHWE–PHWO when the temperature was raised might be explained in the same way (decreased reaction

**Table 2** PHWE–PHWO of the soil sample. Percentage conversion of PAHs (%RSD) under various oxidation conditions ( $n = 4$ ). Nominal flow in extraction was 1.0 ml min<sup>-1</sup> and in oxidation 2.0 ml min<sup>-1</sup> (oxidant flow 1.0 ml min<sup>-1</sup>). PHWE was performed at 300 °C for 20 min

Compound	A <sup>a</sup>	B <sup>b</sup>	C <sup>c</sup>	D <sup>d</sup>	E <sup>e</sup>	F <sup>f</sup>
Naphthalene	ND	ND	89.3 (5)	77.8 (16)	95.3 (5)	87.8 (1)
Acenaphthylene	ND	ND	96.7 (1)	97.1 (0.1)	96.6 (1)	96.2 (5)
Acenaphthene	ND	ND	85.1 (16)	65.1 (18)	81.8 (19)	85.1 (16)
Fluorene	ND	ND	77.7 (3)	88.2 (7)	94.1 (3)	93.0 (11)
Phenanthrene + Anthracene <sup>g</sup>	98.9 (0.1)	99.3 (1)	97.3 (0.1)	96.4 (1)	97.4 (1)	94.0 (5)
Fluoranthene	98.6 (1)	99.4 (1)	92.7 (0.4)	92.7 (1)	96.1 (3)	92.5 (7)
Pyrene	98.3 (1)	99.3 (1)	95.2 (1)	96.7 (1)	96.7 (3)	90.4 (5)
Benzo(a)anthracene + chrysene <sup>g</sup>	88.5 (3)	98.6 (1)	97.6 (0.2)	95.1 (1)	97.2 (1)	94.5 (2)
Benzo(b)fluoranthene + benzo(k)fluoranthene <sup>g</sup>	66.1 (10)	95.5 (2)	95.5 (0.4)	94.3 (1)	95.8 (1)	94.5 (2)
Benzo(a)pyrene	39.5 (25)	92.1 (9)	93.0 (1)	92.4 (3)	94.8 (2)	94.4 (7)
Indeno-1,2,3(c,d)-pyrene	23.5 (19)	91.0 (6)	94.9 (1)	98.0 (2)	97.3 (2)	98.4 (3)
Benzo(g,h,i)perylene	28.1 (17)	91.1 (5)	95.5 (1)	99.0 (2)	97.8 (2)	98.4 (3)

<sup>a</sup> A) Oxidation at 100 °C,  $c(\text{oxidant}) = 21.1$  g l<sup>-1</sup>,  $P \sim 150$  bar, reaction time = 7.9 min. <sup>b</sup> B) Oxidation at 150 °C,  $c(\text{oxidant}) = 21.1$  g l<sup>-1</sup>,  $P \sim 150$  bar, reaction time = 7.6 min. <sup>c</sup> C) Oxidation at 225 °C,  $c(\text{oxidant}) = 21.1$  g l<sup>-1</sup>,  $P \sim 150$  bar, reaction time = 6.9 min. <sup>d</sup> D) Oxidation at 300 °C,  $c(\text{oxidant}) = 21.1$  g l<sup>-1</sup>,  $P \sim 150$  bar, reaction time = 5.9 min. <sup>e</sup> E) Oxidation at 300 °C,  $c(\text{oxidant}) = 52.8$  g l<sup>-1</sup>,  $P \sim 150$  bar, reaction time = 5.9 min. <sup>f</sup> F) Oxidation at 360 °C,  $c(\text{oxidant}) = 52.8$  g l<sup>-1</sup>,  $P \sim 250$  bar, reaction time = 4.8 min. <sup>g</sup> See footnote *b* of Table 1.

**Table 3** PHWE–PHWO of the soil sample. Percentage conversion of PAHs (%RSD) under various oxidation conditions ( $n = 4$ ). Nominal flow in extraction was 1.0 ml min<sup>-1</sup> and in oxidation 5.0 ml min<sup>-1</sup> (oxidant flow 4.0 ml min<sup>-1</sup>). PHWE was performed at 300 °C for 20 min

Compound	A <sup>a</sup>	B <sup>b</sup>	C <sup>c</sup>	D <sup>d</sup>	E <sup>e</sup>
Naphthalene	ND	ND	ND	ND	97.5 (5)
Acenaphthylene	84.4 (27)	ND	98.1 (2)	ND	ND
Acenaphthene	86.1 (14)	ND	ND	ND	94.1 (11)
Fluorene	86.9 (21)	ND	97.7 (2)	ND	97.6 (2)
Phenanthrene + Anthracene <sup>f</sup>	98.9 (0.1)	ND	99.2 (1)	ND	95.9 (3)
Fluoranthene	98.9 (1)	ND	99.1 (2)	ND	92.1 (7)
Pyrene	98.8 (1)	99.8 (0.4)	99.2 (1)	ND	99.7 (0.1)
Benzo(a)anthracene + chrysene <sup>f</sup>	93.9 (6)	99.1 (1)	98.4 (2)	ND	93.3 (2)
Benzo(b)fluoranthene + benzo(k)fluoranthene <sup>f</sup>	71.2 (39)	96.6 (0.3)	93.7 (9)	ND	94.0 (2)
Benzo(a)pyrene	83.1 (31)	97.6 (1.5)	88.3 (22)	ND	94.3 (4)
Indeno-1,2,3(c,d)-pyrene	74.9 (50)	97.1 (3)	87.3 (25)	ND	98.0 (0.4)
Benzo(g,h,i)perylene	73.0 (59)	97.1 (3)	86.5 (26)	ND	98.6 (0.3)

<sup>a</sup> A) Oxidation at 100 °C,  $c(\text{oxidant}) = 52.8$  g l<sup>-1</sup>,  $P \sim 150$  bar, reaction time = 3.2 min. <sup>b</sup> B) Oxidation at 150 °C,  $c(\text{oxidant}) = 52.8$  g l<sup>-1</sup>,  $P \sim 150$  bar, reaction time = 3.0 min. <sup>c</sup> C) Oxidation at 225 °C,  $c(\text{oxidant}) = 52.8$  g l<sup>-1</sup>,  $P \sim 150$  bar, reaction time = 2.8 min. <sup>d</sup> D) Oxidation at 300 °C,  $c(\text{oxidant}) = 52.8$  g l<sup>-1</sup>,  $P \sim 150$  bar, reaction time = 2.4 min. <sup>e</sup> E) Oxidation at 360 °C,  $c(\text{oxidant}) = 52.8$  g l<sup>-1</sup>,  $P \sim 250$  bar, reaction time = 1.9 min. <sup>f</sup> See footnote *b* of Table 1.

**Table 4** PHWE and PHWE–PHWO of the soil sample. Peak areas of organic compounds relative to those of the ISTD in percentages. RSDs (in %) are given in parentheses.

Compound	PHWE (300 °C, 20 min)	PHWE–SCWO				
		225 °C, $c(\text{H}_2\text{O}_2)$ = 21.1 g l <sup>-1</sup>	300 °C, $c(\text{H}_2\text{O}_2)$ = 21.1 g l <sup>-1</sup>	300 °C, $c(\text{H}_2\text{O}_2)$ = 52.8 g l <sup>-1</sup>	360 °C, $c(\text{H}_2\text{O}_2)$ = 52.8 g l <sup>-1</sup>	360 °C, $c(\text{H}_2\text{O}_2)$ = 52.8 g l <sup>-1a</sup>
Benzaldehyde	5.2 (10)	ND	6.4 (26)	2.3 (21)	3.5 (38)	ND
Phenol	27.3 (24)	ND	39.7 (13)	7.2 (20)	5.4 (47)	ND
Benzoic acid	0.3 (50)	11.9 (20)	296.8 (16)	70.7 (8)	461.8 (8)	86.8 (54)
Quinoline	5.0 (20)	ND	ND	ND	ND	ND
1[3H]-Isobenzofuranone	ND	ND	71.3 (9)	21.0 (12)	42.3 (11)	22.5 (44)
1,1'-Biphenyl	8.4 (31)	ND	ND	ND	ND	ND
Dibenzofuran	33.1 (11)	ND	15.3 (28)	7.0 (37)	18.2 (40)	10.7 (71)
9H-Fluoren-9-one	83.4 (13)	13.8 (15)	38.1 (7)	18.6 (37)	38.6 (44)	36.1 (10)
9H-Xanthen-9-one	ND	ND	17.3 (18)	4.7 (22)	14.6 (23)	9.3 (24)
9,10-Anthracenedione	18.9 (53)	26.6 (2)	45.6 (5)	22.8 (25)	70.6 (10)	79.7 (1)

<sup>a</sup> The nominal flow from the pump delivering oxidant was 4.0 ml min<sup>-1</sup> (1.0 ml min<sup>-1</sup> in other experiments).

**Table 5** TOC content of the effluent (%RSD) under various conditions ( $n = 4$ ). Corresponding reaction times can be found in Tables 2 and 3. Oxidant concentration was 52.8 g l<sup>-1</sup>.

Experimental conditions	TOC in mg (%RSD)
PHWE (no SCWO step), $T = 300$ °C, flow = 1.0 ml min <sup>-1</sup> , $P \sim 150$ bar	6.7 (1)
PHWE–SCWO, $T = 100$ °C, flow (oxidant) = 1.0 ml min <sup>-1</sup> , $P \sim 150$ bar	7.5 (5)
<sup>a</sup> PHWE–SCWO, $T = 100$ °C, flow (oxidant) = 4.0 ml min <sup>-1</sup> , $P \sim 150$ bar	1.5 (51)
PHWE–SCWO, $T = 150$ °C, flow (oxidant) = 1.0 ml min <sup>-1</sup> , $P \sim 150$ bar	7.4 (4)
PHWE–SCWO, $T = 150$ °C, flow (oxidant) = 4.0 ml min <sup>-1</sup> , $P \sim 150$ bar	2.4 (23)
PHWE–SCWO, $T = 225$ °C, flow (oxidant) = 1.0 ml min <sup>-1</sup> , $P \sim 150$ bar	8.1 (6)
PHWE–SCWO, $T = 225$ °C, flow (oxidant) = 4.0 ml min <sup>-1</sup> , $P \sim 150$ bar	1.4 (13)
PHWE–SCWO, $T = 300$ °C, flow (oxidant) = 1.0 ml min <sup>-1</sup> , $P \sim 150$ bar	2.8 (8)
PHWE–SCWO, $T = 300$ °C, flow (oxidant) = 4.0 ml min <sup>-1</sup> , $P \sim 150$ bar	3.0 (7)
PHWE–SCWO, $T = 360$ °C, flow (oxidant) = 1.0 ml min <sup>-1</sup> , $P \sim 250$ bar	4.9 (5)
PHWE–SCWO, $T = 360$ °C, flow (oxidant) = 4.0 ml min <sup>-1</sup> , $P \sim 250$ bar	4.9 (4)

<sup>a</sup> The result of the analysis is erratic to some degree; see Results for further information.

time and more rapid decomposition of persulfate) as the decrease in PAH conversions at elevated temperatures. Under some conditions we also found other compounds, which could not be identified, and are not listed in Table 4. The compounds not identified with certainty were the most abundant with both oxidant flows at 100 °C where several hydrocarbons were detected. The chromatograms were the 'cleanest' with oxidant flow of 4.0 ml min<sup>-1</sup> at 225 and 300 °C where only a few unidentified peaks were found in low concentrations.

The TOC content of the effluent under various conditions is presented in Table 5. The best TOC removal (~80% relative to the PHWE result) was obtained at 225 °C with oxidant flow rate of 4.0 ml min<sup>-1</sup> and concentration of 52.8 g l<sup>-1</sup>. However, considerable amounts of organics were left in the effluent and, in this respect, it can be concluded that only limited oxidation was achieved with potassium persulfate as oxidant. For comparison, in our earlier study with on-line coupled PHWE–SCWO equipment and hydrogen peroxide as oxidant in oxidation of PAHs, TOC content of the effluent was decreased by ca. 91% under optimized conditions.<sup>36</sup> Because the tube, especially the parts beyond the heated region, was not flushed

with dichloromethane, some compounds may have got trapped there, with a resulting effect on the TOC removal value. Many products formed during oxidation are more polar (favoring water phase) than the starting compounds. This may explain the sometimes higher TOC contents of PHWE–PHWO samples than of the PHWE sample. Furthermore, some crystals were formed at the bottom of the test tubes during TOC analysis of the samples taken after PHWE–PHWO treatment at 100 °C with 4.0 ml min<sup>-1</sup> oxidant flow. This constitutes clear evidence that some compounds were not totally soluble in water under the conditions employed, reducing the reliability of the results.

Potassium persulfate concentration does not need to be as high as it was during the whole PHWE–SCWO procedure to get good conversions for the organics. This is because most of the organics are extracted at the beginning of PHWE; at the end of the extraction the concentration of the organics is lower and so also the need for oxidant. No gradient in oxidant concentration was developed because the extraction profile of the organics was not studied in detail. A clear disadvantage of using potassium persulfate as oxidant is that sulfate is released to water. The formation of sulfate was studied in detail in our earlier study.<sup>27</sup> The sulfate could be removed by precipitation or by biological or ion exchange methods.

Technically the PHWE–PHWO equipment was capable of safe and effective extraction of organic compounds from the soil. Overall, the recoveries with PHWE were better than those obtained with Soxhlet extraction. In the PHWE–PHWO studies excellent conversions were obtained for the PAHs and, under optimized conditions, the TOC content was clearly decreased. However, considerable amounts of organics were still left in the effluent.

## Acknowledgments

We thank Dr. Bert van Bavel of the University of Umeå (Sweden) for submitting the soil sample. Financial support from the Academy of Finland is greatly appreciated (projects 52746 and 48865).

## References

- J. Jacob, *Pure Appl. Chem.*, 1996, **68**, 301–308.
- T. Hyötyläinen and A. Oikari, *Chemosphere*, 1999, **38**, 1135–1144.
- E. U. Franck, *Pure Appl. Chem.*, 1970, **24**, 13–30.
- M. Uematsu and E. U. Franck, *J. Phys. Chem. Ref. Data*, 1980, **9**, 1291–1306.

- 5 K. H. Dudziak and E. U. Franck, *Ber. Bunsenges. Phys. Chem.*, 1966, **70**, 1120–1128.
- 6 T. Yamaguchi, *J. Mol. Liq.*, 2001, **90**, 313–322.
- 7 Y. E. Gorbaty and G. V. Bondarenko, *J. Supercrit. Fluids*, 1998, **14**, 1–8.
- 8 D. J. Miller, S. B. Hawthorne, A. M. Gizir and A. A. Clifford, *J. Chem. Eng. Data*, 1998, **43**, 1043–1047.
- 9 J. F. Connolly, *J. Chem. Eng. Data*, 1966, **11**, 13–16.
- 10 H. A. Pray, C. E. Schweickert and B. H. Minnich, *Ind. Eng. Chem.*, 1952, **44**, 1146–1151.
- 11 F. J. Armellini and J. W. Tester, *J. Supercrit. Fluids*, 1994, **7**, 147–158.
- 12 D. J. Miller and S. B. Hawthorne, *J. Chem. Eng. Data*, 2000, **45**, 78–81.
- 13 A. J. M. Lagadec, D. J. Miller, A. V. Lilke and S. B. Hawthorne, *Environ. Sci. Technol.*, 2000, **34**, 1542–1548.
- 14 K. Hartonen, K. Inkala, M. Kangas and M.-L. Riekkola, *J. Chromatogr. A*, 1997, **785**, 219–226.
- 15 K. Hartonen, G. Meissner, T. Kesälä and M.-L. Riekkola, *J. Microcolumn Sep.*, 2000, **12**, 412–418.
- 16 B. van Bavel, K. Hartonen, C. Rappe and M.-L. Riekkola, *Analyst*, 1999, **124**, 1351–1354.
- 17 J. J. Langenfeld, S. B. Hawthorne, D. J. Miller and J. Pawliszyn, *Anal. Chem.*, 1994, **66**, 909–916.
- 18 M. Modell, *Standard Handbook of Hazardous Waste Treatment and Disposal*, ed. H. M. Freeman, McGraw-Hill, NY, 1988, 153–168.
- 19 C. A. Blaney, L. Li, E. F. Gloyna and S. U. Hossain, *Supercritical Water Oxidation of Pulp and Paper Mill Sludge as an Alternative to Incineration*, in *ACS Symposium Series*, American Chemical Society, Washington DC, 1995, vol. 608, pp. 444–455.
- 20 A. Shanableh and Y. Shimizu, *Water Sci. Technol.*, 2000, **41**, 84–92.
- 21 L. Lei, X. Hu, H. P. Chu, G. Chen and P. L. Yue, *Water Sci. Technol.*, 1997, **35**, 311–319.
- 22 Q. Zhang and K. T. Chuang, *AIChE J.*, 1999, **45**, 145–150.
- 23 A. Alejandre, F. Medina, P. Salagre, A. Fabregat and J. E. Sueiras, *Appl. Catal. B: Environmental*, 1998, **18**, 307–315.
- 24 D. B. Mitton, J.-H. Yoon, J. A. Cline, H.-S. Kim, N. Eliaz and R. M. Latanasion, *Ind. Eng. Chem. Res.*, 2000, **39**, 4689–4696.
- 25 P. Kritzer, N. Boukis and E. Dinjus, *J. Supercrit. Fluids*, 1999, **15**, 205–227.
- 26 J. Kronholm, P. Jyske and M.-L. Riekkola, *Ind. Eng. Chem. Res.*, 2000, **39**, 2207–2213.
- 27 J. Kronholm, H. Metsälä, K. Hartonen and M.-L. Riekkola, *Environ. Sci. Technol.*, 2001, **35**, 3247–3251.
- 28 D. A. House, *Chem. Rev.*, 1962, **62**, 185–203.
- 29 *Gmelins Handbuch der Anorganischen Chemie*, Verlag Chemie, G.M.B.H., Berlin, 1938.
- 30 R. M. Powell, B. E. Bledsoe, G. P. Curtis and R. L. Johnson, *Environ. Sci. Technol.*, 1989, **23**, 1246–1249.
- 31 F. Martin, C. Saiz-Jimenez and F. J. Gonzales-Vila, *Soil Sci.*, 1981, **132**, 200–203.
- 32 C. Cuypers, T. Grotenhuis, J. Joziassse and W. Rulkens, *Environ. Sci. Technol.*, 2000, **34**, 2057–2063.
- 33 T. M. Young and W. J. Weber, *Environ. Sci. Technol.*, 1995, **29**, 92–97.
- 34 B. Misch, A. Firus and G. Brunner, *J. Supercrit. Fluids*, 2000, **17**, 227–237.
- 35 J. Kronholm, T. Kuosmanen, K. Hartonen and M.-L. Riekkola, Destruction of PAHs from Soil by Using Pressurized Hot Water Extraction Coupled with Supercritical Water Oxidation, *Waste Manage.*, 2002, in press.
- 36 J. Kronholm, J. Kalpala, K. Hartonen and M.-L. Riekkola, Pressurized Hot Water Extraction Coupled with Supercritical Water Oxidation in Remediation of Sand and Soil Containing PAHs, *J. Supercrit. Fluids*, 2002, in press.
- 37 T. Andersson, K. Hartonen, T. Hyötyläinen and M.-L. A. Riekkola, Novel Extraction Vessel Design in the Pressurised Hot Water Extraction and Thermal Desorption of PAHs from Sediment, *Anal. Chim. Acta*, submitted.
- 38 S. B. Hawthorne, Y. Yan and D. J. Miller, *Water Anal. Chem.*, 1994, **66**, 2912–2920.
- 39 S. B. Hawthorne and C. B. Grabanski, *Environ. Sci. Technol.*, 2000, **34**, 4348–4353.
- 40 S. B. Hawthorne, C. B. Grabanski, E. Martin and D. J. Miller, *J. Chromatogr. A*, 2000, **892**, 421–433.
- 41 P. D. Goulden and D. H. J. Anthony, *Anal. Chem.*, 1978, **50**, 953–958.





# Efficient solvent-free microwave phosphorylation of microcrystalline cellulose

Natalia Gospodinova,<sup>\*a</sup> Axelle Grelard,<sup>b</sup> Marc Jeannin,<sup>c</sup> Gabrielle C. Chitanu,<sup>d</sup> Adrian Carpov,<sup>d</sup> Valérie Thiéry<sup>\*a</sup> and Thierry Besson<sup>\*a</sup>

<sup>a</sup> Laboratoire de Génie Protéique et Cellulaire, EA 3169, Groupe de Chimie Organique, UFR Sciences Fondamentales et Sciences pour l'Ingénieur, Université de La Rochelle, Avenue Michel Crépeau, F-17042 La Rochelle Cedex 1, France. E-mail: ngospodi@univ-lr.fr, tbesson@univ-lr.fr, vthiery@univ-lr.fr

<sup>b</sup> Centre Commun d'Analyse, Université de La Rochelle, 5 Perspective de l'Océan, 17071 La Rochelle Cedex 9, France

<sup>c</sup> Laboratoire d'Etude des Matériaux en Milieux Agressifs, UFR Sciences Fondamentales et Sciences pour l'Ingénieur, Université de La Rochelle, Avenue Michel Crépeau, F-17042 La Rochelle cedex 1, France

<sup>d</sup> Institute of Macromolecular Chemistry "Petru Poni", Aleea Grigore Ghica Voda, 41A, 6600 Iasi, Romania

Received 10th January 2002

First published as an Advance Article on the web 16th April 2002

Environmentally friendly microwave phosphorylation of microcrystalline cellulose is herein described for the first time. Microwave irradiation is found to offer an efficient solvent-free procedure for cellulose modification without its pre-treatment (swelling in appropriate solvent).

## Introduction

Cellulose is the most abundant compound among naturally occurring polysaccharides. It is renewable, recyclable and biodegradable. By introduction of various functional groups onto the main polysaccharide chain, additional properties can be defined. Thus, promising properties of phosphorylated polysaccharides such as: high adsorption of serum protein by phosphorylated cellulose,<sup>1a</sup> efficient adsorption of heavy-metal ions by chitin phosphate,<sup>1b</sup> effectiveness of phosphorus-containing substituents as flame retardants for cellulose,<sup>1c</sup> anticoagulant capacity of oat spelt xylan phosphate,<sup>1d</sup> high performance electro-rheological effect of anhydrous suspensions of phosphorylated cellulose particles,<sup>1e</sup> excellent adhesion and efficient corrosion inhibition capabilities of phosphorylated hydroxypropyl cellulose derivatives<sup>1f</sup> have been reported.

Despite considerable interest in cellulose phosphorylation during the 1930s,<sup>2a</sup> many publications on cellulose phosphorylation have appeared since then. Some general observations based on the most recent data (Table 1) may be briefly formulated: (a) phosphorylation of cellulose by phosphorus(v) derivatives in heterogeneous conditions<sup>1a,2b–e</sup> is characterised by a low degree of substitution (DS, number of P atoms per cellulose repeating unit) of hydroxy functions of cellulose (DS = 0.2–0.6); (b) reactivity of phosphorus(III) compounds is higher than of phosphorus(V) ones: thus, the DS of product obtained in the presence of phosphorous acid (H<sub>3</sub>PO<sub>3</sub>) (DS = 0.8,<sup>2d</sup> and 2.0<sup>2e</sup>) is higher when compared to cellulose phosphorylated with phosphorus oxychloride (DS = 0.2<sup>2c</sup>), phosphorus pentoxide (DS = 0.6<sup>1a</sup>) or dihydrogen phosphate with urea as coupling agent (DS = 0.22<sup>b</sup>); (c) the relatively high degree of substitution of hydroxy functions of cellulose has been achieved by phosphorylation of soluble cellulose derivatives in homogeneous conditions, phosphorylation of hydroxypropyl cellulose in DMF (DS = 1.3<sup>1f</sup>), or by pre-treatment of

native cellulose by swelling in appropriate solvent such as a 70% aqueous solution of zinc chloride (DS = 2.0<sup>2e</sup>).

It is well known that the accessibility of the hydroxy functions of cellulose strongly affects the efficiency of cellulose functionalization.<sup>3</sup> The advantages of synthesis performed in homogeneous conditions were underlined by several authors in the case of cellulose derivatives. However, studies concerning the synthesis from native cellulose are rather limited. Considering the fact that cellulose chains do not change or lose their characteristic rigidity during the solvation process, the use of *N,N*-dimethylacetamide/lithium chloride and *N*-methylpyrrolidone/lithium chloride is particularly efficient.

As an alternative to conventional heating techniques, microwave irradiation can provide a fast and efficient synthesis method.<sup>4a</sup> In the course of our previous work on the application of microwave irradiation in organic chemistry, we demonstrated that many reactions could be run in a focused microwave oven thereby achieving striking reductions in shorter reaction times, better yields and cleaner reactions than for purely conventional

## Green Context

Cellulose is an abundant and renewable feedstock which will become more important to the chemical and allied industries as petrochemicals become scarce and expensive. Functionalisation of such materials is often necessary so as to add value for numerous applications including adsorption, flame retardancy and corrosion inhibition. In this paper a novel method of phosphorylation is described. The microwave activation method is both rapid and solvent free. Furthermore, the degree of substitution that can be achieved exceeds that from using more conventional methods.

JHC

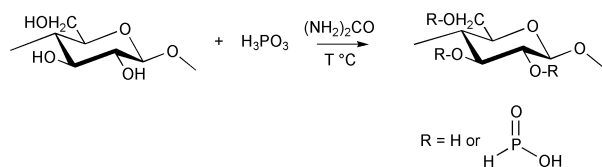
**Table 1** Data on cellulose phosphorylation

Type of cellulose	Reaction conditions	Degree of substitution <sup>a</sup>	Reference
Cellulose-membrane	DMF, phosphorus pentoxide, 25 °C, 48 h	0.6	1a
Hydroxypropyl cellulose	DMF, poly(phosphoric) acid and triethylamine, 120 °C, 6 h	1.3	1f
Poplin cellulose	H <sub>2</sub> O, dihydrogen phosphate and urea at 25 °C, post-treatment at 170 °C, 10 min	0.2	2b
Cotton cellulose	DMF, phosphorus oxychloride, 100 °C, 2 h	0.2	2c
Cotton cellulose	Phosphorous acid, 140 °C, 7 h	0.8	2d
Paper cellulose after swelling in a 70% aqueous solution of zinc chloride	Phosphorous acid and urea, 150 °C, 8 h	2.0	2e
Microcrystalline cellulose	Phosphorous acid and urea, microwave irradiation, 85 °C, 6 h	0.6	Present work
Microcrystalline cellulose	Phosphorous acid and urea, microwave irradiation, 105 °C, 2 h	2.8	Present work

<sup>a</sup> Number of P atoms per cellulose repeating unit

heating processes.<sup>4b,c</sup> It is reasonable to suppose that the increase of the diffusion rate and sorption of polar molecules in cellulose could be enhanced if microwaves induce orientation of hydroxy groups by resonance absorption of microwave energy. Such orientation could therefore be maximum (maximum of dielectric loss) when the frequency of the electromagnetic waves is coincident with the frequency of macromolecular motion, or  $\tau(T) = \beta/2\pi f_{\max}$ , where  $\tau(T)$  is the relaxation time at temperature  $T$ ,  $f_{\max}$  is the frequency of the electrical field, corresponding to dielectric loss maximum, and  $\beta$  characterises the asymmetry of the relaxation process in relation to this in liquids ( $\beta = 1$ ).<sup>5</sup> The relaxation time depends on the temperature according to Arrhenius law:  $\tau(T) = \tau_0 \exp(E/RT)$ , where  $E$  is the activation energy. At high microwave frequencies, the temperature range corresponding to segmental motion in amorphous polymers is situated above their decomposition temperature. However, localised, thermally activated motions (secondary relaxation transitions) are characterised by a much lower temperature range. An extensive study of secondary relaxation processes in cellulose over a large frequency range ( $10^{-2}$ – $10^6$  Hz) of electric field have recently been performed.<sup>6a,b</sup>

By using the values of  $\beta$ ,  $\tau_0$  and  $E$ , presented in these works, we have calculated the temperatures corresponding to the dielectric loss maximum and, hence, to the maximum of hydroxy group orientation at the typical frequency of microwave assisted synthesis ( $2.54 \times 10^9$  Hz). As a result, temperatures of 112 and 150 °C are calculated. The appropriate temperature range was used for comparative study of solvent-free phosphorylation of microcrystalline cellulose without its swelling in an aqueous solution of zinc chloride under both microwave irradiation and conventional heating. A much higher efficiency of microwave cellulose phosphorylation compared with conventional heating was demonstrated (Table 1). Phosphorous acid monosubstituted esters of cellulose (Scheme 1) of various degrees of substitution (0.2–2.8) were obtained by this simple procedure.



## Results and discussion

We investigated the effect of temperature and reaction time on the DS of cellulose by conventional heating and microwave irradiation. The temperature range between 75 and 150 °C was

chosen: 75 °C is the lowest limit required for dissolving urea in molten H<sub>3</sub>PO<sub>3</sub> and cellulose can be warmed up to 150 °C without substantial formation of degradation products.

The relationship between the reaction conditions and the DS of the product is shown in Fig. 1. It can be observed that when using conventional heating the maximum DS of cellulose, corresponding to a reaction time of 360 min, varies in the range of 0.2 and 1.4 depending on reaction temperature.

More extensive substitution of hydroxy functions in cellulose was achieved by using microwave irradiation. In contrast to conventional heating, the DS of cellulose increased dramatically above  $\approx 100$  °C, for example, highly phosphorylated cellulose (DS = 2.8) can be obtained after 120 min irradiation at 105 °C. These results are in accordance with the considerations, presented above, about supposed activation of diffusion and sorption of polar molecules in cellulose by microwave induced orientation of hydroxy groups.

In order to elucidate the structure of phosphorylated cellulose FT-IR, <sup>31</sup>P NMR and solid-state CP/MAS <sup>13</sup>C NMR spectroscopy studies were performed. Strong absorptions at 2370, 1210 and 970 cm<sup>-1</sup> were observed in the FT-IR spectrum of phosphorylated cellulose. According to published data<sup>2e</sup> these bands were attributed to P–H, P=O and P–O–C groups, respectively.

The peaks in the solid-state CP/MAS <sup>13</sup>C NMR spectra of native and substituted cellulose have been assigned on the basis of published solid state NMR data of cellulose nitrates.<sup>7a</sup> The doublet at 106, 105 ppm was assigned to C1. The peaks at 89 and 83 ppm were assigned to C4 in the crystalline and amorphous regions, respectively; the peaks at 65 and 64 ppm were assigned to crystalline and amorphous C6, respectively. The peaks in the 75–72 ppm region were assigned to C2, C3 and C5 resonances.

Thus, the decrease in the resonance assigned to crystalline C6 and C4 corresponds to substitution at a C6. A new resonance at 103 ppm may be assigned to phosphorylation of C2. The increase of intensity at 82 ppm was assigned to the effect of phosphorylation at C3.

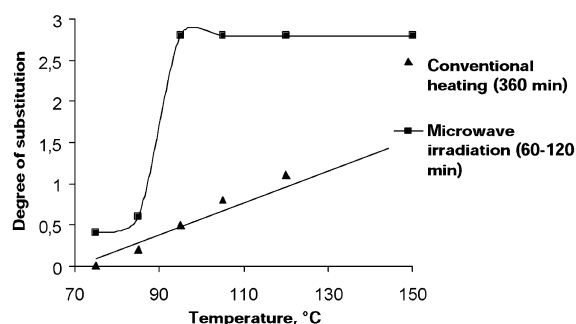


**Fig. 1** Relationship between the reaction conditions and the DS of cellulose.

$^{31}\text{P}$  NMR spectra of the same samples were also studied. According to published  $^{31}\text{P}$  NMR data on phosphorous organic derivatives, the observed resonances in the 2.5–7.5 ppm region correspond to those of monosubstituted phosphorous acid esters.<sup>7b</sup> The peaks corresponding to the three positions of substitution were even observed in the spectrum of phosphorylated cellulose with DS = 0.2. A signal at 2.6 ppm was assigned to P–O–C6. The doublets at 5.1–5.2 and at 7.5–7.6 ppm were assigned to P–O–C2 and P–O–C3. All the signals split into doublets when proton decoupling is not applied. This result confirms the formation of monosubstituted phosphorous acid esters of cellulose (see Scheme 1).

In conclusion, we present here for the first time the efficient solvent-free microwave phosphorylation of cellulose. This environmentally friendly process leads to monosubstituted phosphorous acid esters of cellulose of various degrees of substitution of hydroxy functions (0.2–2.8) without pre-treatment (swelling in an appropriate solvent). Considerable improvement in the degree of substitution of cellulose in comparison with conventional heating processes leads to a promising example of the usefulness of microwaves in the field of cellulose modification.

## Experimental

Commercial microcrystalline cellulose (Avicel), phosphorous acid and urea were used without further purification.

Focused microwave phosphorylation was carried out at atmospheric pressure with a Synthwave S402 Prolabo microwave reactor (300 W, monomode system), which has quartz reactors, visual control, irradiation monitored by PC computer, infrared measurement and continuous feedback temperature control (by PC).

A mixture of the urea (29.0 mmol), phosphorous acid (17.6 mmol) and cellulose (1.8 mmol) was placed under argon atmosphere in a quartz vial (10 ml) inside the oven. The irradiation was programmed to obtain a constant temperature (75, 85, 95, 105, 120 and 150 °C) with a maximal power output of 12 W. After cooling, the mixture was dissolved in water, precipitated with ethanol, filtered and dried. The procedure of purification was repeated three times. Phosphorylation under conventional heating was performed at the same temperatures and reactant quantity.

X-Ray energy dispersion spectrometry analysis (scanning electron microscope, equipped with a LinkSis 300 system,

JEOL 5410 LV instrument) was used for phosphorus, oxygen and carbon content characterisation of native and phosphorylated cellulose. Fourier transform infrared (FTIR) spectra of native and phosphorylated cellulose were recorded on a Paragon 1000 FT-IR spectrometer using KBr pellets.  $^{13}\text{C}$  and  $^{31}\text{P}$  NMR spectra were recorded on a JNM-LA400 JEOL spectrometer. Solid-state  $^{13}\text{C}$  cross-polarised magic angle spinning (CP/MAS) NMR spectra were acquired at a frequency of 100.4 MHz at room temperature. All chemical shifts are referenced to hexamethylbenzene (HMB).  $^{31}\text{P}$  NMR spectra were recorded at 161.7 MHz in  $\text{D}_2\text{O}$ . All chemical shifts are referenced to  $\text{H}_3\text{PO}_4$ .

## References

- (a) S. S. Kim, W. Y. Jeong, B. C. Shin, S. Y. Oh, H. W. Kim and J. M. Rhee, *J. Biomed. Mater. Res.*, 1998, **40**, 401; (b) N. Nishi, Sh-Ic. Nishimura, A. Ebina, A. Tsutsumi and S. Tokura, *Int. J. Biol. Macromol.*, 1984, **6**, 53; (c) B. Gilliland and B. Smith, *J. Appl. Polym. Sci.*, 1972, **16**, 1801; (d) R. Dace, E. McBride, K. Brooks, J. Gander, M. Buszko and V. M. Doctor, *Thrombosis Res.*, 1997, **87**, 113; (e) B. G. Ahn, U. S. Choi and O. K. Kwon, *Polym. Int.*, 2000, **49**, 567; (f) T. Kowalik, H.-J. Adler, A. Plagge and M. Stratmann, *Macromol. Chem. Phys.*, 2000, **201**, 2064.
- (a) G. Champetier and G. Urbain, *C. R. Acad. Sci.*, 1933, **27**, 930; (b) P. J. Baugh, A. G. Bradbury and J. B. Lawton, *J. Carbohydr. Res.*, 1978, **63**, 215; (c) T. L. Vigo and C. M. Welch, *Carbohydr. Res.*, 1974, **32**, 331; (d) K. Petrov, E. Nifantiev, I. Sopikova and M. Belavintzev, *Visokomol. Soed.*, 1963, **5**, 90 (*Chem. Abstr.*, 1964, **60**, 10913); (e) N. Inagaki, S. Nakamura, H. Asai and K. Katsura, *J. Appl. Polym. Sci.*, 1976, **20**, 2829.
- M. Diamantoglou and E. F. Kindinger, in *Cellulose and Cellulose Derivatives: Physico-chemical Aspect and Industrial Application*, ed. J. F. Kennedy, G. O. Phillips and P. O. Williams, Cambridge-Woodhead, Abington, 1995, pp. 141–152.
- (a) G. Majetich and K. Wheless, in *Microwave-Enhanced Chemistry, Fundamentals, Samples Preparation and Application*, ed. American Chemical Society, Washington, DC, 1997, p. 455; (b) J. Guillard and T. Besson, *Tetrahedron*, 1999, **55**, 5139 and references therein; (c) S. Frère, V. Thiéry and T. Besson, *Tetrahedron Lett.*, 2001, **42**, 2791.
- J. D. Ferry, in *Viscoelastic Properties of Polymers*, Wiley, New York, 3rd edn., 1980.
- (a) D. Meissner, J. Einfeld and A. Kwasniewski, *J. Non-Cryst. Solids*, 2000, **275**, 199 and references therein; (b) A. De La Rosa, L. Heux and J. Y. Cavallé, *Polymer*, 2001, **42**, 5371 and references therein.
- (a) P. M. Patterson, D. J. Patterson, J. Blackwell, J. L. Koenig, A. M. Jamieson, Y. P. Carignan and E. V. Turngren, *J. Polym. Sci. Polym. Phys. Ed.*, 1985, **23**, 483; (b) L. Kolovith, E. Ingall and R. Benner, *Limnol. Oceanogr.*, 2001, **46**, 309.



# Methanesulfonate and *p*-toluenesulfonate salts of the *N*-methyl-*N*-alkylpyrrolidinium and quaternary ammonium cations: novel low cost ionic liquids

J. Golding,<sup>a</sup> S. Forsyth,<sup>a</sup> D. R. MacFarlane,<sup>a</sup> M. Forsyth<sup>b</sup> and G. B. Deacon.<sup>a</sup>

<sup>a</sup> Centre for Green Chemistry, School of Chemistry, Monash University, Clayton, Victoria 3800, Australia

<sup>b</sup> Department of Materials Engineering, Monash University, Clayton, Victoria 3800, Australia. E-mail: s.forsyth@sci.monash.edu.au

Received 29th January 2002

First published as an Advance Article on the web 17th April 2002

The preparation and characterization of a series of novel salts, based on the *N*-methyl-*N*-alkylpyrrolidinium or quaternary ammonium organic cations coupled with sulfonate type anions, namely the mesylate ( $\text{CH}_3\text{SO}_3^-$ ) and tosylate ( $\text{CH}_3\text{C}_6\text{H}_4\text{SO}_3^-$ ) anions are reported. These salts are analogues of the previously described organic cation bis(trifluoromethanesulfonyl)amide (TFSA) salts that form useful ionic liquids of interest in “Green” synthesis. Several of the salts are liquid below 50 °C, *e.g.* tributylhexylammonium tosylate and ethylmethylpyrrolidinium mesylate and one is liquid at and below room temperature (tributylhexylammonium mesylate). These new salts have a cost advantage over salts of the TFSA<sup>-</sup>, PF<sub>6</sub><sup>-</sup> and CF<sub>3</sub>SO<sub>3</sub><sup>-</sup> anions. Electrochemical and thermal properties have been investigated. The salts are stable to beyond 100 °C and exhibit electrochemical potential windows of at least  $\pm 2$  V vs. Ag/Ag<sup>+</sup>. Some of the salts exhibit multiple crystalline phases below their melting points, potentially indicative of plastic crystal behaviour, whilst others showed more simple solid–liquid behaviour. Many of the salts were found to be glass forming.

## Introduction

It has become evident that for the widespread acceptance of ionic liquids for solvent replacement, their recyclability has to be proven, and their cost reduced.<sup>1</sup> Recycling of solvents may never be widely accepted in some industries (for example pharmaceuticals) as the costs to ensure purity in order to satisfy statutory bodies are seen as prohibitive. Ionic liquids must not only equal traditional solvents but, in fact, out-perform them in order to become more widely used. Whilst the short-term effectiveness of ionic liquids is limited by their variety and availability, they will certainly replace traditional solvents in some processes in the long run particularly as the desirable properties—low vapour pressure, fluidity, chemical and thermal stability<sup>1</sup> are better understood and indeed improved. In addition, important reaction specific effects are being discovered as a variety of reactions are tested in ionic liquids. For example, in a recent report from this laboratory the synthesis of cyclotrimeratrylene (CTV) in high yield in an ionic liquid was described.<sup>2</sup> This used tributylhexylammonium bis(trifluoromethanesulfonyl)amide (otherwise known as N<sub>6444</sub>TFSA), one of the strongly hydrophobic family of ionic liquids based on TFSA<sup>-</sup> and related ions.<sup>3–5</sup> The high yield in this CTV formation reaction was hypothesized to be a result of the fact that the reaction produces water and that, in the strongly hydrophobic environment of the ionic liquid, the equilibrium water activity is very low. Thus by ensuring water loss to a flowing air stream, the reaction was driven to high yield rather than being allowed to reach equilibrium with a high water activity.

In order for ionic liquids to become ‘cheap, popular, simple and effective’ replacements for solvents in synthetic chemistry and also in the area of electrolytes, it is an imperative that a range of salts becomes available for the wide variety of solvent uses. The mesylate ( $\text{CH}_3\text{SO}_3^-$ ) and tosylate ( $\text{CH}_3\text{C}_6\text{H}_4\text{SO}_3^-$ ) anions are relatively cheap, and considered extremely stable

both electrochemically, chemically and thermally.<sup>4</sup> The mesylate anion was shown to form low melting compounds of the ethylmethyl and butylmethyl imidazolium cations.<sup>4</sup> *N,N*-dimethylpyrrolidinium *p*-toluenesulfonate (P<sub>11</sub>Tos) has been reported by Eliel *et al.*,<sup>6</sup> with this cation being shown to be vulnerable to ring opening by strong nucleophilic attack (azide or methanethiolate). In this paper we explore the salts of these anions with a range of cations previously shown<sup>3</sup> to be useful in forming room temperature ionic liquids.

## Experimental

The various alkyl iodides (Aldrich/BDH/Fluka), *i*-PrOH (BDH), *p*-toluenesulfonic acid ( $\text{CH}_3\text{C}_6\text{H}_4\text{SO}_3\text{H}$ , Unilab), methanesulfonic acid (70%  $\text{CH}_3\text{SO}_3\text{H}$  in  $\text{H}_2\text{O}$ , Aldrich) and 1-methylpyrrolidine (Aldrich) were used as received. Melting points were measured using capillary tube apparatus, and are quoted as ranges from the visual observation of onset to completion of the melt. Differential scanning calorimetry (DSC) was carried out on a Perkin-Elmer DSC-7 with ambient

## Green Context

**This paper describes some novel low-cost ionic liquids. These are based on tosylate and mesylate anions, which are both considerably less expensive than the commonly used TFSA<sup>-</sup> anion. Low melting points, water solubility and good stability (thermal, chemical and electrochemical) add to their advantages. The paper not only adds to our ionic liquids toolkit, it also provides more valuable physical data on these fascinating substances, including electrochemical and thermal properties.** JHC



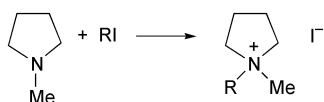
temperatures and above (50–200 °C) calibrated with indium (156.54 °C) and *p*-nitrotoluene (51.64 °C). Thermogravimetric analysis (TGA) was conducted using a STA1500 (Rheometric Scientific) in a nitrogen atmosphere (50 ml min<sup>-1</sup>) between 30 and 500 °C with a temperature rate of 10 °C min<sup>-1</sup>. The instrument was calibrated using four melting points (indium, tin, lead and zinc) and aluminium pans were used in all experiments. <sup>1</sup>H and <sup>13</sup>C NMR spectra were recorded on a Bruker DPX-300 MHz spectrometer, in d<sub>6</sub>-DMSO. Tetramethylsilane (TMS) was used as an internal standard. Infrared spectra were recorded on a Perkin-Elmer FTIR 1600 instrument. Solid samples were examined as KBr discs ~5% w/w, while liquid samples (including Nujol mulls) were examined between sodium chloride plates. Electrospray mass spectrometry was carried out on a Micromass Platform, both positive and negative species were detected with an electrospray source. Samples were dissolved in a 1:1 methanol–water mixture. Electrochemistry was carried out under a nitrogen atmosphere (in a drybox) using a Maclab potentiostat and Maclab software. Electrodes consisted of a glassy carbon working electrode, a platinum wire counter electrode and a silver wire pseudo reference electrode.

For simplicity an acronym is used to describe the various cations prepared consisting of P = pyrrolidinium and N = ammonium, along with a subscript indicating the number of carbons in each of the attached alkyl groups, *e.g.* N<sub>6222</sub> corresponds to the *N,N,N*-triethyl-*N*-hexylammonium cation. Table 1 lists the compounds prepared and the acronyms applied.

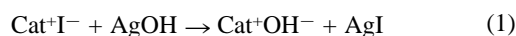
### Synthesis and characterisation

The *N*-alkyl-*N*-methylpyrrolidinium iodides were initially synthesized according to literature methods.<sup>3</sup>

The same method was used in the synthesis of the quaternary ammonium iodides.



*N,N*-alkylmethylpyrrolidinium and *N,N,N*-trialkyl-*N*-hexylammonium *p*-toluenesulfonates and methanesulfonates (Table 1) were prepared in good to very high yields from the corresponding iodide by the reaction sequence:



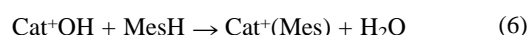
(Cat = P<sub>1n</sub>, N<sub>6mn</sub> (see Table 1); R = *p*-MeC<sub>6</sub>H<sub>4</sub>, Me). A slight excess of freshly prepared silver hydroxide (AgNO<sub>3</sub> and NaOH afforded solid AgOH, which was washed thoroughly to remove any residual salts) was added to *N*-methyl-*N*-alkylpyrrolidinium iodide and the suspension stirred for 1 h. The precipitated solid (AgI and excess AgOH) was filtered off. A slight excess of *p*-toluenesulfonic acid (CH<sub>3</sub>C<sub>6</sub>H<sub>4</sub>SO<sub>3</sub>H) or methanesulfonic acid (70% CH<sub>3</sub>SO<sub>3</sub>H in H<sub>2</sub>O) was added to the filtrate and the water removed by rotary evaporation. The subsequent residue was taken up in acetone and sodium carbonate was added to neutralise and remove excess acid and any residual water. The mixture was then filtered and the solvent evaporated. The product was then dried *in vacuo* for 2 days.

The above method has proven to be reliable and effective in the laboratory for small scale synthesis. For larger scale quantities a silver-free, ion exchange approach has been developed. Two variations using ion-exchange resin have been successful. The first (reactions (3) and (4)) involves preparation of an anion exchange resin loaded with the mesylate or tosylate

anion, as required, by treatment with the concentrated acid. Mixing the resin material with the iodide salt of the desired cation produces rapid displacement of the target anion by the iodide. The resin material is recycled using concentrated base.



Alternatively, the second (reactions (5) and (6)) method uses an hydroxide loaded resin to displace the iodide anion from the iodide salt of the desired cation to produce a hydroxide which is subsequently neutralised with either methanesulfonic acid or tolylsulfonic acid and the water removed by evaporation. The resin material is recycled using concentrated base. The bromide salts have also been found to be useful as a starting material in this approach.



All salts were identified using IR, NMR and mass spectrometry. Microanalyses were obtained for three representative products. All *p*-toluenesulfonates showed ν<sub>as</sub>(SO<sub>3</sub>) at 1219–1199 and ν<sub>s</sub>(SO<sub>3</sub>) at 1037–1031 cm<sup>-1</sup> and methanesulfonates at 1206–1192 and 1056–1040 cm<sup>-1</sup> respectively. Two such bands are as expected for ionic sulfonates.<sup>7</sup> The two aromatic proton resonances of the *p*-toluenesulfonates show variations of only 0.01 and 0.02 ppm over the whole range of compounds (see below). A similar consistency is observed for the ring proton resonances and for δ(Me) of the *N*-alkyl-*N*-methylpyrrolidinium methanesulfonates, but the resonance is significantly shifted for the trialkylhexylammonium salts. Detailed <sup>1</sup>H and <sup>13</sup>C NMR data support the structures of the cations, with appropriate variations upon homologation in the *N*-alkyl-*N*-methylpyrrolidinium series. Identification of the cations and sulfonate anions is also supported by observation of P<sub>1n</sub><sup>+</sup> or N<sub>6mn</sub><sup>+</sup> cations and *p*-MeC<sub>6</sub>H<sub>4</sub>SO<sub>3</sub><sup>-</sup> or MeSO<sub>3</sub><sup>-</sup> in the positive and negative electrospray mass spectra respectively. In some cases additional features, [Cat<sub>2</sub>(O<sub>3</sub>SR)]<sup>+</sup> and [Cat-(O<sub>3</sub>SR)<sub>2</sub>]<sup>-</sup> were also displayed.

### *N,N*-Dimethylpyrrolidinium *p*-toluenesulfonate (P<sub>11</sub>Tos)

P<sub>11</sub>I (2.15 g, 9.5 mmol), AgNO<sub>3</sub> (converted to AgOH) (2.5 g, 14.7 mmol) and CH<sub>3</sub>C<sub>6</sub>H<sub>4</sub>SO<sub>3</sub>H (1.70 g, 9.9 mmol) yielded P<sub>11</sub>Tos (2.45 g, yield 95%). IR (KBr disc) 3422s (br), 3038s, 2972s, 2915s, 1598m, 1478s, 1420m, 1402m, 1310s, 1207vs, 1119vs, 1033vs, 1003vs, 981s, 939s, 897m, 855m, 812s, 732w, 713m, 682vs, 566vs, 462w, 454w, 434w cm<sup>-1</sup>. <sup>1</sup>H NMR (300 MHz, d<sub>6</sub>-DMSO) δ 2.08 (4H, 2 × CH<sub>2</sub>), 2.29 (3H, -SO<sub>3</sub>C<sub>6</sub>H<sub>4</sub>CH<sub>3</sub>), 3.08 (6H, 2 × CH<sub>3</sub>), 3.44 (4H, 2 × CH<sub>2</sub>), 7.11 (2H, 2 × CH) and 7.48 (2H, 2 × CH). <sup>13</sup>C NMR (75 MHz, d<sub>6</sub>-DMSO) δ 20.67 (Tos-CH<sub>3</sub>), 21.30 (2 × CH<sub>2</sub>), 50.92 (2 × CH<sub>3</sub>) and 64.69 (2 × CH<sub>2</sub>), 125.40 (Tos-CH), 127.92 (Tos-CH), 137.40 (Tos-CCH<sub>3</sub>) and 145.84 (Tos-CSO<sub>3</sub><sup>-</sup>). Electrospray mass spectrum: ES<sup>+</sup> *m/z* 100 (100%, P<sub>11</sub><sup>+</sup>), 371 (5%, [P<sub>11</sub><sup>+</sup>]<sub>2</sub>[CH<sub>3</sub>C<sub>6</sub>H<sub>4</sub>SO<sub>3</sub><sup>-</sup>]). ES<sup>-</sup> *m/z* 172 (100%, CH<sub>3</sub>C<sub>6</sub>H<sub>4</sub>SO<sub>3</sub><sup>-</sup>), 442 (5%, [P<sub>11</sub><sup>+</sup>][CH<sub>3</sub>C<sub>6</sub>H<sub>4</sub>SO<sub>3</sub><sup>-</sup>]<sub>2</sub>). Microanalysis: found: C 57.38, H 8.03, N 5.15; requires: C 57.56, H 7.75, N 5.17%.

### *N*-Ethyl-*N*-methylpyrrolidinium *p*-toluenesulfonate (P<sub>12</sub>Tos)

P<sub>12</sub>I (2.30 g, 9.5 mmol), AgNO<sub>3</sub> (converted to AgOH) (2.5 g, 14.7 mmol) and CH<sub>3</sub>C<sub>6</sub>H<sub>4</sub>SO<sub>3</sub>H (1.70 g, 9.9 mmol) yielded P<sub>12</sub>Tos (2.55 g, yield 94%). IR (KBr disc) 3424s (br), 3028s, 2982s, 1655w, 1598m, 1481s, 1463s, 1413s, 1386s, 1367m, 1344m, 1299m, 1205vs (br), 1118vs, 1033vs, 1008vs, 938s,

916m, 856w, 817vs, 714m, 680vs, 566vs, 451w  $\text{cm}^{-1}$ .  $^1\text{H}$  NMR (300 MHz,  $d_6$ -DMSO)  $\delta$  1.26 (3H,  $\text{CH}_3$ ), 2.07 (4H,  $2 \times \text{CH}_2$ ), 2.28 (3H,  $-\text{SO}_3\text{C}_6\text{H}_4\text{CH}_3$ ), 2.95 (3H,  $\text{NCH}_3$ ), 3.40 (6H,  $2 \times \text{CH}_2$  and  $\text{NCH}_2$ ), 7.11 (2H,  $2 \times \text{Tos-CH}$ ) and 7.48 (2H,  $2 \times \text{Tos-CH}$ ).  $^{13}\text{C}$  NMR (75 MHz,  $d_6$ -DMSO)  $\delta$  8.74 (alkyl- $\text{CH}_3$ ), 20.67 (Tos- $\text{CH}_3$ ), 21.01 ( $2 \times \text{CH}_2$ ), 46.87 ( $\text{NCH}_2$ ), 58.30 ( $\text{NCH}_3$ ), 62.82 ( $2 \times \text{CH}_2$ ), 125.40 (Tos-CH), 127.92 (Tos-CH), 137.42 (Tos- $\text{CCH}_3$ ) and 145.86 (Tos- $\text{CSO}_3^-$ ). Electrospray mass spectrum:  $\text{ES}^+ m/z$  114 (100%,  $\text{P}_{12}^+$ ).  $\text{ES}^- m/z$  171 (100%,  $\text{CH}_3\text{C}_6\text{H}_4\text{SO}_3^-$ ).

#### ***N*-Methyl-*N*-propylpyrrolidinium *p*-toluenesulfonate ( $\text{P}_{13}\text{Tos}$ )**

$\text{P}_{13}\text{I}$  (2.42 g, 9.5 mmol),  $\text{AgNO}_3$  (converted to  $\text{AgOH}$ ) (2.5 g, 14.7 mmol) and  $\text{CH}_3\text{C}_6\text{H}_4\text{SO}_3\text{H}$  (1.80 g, 10.1 mmol) yielded  $\text{P}_{13}\text{Tos}$  (2.73 g, yield 96%). IR (KBr disc) 3457s (br), 3025s, 2970vs, 2883s, 1599m, 1475s, 1385s, 1343m, 1219s (br), 1125vs, 1037vs, 1010vs, 975s, 944s, 908m, 816s, 763m, 711m, 686vs, 637m, 565vs, 494m, 450m  $\text{cm}^{-1}$ .  $^1\text{H}$  NMR (300 MHz,  $d_6$ -DMSO)  $\delta$  0.90 (3H,  $\text{CH}_3$ ), 1.71 (2H,  $\text{CH}_2$ ), 2.07 (4H,  $2 \times \text{CH}_2$ ), 2.29 (3H  $-\text{SO}_3\text{C}_6\text{H}_4\text{CH}_3$ ), 2.97 (3H,  $\text{NCH}_3$ ), 3.25 (2H,  $\text{NCH}_2$  and solvent shoulder), 3.43 (4H,  $2 \times \text{CH}_2$ ), 7.12 (2H,  $2 \times \text{Tos-CH}$ ) and 7.47 (2H,  $2 \times \text{Tos-CH}$ ).  $^{13}\text{C}$  NMR (75 MHz,  $d_6$ -DMSO)  $\delta$  10.08 (alkyl- $\text{CH}_3$ ), 16.45 (alkyl- $\text{CH}_2$ ), 20.66 (Tos- $\text{CH}_3$ ), 21.00 ( $2 \times \text{CH}_2$ ), 46.87, 58.30 ( $2 \times \text{CH}_3$ ), 63.31 ( $2 \times \text{CH}_2$ ), 125.40 (Tos-CH), 127.90 (Tos-CH), 137.39 (Tos  $\text{CCH}_3$ ) and 145.81 (Tos- $\text{CSO}_3^-$ ). Electrospray mass spectrum:  $\text{ES}^+ m/z$  128 (100%,  $\text{P}_{13}^+$ ).  $\text{ES}^- m/z$  171 (100%,  $\text{CH}_3\text{C}_6\text{H}_4\text{SO}_3^-$ ).

#### ***N*-Butyl-*N*-methylpyrrolidinium *p*-toluenesulfonate ( $\text{P}_{14}\text{Tos}$ )**

$\text{P}_{14}\text{I}$  (2.56 g, 9.5 mmol),  $\text{AgNO}_3$  (converted to  $\text{AgOH}$ ) (2.5 g, 14.7 mmol) and  $\text{CH}_3\text{C}_6\text{H}_4\text{SO}_3\text{H}$  (1.80 g, 10.1 mmol) yielded  $\text{P}_{14}\text{Tos}$  (2.77 g, yield 93%). IR (KBr disc) 3445m (br), 3031s, 2963s, 2875s, 1650w, 1597m, 1475s, 1436s, 1383s, 1355m, 1307m, 1196vs (br), 1122vs, 1031s, 1008s, 967m, 933s, 900m, 817s, 744m, 711m, 682vs, 636m, 565vs, 447m  $\text{cm}^{-1}$ .  $^1\text{H}$  NMR (300 MHz,  $d_6$ -DMSO)  $\delta$  0.92 (3H,  $\text{CH}_3$ ), 1.30 (2H,  $\text{CH}_2$ ), 1.67 (2H,  $\text{CH}_2$ ), 2.07 (4H,  $2 \times \text{CH}_2$ ), 2.28 (3H  $-\text{SO}_3\text{C}_6\text{H}_4\text{CH}_3$ ), 2.97 (3H,  $\text{NCH}_3$ ), 3.28 (2H,  $\text{NCH}_2$  and solvent shoulder), 3.44 (4H,  $2 \times \text{CH}_2$ ), 7.10 (2H,  $2 \times \text{Tos-CH}$ ) and 7.47 (2H,  $2 \times \text{Tos-CH}$ ).  $^{13}\text{C}$  NMR (75 MHz,  $d_6$ -DMSO)  $\delta$  13.39 (alkyl- $\text{CH}_3$ ), 19.22 (alkyl- $\text{CH}_2$ ), 20.68 (Tos- $\text{CH}_3$ ), 21.02 ( $2 \times \text{CH}_2$ ), 24.84 (alkyl- $\text{CH}_2$ ), 47.40, 62.81 ( $\text{NCH}_3$ ), 63.32 ( $2 \times \text{CH}_2$ ), 125.41 (Tos-CH), 127.92 (Tos-CH), 137.41 (Tos- $\text{CCH}_3$ ) and 145.81 (Tos- $\text{CSO}_3^-$ ). Electrospray mass spectrum:  $\text{ES}^+ m/z$  142 (100%,  $\text{P}_{14}^+$ ), 455 (10%,  $[\text{P}_{14}^+]_2[\text{CH}_3\text{C}_6\text{H}_4\text{SO}_3^-]$ ).  $\text{ES}^- m/z$  171 (100%,  $\text{CH}_3\text{C}_6\text{H}_4\text{SO}_3^-$ ), 484 (40%,  $[\text{P}_{14}^+][\text{CH}_3\text{C}_6\text{H}_4\text{SO}_3^-]_2$ ). Microanalysis: found: C 60.59, H 8.85, N 4.34; requires: C 61.34, H 8.63, N 4.47%.

#### ***N*-Hexyl-*N*-methylpyrrolidinium *p*-toluenesulfonate ( $\text{P}_{16}\text{Tos}$ )**

$\text{P}_{16}\text{I}$  (2.82 g, 9.5 mmol),  $\text{AgNO}_3$  (converted to  $\text{AgOH}$ ) (2.5 g, 14.7 mmol) and  $\text{CH}_3\text{C}_6\text{H}_4\text{SO}_3\text{H}$  (1.80 g 10.1 mmol) yielded  $\text{P}_{16}\text{Tos}$  (3.01 g, yield 93%). IR (KBr disc) 3506m (br), 3024m, 2955s, 2925s, 2859s, 1654m, 1599m, 1469s, 1402m, 1380m, 1200s (br), 1119s, 1033s, 1009s, 938m, 853w, 818s, 730w, 712m, 681s, 564s  $\text{cm}^{-1}$ .  $^1\text{H}$  NMR (300 MHz,  $d_6$ -DMSO)  $\delta$  0.88 (3H,  $\text{CH}_3$ ), 1.29 (6H,  $3 \times \text{CH}_2$ ), 1.67 (2H,  $\text{CH}_2$ ), 2.07 (4H,  $2 \times \text{CH}_2$ ), 2.28 (3H,  $-\text{SO}_3\text{C}_6\text{H}_4\text{CH}_3$ ), 2.97 (3H,  $\text{NCH}_3$ ), 3.27 (2H,  $\text{NCH}_2$  and solvent shoulder), 3.43 (4H,  $2 \times \text{CH}_2$ ), 7.11 (2H,  $2 \times \text{Tos-CH}$ ) and 7.48 (2H,  $2 \times \text{Tos-CH}$ ).  $^{13}\text{C}$  NMR (75 MHz,  $d_6$ -DMSO)  $\delta$  13.72 (alkyl- $\text{CH}_3$ ), 20.67 (alkyl- $\text{CH}_2$ ), 21.02 ( $2 \times$

$\text{CH}_2$ ), 21.77 (Tos- $\text{CH}_3$ ), 22.79, 25.48, 30.58, (alkyl- $\text{CH}_2$ ), 47.44, 63.04 ( $\text{NCH}_3$ ), 63.32 ( $2 \times \text{CH}_2$ ), 125.41 (Tos-CH), 127.90 (Tos-CH), 137.38 (Tos- $\text{CCH}_3$ ) and 145.81 (Tos- $\text{CSO}_3^-$ ). Electrospray mass spectrum:  $\text{ES}^+ m/z$  170 (100%,  $\text{P}_{16}^+$ ), 511 (7.5%,  $[\text{P}_{16}^+]_2[\text{CH}_3\text{C}_6\text{H}_4\text{SO}_3^-]$ ).  $\text{ES}^- m/z$  171 (100%,  $\text{CH}_3\text{C}_6\text{H}_4\text{SO}_3^-$ ), 512 (25%,  $[\text{P}_{16}^+][\text{CH}_3\text{C}_6\text{H}_4\text{SO}_3^-]_2$ ).

#### ***N*-Hexyl-*N,N,N*-triethylammonium *p*-toluenesulfonate ( $\text{N}_{6222}\text{Tos}$ )**

$\text{N}_{6222}\text{I}$  (2.97 g, 9.5 mmol)  $\text{AgNO}_3$  (converted to  $\text{AgOH}$ ) (2.5 g, 14.7 mmol) and  $\text{CH}_3\text{C}_6\text{H}_4\text{SO}_3\text{H}$  (1.80 g 10.1 mmol) yielded  $\text{N}_{6222}\text{Tos}$  (3.03 g, yield 89%). IR (KBr disc) 3402m (br), 2953m, 2924m, 2863m, 1655m, 1624m, 1482m, 1459m, 1397m, 1205vs, 1123s, 1036s, 1013s, 941w, 818m, 683s, 566s  $\text{cm}^{-1}$ .  $^1\text{H}$  NMR (300 MHz,  $d_6$ -DMSO)  $\delta$  0.85 (3H, Hx- $\text{CH}_3$ ), 1.14 (9H,  $3 \times \text{Et-CH}_3$ ), 1.29 (6H,  $3 \times \text{Hx-CH}_2$ ), 1.55 (2H, Hx- $\text{CH}_2$ ), 2.28 (3H  $-\text{SO}_3\text{C}_6\text{H}_4\text{CH}_3$ ), 3.09 (2H, Hx- $\text{CH}_2$ ), 3.26 (6H,  $3 \times \text{Et-CH}_2$ ), 7.10 (2H,  $2 \times \text{Tos-CH}_2$ ) and 7.47 (2H,  $2 \times \text{Tos-CH}_2$ ).  $^{13}\text{C}$  NMR (75 MHz,  $d_6$ -DMSO)  $\delta$  7.05 (Hx- $\text{CH}_3$ ), 13.70 (Et- $\text{CH}_3$ ), 20.66 (alkyl- $\text{CH}_2$ ), 20.79 (alkyl- $\text{CH}_2$ ), 21.81 (alkyl- $\text{CH}_2$ ), 25.37 (alkyl- $\text{CH}_2$ ), 30.56 (alkyl- $\text{CH}_2$ ), 51.89 (Hx,  $\text{NCH}_2$ ), 55.95 (Et,  $\text{NCH}_2$ ), 125.41 (Tos-CH), 127.89 (Tos-CH), 137.36 (Tos- $\text{CCH}_3$ ); Tos- $\text{CSO}_3^-$  not observed. Electrospray mass spectrum:  $\text{ES}^+ m/z$  186 (100%,  $\text{N}_{6222}^+$ ).  $\text{ES}^- m/z$  171 (100%,  $\text{CH}_3\text{C}_6\text{H}_4\text{SO}_3^-$ ), 528 (5%,  $[\text{N}_{6222}^+][\text{CH}_3\text{C}_6\text{H}_4\text{SO}_3^-]_2$ ).

#### ***N*-Hexyl-*N,N,N*-tributylammonium *p*-toluenesulfonate ( $\text{N}_{6444}\text{Tos}$ )**

$\text{N}_{6444}\text{I}$  (3.77 g, 9.5 mmol),  $\text{AgNO}_3$  (converted to  $\text{AgOH}$ ) (2.5 g, 14.7 mmol) and  $\text{CH}_3\text{C}_6\text{H}_4\text{SO}_3\text{H}$  (1.70 g 9.9 mmol) yielded  $\text{N}_{6444}\text{Tos}$  (3.56 g, yield 85%). IR (KBr disc) 3450m (br), 2960s, 2873s, 1638m, 1491s, 1466s, 1383s, 1199vs, 1121s, 1035s, 1013s, 946w, 878m, 816s, 740m, 712m, 680s, 565s  $\text{cm}^{-1}$ .  $^1\text{H}$  NMR (300 MHz,  $d_6$ -DMSO)  $\delta$  0.92 (12H,  $4 \times \text{CH}_3$ ), 1.29 (12H,  $6 \times \text{CH}_2$ ), 1.56 (8H,  $4 \times \text{CH}_2$ ), 2.28 (3H,  $-\text{SO}_3\text{C}_6\text{H}_4\text{CH}_3$ ), 3.16 (8H,  $4 \times \text{CH}_2$ ), 7.10 (2H,  $2 \times \text{Tos-CH}_2$ ) and 7.47 (2H,  $2 \times \text{Tos-CH}_2$ ).  $^{13}\text{C}$  NMR (75 MHz,  $d_6$ -DMSO)  $\delta$  13.39 (Hx- $\text{CH}_3$ ), 13.71 (Bu- $\text{CH}_3$ ), 19.14 (alkyl- $\text{CH}_2$ ), 20.69 (alkyl- $\text{CH}_2$ ), 20.96 (alkyl- $\text{CH}_2$ ), 21.84 (alkyl- $\text{CH}_2$ ), 23.04 (alkyl- $\text{CH}_2$ ), 25.40 (alkyl- $\text{CH}_2$ ), 30.53 (alkyl- $\text{CH}_2$ ), 57.50 (Hx,  $\text{NCH}_2$ ), 57.71 (Bu,  $\text{NCH}_2$ ), 125.45 (Tos-CH), 127.89 (Tos-CH), 137.37 (Tos- $\text{CCH}_3$ ), 145.96 (Tos- $\text{CSO}_3^-$ ). Electrospray mass spectrum:  $\text{ES}^+ m/z$  270 (100%,  $\text{N}_{6444}^+$ ).  $\text{ES}^- m/z$  171 (100%,  $\text{CH}_3\text{C}_6\text{H}_4\text{SO}_3^-$ ).

#### ***N,N*-Dimethylpyrrolidinium methanesulfonate ( $\text{P}_{11}\text{Mes}$ )**

$\text{P}_{11}\text{I}$  (2.15 g, 9.5 mmol),  $\text{AgNO}_3$  (converted to  $\text{AgOH}$ ) (2.5 g, 14.7 mmol) and 70% aqueous  $\text{CH}_3\text{SO}_3\text{H}$  (1.40 g) yielded  $\text{P}_{11}\text{Mes}$  (1.63 g, yield 88%). IR (Nujol mull) 3420 m (br), 3024s, 2926s, 2853s, 1654w, 1467s, 1429m, 1376s, 1332s, 1313w, 1192s (br), 1040s, 1011m, 983w, 938m, 817w, 767s, 722w  $\text{cm}^{-1}$ .  $^1\text{H}$  NMR (300 MHz,  $d_6$ -DMSO)  $\delta$  2.09 (4H,  $2 \times \text{CH}_2$ ), 2.31 (3H,  $\text{CH}_3\text{SO}_3^-$ ), 3.10 (6H,  $2 \times \text{CH}_3$ ) and 3.47 (4H,  $2 \times \text{CH}_2$ ).  $^{13}\text{C}$  NMR (75 MHz,  $d_6$ -DMSO)  $\delta$  21.29 ( $2 \times \text{CH}_2$ ), 50.87 ( $2 \times \text{CH}_3$ ) and 64.64 ( $2 \times \text{CH}_2$ );  $\text{CH}_3\text{SO}_3^-$  not observed. Electrospray mass spectrum:  $\text{ES}^+ m/z$  100 (100%,  $\text{P}_{11}^+$ ), 295 (5%,  $[\text{P}_{11}^+]_2[\text{CH}_3\text{SO}_3^-]$ ).  $\text{ES}^- m/z$  95 (100%,  $\text{CH}_3\text{SO}_3^-$ ). Microanalysis: found: C 42.05, H 9.00, N 6.88, requires: C 43.08, H 8.72, N 7.18%.

#### ***N*-Ethyl-*N*-methylpyrrolidinium methanesulfonate ( $\text{P}_{12}\text{Mes}$ )**

$\text{P}_{12}\text{I}$  (2.30 g, 9.5 mmol),  $\text{AgNO}_3$  (converted to  $\text{AgOH}$ ) (2.5 g, 14.7 mmol) and 70% aqueous  $\text{CH}_3\text{SO}_3\text{H}$  (1.70 g) yielded

**P<sub>12</sub>Mes** (1.77 g, yield 89%). IR (Nujol mull) 3418m (br), 2926s, 2853s, 1644w (br), 1460s, 1376s, 1255w, 1198s, 1074w, 1045w, 790s, 722w cm<sup>-1</sup>. <sup>1</sup>H NMR (300 MHz, d<sub>6</sub>-DMSO)  $\delta$  1.27 (3H, CH<sub>3</sub>), 2.08 (4H, 2  $\times$  CH<sub>2</sub>), 2.32 (3H, CH<sub>3</sub>SO<sub>3</sub><sup>-</sup>), 2.98 (3H, NCH<sub>3</sub>) and 3.42 (6H, NCH<sub>2</sub>, 2  $\times$  CH<sub>2</sub> and solvent shoulder). <sup>13</sup>C NMR (75 MHz, d<sub>6</sub>-DMSO)  $\delta$  8.75 (CH<sub>3</sub>), 20.99 (2  $\times$  CH<sub>2</sub>), 46.81 (NCH<sub>3</sub>), 58.21 (NCH<sub>2</sub>) and 62.77 (2  $\times$  NCH<sub>2</sub>); CH<sub>3</sub>SO<sub>3</sub><sup>-</sup> not observed. Electrospray mass spectrum: ES+ *m/z* 114 (100%, P<sub>12</sub><sup>+</sup>), 323 (5%, [P<sub>12</sub><sup>+</sup>]<sub>2</sub>[CH<sub>3</sub>SO<sub>3</sub><sup>-</sup>]). ES- *m/z* 95 (100%, CH<sub>3</sub>SO<sub>3</sub><sup>-</sup>).

#### ***N*-Methyl-*N*-propylpyrrolidinium methanesulfonate (P<sub>13</sub>Mes)**

P<sub>13</sub>I (2.42 g, 9.5 mmol), AgNO<sub>3</sub> (converted to AgOH) (2.5 g, 14.7 mmol) and 70% aqueous CH<sub>3</sub>SO<sub>3</sub>H (1.80 g) yielded P<sub>13</sub>Mes (1.94 g, yield 92%). IR (KBr disc) 3443s (br), 3015m, 2976m, 2886m, 1638m, 1471m, 1420m, 1330s, 1195vs (br), 1056vs, 1006w, 966w, 941w, 905vw, 784s, 561s, 536s cm<sup>-1</sup>. <sup>1</sup>H NMR (300 MHz, d<sub>6</sub>-DMSO)  $\delta$  0.91 (3H, CH<sub>3</sub>), 1.72 (2H, CH<sub>2</sub>), 2.08 (4H, 2  $\times$  CH<sub>2</sub>), 2.30 (3H, CH<sub>3</sub>SO<sub>3</sub><sup>-</sup>), 2.98 (3H, NCH<sub>3</sub>), 3.26 (2H, NCH<sub>2</sub> and solvent shoulder) and 3.45 (4H, 2  $\times$  CH<sub>2</sub>). <sup>13</sup>C NMR (75 MHz, d<sub>6</sub>-DMSO)  $\delta$  10.57 (CH<sub>3</sub>), 16.46 (CH<sub>2</sub>), 21.01 (2  $\times$  CH<sub>2</sub>), 47.47 (NCH<sub>3</sub>), 63.32 (2  $\times$  NCH<sub>2</sub>) and 64.41 (NCH<sub>2</sub>); CH<sub>3</sub>SO<sub>3</sub><sup>-</sup> not observed. Electrospray mass spectrum: ES+ *m/z* 128 (100%, P<sub>13</sub><sup>+</sup>), 351 (5%, [P<sub>13</sub><sup>+</sup>]<sub>2</sub>[CH<sub>3</sub>SO<sub>3</sub><sup>-</sup>]). ES- *m/z* 95 (100%, CH<sub>3</sub>SO<sub>3</sub><sup>-</sup>).

#### ***N*-Butyl-*N*-methylpyrrolidinium methanesulfonate (P<sub>14</sub>Mes)**

P<sub>14</sub>I (2.56 g, 9.5 mmol), AgNO<sub>3</sub> (converted to AgOH) (2.5 g, 14.7 mmol) and 70% aqueous CH<sub>3</sub>SO<sub>3</sub>H (1.40 g) yielded P<sub>14</sub>Mes (2.03 g, yield 90%). IR (neat solid) 3451s (br), 3018m, 2962s, 2940s, 2876m, 1652w, 1468m, 1416m, 1380w, 1322m, 1306m, 1247m, 1206vs (br), 1081m, 1062m, 1052m, 1040s, 1008w, 965w, 932m, 791m, 796m, 561s, 550s, 484s cm<sup>-1</sup>. <sup>1</sup>H NMR (300 MHz, d<sub>6</sub>-DMSO)  $\delta$  0.93 (3H, CH<sub>3</sub>), 1.32 (2H, CH<sub>2</sub>), 1.68 (2H, CH<sub>2</sub>), 2.08 (4H, 2  $\times$  CH<sub>2</sub>), 2.30 (3H, CH<sub>3</sub>SO<sub>3</sub><sup>-</sup>), 2.98 (3H, NCH<sub>3</sub>), 3.30 (2H, NCH<sub>2</sub> and solvent shoulder) and 3.45 (4H, 2  $\times$  CH<sub>2</sub>). <sup>13</sup>C NMR (75 MHz, d<sub>6</sub>-DMSO)  $\delta$  13.39 (CH<sub>3</sub>), 19.22 (CH<sub>2</sub>), 21.01 (2  $\times$  CH<sub>2</sub>), 24.84 (CH<sub>2</sub>), 47.38 (NCH<sub>3</sub>), 62.77 (NCH<sub>2</sub>) and 63.30 (2  $\times$  NCH<sub>2</sub>); CH<sub>3</sub>SO<sub>3</sub><sup>-</sup> not observed. Electrospray mass spectrum: ES+ *m/z* 142 (100%, P<sub>14</sub><sup>+</sup>), 379 (5%, [P<sub>14</sub><sup>+</sup>]<sub>2</sub>[CH<sub>3</sub>SO<sub>3</sub><sup>-</sup>]). ES- *m/z* 95 (100%, CH<sub>3</sub>SO<sub>3</sub><sup>-</sup>), 332 (5%, [P<sub>14</sub><sup>+</sup>][CH<sub>3</sub>SO<sub>3</sub><sup>-</sup>]).

#### ***N*-Hexyl-*N*-methylpyrrolidinium methanesulfonate (P<sub>16</sub>Mes)**

P<sub>16</sub>I (2.82 g, 9.5 mmol), AgNO<sub>3</sub> (converted to AgOH) (2.5 g, 14.7 mmol) and 70% aqueous CH<sub>3</sub>SO<sub>3</sub>H (1.80 g) yielded P<sub>16</sub>Mes (1.87 g, yield 74%). IR (Nujol mull) 3454 m (br), 2919vs (br), 1652 m (br), 1464vs, 1377s, 1323w, 1308w, 1193s (br), 1040s, 938m, 767s, 727w cm<sup>-1</sup>. <sup>1</sup>H NMR (300 MHz, d<sub>6</sub>-DMSO)  $\delta$  0.88 (3H, CH<sub>3</sub>), 1.31 (6H, 3  $\times$  CH<sub>2</sub>), 1.69 (2H, CH<sub>2</sub>), 2.08 (4H, 2  $\times$  CH<sub>2</sub>), 2.30 (3H, CH<sub>3</sub>SO<sub>3</sub><sup>-</sup>), 2.98 (3H, NCH<sub>3</sub>), 3.30 (2H, NCH<sub>2</sub> and solvent shoulder) and 3.45 (4H, 2  $\times$  CH<sub>2</sub>). <sup>13</sup>C NMR (75 MHz, d<sub>6</sub>-DMSO)  $\delta$  13.72 (CH<sub>3</sub>), 21.00 (2  $\times$  CH<sub>2</sub>), 21.77 (CH<sub>2</sub>), 22.79 (CH<sub>2</sub>), 25.47 (CH<sub>2</sub>), 30.57 (CH<sub>2</sub>), 47.40 (NCH<sub>3</sub>), 62.95 (NCH<sub>2</sub>) and 63.28 (2  $\times$  NCH<sub>2</sub>); CH<sub>3</sub>SO<sub>3</sub><sup>-</sup> not observed. Electrospray mass spectrum: ES+ *m/z* 170 (100%, P<sub>16</sub><sup>+</sup>), 435 (7.5%, [P<sub>16</sub><sup>+</sup>]<sub>2</sub>[CH<sub>3</sub>SO<sub>3</sub><sup>-</sup>]), 454 (5%, [P<sub>16</sub><sup>+</sup>]<sub>2</sub>[CH<sub>3</sub>SO<sub>3</sub><sup>-</sup>]-H<sub>2</sub>O). ES- *m/z* 95 (100%, CH<sub>3</sub>SO<sub>3</sub><sup>-</sup>), 360 (5%, [P<sub>16</sub><sup>+</sup>][CH<sub>3</sub>SO<sub>3</sub><sup>-</sup>]).

#### **Preparation of *N*-hexyl-*N,N,N*-triethylammonium methanesulfonate (N<sub>6222</sub>Mes)**

N<sub>6222</sub>I (2.97 g, 9.5 mmol), AgNO<sub>3</sub> (converted to AgOH) (2.5 g, 14.7 mmol) and 70% aqueous CH<sub>3</sub>SO<sub>3</sub>H (2.40 g) yielded N<sub>6222</sub>Mes (1.80 g, yield 67%). IR (KBr disc) 3445 m (br), 3011m, 2935m, 2869w, 1638w, 1460m, 1420m, 1397m, 1330s, 1201vs (br), 1056vs, 964w, 785s, 561s, 536s cm<sup>-1</sup>. <sup>1</sup>H NMR (300 MHz, d<sub>6</sub>-DMSO)  $\delta$  0.88 (3H, CH<sub>3</sub>), 1.31 (6H, 3  $\times$  CH<sub>2</sub>), 1.69 (2H, CH<sub>2</sub>), 2.08 (4H, 2  $\times$  CH<sub>2</sub>), 2.74 (3H, CH<sub>3</sub>SO<sub>3</sub><sup>-</sup>), 2.74 (3H, NCH<sub>3</sub>), 3.30 (2H, NCH<sub>2</sub> and solvent shoulder) and 3.45 (4H, 2  $\times$  CH<sub>2</sub>). <sup>13</sup>C NMR (75 MHz, d<sub>6</sub>-DMSO)  $\delta$  13.72 (4  $\times$  CH<sub>3</sub>), 21.00 (CH<sub>2</sub>), 21.77 (CH<sub>2</sub>), 22.79 (CH<sub>2</sub>), 25.47 (CH<sub>2</sub>), 30.57 (CH<sub>2</sub>), 47.40 (CH<sub>3</sub>SO<sub>3</sub><sup>-</sup>), 62.95 (NCH<sub>2</sub>) and 63.28 (3  $\times$  NCH<sub>2</sub>). Electrospray mass spectrum: ES+ *m/z* 186 (100%, N<sub>6222</sub><sup>+</sup>), 467 (5%, [N<sub>6222</sub><sup>+</sup>]<sub>2</sub>[CH<sub>3</sub>SO<sub>3</sub><sup>-</sup>]). ES- *m/z* 95 (100%, CH<sub>3</sub>SO<sub>3</sub><sup>-</sup>), 376 (15%, [N<sub>6222</sub><sup>+</sup>][CH<sub>3</sub>SO<sub>3</sub><sup>-</sup>]).

#### **Preparation of *N*-hexyl-*N,N,N*-tributylammonium methanesulfonate (N<sub>6444</sub>Mes)**

N<sub>6444</sub>I (3.77 g, 9.5 mmol), AgNO<sub>3</sub> (converted to AgOH) (2.5 g, 14.7 mmol) and 70% aqueous CH<sub>3</sub>SO<sub>3</sub>H (3.00 g) yielded N<sub>6444</sub>Mes (3.26 g, yield 94%). IR (neat liquid) 3456w (br), 2960s, 2934s, 2874m, 1655vw, 1467m, 1381m, 1321m, 1199s, 1111m, 1072s, 1039s, 877m, 792w, 763m, 428s cm<sup>-1</sup>. <sup>1</sup>H NMR (300 MHz, d<sub>6</sub>-DMSO)  $\delta$  0.93 (12H, 4  $\times$  CH<sub>3</sub>), 1.29 (12H, 6  $\times$  CH<sub>2</sub>), 1.57 (8H, 4  $\times$  CH<sub>2</sub>), 2.74 (3H, CH<sub>3</sub>SO<sub>3</sub><sup>-</sup>), 3.17 (8H, 4  $\times$  NCH<sub>2</sub>). <sup>13</sup>C NMR (75 MHz, d<sub>6</sub>-DMSO)  $\delta$  13.83 (3  $\times$  CH<sub>3</sub>), 14.15 (CH<sub>3</sub>), 19.57 (3  $\times$  CH<sub>2</sub>), 21.36 (CH<sub>2</sub>), 22.25 (CH<sub>2</sub>), 23.47 (3  $\times$  CH<sub>2</sub>), 25.83 (CH<sub>2</sub>), 30.94 (CH<sub>2</sub>), 40.09 (CH<sub>3</sub>SO<sub>3</sub><sup>-</sup>), 58.14 (4  $\times$  NCH<sub>2</sub>). Electrospray mass spectrum: ES+ *m/z* 270 (100%, N<sub>6444</sub><sup>+</sup>), ES- *m/z* 95 (100%, CH<sub>3</sub>SO<sub>3</sub><sup>-</sup>), 460 (5%, [N<sub>6222</sub><sup>+</sup>][CH<sub>3</sub>SO<sub>3</sub><sup>-</sup>]).

## **Results and discussion**

### **Thermal analysis**

Thermal data derived from the DSC traces are summarized in Table 1. Illustrative DSC thermograms obtained on warming are shown in Fig. 1. The quarternary ammonium salts (N<sub>6444</sub> and N<sub>6222</sub> of both tosylate and mesylate) evidence what may be considered to be classical thermal behaviour, showing either a melting endotherm alone (*e.g.* N<sub>6222</sub>Tos) or a glass transition, subsequent crystallization and a final melting transition (*e.g.* N<sub>6444</sub>Tos). The broadness of the final melting peak in some cases (*e.g.* N<sub>6222</sub>Mes) may indicate the onset of one or more solid–solid transitions coincident with the melting point; these are a major feature of the solid state behaviour of other salts of the same anions as discussed further below. The pyrrolidinium salts of the mesylate and tosylate anions also show examples of such a convergence of melting and solid–solid transitions. In particular the P<sub>11</sub>Tos shows a convoluted peak appearing at ~150 °C, demonstrating a blurring of solid–solid transitions and final melting. A distinct shoulder is evident on the initial peak which in turn, overlays the melting endotherm. Broad, shouldered peaks are also evident for the P<sub>12</sub>, P<sub>13</sub> and P<sub>14</sub> tosylate salts. The P<sub>16</sub>Tos exhibits two small solid–solid transitions below what is still a relatively broad melting peak.

The mesylate salts of the same series of cations (P<sub>11</sub>–P<sub>16</sub>) tend to show a more distinct separation of submelting and melting transitions. This is clearly evident in the case of P<sub>11</sub>Mes, however P<sub>12</sub>, P<sub>13</sub> and P<sub>14</sub> mesylates have relatively broad melts compared with the rest of the series. Somewhat intriguingly, P<sub>13</sub>Mes shows more classical thermal behaviour (*T<sub>g</sub>*, crystallization and melting) whereas other salts of this cation (*e.g.* with



**Table 1** Compounds prepared in the *p*-toluenesulfonate and methanesulfonate families of organic salts and their thermal properties

Compound (name)	Acronym	$T_g/^\circ\text{C}$ ( $\pm 2^\circ\text{C}$ )	$T_x/^\circ\text{C}$ ( $\pm 2^\circ\text{C}$ )	$T_{8-9}/^\circ\text{C}$ ( $\pm 2^\circ\text{C}$ )	$T_m/^\circ\text{C}$ ( $\pm 2^\circ\text{C}$ )	$\Delta S_f/\text{J K}^{-1} \text{mol}^{-1}$ ( $\pm 10\%$ )
<i>N,N</i> -Dimethylpyrrolidinium <i>p</i> -toluenesulfonate	P <sub>11</sub> Tos			145	167 <sup>a</sup>	59
<i>N</i> -Methyl- <i>N</i> -ethylpyrrolidinium <i>p</i> -toluenesulfonate	P <sub>12</sub> Tos				120 <sup>a</sup>	71
<i>N</i> -Methyl- <i>N</i> -propylpyrrolidinium <i>p</i> -toluenesulfonate	P <sub>13</sub> Tos		-11		80 <sup>a</sup>	56
<i>N</i> -Methyl- <i>N</i> -butylpyrrolidinium <i>p</i> -toluenesulfonate	P <sub>14</sub> Tos		-11	81	115 <sup>a</sup>	55
<i>N</i> -Methyl- <i>N</i> -hexylpyrrolidinium <i>p</i> -toluenesulfonate	P <sub>16</sub> Tos			-102	91	137
<i>N</i> -Hexyl- <i>N,N,N</i> -triethylammonium <i>p</i> -toluenesulfonate	N <sub>6222</sub> Tos				109	75
<i>N</i> -Hexyl- <i>N,N,N</i> -tributylammonium <i>p</i> -toluenesulfonate	N <sub>6444</sub> Tos	-40	-2		50 <sup>a</sup>	48
<i>N,N</i> -Dimethylpyrrolidinium methanesulfonate	P <sub>11</sub> Mes			88	160/174	200
<i>N</i> -Methyl- <i>N</i> -ethylpyrrolidinium methanesulfonate	P <sub>12</sub> Mes	-106 <sup>b</sup>	-46	-76	7	40 <sup>a</sup>
<i>N</i> -Methyl- <i>N</i> -propylpyrrolidinium methanesulfonate	P <sub>13</sub> Mes	-72	-32			80 <sup>a</sup>
<i>N</i> -Methyl- <i>N</i> -butylpyrrolidinium methanesulfonate	P <sub>14</sub> Mes	-68	-35			63 <sup>a</sup>
<i>N</i> -Methyl- <i>N</i> -hexylpyrrolidinium methanesulfonate	P <sub>16</sub> Mes					86
<i>N</i> -Hexyl- <i>N,N,N</i> -triethylammonium methanesulfonate	N <sub>6222</sub> Mes					62
<i>N</i> -Hexyl- <i>N,N,N</i> -tributylammonium methanesulfonate	N <sub>6444</sub> Mes					N/A <sup>c</sup>

<sup>a</sup> Broad melting transition. <sup>b</sup> Assigned to the glass transition in supercooled phase I. <sup>c</sup> Liquid at room temperature, no melting transition observed.

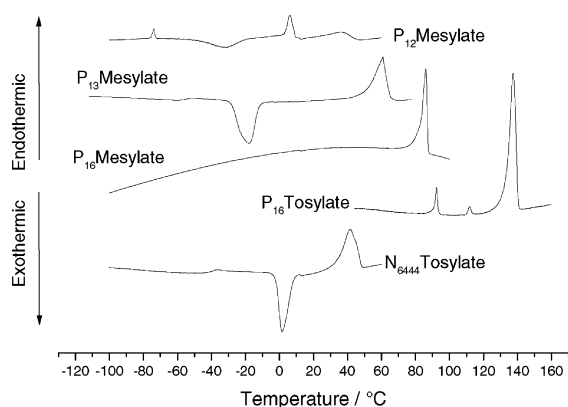


**Fig. 1** Illustrative examples of DSC thermograms of P<sub>12</sub>Mes, P<sub>13</sub>Mes, P<sub>16</sub>Mes, P<sub>16</sub>Tos and N<sub>6444</sub>Tos salts.

PF<sub>6</sub><sup>-</sup>,<sup>8</sup> BF<sub>4</sub><sup>-</sup>,<sup>8</sup> TFSA<sup>-3,9</sup> or dicyanamide<sup>10</sup> anions) have generally been rich in solid–solid transitions.

The N<sub>6222</sub>, P<sub>12</sub> and P<sub>14</sub> mesylates and the N<sub>6444</sub> tosylate members of the families have melting points at or below 60 °C and could therefore be useful for synthetic solvent use in reactions run above 60 °C. A room temperature ionic liquid is available with the N<sub>6444</sub> mesylate which could not be crystallized. Of course, mixtures of these compounds can be expected to form binary mixtures with melting points lower than those for the pure salts.

Figs. 2 and 3 show illustrative thermogravimetric analysis traces for two representatives of the mesylate and tosylate salts respectively. Both examples show only very minor weight loss over the temperature interval 30–300 °C at which point rapid decomposition is observed. The tosylate example is slightly more stable than the mesylate. Stability to around 300 °C is typical of many ionic liquids including the hexafluorophosphate and tetrafluoroborate salts.<sup>11</sup> Aluminium pans, as used in our experiments, have been shown to catalyse the decomposition of hexafluorophosphate salts at lower temperatures than

alumina (Al<sub>2</sub>O<sub>3</sub>) pans.<sup>11</sup> The TFSA and triflate salts are remarkably more stable than any of these with only minor weight loss evident below 350 °C and the main process setting

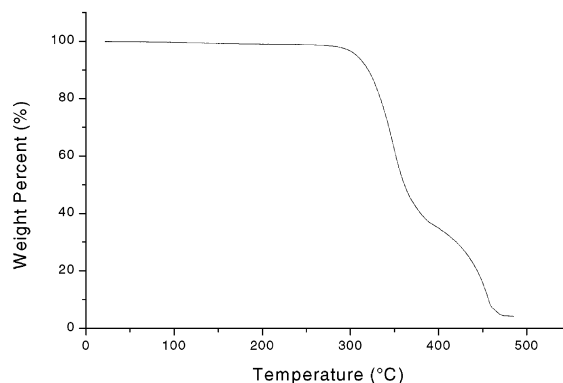


**Fig. 2** Thermogravimetric trace for P<sub>13</sub>Mes showing decomposition weight loss setting in around 300 °C.

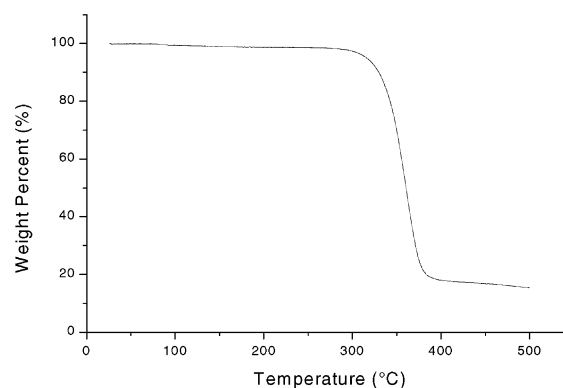


**Fig. 3** Thermogravimetric trace for P<sub>13</sub>Tos showing decomposition weight loss setting in around 300 °C.



in above 400 °C.<sup>5</sup> The difference between the mesylate and the triflate salts is clearly the effect of fluorination on the anion and, given the presence of aliphatic C–H bonds in the cations, it would appear that the effect of fluorination is more than simple replacement with a more stable bond. The electron withdrawing effect of the CF<sub>3</sub> on the negatively charged moiety in each case may stabilize the anion against oxidative processes at that site.

The salts have proven to be quite stable in their liquid states at temperatures in excess of 100 °C and for periods in excess of 5 h. The electrochemical stability measurements described below were carried out at 100 °C and during the course of these extensive sets of measurements no evidence of breakdown was observed.

### Solubility properties

All of the salts reported are at least partially soluble in water as well as alcohols and other polar solvents. This is similar to the analogous triflate (CF<sub>3</sub>SO<sub>3</sub><sup>−</sup>) salts<sup>3</sup> but is in contrast to the analogous TFSA<sup>−</sup> salts in which the anion produces salts, which are not miscible with water. This is most likely the result of fluorination in the TFSA<sup>−</sup> case, which has the effect of inducing a distribution of the net negative charge through the core of the molecule and onto the fluorine atoms. Further discussion of the structure and charge distribution as obtained from quantum chemical calculations of this interesting family of sulfonyl and bis(sulfonyl)amide anions will be published elsewhere.

### Electrochemistry

Representative cyclic voltammograms of these compounds (Figs. 4–6) indicate that both families of ionic liquids have wide electrochemical windows of stability but that the tosylate salts are substantially more electrochemically stable than the analogous mesylate salts. In order that a wide range of salts could be compared in their liquid states all electrochemical cycling measurements were carried out at 100 °C. The mesylate salt of the P<sub>13</sub> cation shows reductive and oxidative limits of approximately −2.25 and +2.30 V, respectively, against a Ag/Ag<sup>+</sup> pseudo-reference electrode. The *p*-toluenesulfonate salt of the same (P<sub>13</sub>) cation exhibits a similar reductive limit of about 2.30 V but increased oxidative stability with an oxidative limit of +3.2 V. The N<sub>6444</sub>Tos salt has an almost identical reductive limit of −2.40 V but the reaction at the oxidative limit is sufficiently sluggish that no rapid process is observed up to +5.00 V (the limit of the measurement). The oxidative limit in both the mesylate and tosylate cases probably represents an oxidation of the anion to a neutral radical species. From the

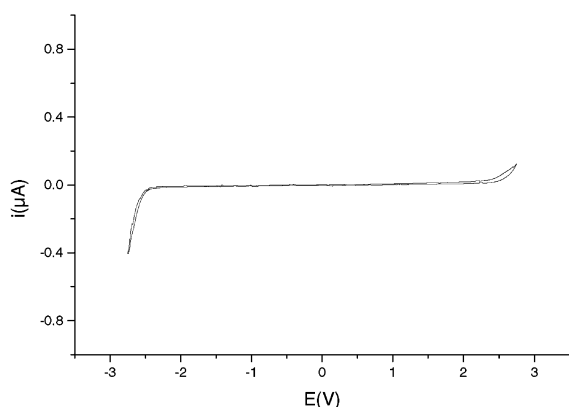


**Fig. 4** Cyclic voltammogram of P<sub>13</sub>Mes carried out at 100 °C vs. Ag/Ag<sup>+</sup> pseudo-reference electrode. GC working and Pt counter electrode.

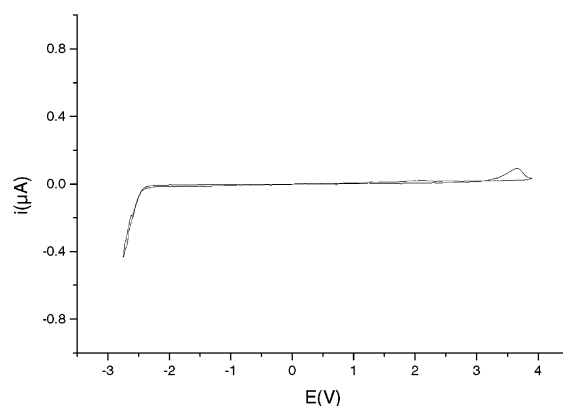


**Fig. 5** Cyclic voltammogram of P<sub>13</sub>Tos carried out at 100 °C vs. Ag/Ag<sup>+</sup> pseudo-reference electrode. GC working and Pt counter electrode.

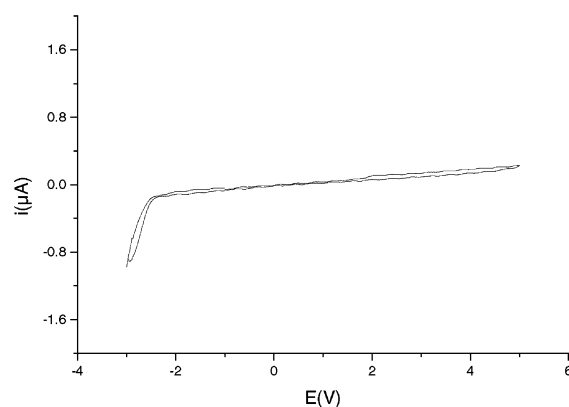


**Fig. 6** Cyclic voltammogram of N<sub>6444</sub>Tos carried out at 100 °C vs. Ag/Ag<sup>+</sup> pseudo-reference electrode. GC working and Pt counter electrode.

differences observed here it would appear that the tosylate is significantly stabilized against this process by the aromatic ring.

### Solid state behaviour

Many of the compounds described here display one or more solid–solid phase transitions in their DSC traces. A number of related pyrrolidinium compounds have previously been shown to exhibit plastic crystal phases in their solid states.<sup>3,8–10</sup> This behaviour has its origins in rotatory motions of one or both of the ions on their lattice sites in the crystal. One of the characteristics of this type of phase behaviour is that the sub-melting solid–solid phase transitions make up a substantial part of the overall entropy of melting (in particular the entropy associated with the rotational motions) such that the residual entropy change,  $\Delta S_f$ , observed on melting is often quite small. Timmermans observed that in molecular plastic crystal compounds  $\Delta S_f$  is often lower than 20 J K<sup>−1</sup> mol<sup>−1</sup>)<sup>12</sup> and MacFarlane *et al.* have hypothesized<sup>3</sup> that in compounds containing molecular ions such as those described here,  $\Delta S_f$  can be as high as 40 J K<sup>−1</sup> mol<sup>−1</sup> if one of the ions is not rotationally activated in the solid state.

The entropies of melting recorded in Table 1 indicate that many of the salts reported here indeed satisfy this criterion for the existence of plastic crystal phases. In particular many of the mesylates have quite low values of  $\Delta S_f$ . While it is normally true that the plastic crystalline phase behaviour is often associated with the observation of a solid–solid phase transition, the observation of such a transition in a thermal trace such as those in Fig. 1 is not a necessary condition for such a phase to exist. In fact, super-cooling of the plastic crystalline phase

below the solid–solid transition point has frequently been observed. Thus, for example, in the case of  $N_{6222}Mes$  the low value of  $\Delta S_f$  is strongly indicative of the existence of a plastic crystalline phase and the absence of an observed solid–solid transition in the thermal trace simply a reflection of the fact that the low-temperature, ordered phase did not form under the conditions of cooling and warming in the experiment. Many of the tosylate salts show one or more solid–solid phase transitions but nonetheless  $\Delta S_f$  values in excess of  $50 \text{ J K}^{-1} \text{ mol}^{-1}$ . This may be another example of the situation where the higher temperature phases reflect rotatory motions of the cation only and  $\Delta S_f$  therefore retains a large contribution from the final onset of motions of the anion.

## Conclusions

The ionic liquids presented here provide further alternatives to traditional solvents for a variety of applications including synthetic uses and electrolytes for electrochemical devices. The tosylate and mesylate anions are both substantially cheaper than the  $TFSA^-$  and  $PF_6^-$  anions and provide relatively low melting, water soluble salts that are thermally, chemically and electrochemically stable. At least one member of the family, *N*-hexyl-*N*-tributylammonium mesylate, is liquid at room temperature.

## Acknowledgements

The support of the Special Research Centre for Green Chemistry and the Australian Research Council is gratefully acknowledged.

## References

- (a) K. R. Seddon, *J. Chem. Tech. Biotechnol.*, 1997, **68**, 351–356; (b) T. Welton, *Chem. Rev.*, 1999, **99**, 2071–2083; (c) J. T. Hamill, C. Hardacre, M. Nieuwenhuyzen, K. R. Seddon, S. A. Thompson and B. Ellis, *Chem. Commun.*, 2000, 1929; (d) M. Torres, A. Stark and K. R. Seddon, *Pure Appl. Chem.*, 2000, **72**, 2275.
- J. L. Scott, D. R. MacFarlane, C. L. Raston and C. Mei Teoh, *Green Chem.*, 2000, **2**, 123–126.
- (a) D. R. MacFarlane, P. Meakin, J. Sun, N. Amini and M. Forsyth, *J. Phys. Chem.*, 1999, **103**, 4164–4170; (b) J. Sun, D. R. MacFarlane and M. Forsyth, *Ionic*, 1997, **3**, 356–362; (c) J. Sun, M. Forsyth and D. R. MacFarlane, *J. Phys. Chem. B*, 1998, **102**, 8858–8864.
- E. I. Cooper and E. J. M. O'Sullivan, *Proc. 8th Int. Symp. Molten Salts*, 1992, 386–396.
- P. Bonhote, A.-P. Dias, N. Papageorgio, K. Kalyanasundaram and M. Gratzel, *Inorg. Chem.*, 1996, **35**, 1168–1178.
- E. L. Eliel, R. O. Hutchins, R. Membane and R. L. Willer, *J. Org. Chem.*, 1976, **41**, 1052–1057.
- J. H. R. Clarke and L. A. Woodward, *Trans. Faraday Soc.*, 1968, **64**, 1041; P. A. Yeats, J. R. Sams and F. Aubke, *Inorg. Chem.*, 1971, **10**, 1877.
- J. Golding, N. Hamid, D. R. MacFarlane, M. Forsyth, C. Forsyth, C. Collins and J. Huang, *Chem. Mater.*, 2001, **13**(2), 558; D. R. MacFarlane and M. Forsyth, *Adv. Mater.*, 2001, **13**, 957; S. Forsyth, J. Golding, D. R. MacFarlane and M. Forsyth, *Electrochim. Acta*, 2001, **46**, 1753–1758.
- (a) J. Huang, M. Forsyth and D. R. MacFarlane, *Solid State Ionics*, 2000, **136**, 447–452; (b) M. Forsyth, J. Huang and D. R. MacFarlane, *J. Mater. Chem.*, 2000, **10**, 2259–2265; (c) D. R. MacFarlane, J. Huang and M. Forsyth, *Nature*, 1999, **402**, 792–794.
- D. R. MacFarlane, G. B. Deacon, S. Forsyth and J. Golding, *Chem Commun.*, 2001, 1430–1431.
- H. L. Ngo, K. LeCompte, L. Hargens and A. B. McEwen, *Thermochim. Acta*, 2000, **357–358**, 97–102.
- J. Timmermans, *J. Mater. Phys. Chem. Solids*, 1961, **18**(11), 1.



# Selective and high yield synthesis of dimethyl carbonate directly from carbon dioxide and methanol

Jun-Chul Choi, Liang-Nian He, Hiroyuki Yasuda and Toshiyasu Sakakura\*

National Institute of Advanced Industrial Science and Technology (AIST), 1-1-1 Higashi, AIST Central 5, Tsukuba 305-8565, Japan. E-mail: t-sakakura@aist.go.jp

Received 17th January 2002

First published as an Advance Article on the web 16th April 2002

Supercritical carbon dioxide is efficiently converted to dimethyl carbonate (DMC) via the reaction with methanol in the presence of a catalytic amount of dialkyltin oxide or its derivatives. The removal of water is the key to accomplishing the high conversion by shifting the equilibrium to dimethyl carbonate. Dehydration is successfully carried out by circulating the reaction mixture through a dehydrating tube packed with molecular sieve 3A. Under the effective dehydration conditions, the DMC yield is almost linearly dependent on the reaction time, catalyst amount, methanol concentration, and CO<sub>2</sub> pressure.

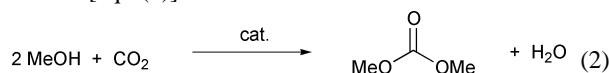
## Introduction

Due to the increasing importance of environmental and resource issues, chemists have recently devoted themselves to the realization of a sustainable society through green chemistry activity.<sup>1</sup> In this context, carbon dioxide is a key molecule because it is a typical renewable resource. The utilization of carbon dioxide is also very attractive for synthetic chemists because of its environmentally benign nature (nontoxic, non-corrosive, and nonflammable). Especially, the utilization as a reaction medium and a phosgene substitute has been attracting much interest.<sup>2–6</sup> On the other hand, dimethyl carbonate (DMC) is a promising target molecule derived from CO<sub>2</sub>. The use of DMC widely covers polycarbonate synthesis, polyurethane synthesis, fuel additives, carbonylating reagents, alkylating reagents, polar solvents, *etc.*<sup>7,8</sup> In addition, DMC synthesis from CO<sub>2</sub> seems reasonable from a thermodynamic view point because the oxidation state of carbon in DMC is the same as in carbon dioxide.

The typical synthetic methods of DMC starting from CO<sub>2</sub> are represented by the following two procedures. The first method is the reaction of methanol with methyl iodide under CO<sub>2</sub>. The consumption of an equimolar amount of methyl iodide for producing one mole of DMC is the disadvantage of this method [eqn. (1)].<sup>9</sup> The second method is DMC synthesis only from



methanol and CO<sub>2</sub> [eqn. (2)]. The problem of this procedure is the low methanol conversion that is ascribed to the thermodynamic limitations and/or deactivation of the catalysts by H<sub>2</sub>O.<sup>10–15</sup> We now wish to report DMC synthesis directly from carbon dioxide and methanol with high methanol conversion by using recyclable inorganic dehydrating agents such as molecular sieves [eqn (2)].

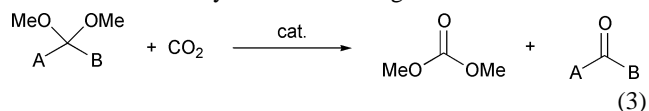


## Results and discussion

### (a) Reaction using orthoesters and acetals

In spite of the many attempts to remove water from the reaction mixture of eqn. (2) using dehydrating agents such as molecular

sieves, MgSO<sub>4</sub>, Na<sub>2</sub>SO<sub>4</sub>, dicyclohexylcarbodiimide, *etc.*, no successful results have been obtained.<sup>10–15</sup> Hence, we previously reported another methodology to overcome the thermodynamic limitation. Thus, we first dehydrate methanol to form dehydrated derivatives such as the orthoester or acetal and then react the dehydrated derivative with carbon dioxide. Overall, the reaction can be regarded as DMC synthesis from CO<sub>2</sub> and methanol. In this way, there is no need to remove the water from the reaction mixture for the DMC synthesis. Indeed, trimethyl orthoacetate, which is easily hydrolyzed, reacted with carbon dioxide in the presence of a catalytic amount of dibutyltin dimethoxide to give DMC in high yields [eqn. (3): A = Me, B = MeO].<sup>6b</sup> The reaction took place even without adding methanol. The drawbacks of this procedure are the high cost of the starting material and the co-production of methyl acetate, which is hard to recycle to the starting orthoester.



In order to circumvent these problems concerning use of the orthoester, we next investigated the reaction of an acetal [eqn. (3): A, B = Me].<sup>6d,e</sup> The reaction is different from that using the orthoester in that the presence of methanol is inevitable. Indeed, the requirement of methanol is clearly shown in Fig. 1. Thus, the DMC yield is proportional to the methanol concentration. This indicates that DMC is, in fact, formed from methanol and CO<sub>2</sub> according to eqn. (2). The acetal is probably working as a chemical dehydrating agent. The details of the mechanism will

## Green Context

**Dimethyl carbonate (DMC) is a very useful compound for polycarbonate and polyurethane synthesis, and for other applications including fuel additives and as an alkylating agent. It can be synthesised using iodomethane, but this wastes the heavy halogen. The cleanest synthesis would be the direct reaction of methanol with CO<sub>2</sub>, but existing methods are inefficient. Here, a new and highly efficient method of DMC synthesis via this route is described. A recyclable dehydrating agent incorporated in the reactor is used to maintain the activity of the catalyst and achieve high methanol conversion.**

JHC

be discussed in the next section. The merits of using an acetal rather than the orthoester are the low cost of the starting material, and the easy conversion of the co-produced acetone to the starting dimethyl acetal.

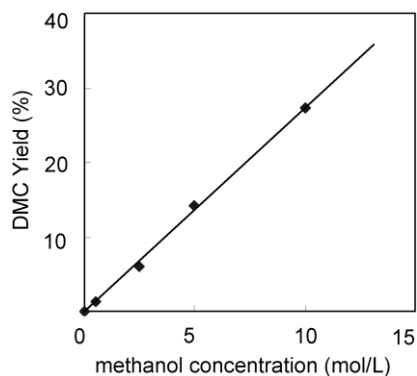
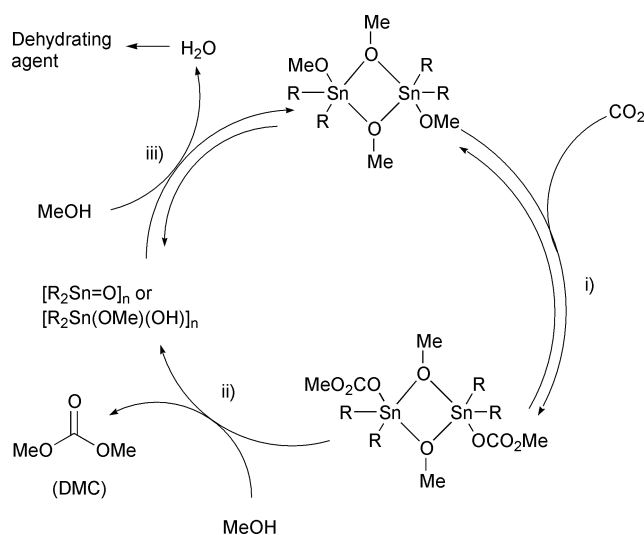


**Fig. 1** Effect of methanol concentration on the dimethyl carbonate synthesis from CO<sub>2</sub>, acetal and methanol. *Reaction conditions:* autoclave (20 cm<sup>3</sup> inner volume), 2,2-dimethoxypropane (10 mmol), dibutyltin dimethoxide (0.2 mmol), methanol, carbon dioxide (total pressure 300 atm), 180 °C, 24 h. Yields are based on the acetal.

### (b) Mechanistic consideration

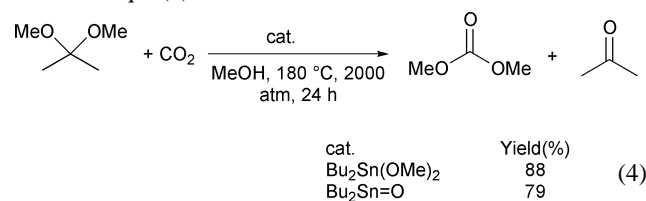
Judging from various spectroscopic studies such as NMR (<sup>1</sup>H, <sup>13</sup>C, <sup>119</sup>Sn), IR and X-ray studies, a plausible catalytic cycle for the tin-catalyzed DMC synthesis using acetals is summarized in Scheme 1.<sup>6c,e,16</sup> The catalytic cycle is comprised of three steps: (i) CO<sub>2</sub> insertion into the terminal methoxide of [R<sub>2</sub>Sn(OMe)<sub>2</sub>]<sub>2</sub>, (ii) the thermolysis of the resulting [R<sub>2</sub>Sn(O-CO<sub>2</sub>Me)(OMe)]<sub>2</sub> leading to DMC, and (iii) regeneration of tin dimethoxide from tin oxide or tin hydroxide. The first and second steps have already been characterized at the molecular level.<sup>6c</sup> As for step (ii), involvement of the intramolecular process was pointed out; a very similar conclusion was recently proposed by another group.<sup>16</sup>

Based on Scheme 1, deactivation of the catalyst by H<sub>2</sub>O would not be the crucial problem limiting the DMC yield because dialkyltin dimethoxide is regenerated from dialkyltin oxide or hydroxide in the presence of methanol and dehydrating agents (step iii). In other words, Bu<sub>2</sub>Sn=O should work as the



**Scheme 1**

active catalyst in place of Bu<sub>2</sub>Sn(OMe)<sub>2</sub>. Indeed, the catalytic activity of Bu<sub>2</sub>Sn=O was very close to that of Bu<sub>2</sub>Sn(OMe)<sub>2</sub> as shown in eqn. (4).



### (c) DMC synthesis directly from MeOH and CO<sub>2</sub>

As discussed in the previous section, the role of acetal in eqn. (4) seems to be a dehydrating agent rather than a substrate. In addition, hydrolysis of the tin catalyst is not the critical problem. These facts strongly prompted us to study DMC synthesis directly from methanol and CO<sub>2</sub> without using acetals. The use of inorganic dehydrating agents such as molecular sieves is more attractive compared with the use of chemical dehydrating agents such as acetals because inorganic dehydrating agents are easily recyclable and do not produce co-products. Although several papers reported such attempts, DMC yields based on methanol have still been very low.<sup>9–15</sup> This is presumably due to the reversibilities of the dehydration under the reaction conditions. In other words, it is difficult to efficiently absorb water from the MeOH/CO<sub>2</sub> mixture at high temperature.

In order to overcome the above problems, a new dehydrating system has been designed. An outline of this system is shown in Fig. 2. In this system, the dehydrating agent, molecular sieve 3A, is separated from the reactor. The dehydrating part is kept at room temperature for improving the dehydrating efficiency. A part of the reaction mixture is circulated through the dehydrating tube by a high-pressure circulation pump. The power of the new dehydrating system is clearly shown in Fig. 3. Thus, the yield of DMC in the absence of the dehydrating tube became steady at a level of a few percent after a very short reaction period. On the other hand, by using the new reactor, the DMC yield increased as the reaction time increased. The yield reached nearly 50% after 72 h. This is the first example of obtaining DMC directly from methanol and CO<sub>2</sub> with a high yield. In addition, the present DMC synthesis is very selective. Indeed, DMC is substantially the sole product as judged by gas chromatography (Fig. 4). It should be noted here that the time dependence with molecular sieve 3A is similar to that observed for the reaction of acetal.<sup>6e</sup> Hence, the dehydration by the new reactor with molecular sieve 3A is as effective as that by acetal. The effect of shape and size of the molecular sieve 3A was also investigated (Table 1). Briefly, these factors did not dramat-

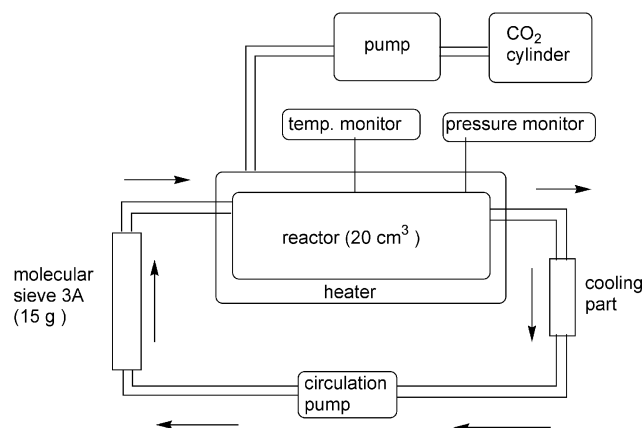


**Fig. 2** Schematic diagram of a batch reactor with internal recycle.



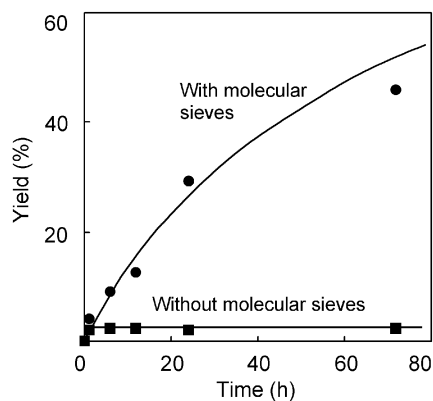


**Fig. 3** Time dependence of dimethyl carbonate synthesis from CO<sub>2</sub> and methanol. *Reaction conditions:* autoclave with internal recycle (see Fig. 2), dibutyltin dimethoxide (2.0 mmol), methanol (100 mmol), molecular sieve 3A (15 g), carbon dioxide (total pressure 300 atm), 180 °C. Yields are based on methanol.

ically affect the DMC yield although too small a size caused a large pressure drop across the dehydrating tube and made it difficult to circulate the reaction mixture.

The efficacy of the dehydration using molecular sieve 3A is also shown significantly by the dependence on the catalyst amount (Fig. 5). In the absence of molecular sieve 3A, the DMC yield was zero-order with respect to the catalyst amount supporting the fact that the yield is thermodynamically controlled. On the other hand, the DMC yield increased with increasing catalyst amount in the presence of molecular sieve 3A, showing that the reaction rate is dependent on the catalyst concentration when water is efficiently removed. A similar relation between the DMC yield and the catalyst amount was observed for the DMC synthesis using acetal as the dehydrating agent.

The effect of CO<sub>2</sub> pressure on the new dehydrating system was also investigated (Fig. 6). The DMC yield is nearly

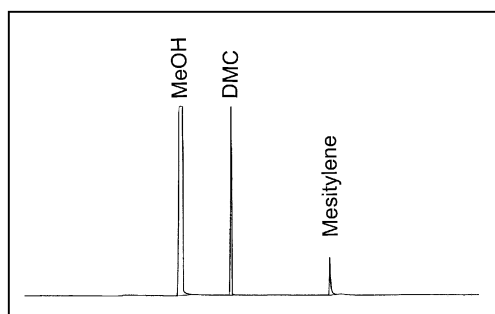


**Fig. 4** GC chart of the reaction mixture. *Reaction conditions:* autoclave with internal recycle (see Fig. 2), dibutyltin dimethoxide (2.0 mmol), methanol (100 mmol), molecular sieve 3A (15 g), carbon dioxide (total pressure 300 atm), 180 °C, 72 h. DMC yield 46% based on starting methanol. GC conditions: TC-WAX (60 m), 40–240 °C, mesitylene as internal GC standard.

**Table 1** Effect of molecular sieve 3A on the DMC synthesis from carbon dioxide and methanol<sup>a</sup>

Entry	Dehydrating agent	DMC yield (%) <sup>b</sup>
1	None	2.1
2	Pellet (1.5 mm diam. × 3.2 mm)	13.3
3	Beads (2 mm)	29.2
4 <sup>c</sup>	Beads (0.3–0.4 mm)	27.0

<sup>a</sup> *Reaction conditions:* autoclave with internal recycle (see Fig. 2), dibutyltin dimethoxide (2.0 mmol), methanol (100 mmol), molecular sieve 3A (15 g), carbon dioxide (total pressure 300 atm), 180 °C, 24 h. <sup>b</sup> Based on methanol <sup>c</sup> Insufficient circulation.

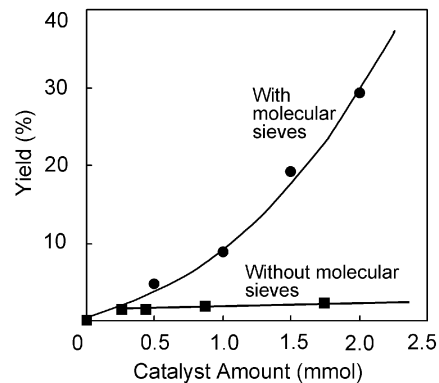


**Fig. 5** Effect of catalyst amount on dimethyl carbonate synthesis from CO<sub>2</sub> and methanol. *Reaction conditions:* autoclave with internal recycle (see Fig. 2), dibutyltin dimethoxide, methanol (100 mmol), molecular sieve 3A (15 g), carbon dioxide (total pressure 300 atm), 180 °C, 24 h. Yields are based on methanol.

proportional to the reaction pressure. A similar relation between the DMC yield and the reaction pressure was observed for DMC synthesis from acetal and CO<sub>2</sub>.<sup>6d,e</sup> There are two factors which can explain the pressure effect: thermodynamics and kinetics. In order to differentiate these factors, the DMC yields at different pressures were plotted vs. the reaction time (Fig. 7) in which the slope of the lines represents the reaction rates. As easily seen, the reaction rate at 300 atm was about three times greater than that at 100 atm proving the importance of the kinetic factor.

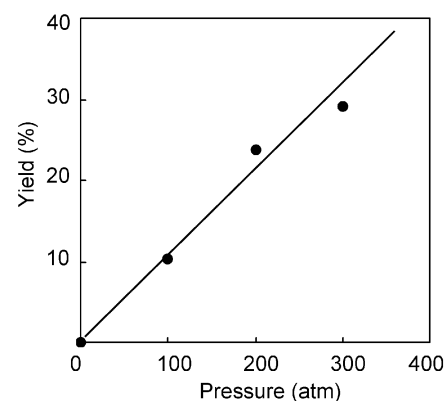


**Fig. 6** Pressure effect on dimethyl carbonate synthesis from CO<sub>2</sub> and methanol. *Reaction conditions:* autoclave with internal recycle (see Fig. 2), dibutyltin dimethoxide (2.0 mmol), methanol (100 mmol), molecular sieve 3A (15 g), carbon dioxide, 180 °C, 24 h. Yields are based on methanol.

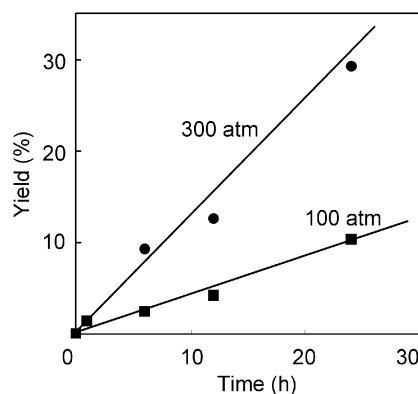


**Fig. 7** Time dependence of dimethyl carbonate synthesis from CO<sub>2</sub> and methanol at different pressures. *Reaction conditions:* autoclave with internal recycle (see Fig. 2), dibutyltin dimethoxide (2.0 mmol), methanol (100 mmol), molecular sieve 3A (15 g), carbon dioxide (total pressure 100 or 300 atm), 180 °C. Yields are based on methanol.

The mechanism of DMC formation by the new reaction system using molecular sieve 3A would be fundamentally the same as that using acetal. Acetal in Scheme 1 can be replaced by molecular sieve 3A. Based on the results of the stoichiometric reaction, DMC formation from  $[\text{R}_2\text{Sn}(\text{OCO}_2\text{Me})(\text{OMe})_2]$  should be slow [Scheme 1, step (ii)].<sup>6c,16</sup> Since  $[\text{R}_2\text{Sn}(\text{OCO}_2\text{Me})(\text{OMe})_2]$  is in equilibrium with  $[\text{R}_2\text{Sn}(\text{OMe})_2]$  [step (i)], the rate of DMC formation should be governed by the concentrations of  $[\text{R}_2\text{Sn}(\text{OMe})_2]$  and  $\text{CO}_2$ . Hence, higher  $\text{CO}_2$  pressure is preferable for achieving higher reaction rates as shown in Figs. 6 and 7.

Finally, the phase behavior of the reaction mixture is summarized as follows based on observations through the sapphire windows. At a relatively low pressure of around 50 atm, two phases (gas–liquid) were clearly observed. With an increase in the pressure, the liquid level rose and the supercritical  $\text{CO}_2$  phase decreased. Eventually, the upper phase disappeared around 200 atm to give a single homogeneous phase (methanol– $\text{CO}_2$  mixture). Based on Figs. 6 and 7, a greater amount of the lower phase is favorable for achieving a higher reaction rate. This is ascribed to a high  $\text{CO}_2$  concentration in the lower phase where DMC is formed.

## Conclusion

We have proved that DMC can be directly synthesized from  $\text{CO}_2$  and methanol with a high methanol conversion. Three important factors for achieving high yields are (a) removal of water from the system, (b) choice of the catalyst, and (c) high  $\text{CO}_2$  pressure. In particular, a new dehydration system using molecular sieves has been proposed. This system is more attractive compared with our previous reports on DMC synthesis using orthoesters or acetals as chemical dehydrating agents since the molecular sieve is easily recyclable, and there is no co-product. We believe that the present paper shows a great possibility of  $\text{CO}_2$  as a phosgene alternative and is encouraging for chemists in the field of  $\text{CO}_2$  utilization. Improvement in the dehydrating method and acceleration of the reaction rate by developing highly active catalysts are the next challenges.

## Experimental

Trimethyl orthoacetate, 2,2-dimethoxypropane, dibutyltin dimethoxide and dibutyltin oxide were purchased from Aldrich Chemical Co. (Milwaukee, WI). Carbon dioxide (Showa Tansan Co., Kawasaki, purity >99.99%) was used without further purification. Reaction products were analyzed by GC using capillary columns: J & W Scientific DB-1 (60 m) and GL Science TC-WAX (60 m) on a Shimadzu GC-9A or GC-17A gas chromatograph equipped with a flame ionization detector (FID) using 1,3,5-trimethylbenzene as an internal standard. GC–MS analysis was performed using a HP-5890 gas chromatograph connected to a HP-5971A mass spectrometer (EI 70 eV).

## General procedure

**(a) Without internal recycle.** In a stainless steel autoclave (20 cm<sup>3</sup> inner volume), carbon dioxide (liquid, 65 atm) was added to a mixture of 2,2-dimethoxypropane (10 mmol), dibutyltin dimethoxide (0.2 mmol), methanol (200 mmol) and 1,3,5-trimethylbenzene (50  $\mu\text{l}$ ) at room temperature. The initial pressure was adjusted to 300 atm at 180 °C and the autoclave was heated at that temperature for 24 h. After cooling, product yield was determined by GC and the products were further

identified using GC–MS by the comparison of retention times and fragmentation patterns with authentic samples.

**(b) With internal recycle.** The reactions using a dehydration tube packed with molecular sieve 3A were carried out in a stirred autoclave shown in Fig. 2. In a stainless steel autoclave (20 cm<sup>3</sup> inner volume), carbon dioxide (liquid, 65 atm) was added to a mixture of dibutyltin dimethoxide (2.0 mmol), methanol (100 mmol) and 1,3,5-trimethylbenzene (50  $\mu\text{l}$ ) at room temperature. The dehydration tube was packed with molecular sieve 3A (15 g). The initial pressure was adjusted to 300 atm at 180 °C and the autoclave was heated at that temperature for 24 h. A part of the reaction mixture was circulated through a high pressure circulation pump (Nitto Koatsu MP-1000). After the reaction, carbon dioxide was released and the resulting liquid was analyzed by GC and GC–MS.

**High pressure NMR and IR.** High-pressure NMR spectra were recorded on a JEOL LA400WB spectrometer (400 MHz for <sup>1</sup>H) using sapphire tubes designed by Horvath and Millar.<sup>17</sup> High-pressure IR spectra were measured on a JASCO FT/IR-5300 using a high pressure cell with zinc sulfide windows.

## Acknowledgments

The authors are indebted to Professor Istvan T. Horvath for generous information about high-pressure NMR tube assembly. The authors also thank the New Energy and Industrial Technology Development Organization (NEDO) of Japan for generous financial support to L.-N. H.

## References

- (a) P. T. Anastas and J. C. Warner, in *Green Chemistry, Theory and Practice*, Oxford University, Oxford, 1998; (b) A. S. Matlack, in *Introduction to Green Chemistry*, Marcel Dekker, Basel, 2001.
- (a) P. G. Jessop, T. Ikariya and R. Noyori, *Science*, 1995, **269**, 1065; (b) P. G. Jessop, T. Ikariya and R. Noyori, *Chem. Rev.*, 1995, **95**, 259; (c) P. G. Jessop, T. Ikariya and R. Noyori, *Chem. Rev.*, 1999, **99**, 475.
- (a) W. Leitner, *Angew. Chem., Int. Ed. Engl.*, 1995, **34**, 2207; (b) *Chemical Synthesis Using Supercritical Fluids*, ed. P. G. Jessop and W. Leitner, Wiley-VCH, Weinheim, 1999.
- D. A. Morgensten, R. M. LeLacheur, D. K. Morita, S. L. Borkovsky, S. Feng, G. H. Brown, L. Luan, M. F. Gross, M. J. Burk and W. Tumas, in *Green Chemistry*, ed. P. T. Anastas and T. C. Williamson, ACS Symposium Series 626; American Chemical Society, Washington, DC, 1996, p. 132.
- M. Aresta and E. Quaranta, *CHEMTECH*, 1997, 32.
- (a) J.-C. Choi, Y. Kobayashi and T. Sakakura, *J. Org. Chem.*, 2001, **66**, 5262; (b) T. Sakakura, Y. Saito, M. Okano, J.-C. Choi and T. Sako, *J. Org. Chem.*, 1998, **63**, 7095; (c) J.-C. Choi, T. Sakakura and T. Sako, *J. Am. Chem. Soc.*, 1999, **121**, 3793; (d) T. Sakakura, J.-C. Choi, Y. Saito, T. Masuda, T. Sako and T. Oriyama, *J. Org. Chem.*, 1999, **64**, 4506; (e) T. Sakakura, J.-C. Choi, Y. Saito and T. Sako, *Polyhedron*, 2000, **19**, 573; (f) L.-N. He, J.-C. Choi and T. Sakakura, *Tetrahedron Lett.*, 2001, **42**, 2169; (g) M. Abila, J.-C. Choi and T. Sakakura, *Chem. Commun.*, 2001, 2238.
- M. A. Pacheco and C. L. Marshall, *Energ. Fuels*, 1997, **11**, 2.
- (a) A.-A. Shaikh and S. Sivaram, *Chem. Rev.*, 1996, **96**, 951; (b) P. Tundo, M. Selva and S. Memoli, *ACS Symp. Ser.*, 2000, **767**, 87; (c) P. Tundo, *Pure Appl. Chem.*, 2000, **72**, 1793.
- (a) S.-i. Fujita, B. M. Bhanage, Y. Ikushima and M. Arai, *Green Chem.*, 2001, **3**, 87; (b) S. Fang and K. Fujimoto, *Appl. Catal. A*, 1996, **142**, L1.
- S. Sakai, T. Fujinami, T. Yamada and S. Furusawa, *Nippon Kagaku Kaishi*, 1975, 1789.
- N. Yamazaki, S. Nakahama and F. Higashi, *Rep. Asahi Glass Found. Ind. Technol.*, 1978, **33**, 31.
- (a) J. Kizlink and I. Pastucha, *Collect. Czech. Chem. Commun.*, 1995, **60**, 687; (b) J. Kizlink and I. Pastucha, *Collect. Czech. Chem.*

- Commun.*, 1994, **59**, 2116; (c) J. Kizlink, *Collect. Czech. Chem. Commun.*, 1993, **58**, 1399.
- 13 (a) Y. Ikeda, T. Sakahori, K. Tomishige and K. Fujimoto, *Catal. Lett.*, 2000, **66**, 59; (b) K. Tomishige, T. Sakahori, Y. Ikeda and K. Fujimoto, *Catal. Lett.*, 1999, **58**, 225; (c) K. Tomishige, Y. Ikeda, T. Sakahori and K. Fujimoto, *J. Catal.*, 2000, **192**, 355.
- 14 T. Zhao, Y. Han and Y. Sun, *Fuel Proc. Tech.*, 2000, **62**, 187.
- 15 N. S. Isaacs, B. O'Sullivan and C. Verhaelen, *Tetrahedron*, 1999, **55**, 11949.
- 16 D. Ballivet-Tkatchenko, O. Douteau and S. Stutzmann, *Organometallics*, 2000, **19**, 4563.
- 17 I. T. Horvath and J. M. Millar, *Chem. Rev.*, 1991, **91**, 1339.



# Selective partial oxidation in supercritical water: the continuous generation of terephthalic acid from *para*-xylene in high yield

Paul A. Hamley,<sup>a</sup> Thomas Ilkenhans,<sup>a</sup> Jeremy M. Webster,<sup>a</sup> Eduardo Garcia-Verdugo,<sup>a</sup> Eleni Venardou,<sup>a</sup> Matthew J. Clarke,<sup>a</sup> Rita Auerbach,<sup>a</sup> W. Barry Thomas,<sup>b</sup> Keith Whiston<sup>b</sup> and Martyn Poliakoff<sup>\*a</sup>

<sup>a</sup> School of Chemistry, The University of Nottingham, Nottingham, UK NG7 2RD.

E-mail: Martyn.poliakoff@nottingham.ac.uk

<sup>b</sup> DuPont Polyester Technologies, PO Box 2002, Wilton, Middlesbrough, UK TS90 8JF

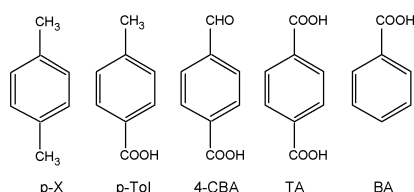
Received 27th February 2002

First published as an Advance Article on the web 24th April 2002

The continuous selective oxidation of *p*-xylene (*p*-X) by O<sub>2</sub> (generated by thermal decomposition of aqueous H<sub>2</sub>O<sub>2</sub>) catalyzed by MnBr<sub>2</sub> in supercritical H<sub>2</sub>O at *ca.* 400 °C is reported for the first time. The selectivity for terephthalic acid (TA) is >90%. Compared to existing industrial processes, the reaction has the potential for a significant increase in energy efficiency and a substantial reduction in waste. This reaction is significant because the presence of H<sub>2</sub>O lowers the catalytic activity of MnBr<sub>2</sub> in the conventional route to TA *via* oxidation of *p*-X in CH<sub>3</sub>COOH.

## Introduction

Terephthalic acid, TA, is a major commodity chemical and an important intermediate for the production of polyester polymers. The various routes for the manufacture of TA have recently been reviewed.<sup>1</sup> Current state-of-the-art technology involves the continuous liquid phase oxidation of *p*-xylene (*p*-X) using molecular O<sub>2</sub> in a lower (*e.g.* C<sub>2</sub>–C<sub>6</sub>) aliphatic monocarboxylic acid, *e.g.* CH<sub>3</sub>CO<sub>2</sub>H, with a homogeneous heavy metal catalyst system usually incorporating a promoter, *e.g.* bromine. CH<sub>3</sub>CO<sub>2</sub>H is particularly useful as the solvent since it is relatively resistant to oxidation and increases the activity of the catalytic pathway. The reaction is typically carried out on a very large scale in a stirred reactor at 150–250 °C and 0.6–3 MPa and the optimized process is highly selective with a yield of TA of at least 95%. The oxidation is a free radical process, the mechanism of which has been investigated in detail;<sup>2</sup> key intermediates include *p*-toluic acid (*p*-Tol) and 4-carboxybenzaldehyde (4-CBA). In addition, benzoic acid (BA) can be formed *via* decarboxylation of TA and other intermediates.



Generally, the TA obtained in the commercial oxidation is insufficiently pure for direct use in polyester production since it contains 4-CBA as a major impurity along with various colour-forming precursors and coloured impurities. 4-CBA is usually present because a substantial proportion of the TA precipitates during the course of the reaction and, although 4-CBA may be below its solubility limit, it tends to co-precipitate with TA. Thus, the crude TA has to be purified before it can be used in production of polyester. Purification typically involves dissolving the impure TA in water at high temperature, followed by hydrogenation in the presence a supported noble metal catalyst.

This step reduces the 4-CBA to *p*-Tol and converts the various coloured impurities to colourless products. The purified TA is then recovered from solution by a series of crystallisation, solid–liquid separation and drying steps. *p*-Tol is considerably more soluble than TA in H<sub>2</sub>O and remains in the aqueous mother liquor following crystallisation of TA.<sup>3,4</sup>

High purity TA can be obtained by carrying out the oxidation in a different, continuous process<sup>5</sup> with a high solvent:*p*-X ratio. Co-precipitation of 4-CBA with TA is largely avoided since the TA is not allowed to precipitate in any quantity during the reaction. Furthermore, the conditions necessary to achieve this also promote oxidation of 4-CBA and other intermediates to a greater extent than conventionally. However, a continuous process of this type necessarily involves using substantial amounts of organic solvent. Such solvents are relatively costly and, due to environmental restrictions, may require recovery and recycling. In addition, CH<sub>3</sub>CO<sub>2</sub>H is flammable when mixed with air or O<sub>2</sub> under typical reaction conditions; this means that a proportion of the organic solvent may be ‘lost’ due to oxidation during the process.

Supercritical H<sub>2</sub>O, scH<sub>2</sub>O (*T*<sub>c</sub> = 374 °C, *p*<sub>c</sub> = 22.1 MPa) has been widely investigated as a medium for the *total* oxidation of organic waste because of the relatively high solubility of many organic compounds in scH<sub>2</sub>O and its complete miscibility with

## Green Context

The use of supercritical or high temperature water as a medium for the total oxidation of organics is well known as a method of waste destruction. However, the selective oxidation of hydrocarbons in this medium has received little attention, despite the potential benefits of water as a reaction medium. This article describes a very efficient and high yielding continuous oxidation of *p*-xylene to terephthalic acid using oxygen in supercritical water. The selectivity to product is very high, and over-oxidation is not a problem. In contrast to the current commercial process, solvent oxidation does not occur, providing a clean and effective route to this important product. *DJM*



O<sub>2</sub>.<sup>6–8</sup> In 1998, Holliday *et al.* described a batch process for the synthesis of, *inter alia*, aromatic carboxylic acids from alkyl aromatics in a reaction medium of sub-critical H<sub>2</sub>O using molecular O<sub>2</sub> as the oxidant.<sup>9</sup> In particular, they reported that TA could be generated at ≤64% yield by the selective oxidation of *p*-X at 300–330 °C with O<sub>2</sub> gas as the oxidant and MnBr<sub>2</sub> as the most effective catalyst. A recent paper by Dunn and Savage<sup>10</sup> confirms these findings and explored the reaction conditions in greater depth. It also suggested that Holliday's analytical method might not have distinguished between TA and other acids formed as part of the oxidation process. Both of these studies<sup>9,10</sup> were carried out in sealed autoclaves as batch reactions and represent the first examples of selective oxidation in near-critical or scH<sub>2</sub>O. If the reaction could be made continuous and more selective, it would be potentially attractive for the manufacture of TA, as the need for the CH<sub>3</sub>CO<sub>2</sub>H solvent would be eliminated and the higher temperatures could give enhanced energy recovery. Recently, one of the first examples of continuous partial oxidation in scH<sub>2</sub>O was reported;<sup>11</sup> the oxidation of cyclohexane, which was relatively unselective both uncatalysed and in reactors lined with noble metals. Here we report the first results from a long-running and successful project aimed at developing the continuous laboratory scale selective oxidation of *p*-X by O<sub>2</sub> in scH<sub>2</sub>O.

Initially, reactions were tested in a 3 mL batch reactor, made from 316L grade stainless steel, similar to that described elsewhere.<sup>12</sup> These tests showed that, even without any added catalyst, oxidation of *p*-X could yield up to 44% TA (10 min, 308 °C) and, with an MnBr<sub>2</sub> catalyst, up to 70% TA could be generated in H<sub>2</sub>O from *p*-X in the presence of a large excess of O<sub>2</sub> (*p*-X:O<sub>2</sub> 1:36; 10 min, 315 °C, 15.6 MPa). The high excess of O<sub>2</sub> may have been needed because the narrow bore of our batch reactor impedes efficient mixing of the gas and liquid phases. The major difference between our experiments and Holliday's<sup>9</sup> was that we used lower concentrations of MnBr<sub>2</sub> (1000 ppm of bromide as opposed to 7000 ppm) but our overall concentration of *p*-X was also considerably lower.

The continuous oxidation of *p*-X by O<sub>2</sub> was carried out in H<sub>2</sub>O from 200–400 °C and 24–28 MPa with MnBr<sub>2</sub> as the catalyst. The exotherm was minimised by using relatively dilute solutions (<5% organic w/w). Initial experiments were carried out with compressed O<sub>2</sub> but it was found to be difficult to control the gas on the small scale required for this work. Therefore, we have used aqueous H<sub>2</sub>O<sub>2</sub>, which decomposes in the preheater to generate O<sub>2</sub>. Tester and co-workers have shown that there are no significant differences in the oxidation of MeOH in scH<sub>2</sub>O using either O<sub>2</sub> or decomposed H<sub>2</sub>O<sub>2</sub> as the oxidant.<sup>13</sup> The configuration of the system is shown in Fig. 1, where the key feature is the cross-piece, X, where a mixture of scH<sub>2</sub>O and O<sub>2</sub> is contacted with separate streams of *p*-X and a cold solution of MnBr<sub>2</sub>.<sup>14</sup> In the conventional process, Mn<sup>2+</sup> acts as a homogeneous catalyst.<sup>2</sup> However, in scH<sub>2</sub>O, the Mn catalyst can rapidly hydrolyse and dehydrate to form solid oxides like many other transition metal salts.<sup>15–19</sup> The arrangement shown in Fig. 1 allows catalysis to occur before the Mn catalyst has had time to decompose. To demonstrate the need for this configuration, a control experiment was run mixing the catalyst solution (1000 ppm bromide) with H<sub>2</sub>O and high pressure gaseous O<sub>2</sub> prior to preheating to 385 °C and 24 MPa. With 1% *p*-X added downstream of the preheater, the maximum carbon recovery in the solid product was 22–69% w/w with a yield of TA only between 11–18%. Subsequent inspection of the preheater showed significant corrosion to the internal surface of the pipework with a black precipitate (MnO<sub>2</sub> by XRD) coating the pipework. By contrast, up to 90% of the MnBr<sub>2</sub> was recovered in the product solution (Mn: AAS, Br: AgNO<sub>3</sub> titration) by using the mixing arrangement shown in Fig. 1.

The results from a selection of runs are summarised in Table 1. Taken together, the results demonstrate the selective

oxidation of *p*-X to TA can be achieved in scH<sub>2</sub>O. The yield of TA is highly sensitive to a range of variables, including the ratios *p*-X:O<sub>2</sub> and *p*-X:catalyst, the reactor residence time, and the reactor temperature. In general, the selectivities in optimized runs were steady over a period of hours, see Fig. 2, but the overall yields often fluctuated because of minor inconsistencies in the performance of the various components, which are inevitable in so small a reactor of this complexity. Nonetheless, the best yields of TA (examples 10–13) have exceeded 90%, close to those of the current optimized industrial process. The purity of the best recovered samples of TA contained lower levels of oxidation intermediates than commercial crude TA.

Run 1 is a typical unoptimized run with modest overall yield and poor selectivity for TA. Doubling the residence time and increasing the O<sub>2</sub> feed, run 2, reduces the yield of solids but increases the selectivity for TA over the key impurity 4-CBA. By contrast, halving the residence time produces a striking improvement in both the yield and the selectivity for TA, run 3. Increasing the residence time and simultaneously reducing the reactor temperature from 400 to 350 °C, run 4, still gave ca. 50% yield of solid with reasonable selectivity for TA. Reducing the temperature further with low concentrations of catalyst, runs 5–7, almost completely stopped the reaction with no isolable solid products. However, the yield at 300 °C could be restored by increasing the catalyst concentration to 1632 ppm Br; even 45% of the stoichiometric amount of O<sub>2</sub> gave modest amounts of TA, run 8, and 178% O<sub>2</sub> with the mixing zone heated to 378

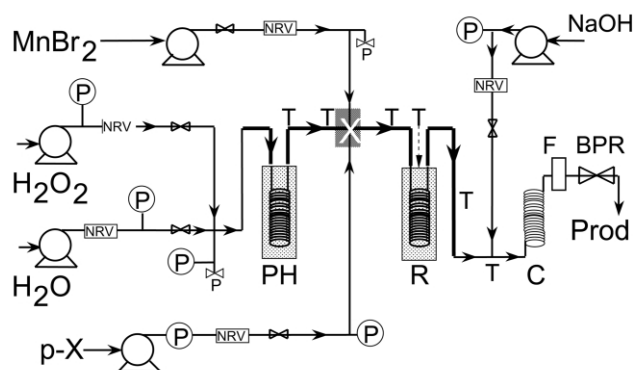


**Fig. 1** Diagram of the continuous reactor for oxidation of *p*-X. A solution of H<sub>2</sub>O<sub>2</sub> is pumped into a tee-piece where it is mixed with cold water. The H<sub>2</sub>O<sub>2</sub>/H<sub>2</sub>O mixture is then heated to ca. 400 °C in the preheater, PH, consisting of a 6 m coil of 1/4 inch o.d. stainless pipe cast into an aluminium block where the H<sub>2</sub>O<sub>2</sub> decomposes to O<sub>2</sub>.<sup>20</sup> The O<sub>2</sub> + H<sub>2</sub>O fluid now passes through the cross-piece, X, where it is contacted with the *p*-X and solution of MnBr<sub>2</sub> catalyst, fed in from their own pumps (the precise mixing geometry is important for the success of the process). The reaction mixture is passed through the reactor, R, which is identical to PH (for short residence times R can be replaced by a short length of Hastelloy tubing). After R, a 4% solution of cold NaOH is injected to prevent precipitation of TA, before the solution passes through the cooling coil, C, and back-pressure regulator, BPR. Other components are labelled as follows: valves ("P" indicates a pressure release valve); F, 0.5 μm filter; NRV, non-return valves; P, pressure transducer; Prod, products; T, thermocouple (the aluminium heater blocks of PH and R also contain thermocouples, not shown); lagged pipework is shown as a thicker line. Br<sup>-</sup> rapidly induces stress-corrosion cracking in stainless steel at high temperatures with corrosion rates being highest in regions of steep thermal gradients.<sup>21</sup> This effect is exacerbated in small-scale apparatus because the temperature gradients are usually steeper than in large equipment. Therefore, Hastelloy is used for the final section of the catalyst feed-pipe and other areas of high corrosion. All pipe work liable to corrosive failure is protected inside wider bore stainless steel pressure tubing to contain any inadvertent leaks. (NB: The Figure is not drawn to scale and safety trips connected to the more critical pressure transducers have been omitted. NaOH would almost certainly not be needed in larger scale apparatus, where the larger bore of the pipe work would reduce the problems of blocking. The NaOH also causes precipitation of the Mn<sup>2+</sup> which can be recovered from the filter, F, as metal oxide/hydroxides. The absence of Mn<sup>2+</sup> in the product solution was confirmed by atomic absorption. The flow rate of NaOH is adjusted to match the expected flow of TA with a × 2 excess of NaOH. PH and R supplied by NWA GmbH; Pumps, Gilson 305 or equivalent; BPR, Tescom, model 26-1722-24-090).

**Table 1** Continuous oxidation of *p*-xylene in scH<sub>2</sub>O at 25.0 MPa

Run	Reactor conditions		Feed		MnBr <sub>2</sub> Catalyst, [Br <sup>-</sup> ]/ppm	Results for product					
	Res. time <sup>a/</sup> min	T/°C	<i>p</i> -X <sup>b</sup> (%)	O <sub>2</sub> <sup>c</sup> (%)		Yield of all solids <sup>d</sup> (%)	Analysis of products <sup>e</sup>				
							TA (%)	4-CBA (%)	<i>p</i> -Tol (%)	BA (%)	By-prods. (%)
1	1.09	400	0.58	87–93	1632	26–37	12.9–25.5	8.0–22.4	14.4–40.8	1.4–5.2	1.1–2.9
2	2.17	400	0.58	111	1632	13–30	9.3–21.3	0–1.6	5.9–12.0	4.9–7.9	0–0.9
3	0.54	400	0.58	115	1632	71	51.9–63.8	0	0–5.95	5.9–11.8	0–1.6
4	2.08	350	0.7	120	975	45–61	45.3–61.2	3.2	6.58–17.6	6.2–9.8	0
5	12.8	300	0.58	149	537	0	0.1–0.4	0	0	0	0.1
6	12.8	250	0.58	149	537	0	0–0.3	0	0–0.14	0	0.2–1.2
7	11.7	200	0.58	149	537	0	0	0	0–13.9	0	0–1.2
8	2.42	300	0.58	45	1632	13–98	13.0–26.4	8.5–11.5	35.4–64.1	2.4–3.7	4.3–5.6
9	2.43	300 <sup>f</sup>	0.58	178	1632	42–81	71.6–81.8	0	0	4.9–7.1	0
10	0.3	400 <sup>g</sup>	0.58	120	1640	72–100	91.8–94.1	0	0	5.8–8.2	0
11	0.3	400 <sup>g</sup>	1.5	180	1640	69–95	92.1–93.8	0	0	6.3–8.0	0
12	0.15	400 <sup>g</sup>	1.5	180	1640	74–90	93.5–95.3	0	0	4.7–6.5	0
13	0.15	400 <sup>g</sup>	2.0	120	1640	79–85	92.1–95.1	0	0	4.9–7.9	0

<sup>a</sup> The residence time was defined as the total reactor volume divided by the volumetric flow-rate. The total volume was taken as the sum of the volume of the tubular reactor, pipework and fittings between the mixing pieces; the first to mix the reactants to initiate the reaction and the second to quench the reaction with the addition of NaOH. The volumetric flow-rate was based on the physical properties of H<sub>2</sub>O at the mixing conditions, as published in International Steam Tables and by the US National Institute of Standards and Technology. <sup>b</sup> *p*-X concentration in reactor (w/w). <sup>c</sup> 3 mol of O<sub>2</sub>, the stoichiometric amount needed to convert *p*-X to TA is taken to be 100%. <sup>d</sup> Yield calculated for aliquots collected over 30 min periods (every 15 min for runs 11–13). <sup>e</sup> Analysis by HPLC of recovered solution (see Experimental section); maximum range of values found by analysing all of the samples collected during the course of a particular run. <sup>f</sup> Mixing zone held at 378 °C. <sup>g</sup> Temperature at mixing piece, followed by a smaller volume reactor, constructed from a 50 cm length of ¼ inch o.d. Hastelloy C276 pipework.

°C, run 9, gave yields comparable to those observed by Holliday *et al.*<sup>9</sup> and by us in batch reactions at similar temperatures.

By contrast, the best yields and selectivities were obtained by using a shorter reactor to give very short residence times, < 20 s. Runs 10–13 all demonstrate more than 90% selectivity for TA, with no detectable 4-CBA or *p*-Tol. The yields are relatively insensitive to changes in residence time and concentration of O<sub>2</sub> at these conditions. The only major impurity identified is BA, which off-line experiments in our batch reactor have shown can be formed in modest amounts by heating TA in scH<sub>2</sub>O. Additional measurements were carried out to confirm the overall mass balance for the continuous oxidation. Thus, a solid product with a composition of 92.1% w/w TA and 7.9% w/w BA was collected over a timed interval of 15 min in run 13. In this period, 0.681 g of *p*-X was fed to the experimental unit and the solid recovered was 1.009 g giving a measured carbon recovery of 97.4%.

Our results suggest that the mechanism of oxidation of TA in scH<sub>2</sub>O is similar to that in CH<sub>3</sub>COOH although the presence of

high amounts of water (> 4–5%) is known<sup>2</sup> to reduce the activity of MnBr<sub>2</sub> drastically at 200 °C. We suggest that the catalyst is not deactivated so strongly in scH<sub>2</sub>O because the polarity of the supercritical fluid is lower than that of liquid H<sub>2</sub>O. The concentration of MnBr<sub>2</sub> is substantially less than that used by Holliday *et al.*<sup>9</sup> but our concentration of *p*-X is also substantially lower.

In this paper, we have shown for the first time that it is possible to oxidize *p*-X continuously in scH<sub>2</sub>O with high selectivity for TA. Most of the experimental difficulties associated with the small-scale of our apparatus have been overcome and a systematic investigation of reaction conditions is now possible. Even without complete optimization, the process generates almost no 4-CBA, one of the most problematic impurities in current commercial processes for manufacturing TA. Furthermore, the process totally eliminates the use of organic solvents and has promise as a potentially cleaner route to manufacture of TA.

## Experimental

**CAUTION:** This type of oxidation is potentially extremely hazardous, and **must** be approached with care and a thorough safety assessment must be made.

Before each run, the apparatus was hydrostatically pressure tested when cold, and was then heated with a flow of pure water (5–10 ml min<sup>-1</sup>). Once the operating temperature had been reached, the pumps for *p*-X, H<sub>2</sub>O<sub>2</sub>, MnBr<sub>2</sub> and NaOH were started. Typically, an experiment was run for 4–8 h. The products were collected for sequential periods of 15–60 min and analysed. A weighed portion of the product solution was acidified with 2 M HNO<sub>3</sub> (alternatively H<sub>2</sub>SO<sub>4</sub> or HCl could be used) to precipitate TA and other components. The solid was filtered off, washed with cold distilled H<sub>2</sub>O and air dried in a desiccator over silica gel and weighed. Purity was verified principally by HPLC. The TA was recovered and the yield calculated as a percentage of the stoichiometric amount expected from the measured amount of *p*-X pumped into the apparatus.

As pointed out by Dunn and Savage,<sup>10</sup> reproducible analysis of TA is quite challenging. The selectivity was determined by

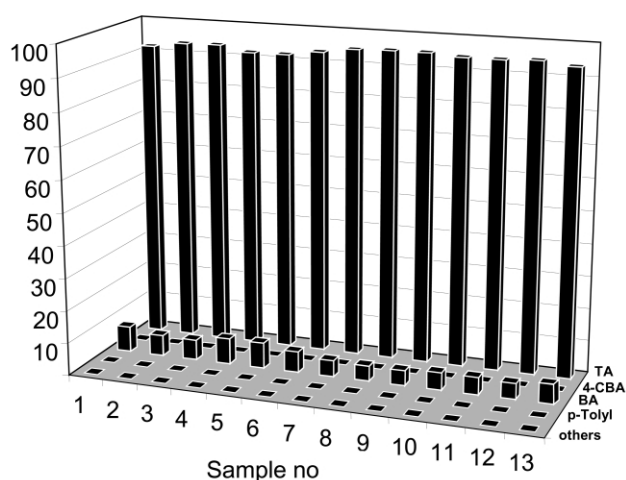


**Fig. 2** Plot showing the variation in selectivity observed during a continuous run. Samples were collected at 15 min intervals after the reactor had reached stable conditions, as listed in run 13 in Table 1. Others refers to the by-products as listed in the Experimental section.

direct injection of the solution recovered from the reactor onto an HPLC column using a method specially developed for these experiments. Gradient elution with solvents CH<sub>3</sub>CN (16.7%) and buffer (83.3 to 60% and back to 83.3%) was used. The stock buffer solution was prepared by dissolving 15 g anhydrous CH<sub>3</sub>CO<sub>2</sub>Na in 250 ml de-ionised water, before adding CH<sub>3</sub>CO<sub>2</sub>H (50%, 100 ml). The pH was adjusted to 3.9 ± 0.01 with 5% CH<sub>3</sub>CO<sub>2</sub>H, before diluting to 500 ml. The dilute buffer was prepared by diluting 30 mL of the stock buffer solution to 500 ml with de-ionised water. The injection volume with needle wash was 1 µL. A Waters Xterra reverse phase C18 column, maintained at 40 °C, was used (flow rate 0.7 ml min<sup>-1</sup>, run time 14 min; UV detection at 230 nm). The oxidation intermediates analysed were 4-carboxybenzaldehyde (4-CBA), *p*-toluic acid (*p*-Tol) and benzoic acid (BA). In addition, some samples were analysed for minor by-products, including 2,6-dicarboxyfluorenone, isophthalic acid, benzene-1,2,4-tricarboxylic acid, 2,4',5'-tricarboxybiphenyl, diphenic acid, 4,4'-dicarboxybenzophenone, 2,6-dicarboxyanthraquinone, 2,6-dicarboxyfluorene and 2,6-dicarboxyanthracene. GC analysis was also used on some samples to determine volatile components, *e.g.* unreacted *p*-X.

## Acknowledgements

We thank EPSRC (Grant Nos GR/K84929 & GR/N06892), ICI Engineering Technology, DuPont Polyester Technologies, NWA GmbH and the Gatsby Foundation for their support. We are grateful to Dr C. Boix, Dr A. Cabañas, Dr J. A. Darr, Dr M. W. George, Dr D. A. Graham, Dr D. H. Gregory, Mr M. Guyler, Dr S. M. Howdle, Dr G. H. Jones, Dr P. Kritzer, Dr E. Lester, Dr R. Oliver, Dr W. Partenheimer, Prof. G. Pattenden, Dr K.-H. Pickel, Dr R. J. Pulham, Dr J. Runnacles, Dr P. Saxton and Mr. K. Stanley for their help and advice.

## References

- 1 K. Weissermel and H.-J. Arpe, in *Industrial Organic Chemistry*, Weinheim, 1997.
- 2 W. Partenheimer, *Catal. Today*, 1995, **23**, 69.
- 3 E. Hindmarsh, J. A. Turner and A. M. Ure, Process for the production of terephthalic acid, *Eur. Pat.*, EP-A-0502628, 1991.
- 4 E. Hindmarsh, J. A. Turner and D. Parker, Process for the production of terephthalic acid, *Eur. Pat.*, EP-A-0498591, 1991.
- 5 J. A. Turner, D. J. Royall, D. S. Hugall, G. H. Jones and D. Woodcock, Process for the production of terephthalic acid, *World. Pat.*, WO-A-98/38150, 1998.
- 6 R. W. Shaw, T. B. Brill, A. A. Clifford, C. A. Eckert and E. U. Franck, *Chem. Eng. News*, 1991, **69**, 26.
- 7 P. E. Savage, *Chem. Rev.*, 1999, **99**, 603.
- 8 P. E. Savage, S. Gopalan, T. I. Mizan, C. J. Martino and E. E. Brock, *AIChE J.*, 1995, **41**, 1723.
- 9 R. L. Holliday, B. Y. M. Jong and J. W. Kolis, *J. Supercrit. Fluids*, 1998, **12**, 255.
- 10 J. B. Dunn and P. E. Savage, *Ind. Eng. Chem. Res.*, 2002, released on the web.
- 11 R. Richter and H. Vogel, *Chem. Ing. Tech.*, 2001, **73**, 1165.
- 12 P. Aleman, C. Boix and M. Poliakoff, *Green Chem.*, 1999, **1**, 65.
- 13 B. D. Phenix, J. L. DiNaro, J. W. Tester, J. B. Howard and K. A. Smith, *Ind. Eng. Chem. Res.*, 2002, **41**, 624.
- 14 D. A. Graham, P. A. Hamley, T. Ilkenhans, M. Poliakoff and D. Woodcock, Production of Aromatic Carboxylic Acids, *World Pat.*, WO 02/02201, 2002.
- 15 T. Adschiri, K. Kanazawa and K. Arai, *J. Am. Ceram. Soc.*, 1992, **75**, 1019.
- 16 R. L. J. Smith, P. Atmaji, Y. Hakuta and K. Arai, in *Separation of metals from sim waste streams*, ed. P. Rudolph von Rohr and C. Trepp, Elsevier, Netherlands, 1996.
- 17 A. Cabañas, J. A. Darr, E. Lester and M. Poliakoff, *Chem. Commun.*, 2000, 901.
- 18 A. Cabañas and M. Poliakoff, *J. Mater. Chem.*, 2001, **11**, 1408.
- 19 K. J. Ziegler, R. C. Doty, K. P. Johnston and B. A. Korgel, *J. Am. Chem. Soc.*, 2001, **123**, 7797.
- 20 E. Croiset, S. F. Rice and R. G. Hanush, *AIChE J.*, 1997, **43**, 2343.
- 21 P. Kritzer, N. Boukis and E. Dinjus, *J. Supercrit. Fluids*, 1999, **15**, 205.



# Aminoalkyl modified polysilsesquioxanes; synthesis, characterisation and catalytic activity in comparison to related aminopropyl modified silicas

Nazli Al-Haq, Ramkrishna Ramnauth, Stefan Kleinebiekel, Duan Li Ou, Alice C. Sullivan\* and John Wilson

Department of Chemistry, Queen Mary and Westfield College, Mile End Road, London, UK  
E1 4NS. E-mail: a.c.sullivan@qmul.ac.uk

Received 22nd January 2002

First published as an Advance Article on the web 17th April 2002

In this paper we report on the sol-gel synthesis and characterisation (by  $^{29}\text{Si}$  CPMAS and SPE MAS,  $^{13}\text{C}$  CPMAS NMR and elemental analysis as well as nitrogen sorption porosimetry) of new aminopropylated polysilsesquioxanes of types  $[(\text{RO})_{3-n}\text{O}_{n/2}\text{SiC}_6\text{H}_4\text{SiO}_{n/2}(\text{OR})_{3-n}]_x[(\text{RO})_{3-n}\text{SiO}_{n/2}(\text{CH}_2)_3\text{NH}_2]_y$  and  $[(\text{RO})_{3-n}\text{O}_{n/2}\text{SiC}_6\text{H}_4\text{SiO}_{n/2}(\text{OR})_{3-n}]_x[(\text{RO})_{3-n}\text{SiO}_{n/2}(\text{CH}_2)_3\text{NH}_2]_y[(\text{RO})_{4-n}\text{O}_{n/2}\text{Si}]_z$  and  $[(\text{RO})_{6-2n}\text{O}_n\text{Si}_2\text{C}_6\text{H}_4]_x[(\text{RO})_{3-n}\text{SiO}_{n/2}(\text{CH}_2)_2\text{NH}(\text{CH}_2)_2\text{NH}_2]_y$ . The catalytic activity of these new polysilsesquioxane supported solid bases in Knoevenagel condensation reactions is described and compared with related aminopropylated silica systems.

## Introduction

The idea underpinning work in this paper was that homogeneously dispersed hydrophobic (organic) regions in polysilsesquioxanes,  $[(\text{RO})_{3-n}\text{O}_{n/2}\text{Si}-\text{Z}-\text{SiO}_{n/2}(\text{OR})_{3-n}]_x$  where Z is an organic spacer, might offer advantages over related purely inorganic support materials *e.g.* mesoporous silicas, for chemistry involving organic substrates. We report here on the assessment of this idea using a new series of solid-bases, aminopropylated polysilsesquioxanes,  $[(\text{RO})_{3-n}\text{O}_{n/2}\text{SiC}_6\text{H}_4\text{SiO}_{n/2}(\text{OR})_{3-n}]_x[(\text{RO})_{3-n}\text{SiO}_{n/2}(\text{CH}_2)_3\text{NH}_2]_y$ , as a catalytic model. Prior to undertaking this study we investigated the relative efficiency of porous silicas and polysilsesquioxanes  $[(\text{RO})_{3-n}\text{O}_{n/2}\text{SiCH}_2\text{C}_6\text{H}_4\text{CH}_2\text{SiO}_{n/2}(\text{OR})_{3-n}]_x^1$  for partition of aromatic compounds from water (details below). The results show that initial uptake is accomplished much faster by hydrophobic porous polysilsesquioxanes than porous inorganic silicas. The initial positive indications that polysilsesquioxanes offer effective partition suggested that functional polysilsesquioxanes might offer effective catalytic media for organic substrates. Macquarrie *et al.* have published extensively on Knoevenagel condensation chemistry catalysed by aminopropyl modified silicas.<sup>2-4</sup> Given that these studies provide an excellent basis for qualitative comparison, we set out to prepare a related series of aminopropyl modified polysilsesquioxanes and to use Knoevenagel condensation chemistry as a means of assessing their base-catalytic activities.

## Results and discussion

The presence of organic framework fragments Z in porous T-functional polysilsesquioxanes  $[(\text{RO})_{3-n}\text{O}_{n/2}\text{Si}-\text{Z}-\text{SiO}_{n/2}(\text{OR})_{3-n}]_x$  should provide pore environments which are more lipophilic than is the case for purely inorganic porous silica. We tested this idea in a simple experiment involving 10 cm<sup>3</sup> aliquots of saturated aqueous naphthalene solution and 0.1 g of a particular porous material. The UV spectrum of the solution

(filtered through 0.2  $\mu\text{m}$  membrane) was recorded after 1 and 16 h. Porous materials used included microporous polysilsesquioxanes  $[(\text{HO})_{3-n}\text{O}_{n/2}\text{CH}_2\text{SiC}_6\text{H}_4\text{CH}_2\text{SiO}_{n/2}(\text{OH})_{3-n}]_x$ , X1, ( $n = 2.25$ ) from deconvoluted NMR with average pore size 20  $\text{\AA}$ , (X1 prepared from 1,4-bis( $\text{Cl}_3\text{SiCH}_2$ )<sub>2</sub> $\text{C}_6\text{H}_4$ ),<sup>1</sup> 1,4-bis(trichlorosilylmethyl)benzene); microporous silica  $[(\text{EtO})_{4-n}\text{O}_{n/2}\text{Si}]_x$  (543 m<sup>2</sup> g<sup>-1</sup>), average pore size 20  $\text{\AA}$  (from acid catalysed sol-gel processed TEOS,  $(\text{EtO})_4\text{Si}$ , tetraethylorthosilicate) and the commercial silica Merck K-100 (316 m<sup>2</sup>g<sup>-1</sup>). The extent of partition of naphthalene from the aqueous solution was monitored by the change in absorbance of the  $\pi-\pi^*$  transition. The results are illustrated in spectra shown in Fig. 1.

While it is apparent that up-take of naphthalene by the porous silicas investigated is slow even after 16 h, the naphthalene was readily taken up by the polysilsesquioxane in the same period. Thus the lipophilic characteristics of the pore environment in the polysilsesquioxane apparently affords a pronounced partition effect. This observation suggested that comparisons of catalytic behaviour between related functional silicas and polysilsesquioxanes would be worthy of study. To assess this we decided to prepare a series of aminopropyl modified polysilsesquioxanes and to use Knoevenagel condensation chemistry analogous to that already reported for aminopropyl modified silicas, as a means of assessing their base-catalytic activities.

## Green Context

The development of efficient base catalysts is relevant to providing clean C-C bond forming reactions. This article describes some advances in the preparation of amine-silica composite materials which are known to be good base catalysts. The incorporation of organic groups in the walls of the materials helps to promote mass transport to the active site, and thus aids catalytic activity. *DJM*



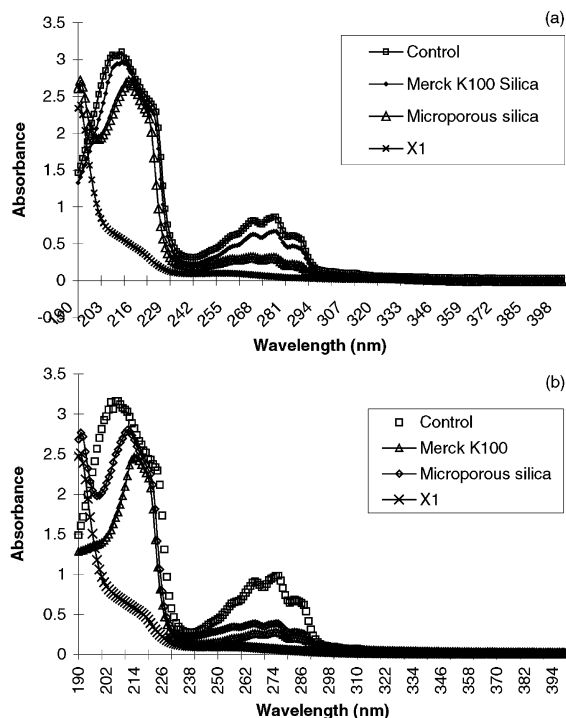


**Fig. 1** (a) UV-vis saturated aqueous naphthalene over porous silicas and polysilsesquioxane, X1 (0.1 g) after 1 h and (b) after 16 h.

### Synthesis and characterisation of aminopropyl modified polysilsesquioxane

A series of aminopropyl modified polysilsesquioxanes  $[(RO)_{3-n}O_{n/2}Si_2C_6H_4SiO_{n/2}(OR)_{3-n}]_x[(RO)_{3-n}SiO_{n/2}(CH_2)_3NH_2]_y$ , APPS, were prepared using  $NH_3$  (aq) catalysed co-polymerisation of the precursors 1,4-bis(triethoxysilyl)benzene, 1,4-((EtO)<sub>3</sub>Si)<sub>2</sub>C<sub>6</sub>H<sub>4</sub>, BTESB<sup>5</sup> and aminopropyltriethoxysilane, AMPS. In addition the material EDEPS, ethylenediaminoethyl modified polysilsesquioxane was prepared from *N*-(3-trimethoxysilylethyl)ethylenediamine, TMSEEDA, and BTESB (see Table 1).

For the sol-gel conditions studied using the BTESB:AMPS system, high surface area materials were only obtained where a BTESB:AMPS ratio of one or greater was used. Thus materials

APPS-4 and APPS-5 were found to have very low surface area and were not further investigated. Spectroscopic details <sup>13</sup>C and <sup>29</sup>Si CP MAS NMR of APPS-1, APPS-3, APPSS-1 and EDEPS-1 are summarised in Table 2.

The <sup>13</sup>C data show the expected organic fragments. The absence of residual ethoxy or methoxy groups (see Fig. 2) indicates that hydrolysis is essentially complete.

In contrast to the efficient hydrolysis step the <sup>29</sup>Si spectra show T<sup>1</sup>, T<sup>2</sup> and T<sup>3</sup> environments for APPS and EDEPS aterials and in addition Q<sup>3</sup>, and Q<sup>4</sup> for APPSS-1, indicating that condensation is incomplete. Deconvolution of the <sup>29</sup>Si CP MAS spectra (details in Table 3) allowed the overall levels of condensation in these materials to be calculated and the values of mostly ~70% are close to those reported for the unfunctionalised polysilsesquioxane itself prepared under base catalysed conditions.<sup>5</sup> Condensation of the T environments in APPSS-1 (60%) was significantly lower than for materials without added TEOS. The average formulae for the materials given in Table 3 are based on measured levels of condensation and measured percentages of carbon and nitrogen. Its noteworthy that the measured mol% of components in the materials after processing and washing is generally close to the mol% of precursors taken. An exception is the Q<sup>n</sup> component of APPSS-1 where the measured Q<sup>n</sup> mol% in the processed material (from <sup>29</sup>Si SPE MAS NMR) represents half of that used. This implies that some soluble Q<sup>n</sup> oligomers are removed at the washing stage.

### Textural studies

Specific surface area measurements were performed on all materials and porosity measurements on samples of APPS-1, APPS-3 and APPSS-1 using nitrogen sorption porosimetry. The results are summarized in Table 4 with isotherms and pore size distributions depicted in Figs. 3 and 4.

For the BTESB:AMPS series the specific surface areas decrease as mol% of AMPS employed increased. Addition of TEOS to the mixture apparently altered this trend with APPSS-1 having a significantly higher surface area than APPS-3. The porosity studies show that materials with large micropores are formed. For APPSS-1 a typical type E hysteresis,<sup>6</sup> suggesting ink-bottle shape pore structure, is seen and the pore size distribution is relatively narrow. APPS-1 and APPS-3 show a bimodal distribution of pores. It is noteworthy that the bimodal

**Table 1** Xerogels used in this study<sup>a</sup>

Xerogel	APPS-1 <sup>b</sup>	APPS-2 <sup>b</sup>	APPS-3 <sup>b</sup>	APPS-4 <sup>b</sup>	APPS-5 <sup>b</sup>	APPSS-1 <sup>c</sup>	EDEPS-1 <sup>d</sup>	PPS <sup>e</sup>
Ratios	1:4	1:2	1:1	2:1	4:1	1:1:1	1:4	1:4

<sup>a</sup> Precursor ratios given with BTESB last. Solvent THF, catalyst  $NH_3$  (aq); see experimental section for conditions used. <sup>b</sup> APPS = aminopropylated polysilsesquioxane from 3-aminopropyl(triethoxy)silane (AMPS) and 1,4-bis(triethoxysilyl)benzene (BTESB). <sup>c</sup> APPSS prepared from AMPS, TEOS (tetraethoxysilane) and BTESB. <sup>d</sup> EDEPS = ethylenediaminoethyl modified polysilsesquioxane from *N*-(3-trimethoxysilylethyl)ethylenediamine (TMSEEDA) and BTESB. <sup>e</sup> PPS = *n*-propyl modified polysilsesquioxane prepared from *n*-propyltriethoxysilane and BTESB.

**Table 2** Solid state NMR spectroscopic data

NMR	Assignments	APPS-1	APPS-2	APPS-3	APPSS-1	EDEPS-1
<sup>29</sup> Si CP MAS	T <sup>1</sup>	-63.24	-63.70	-59.54	-62.92	-63.172
	T <sup>2</sup>	-70.75	-70.78	-69.58	-70.55	-71.863
	T <sup>3</sup>	-79.03	-78.20	-79.52	-79.69	-79.441
	Q <sup>3</sup>	—	—	—	-100.84	—
<sup>13</sup> C CP MAS	ArC	133.51	133.74	134.51	133.61	133.85
	NH <sub>2</sub> CH <sub>2</sub> CH <sub>2</sub> NH	—	—	—	—	48.9
	NHCH <sub>2</sub> CH <sub>2</sub> Si	—	—	—	—	21.77
	CH <sub>2</sub> NH <sub>2</sub>	43.37	43.54	44.03	43.23	39.00
	CH <sub>2</sub> CH <sub>2</sub> CH <sub>2</sub>	24.99	25.09	24.81	24.95	—
	SiCH <sub>2</sub>	10.31	11.09	10.40	10.40	11.22

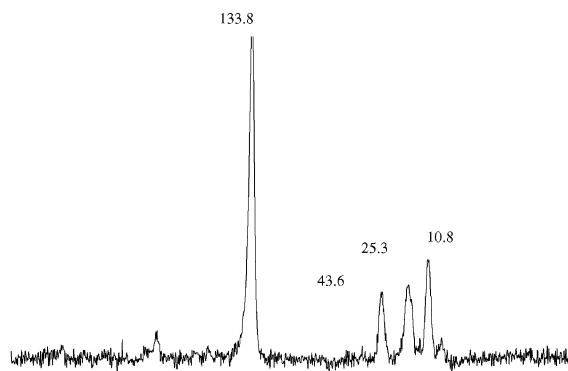
**Table 3** Average stoichiometric formula from deconvoluted  $^{29}\text{Si}$  CP MAS NMR spectra and elemental analysis

Material	Formula from deconvoluted $^{29}\text{Si}$ NMR and C:N ratios	$\alpha^a$	$\beta^b$	C:N		Loading of amino groups/ mmol g $^{-1}$
				Calc.	Found	
APPS-1	$[(\text{RO})_6 - 2n\text{O}_n\text{Si}_2\text{C}_6\text{H}_4]_x[(\text{RO})_3 - n\text{SiO}_{n/2}(\text{CH}_2)_3\text{NH}_2]_y^c$ $[(\text{RO})_{1.62}\text{O}_{2.19}\text{Si}_2\text{C}_6\text{H}_4]_x[(\text{RO})_{0.81}\text{SiO}_{1.10}(\text{CH}_2)_3\text{NH}_2]_y^d$ $[(\text{HO})_{1.62}\text{O}_{2.19}\text{Si}_2\text{C}_6\text{H}_4]_{3.77}[(\text{HO})_{0.81}\text{SiO}_{1.10}(\text{CH}_2)_3\text{NH}_2]^e$ $\text{C}_{25.62}\text{H}_{30.09}\text{O}_{16.31}\text{Si}_{8.54}\text{N}$	73		22.00	22.00	1.2
APPS-3	$[(\text{RO})_6 - 2n\text{O}_n\text{Si}_2\text{C}_6\text{H}_4]_x[(\text{RO})_3 - n\text{SiO}_{n/2}(\text{CH}_2)_3\text{NH}_2]_y^c$ $[(\text{RO})_{1.8}\text{O}_{2.1}\text{Si}_2\text{C}_6\text{H}_4]_x[(\text{RO})_{0.9}\text{SiO}_{1.05}(\text{CH}_2)_3\text{NH}_2]_y^d$ $[(\text{HO})_{1.8}\text{O}_{2.1}\text{Si}_2\text{C}_6\text{H}_4]_{10.86}[(\text{HO})_{0.9}\text{SiO}_{1.05}(\text{CH}_2)_3\text{NH}_2]^e$ $\text{C}_{8.16}\text{H}_{13.89}\text{O}_{5.30}\text{Si}_{2.70}\text{N}$	70		7.00	7.01	3.5
APPSS-1	$[(\text{RO})_6 - 2n\text{O}_n\text{Si}_2\text{C}_6\text{H}_4]_x[(\text{RO})_3 - n\text{SiO}_{n/2}(\text{CH}_2)_3\text{NH}_2]_y[(\text{RO})_4 - n\text{O}_{n/2}\text{Si}]_z^c$ $[(\text{RO})_{2.4}\text{O}_{1.8}\text{Si}_2\text{C}_6\text{H}_4]_x[(\text{RO})_{1.2}\text{SiO}_{0.9}(\text{CH}_2)_3\text{NH}_2]_y[(\text{RO})_{0.72}\text{O}_{1.64}\text{Si}]_z^d$ $[(\text{HO})_{2.4}\text{O}_{1.8}\text{Si}_2\text{C}_6\text{H}_4]_{10.99}[(\text{HO})_{1.2}\text{SiO}_{0.9}(\text{CH}_2)_3\text{NH}_2]_y[(\text{HO})_{0.72}\text{O}_{1.64}\text{Si}]_{0.5}^e$ $\text{C}_{8.94}\text{H}_{15.9}\text{O}_{7.44}\text{Si}_{3.48}\text{N}$	60	82	7.66	7.66	2.8
EDEPS-1	$[(\text{RO})_6 - 2n\text{O}_n\text{Si}_2\text{C}_6\text{H}_4]_x[(\text{RO})_3 - n\text{SiO}_{n/2}(\text{CH}_2)_3\text{NH}(\text{CH}_2)_2\text{NH}_2]_y^c$ $[(\text{RO})_{1.8}\text{O}_{2.1}\text{Si}_2\text{C}_6\text{H}_4]_x[(\text{RO})_{0.9}\text{SiO}_{1.05}(\text{CH}_2)_3\text{NH}(\text{CH}_2)_2\text{NH}_2]_y^d$ $[(\text{HO})_{1.8}\text{O}_{2.1}\text{Si}_2\text{C}_6\text{H}_4]_{3.75}[(\text{HO})_{0.9}\text{SiO}_{1.05}(\text{CH}_2)_3\text{NH}(\text{CH}_2)_2\text{NH}_2]^e$ $\text{C}_{27.5}\text{H}_{35.65}\text{O}_{16.58}\text{Si}_{8.5}\text{N}_2$	70		11.78	11.78	1.1

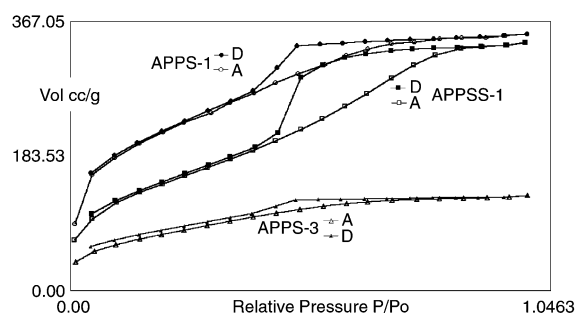
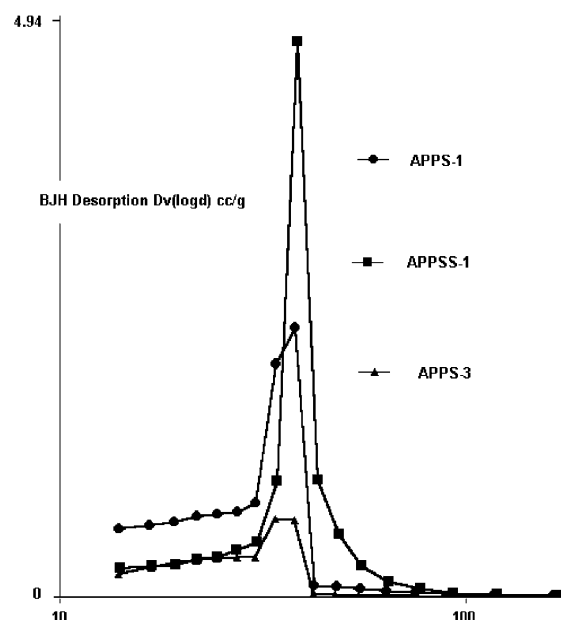
$^a$  FT $2\alpha$  = Overall% condensation of T $^n$  sites.  $^b$   $\beta$  = Overall% condensation of Q $^n$  sites.  $^c$  General formula of materials.  $^d$  Formula incorporating degrees of condensation.  $^e$  Formula incorporating degrees of condensation and fitted to measured C:N and T $^n$ /Q $^n$  ratios for APPSS-1.

distribution is increasingly evident for the higher aminopropyl loading. In contrast APPSS-1 from BTESB:AMPS:TEOS, 1:1:1, has a narrow pore size distribution.

A scanning electron micrograph of APPS-1 is shown in Fig. 5 and indicates a loose nano-particulate type surface texture. This contrasts with the rough polymeric surface texture of acid catalysed polysilsesquioxanes from BTESB and is in keeping with expected differences in textural properties of acid and base catalysed sol-gel processing.<sup>7</sup>

**Fig. 2**  $^{13}\text{C}$  CPMAS NMR spectrum of APPS-3.**Table 4** Porosity measurement results

Entry	BET SA/m $^2$ g $^{-1}$	Micropore SA (t-method)/m $^2$ g $^{-1}$	Total pore volume/cm $^3$ g $^{-1}$	Average pore diameter/ $\text{\AA}$
APPS-1	741	602	0.54	29
APPS-2	525	—	—	—
APPS-3	281	212	0.2	28
APPS-4	21	—	—	—
APPS-5	6	—	—	—
APPSS-1	529	513	0.52	39
EDEPS-1	366	288	0.31	35

**Fig. 3** Nitrogen sorption-desorption isotherms and pore size distribution for APPS-1, APPS-3 and APPSS-1.**Fig. 4** Nitrogen sorption-desorption isotherms and pore size distribution for APPS-1, APPS-3 and APPSS-1.

### Knoevenagel condensation reactions catalysed by APPS-1

Of the many reports in the literature on heterogeneous catalysis of Knoevenagel condensations of aldehydes ketones,<sup>8</sup> the work by Macquarrie and Clark using  $\gamma$ -aminopropylsilica<sup>2</sup> and aminopropyl functionalised MCMs<sup>3</sup> is most relevant to this

**Table 5** Results for Knoevenagel condensation reactions (20 mmol quantities of reagents and 0.2 g catalyst, either in refluxing toluene (20 cm<sup>3</sup>) with removal of water or at room temperature as indicated) catalysed by APPS-1, APPSS-1, or EDEPS

Entry	R	R'	X	Y	Catalyst	t/h	T/°C	Yield (%) <sup>a</sup>	mp/°C <sup>b</sup>	Lit. <sup>9</sup> mp/°C	TON <sup>c</sup> (No. runs)
1	Ph	H	CN	CO <sub>2</sub> Et	APPS-1 <sup>d</sup>	3	20/110	98	52–53	51–53	1363 (16)
					APPSS-1(3)	110	110	99			177 (5)
					EDEPS-1	3	110	98			
					APPS-4	24	110	33			
					PPS	48	110	0			
2	Ph	H	MeCO	CO <sub>2</sub> Et	APPS-1	24	20	70	58–59	59–60	—
3	Ph	H	MeCO	PhCO	APPS-1	24	110	90	98–110	99–100	—
4	Ph	H	MeCO	MeCO	APPS-1	24	110	89	—	—	—
5	Ph	Me	CN	CO <sub>2</sub> Et	APPS-1	48	110	94	45–46	46–47	245 (3)
					APPSS-1	48	110	92			
					EDEPS-1	48	110	66			
6	Ph	Ph	CN	CO <sub>2</sub> Et	APPS-1	48	110	53	98–99	97–99	—
7	Et	Et	CN	CO <sub>2</sub> Et	APPS-1	24	110	94	—	—	326 (4)
					APPSS-1	24	110	89			
					EDEPS-1	24	110	75			
8	C <sub>5</sub> H <sub>10</sub>		CN	CO <sub>2</sub> Et	APPS-1	24	110	98	—	—	—
9	Ph	H	CN	CN	APPS-1	8	110	98	81–82	83	572 (7)
					APPSS-1	6	110	99			
					EDEPS-1	6	110	73			
10	Et	Et	CN	CN	APPS-1	8	110	80	—	—	—

<sup>a</sup> Conversions were measured using GC–MS. <sup>b</sup> Melting points of isolated products. <sup>c</sup> TONs shown reflect mol of product per mol NH<sub>2</sub> for the number of runs shown. Each run was carried in refluxing toluene for the times shown and with removal of water. No loss or increase of activity was observed from one run to the next. <sup>d</sup> This reaction was also shown to be complete within 5 min at room temperature.

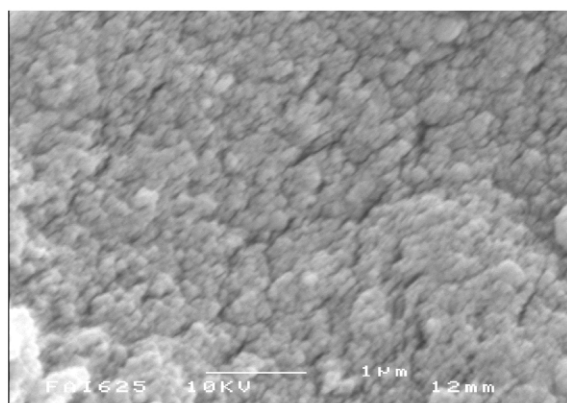


**Fig. 5** Scanning electron micrograph of APPS-1.

paper. These authors point out that for many available catalysts conversions are relatively poor for the most demanding reaction partners, for example, when aromatic ketones are involved. They found  $\gamma$ -aminopropylsilica and aminopropyl functionalised MCMs to be excellent catalysts for condensations involving aliphatic aldehydes and ketones (*e.g.* yields >90% for R,R' = *c*-C<sub>5</sub>H<sub>10</sub>) and reasonably effective catalysts when aromatic aldehydes and ketones are employed (yields ~55–68% for R = Ph, R' = Me). In addition Macquarrie reported that a catalyst prepared from AMPs, phenyl triethoxysilane and TEOS gave significantly better conversions than the aminopropylated silicas for the substrates ethylcyanoacetate/acetophenone (86%) as well as ethylcyanoacetate/pentan-3-one (96%).<sup>4</sup> The new aminopropyl polysilsesquioxane materials APPS-1, APPSS-1 and EDEPS-1 described in this paper were assessed as catalysts for the range of Knoevenagel substrates shown in Table 5.

In order to rule out possible contributions to the catalysis from trace ammonium hydroxide retention after materials processing and washing (although there was no evidence for this from infrared spectra), a blank catalyst, PPS, was prepared

using the base catalytic conditions described for APPS-1 but with BTESB and propyltriethoxysilane instead of BTESB and AMPS. This material was found to be completely inactive for Knoevenagel condensation of benzaldehyde and ethylcyanoacetate.

Yields of condensed products compare well with those reported for aminopropyl modified silicas and are particularly good for some aromatic ketones. In particular the conversion for acetophenone (94%) is higher than that reported for either aminopropylated silica or MCMs and compares well with results on silica modified with aminopropyl and phenyl groups.<sup>4</sup> The reaction profile for entry 7, Table 5, is shown in Fig. 6. The reaction appears to go somewhat slower than that reported for the catalyst based on silica modified with aminopropyl and phenyl groups.<sup>4</sup>

We recorded very high turnover numbers for the catalyst APPS-1 with benzaldehyde and cyanoethylacetate without any loss in activity observed after sixteen runs. The catalyst appeared to be equally active for these reagents in toluene at 20 and 110 °C. It is noteworthy that APPS-4 which has substantially lower surface area than APPS-1 gave a significantly lower conversion with benzaldehyde and cyanoethylacetate compared to APPS-1.

It is also noteworthy that conversion decreased when EDEPS was used as catalyst. The effect of solvent polarity on catalytic activity of APPS-1 (see Fig. 7) followed previously observed

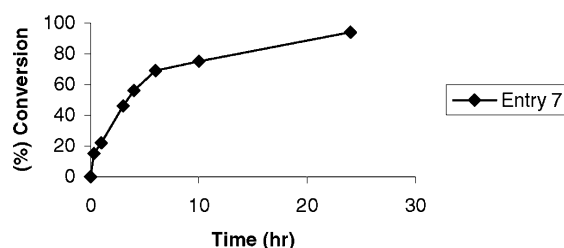


**Fig. 6** The reaction progress between 3-pentanone and ethyl cyanoacetate (with removal of water) (Table 5, entry 7).

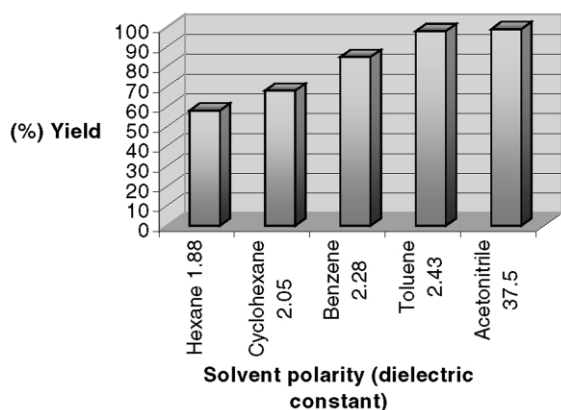


**Fig. 7** Effect of solvent polarity on % conversion for Knoevenagel reaction (1) with APPS-1.

trends for aminopropylated silica catalysts with more polar solvents leading to higher conversions.

Further work on these aminopropyl polysilsesquioxanes and related systems is now in progress.

## Experimental

Reagents obtained commercially were used without any further purification. Manipulations of moisture-sensitive compounds were carried out under an atmosphere of dinitrogen using standard Schlenk-line techniques. Solvents were refluxed over an appropriate drying agent and degassed prior to use. Solution state NMR spectra were recorded in  $\text{CDCl}_3$  solutions using a Jeol EX-270 MHz NMR Spectrometer, with tetramethylsilane as the internal standard. All solid state NMR spectra were recorded on a Bruker MSL 300 MHz spectrometer, spinning speed 4.7 kHz. ( $^{29}\text{Si}$  CPMAS, frequency 59.6 MHz;  $^{13}\text{C}$  CP MAS NMR, frequency 75.5 MHz; Typical conditions for CP MAS were ( $^{29}\text{Si}$ : 5 ms contact time, 1 s delay,  $90^\circ$  pulse for 4.5  $\mu\text{s}$ ,  $^{13}\text{C}$ : 1 ms contact time, 2 s delay,  $90^\circ$  pulse for 4.8  $\mu\text{s}$ .  $^{29}\text{Si}$  SPE MAS spectra were acquired using a 1 min recycle delay, with  $40^\circ$  pulse. Elemental analyses were obtained from the analytical services at Queen Mary, University of London. Surface area measurements were recorded using a Micromeritics Flowsorb II 2300 Surface area Analyser and nitrogen sorption porosimetry measurements were performed using a Quanta Chrome Autosorb 1MP system. The xerogels were ground into fine powders then degassed for several hours prior to analysis. Surface areas were determined by the BET method.<sup>10</sup> Pore size distributions in the mesopore region were determined by the BJH method.<sup>11</sup> The de-Boer t-method<sup>12</sup> was used to evaluate the micropore volume.

Starting reagents  $(\text{EtO})_3\text{SiC}_6\text{H}_4\text{Si}(\text{OEt})_3$ , 1,4-bis(triethoxysilyl)-benzene (BTESB) and 1,4-bis( $\text{Cl}_3\text{SiCH}_2$ ) $_2\text{C}_6\text{H}_4$ ) 1,4-bis(trichlorosilylmethyl)benzene, were synthesised as previously described.<sup>1,4</sup>

### Preparation of APPS-1 [co-polymerization of AMPS/BTESB (1:4)]

The reagents 1,4-bis(triethoxysilyl)benzene (2.99 g, 7.45 mmol), 3-aminopropyl(triethoxy)silane (0.41 g, 1.86 mmol), THF (37 ml) and conc.  $\text{NH}_3$  (aq) (1.0  $\text{cm}^3$ ) and water (2  $\text{cm}^3$ ) were combined under  $\text{N}_2$ . The mixture was stirred for 30 min to give a clear solution. The sol was left under dinitrogen for 48 h

at room temperature. The gel obtained was air-dried for 1 week and then dried at  $60^\circ\text{C}$  in an oven for 24 h. A transparent glass was produced, which was washed with water (50  $\text{cm}^3$ ), ethanol (50  $\text{cm}^3$ ) and ether (50  $\text{cm}^3$ ) and then dried at  $60^\circ\text{C}$  in an oven for 24 h. The glass was crushed to fine powder and heated to  $120^\circ\text{C}$  under vacuum for several hours to remove any volatiles ( $\text{SA} = 741 \text{ m}^2 \text{ g}^{-1}$ ).

### Preparation of APPS-3 [co-polymerization of AMPS/BTESB (1:1)]

The material was prepared as described for APPS-1 using 1,4-bis(triethoxysilyl)benzene (2.99 g, 7.45 mmol) and 3-aminopropyl(triethoxy)silane (1.64 g, 7.45 mmol) ( $\text{SA} = 281 \text{ m}^2 \text{ g}^{-1}$ ).

### Preparation of APPS-1 [co-polymerization of AMPS/BTESB/TEOS (1:1:1)]

The reagents 1,4-bis(triethoxysilyl)benzene (2.99 g, 7.45 mmol), 3-aminopropyl(triethoxy)silane (1.64 g, 7.45 mmol), tetraethoxysilane (1.55 g, 7.45 mmol) THF (37  $\text{cm}^3$ ) and concentrated  $\text{NH}_3$  (aq) (1.0  $\text{cm}^3$ ) and water (2  $\text{cm}^3$ ) were combined under  $\text{N}_2$ . The mixture was stirred for 30 min to give a clear solution. The sol was left under dinitrogen for 24 h. The gel obtained was air dried for 1 week and then dried at  $60^\circ\text{C}$  in an oven for 24 h. An opaque glass was produced, which was washed with water (50  $\text{cm}^3$ ), ethanol (50  $\text{cm}^3$ ) and ether (50  $\text{cm}^3$ ) and then dried at  $60^\circ\text{C}$  in an oven for 24 h. The glass was crushed to a fine powder and heated to  $120^\circ\text{C}$  under vacuum for several hours to remove any volatiles ( $\text{SA} = 529 \text{ m}^2 \text{ g}^{-1}$ ).

### Preparation of EDAPPS-1 [co-polymerization of BTESB/DAPTS (4:1)]

The reagents 1,4-bis(triethoxysilyl)benzene (2.99 g, 7.45 mmol), *N*-(3-trimethoxysilylethyl)ethylenediamine, (0.41 g, 1.86 mmol), THF (37  $\text{cm}^3$ ), concentrated  $\text{NH}_3$  (aq) (1.0  $\text{cm}^3$ ) and water (2  $\text{cm}^3$ ) were combined under  $\text{N}_2$ . The mixture was stirred for 30 min to give a clear solution. The sol was left under dinitrogen for 48 h, but since there was no sign of gelation additional  $\text{NH}_3$  (aq) (1.0  $\text{cm}^3$ ) was added. After 24 h the gel obtained was air dried for 1 week and then dried at  $60^\circ\text{C}$  in an oven for 24 h. A transparent glass was produced, which was washed with water (50  $\text{cm}^3$ ), ethanol (50  $\text{cm}^3$ ) and ether (50  $\text{cm}^3$ ) and then dried at  $60^\circ\text{C}$  in an oven for 24 h. The glass was crushed in to fine powder and heated to  $120^\circ\text{C}$  under vacuum for several hours to remove any volatiles ( $\text{SA} = 359 \text{ m}^2 \text{ g}^{-1}$ ).

### Preparation of PPS-1 (propylpolysilsesquioxane) [co-polymerisation of BTESB-propyltriethoxysilane (4:1)]

The reagent 1,4-bis(triethoxysilyl)benzene (2.99 g, 7.45 mmol, 3.33  $\text{cm}^3$ ), propyltriethoxysilane (0.38 g, 1.86 mmol, 0.43  $\text{cm}^3$ ), THF (37  $\text{cm}^3$ ) and concentrated  $\text{NH}_3$  (aq) (1.0  $\text{cm}^3$ ) were combined under  $\text{N}_2$ . The mixture was stirred for 30 min to give a clear solution. The sol was left under dinitrogen for 24 h. The gel obtained was air dried for 1 week and then dried at  $60^\circ\text{C}$  in an oven for 24 h. A transparent glass was produced, which was



washed with distilled water (50 cm<sup>3</sup>), ethanol (50 cm<sup>3</sup>) and ether (50 cm<sup>3</sup>), then dried at 60 °C in an oven for 24 h. The glass was crushed in to fine powder and heated to 120 °C under vacuum for several hours to remove any volatiles.

### General procedure for the Knoevenagel condensation reactions

A typical Knoevenagel reaction was carried out as follows: 20 mmol of the two reactants and catalyst (0.20 g) were combined in 20 cm<sup>3</sup> of toluene. The mixture was either heated to reflux (with a Dean and Stark trap for the removal of water) or simply stirred at room temperature. Samples for GC–MS analysis were taken at intervals. Standard work-up and purification was carried out in most cases and product identity further confirmed by NMR and mp.

### Acknowledgements

We thank the EPSRC for funding, Abil Aliev, Peter Haycock and Harold Toms of the ULIRS High Field NMR Services at QMW and UCL, Andy Cakebread and Roger Tye of the ULIRS

GC–MS service at Kings College London. N. Al-Haq thanks Valachemi in Teheran for financial assistance.

### References

- 1 S. W. Carr, M. Motevalli, D. Li Ou and A. C. Sullivan, *J. Organomet. Chem.*, 1993, **445**, 35; P. J. Barrie, S. W. Carr, D. Li Ou and A. C. Sullivan, *Chem. Mater.*, 1995, **7**, 265.
- 2 D. J. Macquarrie, J. H. Clark, A. Lambert, J. E. G. Mdoe and A. Priest, *React. Funct. Polym.*, 1997, **35**, 153–158.
- 3 D. J. Macquarrie and D. B. Jackson, *Chem. Commun.*, 1997, 1781.
- 4 D. J. Macquarrie, *Green Chem.*, 1999, **1**, 195.
- 5 K. J. Shea, D. A. Loy and O. Webster, *J. Am. Chem. Soc.*, 1992, **114**, 6700.
- 6 S. J. Gregg and K. S. W. Sing, *Adsorption Surface Area and Porosity* Academic Press, London, 1982.
- 7 C. J. Brinker and G. W. Scherer, *Sol–Gel Science and Technology*, Academic Press, London, 1990.
- 8 E. Angeletti, C. Canepa, G. Martinette and P. Venturello, *J. Chem. Soc., Perkin Trans. 1*, 1989, 105; J. A. Cabello, J. M. Campelo, A. Garcia, D. Luna and J. M. Marinas, *J. Org. Chem.*, 1984, **49**, 5195; F. Texier-Boullet and A. Foucaud, *Tetrahedron Lett.*, 1982, **23**, 4927.
- 9 S. Abdallah-El Ayoubi, F. Texier-Boullet and J. Hamelin, *Synthesis*, 1994, 258; A. C. Cope, C. M. Hofmann, C. Wyckoff and E. Hardenbergh, *J. Am. Chem. Soc.*, 1941, **63**, 3452.
- 10 S. Brunauer, P. H. Emmett and E. Teller, *J. Am. Chem. Soc.*, 1938, **60**, 30911.
- 11 E. P. Barret, L. G. Joyner and P. P. Halenda, *J. Am. Chem. Soc.*, 1951, **73**, 373.
- 12 J. H. de Boer and B. C. Lippert, *J. Catal.*, 1965, **4**, 319.



# Direct, efficient, solvent-free synthesis of 2-aryl-1,2,3,4-tetrahydroquinazolines

Waldo H. Correa, Stavroula Papadopoulos, Peta Radnidge, Brett A. Roberts and Janet L. Scott\*

Centre for Green Chemistry, P.O. Box 23, Monash University, Melbourne, Victoria 3800, Australia. E-mail: janet.scott@sci.monash.edu.au

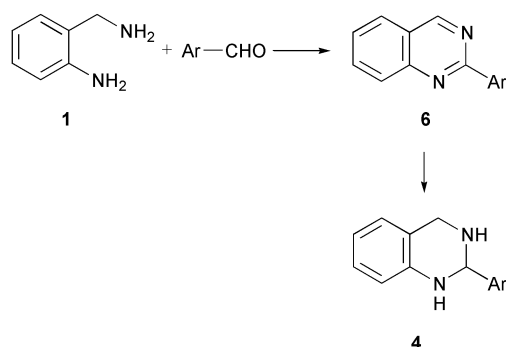
Received (in Cambridge, UK) 18th March 2002

First published as an Advance Article on the web 30th April 2002

2-Aryl-1,2,3,4-tetrahydroquinazolines are synthesised by direct reaction of 2-aminobenzylamine and benzaldehyde derivatives by mixing of the reagents either neat, or as an aqueous slurry. Excellent conversion of starting materials is achieved and no catalysts, derivatisation or auxiliary reagents are required to effect the conversion. Where reaction is sluggish or extent of conversion poor, application of gentle heating to achieve a melt phase results in rapid and clean conversion to the desired tetrahydroquinazoline product.

## Introduction

Many quinazolines **6** and tetrahydroquinazolines **4** are biologically active<sup>1</sup> and derivatives of these are of interest as dihydrofolate reductase inhibitors,<sup>2</sup> antitubercular<sup>3</sup> and anti-bacterial agents.<sup>4</sup>



1,2,3,4-Tetrahydroquinazolines have been prepared by the condensation of 1,3-diamines **1** and *p*-substituted aldehydes such as **2** in refluxing benzene or xylene with azeotropic water removal,<sup>5a</sup> in refluxing ethanol/acetic acid mixtures<sup>5</sup> and by reaction in alkali media.<sup>6</sup> Alternative methods require the conversion of aldehydes, *in situ*, to *N*-(1-chloroalkyl)pyridinium chlorides using thionyl chloride and pyridine followed by reaction with 2-aminobenzylamine to yield hydrochloride salts of **4**.<sup>7</sup> More recently the synthesis of tetrahydroquinazolines by the condensation of 2-aminobenzylamine with aromatic aldehydes in ionic liquids followed by extraction into diethyl ether has been described.<sup>8</sup>

Given the large number of similar condensation reactions that have been reported to proceed readily under solvent-free conditions<sup>9</sup> and the observation that condensation reactions, with suitable thermodynamics, may even proceed in aqueous slurry media,<sup>10</sup> we proceeded to examine the synthesis of tetrahydroquinazolines under simple solvent-free or 'neat' reaction conditions and as aqueous slurries.

These conditions are so simple as to be considered almost facile yet generate product of high purity in excellent conversion and yield. No organic solvents are utilised, no auxiliaries required and energy consumption is kept to a minimum.

## Results and discussion

1,2,3,4-Tetrahydroquinazolines substituted by aryl groups at the 2 position (**4**) are accessible in almost quantitative yield *via* simple mixing of 2-aminobenzylamine **1** and benzaldehyde derivatives **2** directly as solids or as solid plus liquid (Scheme 1). Remarkably many of the product tetrahydroquinazolines may also be prepared by the simple method of slurrying the reagents together in water at ambient temperature in a similar manner to that described by Tanaka and Shiraishi in the synthesis of aromatic Schiff bases.<sup>10b</sup> The reaction occurs at a reasonable rate in spite of the poor aqueous solubility of both reagents. Of the reactions carried out using water as the reaction medium, aldehydes containing an *ortho*-hydroxide substituent resulted in further reaction leading to the di-condensation product **5**. The identities of all products were confirmed by analysis of spectral data and yields and reaction conditions are summarised in Table 1. Clearly, where almost quantitative conversion is achieved under solvent-free reaction conditions, no further purification is required and yield and extent of conversion are interchangeable terms. Isolated yields are thus quoted only for the reactions carried out in aqueous slurries. These are almost certainly related to the scale of the reactions (typically a few hundred milligrams) and higher isolated yields would be expected on scale-up.

In addition, single crystal structures of a number of products were obtained to allow direct identification of the product phase without resort to solution phase spectroscopic analysis (thus

## Green Context

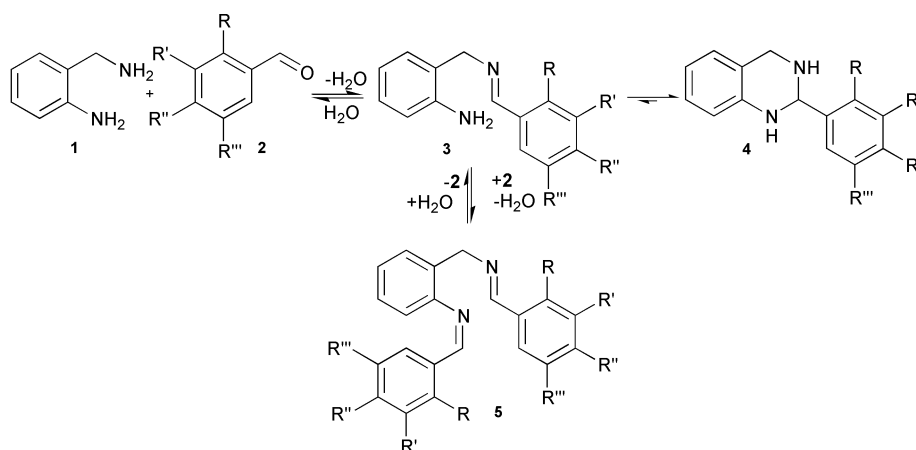
Many quinazolines are biologically active and their derivatives have widespread applications. Their synthesis is *via* a typical condensation reaction method involving a refluxing solvent (e.g. benzene) with azeotropic water removal. Green chemistry teaches us to avoid or at least minimise the use of hazardous solvents including VOCs and the simplest solution, where possible, is to avoid a solvent altogether. Here, remarkably simple and effective solventless methods for quinazoline synthesis are described. No solvents are utilised and no auxiliaries are required. **JHC**

avoiding the possibility that reaction to the product occurs on dissolution). Comparison of the calculated powder X-ray diffraction pattern with that obtained for a solid sample of **4a** from an aqueous slurry reaction indicates that the product isolated is of the same phase as that obtained post recrystallisation as is illustrated in Fig. 1. To ensure that **5** was not an artifact of a further reaction occurring in solution, a sample of **3e** was monitored by  $^1\text{H}$  NMR spectroscopy over a period of one week. No change was noted and the possibility of **5** rapidly forming from **4**, as a result of the reversible nature of the Schiff base formation, thus discounted.<sup>11</sup>

The formation of tetrahydroquinazolines is formally a condensation of the aldehyde and amine to form a Schiff base, **3**, which is in tautomeric equilibrium with the heterocycle, **4**. In products from **2** lacking an *ortho*-hydroxy group, the heterocyclic tautomer (Fig. 2(a)) dominates and no 'chain-tautomer' is detected by solution phase  $^1\text{H}$  NMR analysis, (unlike the analogous benzoxazine derivatives<sup>12</sup>). In products synthesized from **2** with a hydroxy function *ortho* to the aldehyde substituent the 'chain' or Schiff base type tautomer **3** is identified from the single crystal structures, Fig. 2(b). This is in accordance with  $^1\text{H}$  NMR data. The bis-imine **5** (see Fig. 2(c)) is readily distinguished from **4** (or **3**) by  $^1\text{H}$  NMR analysis. A short intramolecular O–H...N hydrogen bond is noted in the

solid-state structure of **3h**, (and **5e** and **5h**). Should this persist in solution, it is likely to stabilize the imine or 'chain open' tautomer relative to the heterocyclic form.<sup>12</sup> This in turn, renders the second amine group open to attack by excess aldehyde and results in preferential formation of the bis-imine products **5**.

As noted previously, grinding of solid reagents yields a viscous liquid melt phase,<sup>13</sup> which may contain dispersed solid material corresponding to one of the reagents. In only one case, **3h**, is no visible phase change noted, and the reaction may be accurately described as a solid–solid reaction. In cases where the reaction is sluggish at ambient temperature, or there remains a significant quantity of solid reagent post mixing, heating the reaction mixture until a melt is obtained results in rapid and almost quantitative conversion to product. Thus the reaction of **1** and **2j** is complete within 10 min at 50 °C but requires 2 d at ambient temperature to achieve a similar extent of conversion. Thermogravimetric analysis (TGA) and simultaneous differential scanning calorimetry (DSC) of reaction mixtures, which convert slowly at room temperature, reveal a distinct endothermic event associated with an increased rate of weight loss as illustrated in Fig. 3. This allows for rapid estimation of the requisite reaction temperature. The products obtained from elevated temperature 'melt' reactions were often glassy on



Scheme 1

Table 1 Solvent free synthesis of 2-aryl-1,2,3,4-tetrahydroquinazolines

R	R'	R''	R'''	Solvent-free									
				Ground (ambient temp.)		Ground and heated <sup>a</sup>				Aqueous slurry (ambient temp.)			
				t/min	Conv. <sup>b</sup> (%)	T/°C	t/min	Conv. <sup>b</sup> (%)	Product	t/min	Yield (conv. <sup>b</sup> ) (%)	Product	
<b>2a</b>	H	H	H	3	99	55	5	99	<b>4a</b>	10	92 (99)	<b>4a</b>	
<b>2b</b>	NO <sub>2</sub>	H	H	45	88	80	10	99	<b>4b</b>	30	86 (95)	<b>4b</b>	
<b>2c</b>	H	NO <sub>2</sub>	H	180	96	55	10	99	<b>4c</b>	120	82 (99)	<b>4c</b>	
<b>2d</b>	H	H	NO <sub>2</sub>	18 h	90	60	10	99	<b>4d</b>	18 h	88 (90)	<b>4d</b>	
<b>2e</b>	OH	H	H	15	99	55	10	99	<b>3e</b>	18 h	92 (99)	<b>5e</b> <sup>c</sup>	
<b>2f</b>	H	H	OH	24 h	80	55	4 h	75	<b>4f</b>	30	77 (99)	<b>4f</b>	
<b>2g</b>	OH	OH	H	12 h	99	55	20	99	<b>3g</b>	120	92 (99)	<b>5g</b> <sup>c</sup>	
<b>2h</b>	OH	H	H	12 h	88	65	60	93	<b>3h</b>	5	96 (99)	<b>5h</b> <sup>c</sup>	
<b>2i</b>	OH	OCH <sub>3</sub>	H	18 h	99	55	10	99	<b>3i</b>	18 h	60 (99)	<b>5i</b> <sup>c</sup>	
<b>2j</b>	H	OCH <sub>3</sub>	OCH <sub>3</sub>	2 d	71	52	5	99	<b>4j</b>	18 h	85 (88)	<b>4j</b>	
<b>2k</b>	H	H	Br	18 h	99	55	20	98	<b>4k</b>	180	84 (99)	<b>4k</b>	
<b>2l</b>	H	Cl	H	2 d	92	50	80	99	<b>4l</b>	24 h <sup>d</sup>	— (88) <sup>e</sup>	<b>4l</b>	
<b>2m</b>	Cl	Cl	H	18 h	95	55	2	97	<b>4m</b>	2 d	74 (95)	<b>4m</b>	

<sup>a</sup> Reactants ground separately prior to heating to melt in oil bath. <sup>b</sup> Determined from  $^1\text{H}$  NMR integrated values and based on consumption of the aldehyde. <sup>c</sup> Yield of the di-condensation product based on limiting reagent. <sup>d</sup> The extent of conversion was determined after 24 h but may have reached this extent significantly earlier. <sup>e</sup> Product did not solidify and could not be isolated except by extraction.

cooling and required crushing or recrystallisation to yield powdered or crystalline material.

Remarkably the reaction proceeded to a high degree of conversion in an aqueous slurry in spite of the extremely low aqueous solubility of all reagents and products. The time required for the reaction was similar to that noted in the neat reaction at ambient temperature, implying that the reaction proceeds *via* a similar route. While the concept of carrying out a condensation reaction in aqueous media may, initially, appear to be counterintuitive, there are a growing number of examples that indicate that many condensation reactions proceed with great facility in aqueous slurries.<sup>10</sup> The advantages of this methodology are obvious: handling of powdered reagents (particularly toxic compounds such as 2-aminobenzylamine) is facilitated, mixing is readily achieved by agitation and heat transfer and thus control (should a reaction prove exothermic) is no different from that used in more traditional solution phase methods. In all the cases tested, except one (**4l**), the product separates from the slurry as a solid which may be isolated by simple filtration followed by drying (clumping may occur necessitating a crushing step prior to filtration—this is readily achieved by choosing an appropriate method of agitation).

In conclusion, a preparatively useful method for the synthesis of tetrahydroquinazolines (or related tautomeric Schiff bases) in exceptionally high yields and at moderate temperatures has been developed. In addition, the optimum reaction temperature is readily determined from simple, quick measurement of the onset temperature of the reaction endotherm by DSC analysis.

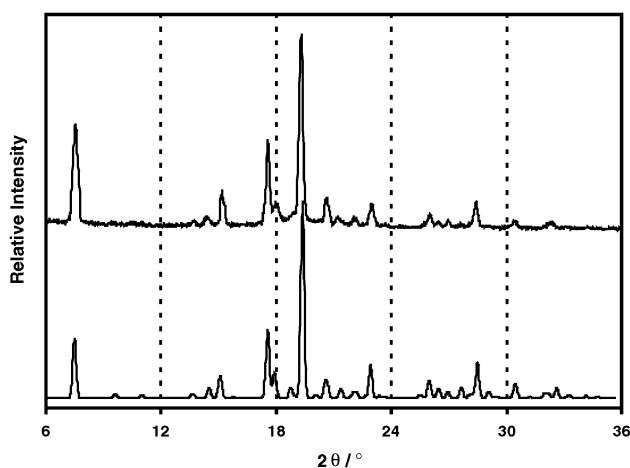


**Fig. 1** Comparison of powder XRD patterns of **4a** immediately after reaction (top) and generated from single crystal diffraction data (below). (Pattern generated from single crystal data is corrected for differences in temperature after determination of unit cell parameters at 294 K.)

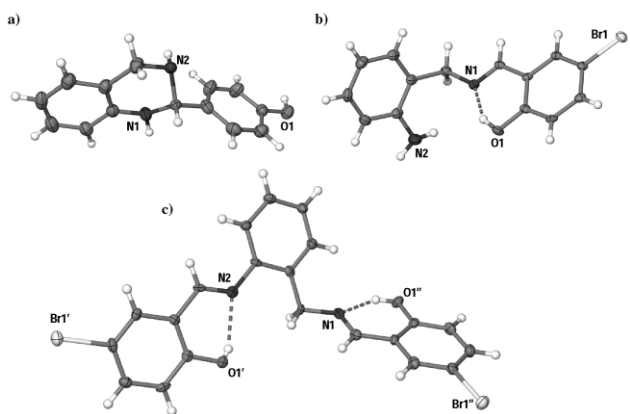


**Fig. 2** Molecular diagrams, derived from single crystal data, of (a) **4f**, (b) **3h** and (c) **5h**. Ellipsoids are represented at the 50% probability level and intramolecular hydrogen bonds indicated as dotted lines.

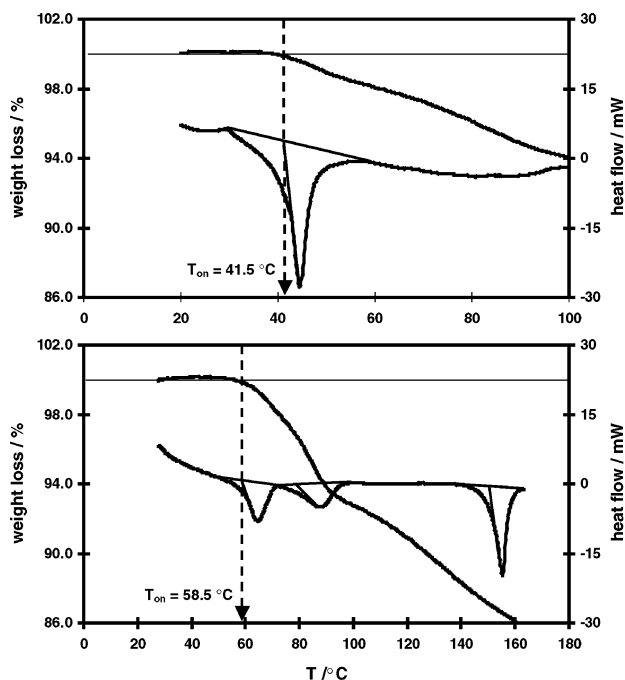


**Fig. 3** Simultaneous TGA and DSC analysis of reaction mixtures of **1** and (a) **2i** and (b) **2h**. In each case, no significant weight loss is noted at temperatures less than that of the onset temperature ( $T_{on}$ ) of the first endotherm. As the reaction under study is a condensation reaction weight loss is associated with the evolution of water. An endotherm corresponding to  $T_{fusion}$  is only noted in the case of formation of **3h** and it is thus reasonable to postulate that the second endotherm noted ( $T_{on} = 77.6\text{ °C}$ ) is due to product crystallization (whether this is a phase change from solid reagents to solid products is, as yet, unknown).

## Experimental

### Molecular characterisation:

<sup>1</sup>H NMR (300 MHz) and <sup>13</sup>C NMR (75 MHz) spectra were recorded on a Varian Mercury 300 MHz spectrometer in CDCl<sub>3</sub> or d<sub>6</sub>-DMSO solution with TMS as reference. Melting points were recorded on an Electrothermal digital melting point apparatus.

X-Ray diffraction data were collected on an Enraf Nonius CCD diffractometer at 123 K using graphite monochromated Mo-K $\alpha$  radiation ( $\lambda = 0.71073\text{ \AA}$ ). Structures were solved by direct methods using the program SHELXS-97<sup>14</sup> and refined by full matrix least squares refinement on  $F^2$  using the programs SHELXL-97<sup>15</sup> and Xseed.<sup>16</sup> Non-hydrogen atoms were refined anisotropically and hydrogen atoms inserted at geometrically determined positions with temperature factors fixed at 1.2 times that of the parent atom except for methyl hydrogen atoms where the temperature factors were constrained to equal 1.5 times that of the parent carbon atom. Hydrogen atoms associated with parent N-atoms were located in electron density difference maps and were refined with simple bond length restraints where required. Where these could not be reliably located they were omitted from the model.

CCDC reference numbers 177047–177053. See <http://www.rsc.org/suppdata/gc/b2/b202729c/> for crystallographic data in CIF or other electronic format.

Powder XRD analysis was performed on a Syntag PAD5 diffractometer at 294 K using Cu-K $\alpha$  radiation ( $\lambda = 1.54059\text{ \AA}$ ) in the range 6–36°  $2\theta$ . The calculated powder X-ray diffraction pattern obtained from a solid sample of reaction product **4a** was compared with that generated from single crystal data using the program LAZYPULVERIX<sup>17</sup> to verify that the product prepared by solvent-free reaction methodology was of the same phase as that obtained post recrystallisation.



## Synthetic procedures

All reagents were of 98% purity or greater and used as purchased from the supplier unless noted otherwise. Grinding experiments were performed with porcelain mortar and pestles, which were acetone rinsed and dried prior to use. Extent of conversion of reagents to products was determined by comparison of integrated values of well-defined product and reagent peaks in  $^1\text{H}$  NMR analysis prior to any purification.

**Method A.** Equimolar quantities of solid **1** and the appropriate benzaldehyde derivative **2** (ca. 250–500 mg scale) were ground together in a mortar and pestle at ambient temperature. In most cases a mutual solution or melt phase formed which hardened with time yielding solid **3**. The time required for product formation varied dependent on the benzaldehyde derivative used and reaction times are recorded below. Extent of conversion was determined by comparison of integrated areas of suitably resolved reagent and product resonances in  $^1\text{H}$  NMR analysis and, where required, the product was recrystallised from an appropriate solvent.

**Method B.** Equimolar quantities of solid **1** and the appropriate benzaldehyde derivative **2** (ca. 100–500 mg scale) were placed in a glass vessel immersed in a preheated oil bath. The temperature varied from 50 to 75 °C and specific temperatures and heating times are recorded below. The melts so formed became progressively more viscous often hardening to a glassy mass as quantitative conversion was achieved. Extent of conversion was determined as described above and, where required, the product was recrystallised from an appropriate solvent.

**Method C.** Equimolar quantities of powdered solid **1** and the appropriate benzaldehyde derivative **2** (ca. 100–500 mg scale) were slurried together in 1 mL of distilled water. Samples of the reagents and products were isolated by filtration and the extent of conversion to product determined as above. In some cases the reagents formed a sticky mass which was broken up by vigorous agitation. Products were isolated by filtration, washed with water, and dried *in vacuo* over silica gel.

### 2-Phenyl-1,2,3,4-tetrahydroquinazoline, **4a**

**A. 1** (1.021 g, 8.35 mmol) and **2a** (0.85 mL, 8.37 mmol) formed a viscous brown liquid which hardened, within 3 min, yielding **4a** in >99% conversion.

**B. 1** (0.1959 g, 1.60 mmol) and **2a** (0.1771 g, 1.67 mmol), heated together at 55 °C, yielded, after 5 min, **4a** in >99% conversion.

**C. 1** (0.2617 g, 1.77 mmol) and **2a** (0.175 mL, 1.72 mmol) yielded, after 5 min, an off-white precipitate, 0.3227 g (92% yield) >99% pure **4a**.

White crystalline material, mp 98.1–101.5 °C (toluene), lit. 98–100 °C<sup>5</sup>

$\delta_{\text{H}}(\text{CDCl}_3)$ : 1.87 (1H, br, NH), 4.00 (1H, d,  $J = 16.8$  Hz), 4.27 (1H, d,  $J = 16.8$  Hz), 4.78 (NH, s), 4.98 (NH, s), 5.25 (1H, s), 6.58–7.51 (Ar-H);  $\delta_{\text{C}}(\text{CDCl}_3)$ : 46.7 (–CH<sub>2</sub>–), 69.9 (–N–CH–N–), 115.3, 118.4, 121.5, 126.4, 126.8, 127.5, 128.7, 128.9, 141.8, 143.9; ESI-MS:  $m/z$  211.0 [M + H<sup>+</sup>]; microanalysis: calc. (found): C 79.97 (79.92), H 6.71 (6.58), N 13.32 (13.57); *Crystal data* for **4a**: C<sub>14</sub>H<sub>14</sub>N<sub>2</sub>,  $M_r = 210.27$ , triclinic, space group  $P\bar{1}$ ,  $a = 9.4360(5)$ ,  $b = 10.4454(5)$ ,  $c = 12.0165(8)$  Å,  $\alpha = 99.837(2)$ ,  $\beta = 98.858(2)$ ,  $\gamma = 101.754(4)^\circ$ ,  $V = 1120.4(1)$  Å<sup>3</sup>,  $Z = 4$ ,  $\mu(\text{Mo-K}\alpha) = 0.075$  mm<sup>–1</sup>. Of 6463 reflections

measured, 4502 were unique with  $2658 I > 2\sigma(I)$ ,  $R$  indices [ $I > 2\sigma(I)$ ]  $R_1 = 0.0822$ ,  $wR_2 = 0.2063$ , GoF on  $F^2 = 1.031$  for 297 refined parameters. As hydrogen atoms associated with N13 and N23 could not be located in electron density difference maps these were omitted from the model.

### 2-(2'-Nitrophenyl)-1,2,3,4-tetrahydroquinazoline, **4b**

**A. 1** (0.4091 g, 3.35 mmol) and **2b** (0.5103 g, 3.38 mmol) formed a sticky pale brown melt which yielded, after 45 min, **4b** in 88% conversion.

**B. 1** (0.0589 g, 0.48 mmol) and **2b** (0.0936 g, 0.48 mmol) heated together at 52 °C, yielded, after 5 min, **4b** in >99% conversion.

**C. 1** (0.2102 g, 1.72 mmol) and **2b** (0.2600 mL, 1.72 mmol) yielded, after 30 min, solid yellow **4b** in 95% conversion.

Orange crystalline material, mp 117.6–119.2 °C (acetone).

$\delta_{\text{H}}(\text{CDCl}_3)$ : 2.8 (1H, br, NH), 3.65 (1H, d,  $J = 16.5$  Hz), 3.96 (1H, d,  $J = 16.5$  Hz), 4.84 (NH, s), 5.10 (NH, s), 5.83 (1H, s), 6.45–8.20 (Ar-H);  $\delta_{\text{C}}(\text{CDCl}_3)$ : 44.9 (–CH<sub>2</sub>–), 64.7 (–N–CH–N–), 115.5, 118.7, 121.8, 124.7, 126.5, 127.7, 129.0, 129.1, 132.8, 136.1, 142.8, 149.5; ESI-MS:  $m/z$  256.1 [M + H<sup>+</sup>]; microanalysis (%): calc. (found): C 65.87 (65.80), H 5.13 (5.07), N 16.46 (16.46), O 12.54 (12.61); *Crystal data* for **4b**: C<sub>14</sub>H<sub>13</sub>N<sub>3</sub>O<sub>2</sub>,  $M_r = 255.27$ , monoclinic, space group  $P2_1/c$ ,  $a = 12.1392(2)$ ,  $b = 7.7897(2)$ ,  $c = 13.5753(3)$  Å,  $\beta = 111.140(8)$ ,  $V = 1197.30(5)$  Å<sup>3</sup>,  $Z = 4$ ,  $\mu(\text{Mo-K}\alpha) = 0.098$  mm<sup>–1</sup>. Of 9206 reflections measured, 2769 were unique with  $2184 I > 2\sigma(I)$ ,  $R$  indices [ $I > 2\sigma(I)$ ]  $R_1 = 0.0450$ ,  $wR_2 = 0.1307$ , GoF on  $F^2 = 1.133$  for 180 refined parameters.

### 2-(3'-Nitrophenyl)-1,2,3,4-tetrahydroquinazoline,<sup>18</sup> **4c**

**A. 1** (0.2010 g, 1.65 mmol) and **2c** (0.2549 g, 1.68 mmol) formed a sticky pale brown melt which yielded, after 45 min, **4c** in 96% conversion.

**B. 1** (0.2051 g, 1.68 mmol) and **2c** (0.2543 g, 1.68 mmol) heated together at 55 °C formed a melt which became progressively more viscous, yielding, after 3 h of heating, **4c** in >99% conversion.

**C. 1** (0.2038 g, 1.67 mmol) and **2c** (0.2504 g, 1.66 mmol) yielded, after 2 h, orange solid **4c** in 99% conversion recrystallised from acetone.

Orange crystalline material, A: mp 96.8–98.8 °C (acetone); B, C: mp 81.9–85.2 °C (ethyl acetate)—the different melting points are due to the occurrence of two polymorphic forms resulting from crystallisation from different solvents. This is confirmed by X-ray powder diffraction analysis:  $2\theta^\circ$  (relative intensity %), Form A: 12.35 (52), 12.50 (47), 14.09 (39), 14.17 (34), 14.75 (22), 15.41 (67), 18.07 (27), 19.04 (62), 19.84 (78), 20.61 (43), 21.36 (33), 22.43 (34), 22.67 (26), 22.80 (27), 23.76 (20), 24.00 (25), 24.06 (29), 24.46 (84), 25.45 (100). Form B: 13.34 (79), 14.66 (57), 14.82 (51), 17.81 (33), 21.53 (46), 24.42 (100).

$\delta_{\text{H}}(\text{CDCl}_3)$ : 3.94 (1H, d,  $J = 16.5$  Hz), 4.23 (1H, d,  $J = 16.5$  Hz), 5.38 (1H, s), 6.66–8.44 (Ar-H);  $\delta_{\text{C}}(\text{CDCl}_3)$ : 45.7 (–CH<sub>2</sub>–), 68.6 (–N–CH–N–), 115.7, 119.0, 121.6, 122.2, 123.6, 126.4, 127.7, 129.8, 133.4, 142.9, 144.1, 148.8; ESI-MS:  $m/z$  256.1 [M + H<sup>+</sup>]; microanalysis (%): calc. (found): C 65.87 (65.92), H 5.13 (5.18), N 16.46 (16.50), O 12.54 (12.49).

## 2-(4'-Nitrophenyl)-1,2,3,4-tetrahydroquinazoline, **4d**

**A. 1** (0.2018 g, 1.65 mmol) and **2d** (0.2504 g, 1.66 mmol) formed a sticky pale brown melt which yielded, after 45 min, **4d**, in 90% conversion.

**B. 1** (0.2022 g, 1.66 mmol) and **2d** (0.2519 g, 1.67 mmol) heated together at 60 °C, yielded, after 3 h, **4d** in >99% conversion.

**C. 1** (0.2035 g, 1.67 mmol) and **2d** (0.2554 g, 1.69 mmol) yielded, after 18 h, bright yellow solid **4d** in 90% conversion.

Orange–yellow crystalline material, mp 97.1–102.0 °C (ethyl acetate), lit. 100–102 °C<sup>5a</sup>

$\delta_{\text{H}}(\text{CDCl}_3)$ : 3.88 (1H, d,  $J = 16.5$  Hz), 4.16 (1H, d,  $J = 16.5$  Hz), 5.39 (1H, s), 6.65–8.27 (Ar–H);  $\delta_{\text{C}}(\text{CDCl}_3)$ : 45.7 (–CH<sub>2</sub>–), 68.7 (–N–CH–N–), 115.7, 119.0, 121.7, 124.1, 126.6, 127.8, 128.2, 142.9, 148.9; ESI-MS:  $m/z$  256.1 [M + H<sup>+</sup>], compound previously reported<sup>5a</sup> with little spectral data.

## 2-[(2'-Aminobenzylimino)methyl]phenol, **3e**

**A. 1** (0.1919 g, 1.57 mmol) and **2e** (0.1989 g, 1.63 mmol) formed a sticky straw coloured melt which yielded, **3e**, 99% conversion.

**B. 1** (0.0855 g, 0.7 mmol) and **2e** (0.0805 g, 0.7 mmol) heated together at 55 °C yielded, after 30 min, **3e** in 99% conversion.

Bright yellow crystals, mp 94.1–98.6 °C, (benzene).

$\delta_{\text{H}}(\text{CDCl}_3)$ : 4.75 (2H, s), 6.78–7.39 (Ar–H), 8.40 (1H, s, –N=CH);  $\delta_{\text{C}}(\text{CDCl}_3)$ : 60.0 (–CH<sub>2</sub>–), 116.2, 117.2, 118.9, 119.0, 119.1, 122.6, 129.1, 129.9, 131.7, 132.6, 144.8, 161.1, 165.9; ESI-MS:  $m/z$  227.1 [M + H<sup>+</sup>]; microanalysis (%): calc. (found): C 74.31 (74.19), H 6.24 (6.17), N 12.38 (12.28), O 7.07 (7.13).

## N-2-[(Salicylideneimino)benzyl]salicylideneimine, **5e**

**C. 1** (0.1431 g, 1.17 mmol) and **2e** (0.1463 g, 1.20 mmol) yielded, after 2 h, bright yellow solid **5e** in 99% conversion.

Yellow crystals, mp 102.8–105.8 °C (dichloromethane/dimethylsulfoxide), lit. 82–83.5 °C.<sup>19</sup>

$\delta_{\text{H}}(\text{CDCl}_3)$ : 4.97 (2H, s), 6.66–7.45 (Ar–H), 8.48 (1H, s, –N=CH), 8.59 (1H, s, –N=CH), 13.08 (1H, s, br, –OH), 13.29 (1H, s, br, –OH);  $\delta_{\text{C}}(\text{CDCl}_3)$ : 41.2 (–CH<sub>2</sub>–), 59.9, 117.2, 117.5, 118.6, 118.8, 119.0, 119.4, 127.4, 128.9, 129.3, 131.7, 132.2, 132.5, 132.7, 133.7, 147.5, 161.2, 163.8, 166.4; ESI-MS:  $m/z$  331.2 [M + H<sup>+</sup>]; compound previously reported<sup>19</sup> with little spectral data, *Crystal data for 5e*: C<sub>21</sub>H<sub>18</sub>N<sub>2</sub>O<sub>2</sub>,  $M_r = 330.37$ , monoclinic, space group  $P2_1/c$ ,  $a = 9.7200(2)$ ,  $b = 14.0370(2)$ ,  $c = 12.2058(1)$  Å,  $\beta = 97.056(2)$ ,  $V = 1652.74(4)$  Å<sup>3</sup>,  $Z = 4$ ,  $\mu(\text{Mo-K}\alpha) = 0.086$  mm<sup>–1</sup>. Of 24372 reflections measured, 4542 were unique with  $2\theta I > 2\sigma(I)$ ,  $R$  indices [ $I > 2\sigma(I)$ ]  $R_1 = 0.047$ ,  $wR_2 = 0.107$ , GoF on  $F^2 = 0.987$  for 228 refined parameters.

## 2-(4'-Hydroxyphenyl)-1,2,3,4-tetrahydroquinazoline, **4f**

**A. 1** (0.2031 g, 1.66 mmol) and **2f** (0.2034 g, 1.67 mmol) formed a sticky straw coloured melt which eventually solidified and ground into a yellow powder of **4f**, 80% conversion.

**B. 1** (0.1950 g, 1.60 mmol) and **2f** (0.1959 g, 1.60 mmol) heated together at 55 °C yielded **4f** in 75% conversion.

**C. 1** (0.2014 g, 1.65 mmol) and **2f** (0.2015 g, 1.65 mmol) yielded, after 30 mins, pale brown solid **4f** in 99% conversion.

Pale brown crystalline material, mp 154.2–155.4 °C (dichloromethane/dimethylsulfoxide).

$\delta_{\text{H}}(\text{DMSO})$ : 3.73 (1H, d,  $J = 16.5$  Hz), 3.98 (1H, d,  $J = 16.5$  Hz), 4.98 (1H, s), 6.46–7.76 (Ar–H), 9.34 (1H, br, –OH);  $\delta_{\text{C}}(\text{CDCl}_3)$ : 45.1 (–CH<sub>2</sub>–), 67.8 (–N–CH–N–), 114.1, 114.7, 115.7, 120.5, 125.5, 125.5, 126.3, 127.9, 133.0, 144.6, 156.7; ESI-MS:  $m/z$  227.1 [M + H<sup>+</sup>], 210.0 [M–OH]; microanalysis (%): calc. (found): C 74.31 (74.17), H 6.24 (6.16), N 12.38 (12.36), O 7.07 (7.12). *Crystal data for 4f*: C<sub>14</sub>H<sub>14</sub>N<sub>2</sub>O,  $M_r = 226.27$ , orthorhombic, space group  $Pbca$ ,  $a = 11.3431(4)$ ,  $b = 8.7088(2)$ ,  $c = 23.4287(5)$  Å,  $V = 2314.4(1)$  Å<sup>3</sup>,  $Z = 8$ ,  $\mu(\text{Mo-K}\alpha) = 0.083$  mm<sup>–1</sup>. Of 13743 reflections measured, 2867 were unique with  $2\theta I > 2\sigma(I)$ ,  $R$  indices [ $I > 2\sigma(I)$ ]  $R_1 = 0.048$ ,  $wR_2 = 0.112$ , GoF on  $F^2 = 1.045$  for 174 refined parameters.

## 2-[(2'-Aminobenzylimino)methyl]-3-hydroxyphenol, **3g**

**A. 1** (0.2064 g, 1.69 mmol) and **2g** (0.2338 g, 1.69 mmol) formed a sticky orange–brown coloured melt which eventually solidified and ground into a deep orange powder of **3g**, 99% conversion.

**B. 1** (0.2021 g, 1.66 mmol) and **2g** (0.2288 g, 1.66 mmol) heated together at 60 °C yielded, after 20 min heating, **3g** in 99% conversion.

Bright orange crystalline material, mp 136.5–137.9 °C (dichloromethane).

$\delta_{\text{H}}(\text{CDCl}_3)$ : 4.73 (2H, s), 6.67–7.16 (Ar–H), 8.21 (1H, s, –C=N–), 13.38 (1H, br, –OH), 13.68 (1H, br, –OH);  $\delta_{\text{H}}(\text{CDCl}_3)$ : 30.1 (–CH<sub>2</sub>–), 58.1 (–N–CH–N–), 116.7, 117.0, 117.1, 118.1, 119.4, 122.6, 129.7, 130.3, 165.7; ESI-MS:  $m/z$  242.3 [M + H<sup>+</sup>]; microanalysis (%) calc. (found): C 69.41 (69.26), H 5.82 (5.79), N 11.56 (11.39), O 13.21 (13.24).

## N-2-[3'-Hydroxysalicylideneimino)benzyl]-3"-hydroxysalicylideneimine, **5g**

**C. 1** (0.2047 g, 1.68 mmol) and **2g** (0.2337 g, 1.69 mmol) formed, after 2 h, deep orange solid **5g** in 99% conversion, mp 118.0–122.4 °C. (decomp.)

$\delta_{\text{H}}(\text{CDCl}_3)$ : 4.04 (2H, s), 6.49–7.03 (Ar–H), 7.81 (1H, s, –C=N–), 7.87 (1H, s, –C=N–); ESI-MS:  $m/z$  363.2 [M + H<sup>+</sup>]; compound previously reported<sup>20</sup> with little spectral data.

## 2-[(2'-Aminobenzylimino)methyl]-4-bromophenol, **3h**

**A. 1** (0.2030 g, 1.66 mmol) and solid **2h** (0.3361 g, 1.67 mmol) yielded, after 12 h, bright yellow **3h**, in 88% conversion.

**B. 1** (0.2062 g, 1.69 mmol) and **2h** (0.3335 g, 1.66 mmol) heated together at 65 °C yielded, bright yellow **3h** in 93% conversion.

Yellow crystals, mp 147.1–152.3 °C (dichloromethane or ethyl acetate).

$\delta_{\text{H}}(\text{CDCl}_3)$ : 4.76 (2H, s), 6.76–7.36 (Ar–H), 8.30 (1H, s, HC=N–), 13.20 (1H, br, –OH);  $\delta_{\text{C}}(\text{CDCl}_3)$ : 59.9 (–CH<sub>2</sub>–), 110.4, 116.3, 119.3, 120.5, 126.8, 130.2, 130.7, 132.6, 133.9, 135.3, 145.2, 160.3, 164.6; ESI-MS:  $m/z$  305.1 [M + H<sup>+</sup>], 288.0 [M–OH]; microanalysis (%): calc. (found): C 55.10 (55.16), H 4.29 (4.26), N 9.18 (9.19), O 5.24 (5.30); *Crystal data for 3h*: C<sub>14</sub>H<sub>13</sub>N<sub>2</sub>OBr,  $M_r = 305.17$ , monoclinic, space group  $P2_1/c$ ,  $a = 24.9478(9)$ ,  $b = 6.0316(2)$ ,  $c = 8.3285(3)$  Å,  $\beta = 98.391(1)$ ,

$V = 1239.82(8) \text{ \AA}^3$ ,  $Z = 4$ ,  $\mu(\text{Mo-K}\alpha) = 3.304 \text{ mm}^{-1}$ . Of 5161 reflections measured, 2494 were unique with  $2155 I > 2\sigma(I)$ ,  $R$  indices [ $I > 2\sigma(I)$ ]  $R_1 = 0.042$ ,  $wR_2 = 0.106$ , GoF on  $F^2 = 1.051$  for 172 refined parameters.

### ***N*-2-[5'-bromosalicylideneimino)benzyl]-5''-bromosalicylideneimine, 5h**

**C. 1** (0.2030 g, 1.66 mmol) and **2h** (0.3353 g, 1.67 mmol) yielded, after 10 min, bright yellow solid **5h** in 99% conversion.

Yellow crystals, mp 150.2–151.9 °C (ethyl acetate).

$\delta_{\text{H}}(\text{CDCl}_3)$ : 4.71 (2H, s), 6.61–7.27 (Ar-H), 8.14 (1H, s, -C=N-), 8.27 (1H, s, -C=N-), 12.80 (1H, br, -OH);  $\delta_{\text{C}}(\text{CDCl}_3)$ : 58.81 (-CH<sub>2</sub>-), 109.1, 109.8, 117.4, 118.0, 118.3, 119.1, 119.5, 126.6, 128.1, 128.4, 130.5, 132.5, 133.4, 134.0, 135.2, 146.0, 159.0, 159.1, 161.3, 164.0; ESI-MS:  $m/z$  488.96 [M + H<sup>+</sup>]; microanalysis (%): calc. (found): C 51.67 (51.69), H 3.30 (3.28), N 5.74 (5.80), O 6.55 (6.61). *Crystal data* for **5h**: C<sub>21</sub>H<sub>16</sub>N<sub>2</sub>Br<sub>2</sub>O<sub>2</sub>,  $M_r = 488.18$ , monoclinic, space group  $P2_1/c$ ,  $a = 24.8822(8)$ ,  $b = 4.6291(2)$ ,  $c = 16.5755(5) \text{ \AA}$ ,  $\beta = 106.263(2)$ ,  $V = 182.8(1) \text{ \AA}^3$ ,  $Z = 4$ ,  $\mu(\text{Mo-K}\alpha) = 4.443 \text{ mm}^{-1}$ . Of 4997 reflections measured, 4997 were unique with  $2316 I > 2\sigma(I)$ ,  $R$  indices [ $I > 2\sigma(I)$ ]  $R_1 = 0.050$ ,  $wR_2 = 0.076$ , GoF on  $F^2 = 0.901$  for 252 refined parameters.

### **2-[(2'-Aminobenzylimino)methyl]-3-methoxyphenol, 3i**

**A. 1** (0.2029 g, 1.66 mmol) and **2i** (0.2536 g, 1.67 mmol) formed a sticky orange-brown coloured melt which, after 18 h, solidified and ground into a deep orange powder of **3i**, 99% conversion.

**B. 1** (0.2008 g, 1.64 mmol) and **2i** (0.2510 g, 1.65 mmol) heated together at 60 °C yielded, after 10 min, **3i** in 99% conversion.

Deep orange crystals, 98.9–102.4 °C (dichloromethane).

$\delta_{\text{H}}(\text{CDCl}_3)$ : 3.91 (3H, s, -OCH<sub>3</sub>), 4.75 (2H, s) 6.75–7.15 (Ar-H), 8.39 (1H, s, HC=N-), 13.59 (1H, br, -OH);  $\delta_{\text{C}}(\text{CDCl}_3)$ : 56.3 (-CH<sub>2</sub>-), 59.9 (-N=C-), 111.9, 114.3, 115.8, 118.2, 118.9, 123.3, 126.7, 127.8, 129.2, 129.9, 144.8, 166.0; ESI-MS:  $m/z$  257.1 [M + H<sup>+</sup>], 240.1 [M-OH]; microanalysis (%): calc. (found): C 70.29 (71.61), H 6.29 (6.60), N 10.93 (10.47), O 12.48 (11.35).

### ***N*-2-[3'-(Methoxysalicylideneimino)benzyl]-3''-methoxysalicylideneimine, 5i**

**C. 1** (0.2007 g, 1.64 mmol) and **2i** (0.2511 g, 1.65 mmol) formed, after 18 h, orange solid **5i** in 99% conversion.

Dull orange solid, mp 94.5–99.9 °C, lit. 101–102 °C.<sup>21</sup>

$\delta_{\text{H}}(\text{CDCl}_3)$ : 3.85 (3H, s, -OCH<sub>3</sub>), 4.75 (2H, s) 6.75–7.03 (Ar-H), 8.48 (1H, s, -C=N-), 8.62 (1H, s, -C=N-), 13.59 (1H, br, -OH), 13.61 (1H, br, -OH); ESI-MS:  $m/z$  391.4 [M + H<sup>+</sup>], 257.1, 240.1 [M - OH].

### **2-(3',4'-Dimethoxyphenyl)-1,2,3,4-tetrahydroquinazoline, 4j**

**A. 1** (0.3344 g, 2.74 mmol) and **2j** (0.5641 g, 2.90 mmol) forming a tan coloured liquid which solidified to a hard, glassy material after 15 min. The extent of conversion to **4j** did not increase beyond 71% even after 2 d.

**B. 1** (0.0589 g, 0.48 mmol) and **2j** (0.0936 g, 0.48 mmol) heated at 52 °C yielded, after 5 min, **4j** in >99% conversion.

**C. 1** (0.1516 g, 1.24 mmol) and **2j** (0.2480 g, 1.28 mmol) yielded, after 19 h, a white solid, **4j** (0.2781 g, 85.4% yield, 88% purity).

White crystals, m.p 89.1–98.7 °C, (acetone).

$\delta_{\text{H}}(\text{CDCl}_3)$ : 3.88 (3H, s), 3.90 (3H, s), 4.01 (1H, d,  $J = 16.5$  Hz), 4.27 (1H, d,  $J = 16.5$  Hz), 4.73 (NH, s), 4.95 (NH, s), 5.17 (1H, s), 6.55–7.49 (Ar-H);  $\delta_{\text{C}}(\text{CDCl}_3)$ : 46.8 (-CH<sub>2</sub>-), 56.1 (-OCH<sub>3</sub>-), 56.2, (-OCH<sub>3</sub>-), 69.7 (-NH-CH-NH-), 109.3, 111.4, 115.2, 118.4, 118.9, 121.4, 126.4, 127.5, 134.5, 143.9, 149.4, 149.5; ESI-MS:  $m/z$  271.2 [M + H<sup>+</sup>]; microanalysis (%): calc. (found): C 71.09 (71.01), H 6.71 (6.76), N 10.36 (10.30), O 11.84 (11.85). *Crystal data* for **4j**: C<sub>16</sub>H<sub>18</sub>N<sub>2</sub>O<sub>2</sub>,  $M_r = 270.32$ , orthorhombic, space group  $Pna2_1$ ,  $a = 20.4722(3)$ ,  $b = 13.2281(2)$ ,  $c = 20.7521(4) \text{ \AA}$ ,  $V = 5619.8(2) \text{ \AA}^3$ ,  $Z = 16$ ,  $\mu(\text{Mo-K}\alpha) = 0.085 \text{ mm}^{-1}$ . Of 30579 reflections measured, 13156 were unique with  $7466 I > 2\sigma(I)$ ,  $R$  indices [ $I > 2\sigma(I)$ ]  $R_1 = 0.0639$ ,  $wR_2 = 0.0959$ , GoF on  $F^2 = 1.032$  for 761 refined parameters.

### **2-(4'-Bromophenyl)-1,2,3,4-tetrahydroquinazoline, 4k**

**A. 1** (0.2017 g, 1.65 mmol) and **2k** (0.3067 g, 1.66 mmol) formed a tan coloured melt which became tacky and solidified to a hard, glassy material after 18 h and was ground into a pale brown powder of **4k**, 99% conversion.

**B. 1** (0.2030 g, 1.66 mmol) and **2k** (0.3093 g, 1.67 mmol), heated together at 55 °C, yielded, after 20 min, **4k** in 98% conversion.

**C. 1** (0.2033 g, 1.66 mmol) and **2k** (0.3086 g, 1.67 mmol) yielded, after 3 h, pale brown solid **4k**, 99% conversion.

Pale brown crystalline material, m.p 82.2–84.9 °C, (ethyl acetate).

$\delta_{\text{H}}(\text{CDCl}_3)$ : 3.93 (1H, d,  $J = 16.5$  Hz), 4.16 (1H, d,  $J = 16.5$  Hz), 5.22 (1H, s), 6.60–7.75 (Ar-H);  $\delta_{\text{C}}(\text{CDCl}_3)$ : 46.0 (-CH<sub>2</sub>-), 69.1 (-NH-CH-NH-), 115.4, 118.6, 121.5, 122.6, 126.5, 127.6, 128.7, 132.0, 140.9, 143.5; ESI-MS:  $m/z$  291.1 [M + H<sup>+</sup>].

### **2-(3'-Chlorophenyl)-1,2,3,4-tetrahydroquinazoline, 4l**

**A. 1** (1.000 g, 8.29 mmol) and **2l** (0.93 mL, 8.21 mmol) yielded, after 2 d, **4l** in 92% conversion.

**B. 1** (0.2019 g, 1.65 mmol) and **2l** (0.20 mL, 1.77 mmol), heated together at 50 °C, yielded a sticky mass in 80 min. <sup>1</sup>H NMR analysis (%) revealed **4l** in 99% conversion.

**C. 1** (0.2067 g, 1.69 mmol) and **2l** (0.2378 g, 1.69 mmol) yielded, after 24 h, **4l**, 88% conversion, this product was difficult to isolate as in solution it is a very viscous liquid.

$\delta_{\text{H}}(\text{CDCl}_3)$ : 3.96 (1H, d,  $J = 16.8$  Hz), 4.23 (1H, d,  $J = 16.5$  Hz), 4.57 (NH, s), 4.98 (NH, s), 5.23 (1H, s), 6.55–8.00 (Ar-H); ESI-MS:  $m/z$  245.0 [M + H<sup>+</sup>].

### **2-(2',3'-Dichlorophenyl)-1,2,3,4-tetrahydroquinazoline, 4m**

**A. 1** (0.1583 g, 1.30 mmol) and **2m** (0.2295 g, 1.31 mmol) formed a tan coloured liquid which became tacky and solidified to a hard, glassy material after 18 h ground into a pale brown powder of **4m**, 95% conversion.

**B. 1** (0.1712 g, 1.4 mmol) and **2m** (0.2458 g, 1.4 mmol), heated together at 55 °C yielded, after 20 min, **4m** in 95% conversion.

**C. 1** (0.1298 g, 1.06 mmol) and **2m** (0.1867 g, 1.07 mmol) yielded, after 3 h, pale brown solid **4m**, 99% conversion.

Pale brown crystals, 111.6–114.3 °C (ethyl acetate).

$\delta_{\text{H}}$ (CDCl<sub>3</sub>): 3.93 (1H, d,  $J = 16.5$  Hz), 4.21 (1H, d,  $J = 16.5$  Hz), 5.67 (1H, s), 6.61–7.58 (Ar-H); ESI-MS:  $m/z$  279.2 [M + H<sup>+</sup>]; microanalysis (%): calc. (found): C 60.23 (60.27), H 4.33 (4.29), N 10.03 (10.01).

## Acknowledgements

This work was supported by an ARC, Special Research Centre grant for the formation of the Centre for Green Chemistry, Monash University.

## References

- L. N. Yakhontov, S. S. Liberman, G. P. Zhikhareva and K. K. Kuz'mina, *Khim.-Farm. Zh.*, 1977, **11**, 14.
- (a) H. Lau, J. T. Ferlan, V. H. Brophy, A. Rosowsky and C. H. Sibley, *Antimicrob. Agents Chemother.*, 2001, **45**, 187; (b) A. H. Calvert, T. R. Jones, P. J. Dady, B. Grzelakowska-Sztabert, R. Paine and G. A. Taylor, *Eur. J. Cancer*, 1980, **16**, 713; (c) A. H. Calvert, T. R. Jones; P. J. Dady, B. Grzelakowska-Sztabert, R. M. Paine, G. A. Taylor and K. R. Harrap, *Eur. J. Cancer*, 1980, **16**, 713; (d) J. B. Hynes, J. M. Buck, L. D'Souza and J. H. Freisheim, *J. Med. Chem.*, 1975, **18**, 1191.
- P. Desai, B. Naik, C. M. Desai and D. Patel, *Asian J. Chem.*, 1998, **10**, 615.
- D. M. Purohit and V. H. Shah, *Indian J. Heterocycl. Chem.*, 1999, **8**, 213.
- (a) G. Kempter, W. Ehrlichmann, M. Plesse and H. U. Lehm, *J. Prakt. Chem.*, 1982, **324**, 832; (b) G. Kempter, H. U. Lehm, M. Plesse, W. Ehrlichmann, A. Jumar and S. Kuehne, *Ger. Pat.*, 203 049, 1983.
- (a) M. Busch, *J. Prakt. Chem. N. F.*, 1895, **51**, 113; (b) M. Busch, *J. Prakt. Chem. N. F.*, 1896, **53**, 414.
- J. S. van den Eynde, J. Godin A. Mayence, A. Maquestiau and E. Anders, *Synthesis*, 1993, **9**, 867.
- T. Kitazuma, F. Zulfiqar and G. Tanaka, *Green Chem.*, 2000, **2**, 133.
- For example, see: (a) F. Toda and K. Tanaka, *Chem. Rev.*, 2000, **100**, 1025; (b) G. W. V. Cave, C. L. Raston and J. L. Scott, *Chem. Commun.*, 2001, 2159.
- (a) J. L. Scott and C. L. Raston, *Green Chem.*, 2000, **2**, 245; (b) K. Tanaka and R. Shiraishi, *Green Chem.*, 2000, **2**, 272.
- After 2 months, the percentage of **5e** in the mixture of **3e** and **5e** increased from 15 to 31%, indicating that the bis reaction product does accumulate in solution, albeit very slowly.
- K. Neuvonen and K. Pihlaja, *Acta Chim. Scand.*, 1993, **47**, 695.
- G. Rothenberg, A. Downie, C. L. Raston and J. L. Scott, *J. Am. Chem. Soc.*, 2001, **123**, 8701.
- G. M. Sheldrick, SHELXS-97, University of Göttingen, 1990.
- G. M. Sheldrick, SHELXL-97, University of Göttingen, 1997.
- L. J. Barbour, X-Seed—a graphical interface to the SHELX program suite, University of Missouri, 1999.
- K. Yvon, W. Jeitschko and E. Parthe, *J. Appl. Crystallogr.*, 1977, **10**, 73.
- J. Lessel, *Arch. Pharm.*, 1994, **327**, 329.
- H. Kanatomi, Y. Demura and I. Murase, *Jpn. Bull. Chem. Soc. Jpn.*, 1975, **48**, 2039.
- M. Sakamoto, M. Kumagai, H. Sakiyama and Y. Nishida, *Synth. React. Inorg. Met.-Org. Chem.*, 1997, **27**, 567.
- D. K. Dey, S. P. Dey, A. Elmali and Y. Elerman, *J. Mol. Struct.*, 2001, **562**, 177.





# *Cassia angustifolia* seed gum as an effective natural coagulant for decolourisation of dye solutions

Rashmi Sanghi,<sup>\*a</sup> Bani Bhattacharya<sup>a</sup> and Vandana Singh<sup>b</sup>

<sup>a</sup> 302 Southern Labs, Facility for Ecological and Analytical Testing, Indian Institute of Technology, Kanpur- 208016, India. E-mail: rsanghi@iitk.ac.in

<sup>b</sup> Chemistry Department, University of Allahabad, Allahabad- 211002, India

Received 3rd January 2002

First published as an Advance Article on the web 25th April 2002

Owing to economic advantages in addition to the potential for improved process robustness and to reduce the pollution load on the environment, particularly in water treatment applications in developing countries, an investigation with biodegradable and eco-friendly naturally occurring seed gum as coagulant was undertaken. Naturally occurring *Cassia angustifolia* (CA) seed gum was evaluated against the chemical coagulant polyaluminium chloride (PAC) for its coagulation ability to remove colour from synthetic dye solutions. Three groups of dyes: Acid Sendula Red, Direct Kahi Green and Reactive Remazol Brilliant Violet were chosen for the case study. For optimum results the variables studied were pH and dosage. CA was found to be a good working substitute alone or in conjunction with a very low dose of PAC for decolourisation of acid and direct, but not for reactive dye solutions. The performance of PAC was better with direct dye and that of CA was better with that of acid dye.

## Introduction

Textile wastewaters present major environmental and health implications. Colour is the first contaminant to be recognized in textile wastewaters and has to be removed before discharging into the receiving water body. The colour if not properly dealt with can have a strong negative impact on the aquatic environment. Hence decolourisation has become an integral part of the textile waste treatment process. Dyestuffs are highly structured polymers<sup>1</sup> with low or no biodegradability. Most of the dyes are hard to degrade<sup>2</sup> by biological means alone and chemical methods like coagulation-flocculation<sup>3</sup> using synthetic coagulants like alum and PAC offer good promise for primary treatment.

Alum is presently the most widely used coagulant. Due to its proven performance in treating wastewater of different characteristics and its low cost, it is extensively used in the drinking water and wastewater treatment. Recently polyaluminium chloride (PAC), a polymerised form of alum, has been increasingly used at treatment plants throughout the world. The advantage of this preformed polymeric aluminium over alum may be due to the partial elimination of polymerisation process that occurs after the coagulant is added to the water.<sup>4</sup>

Though chemical coagulation by alum and PAC may be a method of choice for treating waste waters before being fed to the biological treatment unit, it too has its drawbacks<sup>5</sup> as the effectiveness is strongly pH dependent and finished water may have high residual aluminium concentrations and significant amounts of sludge are produced which complicates handling and disposal procedures. Besides the possibility of Alzheimer's disease due to aluminium, the long-term effects of these chemicals on human health is not known. Further in many developing countries, the cost of importing alum and other required chemicals for conventional treatment might be high and at times prohibitive. To minimize these drawbacks, natural polyelectrolytes,<sup>6–8</sup> which are extracted from plant or animal life can be workable alternatives to synthetic polyelectrolytes. They are biodegradable, safe to human health and have a wider effective dosage range of flocculation for various colloidal suspensions.

Examples of the use of natural polyelectrolytes in drinking water clarification have been recorded throughout human history. Sanskrit writings from India reported that the seeds of Nirmali tree (*Strychnos potatorum*) were used to clarify<sup>9</sup> turbid surface water over 4000 years ago and in the last century Sudanese women discovered clarifying properties in the seeds from *Moringa oleifera*<sup>10</sup> a tree found pantropically throughout India, Asia, sub Saharan Africa and Latin America. Nirmali seeds<sup>11</sup> were found to be anionic polyelectrolytes that destabilize particles in water by interparticle bridging and *Moringa oleifera* has active particle destabilisation proteins. Experiments with extracts from the pulverized stalks, pods, leaves, roots and seeds of the okra<sup>12,13</sup> plant also yielded improved clarification over alum at high turbidity. The reduction in kaolin turbidity by Mesquite bean and *Cactus latifaria* is also comparable to alum coagulation at moderate turbidities. The water soluble proteins, a fraction of which are polar, perhaps contribute to the coagulation ability of the cactus extracts.<sup>14</sup>

Although most seeds contain starch as the principal food reserve, many contain other polysaccharides<sup>15</sup> and have some industrial utility. The first seed gums used commercially were quince, psyllium, flax and locust bean gum.<sup>16</sup> Harvesting of these gums is expensive, but harvesting from annual plants costs much less than from perennial plants or trees. This is clearly demonstrated by the tremendous increase in the use of guar, a gum that is extracted from an annual leguminous plant. Since

## Green Context

The presence of coloured contaminants in textile wastewaters is a major environmental problem and dyes are hard to degrade. Synthetic coagulants are now popular but there are serious health concerns associated with one of the most popular of these, polyaluminium chloride. Here, natural chemical coagulants are tested. It is shown that cassia seed gum can be an effective coagulant and for some dyes can act as a partial or full substitute for synthetic chemical coagulants such as aluminium compounds. *JHC*

the beginning of commercial production in 1953, the use of guar gum<sup>17</sup> has risen rapidly, more so in wastewater treatment technologies. The application of tarota (*Cassia tora*) as coagulant aid has been found<sup>18</sup> to improve treated water turbidity in conjunction with a much lower dosage of alum. With the advent of time and awareness about the hazards of pollution caused by chemicals used to treat wastewater, efforts to explore more seed gums effective for water treatment are underway.

## Results and discussion

Cassia (Caesalpinaceae) is a common annual plant grown in tropical countries and is abundantly available in India. The plants of genus *Cassia* are known to possess medicinal value and are a good source of mucilages, flavonoids, anthraquinones and polysaccharides. The seed gum of *Cassia angustifolia* was investigated for the first time for its potential as a coagulant in wastewater treatment alone and/or in conjunction with PAC. The structure of the polysaccharides obtained from the seeds of *C. angustifolia* has been well elucidated.<sup>19</sup> The polysaccharide was soluble in water and had an ash content of 0.4%. A water-soluble galactomannan consisting of D-galactose and D-mannose in the molar ratio 3:2 has been isolated from the seeds of *C. angustifolia*. The main chain of galactomannan (Fig. 1) was found to consist of (1→4)-linked mannopyranosyl units having β-glycosidic bonds while (1→6)-linked α-glycosidically bonded galactopyranosyl units form the branching points.

A study on the chemical precipitation technique has been carried out to decolourise different dye solutions on a laboratory scale. In this study the coagulation–flocculation test was carried out with aqueous solutions of three synthetic dyes ASR, DKG and RRV to determine the chemicals dosage, pH and dose of cassia alone or in conjunction with PAC, required to obtain optimum results. Coagulation dose and coagulation pH were found to be two of the most important factors influencing the types of hydrolysis products and hence the mechanism of coagulation.

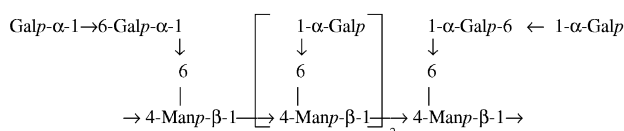


Fig. 1 Chemical structure of *Cassia angustifolia*

### Effect of pH on decolourisation studies

Since pH is an important factor in the flocculation studies, experiments with different dyes were carried out both in acidic (pH 2.5) and basic (pH 10.5) medium. At pH 2.5 the colour removal with 1 ml of PAC stock solution, was 35%, 22% and 16% for acidic, direct and reactive dye, respectively. Decolourisation efficiency was much enhanced under similar conditions but at pH 10 with almost 80%, 99% and 45% for acid, direct and reactive dyes, respectively. Hence all further studies were carried out in basic medium at pH 10.

### Effect of coagulant dosage on decolourisation of dye solutions

Colour removal increased with increase in dosage of coagulant used (Fig. 2). With 2 ml PAC dosage, almost 100% decolourisation was attained for ASR and DKG dyes but not for RRV dye. Similarly CA was effective for ASR and DKG dye but not for RRV dye. The results with the hydrolysed RRV dye were also

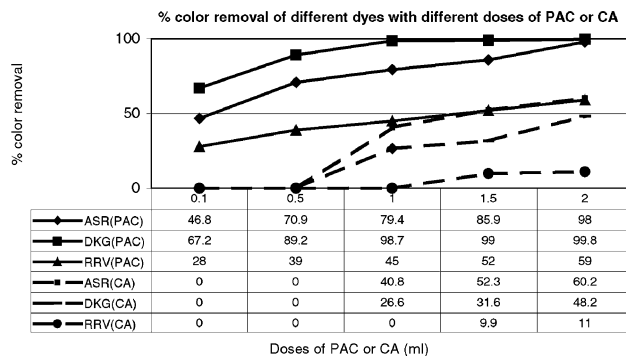


Fig. 2 Decolourisation efficiency of PAC and CA with respect to the three dyes.

not encouraging. RRV in both the hydrolysed and unhydrolysed state formed very poor and light weighted flocs, which settled with difficulty. The colour removal with PAC was in the order DKG > ASR > RRV and with CA was in the order ASR > DKG > RRV. CA was found to work only at a dosage of 1 ml or above. CA was not found to be effective for removal of RRV dye.

### CA as a coagulant aid in conjunction with low dose of PAC

The colour removal by using CA along with a very small dose of PAC (0.1 ml) was studied (Fig. 3). Colour removal enhancement with an added 1.5 ml dose of CA was from 47 to 70% and 67 to 83% for ASR and DKG dyes, respectively. Not much change was observed in the case of reactive RRV dye. The hydrolysed RRV dye showed no colour removal at all. CA was found to be effective only with DKG and ASR dyes (more so with ASR) attaining almost 84% colour removal at 2 ml dose in conjunction with 0.1 ml dose of PAC. For the DKG dye the enhancement in decolourisation on increasing the CA dose was not substantial and no further change was observed on further increasing the dose of CA beyond 2 ml. Perhaps the free OH groups in CA interact with the ASR and DKG dye functionalities but not with that of RRV having vinyl sulfone groups.

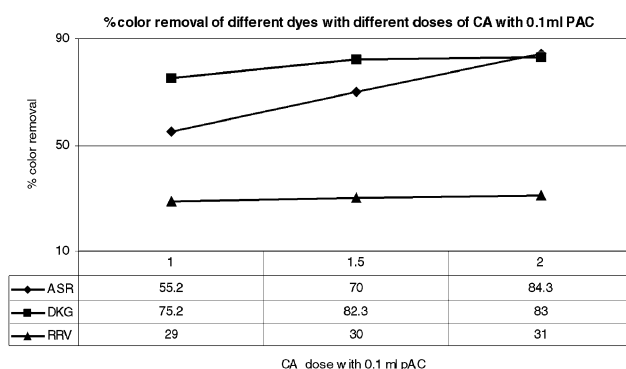


Fig. 3 CA as a coagulant aid in conjunction with a low dose of PAC.

## Experimental

### Isolation of *C. angustifolia* seed gum

The crushed and dried milled seeds (1 kg) were defatted with light petroleum (60–80 °C) and decolourised with ethanol, and then suspended in 1.5% acetic acid for 24 h. The polysaccharide was precipitated by pouring the mucilaginous extract in an

excess of 95% ethanol and the collected polysaccharide was dried over fused calcium chloride under reduced pressure. The desiccated polysaccharide was again dissolved in water and shaken well with chloroform; the denatured protein in the form of gel that collected at the water/chloroform interface was removed. The procedure was repeated four times to obtain polysaccharide free from protein.<sup>20</sup> It was then further purified by complexation with Fehling's solution. The complex thus formed was centrifuged, washed with dilute Fehling's solution and decomposed with 1 M HCl. The polysaccharide was regenerated by pouring the solution into an excess of ethanol with constant stirring. The powdered gum so obtained was used for color removal studies.

PAC-2010 was procured from DSCL (DCM Shriram Consolidated Ltd), N.Delhi India) and the dyes were commercially obtained. PAC was of industrial grade and NaOH used was of reagent grade. Dye stock solutions (20 mg in 1 litre of tap water) of commercially available Direct Kahi Green (DKG), Acid Sandolan Red RSNi (ASR) and Reactive Remazol Brilliant Violet 5R (RRV) dye were prepared. The dyes studied are all commercial dyes and were used without further purification. RRV, a vinyl sulfone dye was purchased from Colour-chem Ltd, Mumbai, ASR from Clariant whereas DKG was obtained as a sample from a local dyeing unit in Panki, Kanpur involved in thread dyeing. Since reactive dyes are used after hydrolysis, RRV dye was also studied in its hydrolysed form. Stock solutions of the coagulant PAC and coagulant aid were prepared. The PAC solution (equivalent to 85 mg l<sup>-1</sup> of Al<sub>2</sub>O<sub>3</sub>) was further diluted ten times. The stock solution (1 g l<sup>-1</sup>) of gum was prepared by dissolving 0.1 g of powder in 100 ml of distilled water. To make it completely water-soluble it was first blended for 5 min, kept in the ultrasonicator for a further 10 min, and then stored in refrigerator.

The dye concentrations were measured at a wavelength corresponding to the maximum absorbance,  $\lambda_{\text{max}}$  by means of a UV-Vis spectrophotometer (Shimadzu UV-160A). The percentage of colour removal was calculated by comparing the absorbance value of the supernatant to the standard curve obtained from a known dye concentration. The pH of the solution was measured with a Digital pH meter (MK VI Systronics). The absorbance, wavelength and pH measured for 20 ppm of acid, direct and reactive dyes were 0.32, 502.2, 7.9; 0.33, 379, 7.86 and 0.25, 559, 7.54, respectively.

150 ml graduated glass bottles were used in the study. Each bottle contained 100 ml of 20 ppm dye stock solution. A period of 1 min was allowed for the flash mixing of the coagulant, NaOH and the dye sample at 100 rpm followed by 20 min of slow agitation at 20 rpm. The solution was then allowed to settle and the time of settlement (approximately 1 h) was recorded.

After 1 h the supernatant was taken for colour analysis by the spectrophotometer.

## Conclusions

It may be concluded that Cassia seed gum can be an effective coagulant aid for direct and acid dyes. It can act as a working substitute, partially or fully, for synthetic chemical coagulants such as PAC. This can, not only reduce the amount of toxic sludge formed after treatment which is difficult to handle and dispose, but also make use of our natural resource in a very constructive and efficient way. There is a need to explore more of such natural resources, which can substitute chemicals for wastewater treatment technologies.

## References

- 1 A. Unden, *Water Sci. Technol.*, 1994, **29**, 179–185.
- 2 G. Mishra and M. Tripathi, *Colourage*, 1993, **10**, 35–38.
- 3 J. K. Edzwald, *Water Sci. Technol.*, 1993, **27**(11), 21–35.
- 4 T. Viraraghvan and C. H. Wimmer, 'Polyaluminium chloride as an alternative to alum coagulation: a case study', *Proc. Can. Soc. Civ. Eng. Annu. Conf.*, 1988, pp. 480–498.
- 5 S. Kawamura, *J. Am. Water Works Assoc.*, 1991, **83**, 89–91.
- 6 K. R. Bulusu, *Environ. Health*, 1963, **10**, 239–264.
- 7 R. Sanghi, *Asian Textile J.*, 2001, **10**(3), 73–75.
- 8 R. Sanghi and A. Singh, *Res. J. Chem. Environ.*, 2001, **5**(2), 35–37.
- 9 A. K. Sen and K. R. Bulusu, *Indian J. Environ. Health*, 1962, **4**, 233–244.
- 10 S. A. A. Jahn, *J. Am. Water Works Assoc.*, 1988, **6**, 43–50.
- 11 P. N. Tripathi, M. Chaudhari and S. D. Bokil, *Indian J. Environ. Health*, 1976, **18**, 272–281.
- 12 M. V. Vaidya and M. V. Nanoti, *Indian J. Environ. Health*, 1989, **31**, 43–48.
- 13 A. A. Samawi and E. M. Shokralla, *J. Environ. Sci. Health, Part A: Environ. Sci. Eng. Toxic Hazard. Subst. Control*, 1996, **31**, 1881–1897.
- 14 A. Diaz, N. Rinem, A. Escorihuela, N. Fernandez, E. Chacin and C. F. Forester, *Process Biochem.*, 1999, **35**, 391–395.
- 15 M. Adinolfi, M. M. Corsaro, R. Lanzetta, M. Parrilli, G. Folkard, W. Grant and J. Sutherland, *Carbohydr. Res.*, 1994, **263**, 103–110.
- 16 R. L. Whistler and C. L. Smart, *Polysaccharide Chemistry*, Academic Press, Inc, New York, 1953.
- 17 *Oil field Chemicals, North America*, C. H. Kline & Co., Fairfield, NJ, 1980.
- 18 V. A. Joshi and M. V. Nanoti, *Indian J. Environ. Protect.*, 1999, **19**, 451–455.
- 19 N. Alam and P. C. Gupta, *Planta Medica*, 1986, **4**, 308–310.
- 20 A. M. Staub, *Methods in Carbohydrate Chemistry*, ed. R. L. Whistler, Academic Press, New York-London, 1965, vol. 5, p. 5.





**Table 1** Conversion of aldehydes into 1,1-diacetates in the presence of H<sub>2</sub>NSO<sub>3</sub>H under ultrasound irradiation or through conventional method

Entry	Aldehyde	Solvent	Time/min		Temp.	Yields <sup>ab</sup> (%)		Mp/°C	
			A	B		A	B	Found	Reported
1	Benzaldehyde ( <b>1a</b> )	Neat	60	10	r. t.	90	94	44–45	44–45 <sup>4</sup>
2	Anisaldehyde ( <b>1b</b> )	Neat	90	23	r. t.	96	98	64–65	64–65 <sup>15</sup>
3	Salicylaldehyde ( <b>1c</b> )	Neat	30	20	r. t.	92	92	104–105	103–104 <sup>15</sup>
4	<i>m</i> -Nitrobenzaldehyde ( <b>1d</b> )	CH <sub>2</sub> Cl <sub>2</sub>	90	25	Reflux	96	97	65–66	64–66 <sup>15</sup>
5	<i>p</i> -Nitrobenzaldehyde ( <b>1e</b> )	CH <sub>2</sub> Cl <sub>2</sub>	60	20	Reflux	98	96	125–127	125–126 <sup>15</sup>
6	<i>o</i> -Nitrobenzaldehyde ( <b>1f</b> )	CH <sub>2</sub> Cl <sub>2</sub>	50	13	Reflux	97	97	90–91	90 <sup>25</sup>
7	Vanillin ( <b>1g</b> )	CH <sub>2</sub> Cl <sub>2</sub>	50	28	Reflux	98	95	92–93	90–91 <sup>15</sup>
8	2,4-Dichlorobenzaldehyde ( <b>1h</b> )	CH <sub>2</sub> Cl <sub>2</sub>	90	40	Reflux	99	98	101–102	
9	3-Chlorobenzaldehyde ( <b>1i</b> )	Neat	40	2	r. t.	96	97	64–65	65–66 <sup>15</sup>
10	4-Chlorobenzaldehyde ( <b>1j</b> )	CH <sub>2</sub> Cl <sub>2</sub>	10	8	r. t.	92	95	82–83	81–82 <sup>19</sup>
11	<i>p</i> -Tolualdehyde ( <b>1k</b> )	Neat	25	12	r. t.	98	98	81–82	81–82 <sup>5</sup>
12	Cinnamaldehyde ( <b>1l</b> )	Neat	20	15	r. t.	98	97	85–86	84–86 <sup>4</sup>
13	Piperonal ( <b>1m</b> )	CH <sub>2</sub> Cl <sub>2</sub>	40	20	r. t.	94	96	79–80	79–80 <sup>19</sup>
14	Furfuraldehyde ( <b>1n</b> )	Neat	30	18	r. t.	87	86	52–53	52–54 <sup>13</sup>
15	<i>p</i> -Dimethylaminobenzaldehyde ( <b>1o</b> )	CH <sub>2</sub> Cl <sub>2</sub>	240	180	r. t.	0	0		

A: without ultrasound irradiation B: under ultrasound irradiation.<sup>a</sup> Yield of pure isolated products. <sup>b</sup> Products characterized by <sup>1</sup>H NMR spectroscopy and comparison with authentic samples

reaction flask was located at the maximum energy area in the cleaner and addition or removal of water was used to control the temperature of the water bath. The products were also characterized by comparison of their melting point with literature values.

#### General procedure for the preparation of 1,1-diacetates through method A

A mixture of the aldehyde (5.00 mmol), acetic anhydride (15.0 mmol) and H<sub>2</sub>NSO<sub>3</sub>H (200 mg) was stirred under different conditions for the length of time given in Table 1. For the reactions with solvent CH<sub>2</sub>Cl<sub>2</sub> (5 ml) was also added. The progress of the reaction was monitored by TLC. After completion, Et<sub>2</sub>O (5 ml) was added to the reaction mixture and the catalyst was filtered off. The catalyst was washed with Et<sub>2</sub>O (2 × 5 ml) and then the filtrate was washed with 5% HCl (10 ml), 5% NaHCO<sub>3</sub> (10 ml) and brine (2 × 10 ml) successively and dried with MgSO<sub>4</sub>. The solvent was evaporated under reduced pressure and the residue was chromatographed on silica gel (light petroleum (bp 60–90 °C) as eluent).

#### General procedure for the preparation of 1,1-diacetates through method B

A mixture of the aldehyde (5.00 mmol), acetic anhydride (15.0 mmol) and H<sub>2</sub>NSO<sub>3</sub>H (200 mg) was put into a conical reactive flask. The flask was located at the maximum energy area in the cleaner and addition or removal of water was used to control the temperature of the water bath. Sonication was performed in a ShangHai Branson-CQX ultrasonic cleaner with a frequency of 25 kHz and a nominal power of 500 W. For the reactions with solvent CH<sub>2</sub>Cl<sub>2</sub> (5 ml) was also added. The progress of the reaction was monitored by TLC. After completion of the reaction, the subsequent steps were the same as in method A.

**3c:** δ<sub>H</sub> 2.09 [6H, s, ArCH(O<sub>2</sub>CCH<sub>3</sub>)<sub>2</sub>], 2.33 (3H, s, 2-CH<sub>3</sub>CO<sub>2</sub>), 7.05–7.69 (4H, m, C<sub>6</sub>H<sub>4</sub>), 7.89 [1H, s, ArCH(OAc)<sub>2</sub>].

**3g:** δ<sub>H</sub> 2.11 [6H, s, ArCH(O<sub>2</sub>CCH<sub>3</sub>)<sub>2</sub>], 2.29 (3H, s, 4-CH<sub>3</sub>CO<sub>2</sub>), 3.85 (3H, s, OCH<sub>3</sub>), 7.00–7.10 (3H, m, C<sub>6</sub>H<sub>3</sub>), 7.65 [1H, s, ArCH(OAc)<sub>2</sub>].

**3h:** δ<sub>H</sub> 2.15 [6H, s, ArCH(O<sub>2</sub>CCH<sub>3</sub>)<sub>2</sub>], 7.28–7.53 (3H, m, C<sub>6</sub>H<sub>3</sub>), 7.93 [1H, s, ArCH(OAc)<sub>2</sub>].

**3m:** δ<sub>H</sub> 2.02 [6H, s, ArCH(O<sub>2</sub>CCH<sub>3</sub>)<sub>2</sub>], 5.87 (2H, s, OCH<sub>2</sub>O), 6.65–6.93 (3H, m, C<sub>6</sub>H<sub>3</sub>), 7.51 [1H, s, ArCH(OAc)<sub>2</sub>].

#### Acknowledgement

The project was supported by National Natural Science Foundation of China (29872011 and 29572039), Educational Ministry of China, Educational Department of Hebei Province (990104), Science and Technology Commission of Hebei Province.

#### References

- 1 T. W. Green and P. G. M. Wuts, *Protective Groups in Organic Synthesis*, John Wiley, New York, 2nd edn., 1991, p. 175.
- 2 P. Cotelle and J. P. Cateau, *Tetrahedron Lett.*, 1992, **33**, 3855.
- 3 T. S. Jin, Y. R. Ma, Z. H. Zhang and T. S. Li, *Org. Prep. Proceed. Int.*, 1998, **30**, 463.
- 4 K. S. Kochhar, B. S. Bal, R. P. Deshpande, S. N. Rajadhyaksha and H. W. Pinnick, *J. Org. Chem.*, 1983, **48**, 1765.
- 5 T. S. Jin, G. Y. Du and T. S. Li, *Indian J. Chem., Sect. B*, 1998, **37**, 939.
- 6 E. R. Perez, A. L. Marrero, R. Perez and M. A. Autie, *Tetrahedron Lett.*, 1995, **36**, 1779.
- 7 B. B. Sinder and S. G. Amin, *Synth. Commun.*, 1978, **8**, 117.
- 8 F. Freeman and E. M. Karcherski, *J. Chem. Eng. Data*, 1997, **22**, 355.
- 9 G. A. Olah and A. K. Mehrotra, *Synthesis*, 1982, 962.
- 10 I. Sciabine, *Bull. Soc. Chem. Fr.*, 1996, 1194.
- 11 J. K. Michie and J. A. Miller, *Synthesis*, 1981, 824.
- 12 H. M. S. Kumar, B. V. S. Reddy, P. T. Reddy and J. S. Yadav, *J. Chem. Res. (S)*, 2000, 86.
- 13 P. Kumar, V. R. Hegda and T. P. Kumar, *Tetrahedron Lett.*, 1995, **36**, 601.
- 14 S. V. N. Raju, *J. Chem. Res. (S)*, 1996, 68.
- 15 Z. H. Zhang, T. S. Li and C. G. Fu, *J. Chem. Res. (S)*, 1997, 174.
- 16 T. S. Jin, G. Y. Du, Z. H. Zhang and T. S. Li, *Synth. Commun.*, 1997, **27**, 2261.
- 17 N. Deka, R. Borah, D. J. Kalita and J. C. Sarma, *J. Chem. Res. (S)*, 1998, 94.
- 18 V. K. Aggarwal, S. Fonquerna and G. P. Vennall, *Synlett*, 1998, 382.
- 19 T. S. Jin, Y. R. Ma, X. Sun, D. Liang and T. S. Li, *J. Chem. Res. (S)*, 2000, 96.
- 20 D. Karmakar, D. Prajapati and J. S. Sandhu, *J. Chem. Res. (S)*, 1998, 382.
- 21 J. L. Luche, *Synthetic Organic Sonochemistry*, Plenum Press, New York, 1998, p. 3.
- 22 T. S. Jin, Y. R. Ma, Z. H. Zhang and T. S. Li, *Synth. Commun.*, 1998, **28**, 3173.
- 23 J. Q. Zhang, *Huaxue Shiji (in Chinese)*, 1996, **37**, 423.
- 24 Y. Luo, M. Liu and J. Fan, *Huaxue Shiji*, 1998, **39**, 407.
- 25 *Dictionary of organic compounds*, Chapman and Hall, New York, 5th edn, 1982, vol. 4, p. 4224.



# Isomerization of *n*-butane by gallium-promoted sulfated zirconia supported on MCM-41

Wei Wang,<sup>a</sup> Chang-Lin Chen,<sup>\*a</sup> Nan-Ping Xu<sup>a</sup> and Chung-Yuan Mou<sup>b</sup>

<sup>a</sup> College of Chemical Engineering, Nanjing University of Technology, Nanjing 210009, China. E-mail: changlinc@yahoo.com

<sup>b</sup> Department of Chemistry, National Taiwan University, 1 Roosevelt Road, Section 4, Taipei, Taiwan

Received 6th February 2002

First published as an Advance Article on the web 13th May 2002

The *n*-butane isomerization reaction on sulfated zirconia (SZ) supported on MCM-41 mesoporous molecular sieve (SZ/MCM-41) was studied at various reaction temperatures in the presence of hydrogen. The catalytic activity was significantly improved with the addition of an appropriate amount of gallium as a promoter. The best conversion was achieved when the catalyst was promoted by 1.7 wt% gallium and calcined at 680 °C. Although the deactivation of these catalysts in the initial stage was observed the deactivated Ga-promoted SZ/MCM-41 catalysts (SZG/MCM-41) could be completely regenerated in air at 450 °C. The Pt-impregnated SZG/MCM-41 catalyst exhibited higher steady conversion compared with the Pt-free form. These halogen-free catalysts have advantages over other strong acid catalysts, in overcoming corrosion and environmental problems.

## Introduction

As an acid-catalyzed reaction, the isomerization reaction of straight-chain hydrocarbons to branched hydrocarbons is an important process for the production of clean-burning fuels in the petrochemical refining industry. For example, isobutene from butane is a key component for the manufacture of valuable gasoline additives such as methyl butyl ether (MTBE) to boost gasoline octane ratings. The current technology for *n*-butane isomerization is based on the Pt/chlorided Al<sub>2</sub>O<sub>3</sub> catalyst, which operates at elevated temperatures and requires constant addition of alkyl chlorides to recover acid functionalities. Owing to the increasingly strict environmental regulations, researchers have paid more attention to solid superacid catalysts to search for stable and environmentally friendly catalysts. Among the solid superacids, sulfated metal oxides, especially sulfated zirconia (SZ), have attracted considerable attention because they are more environmentally benign, and more active and selective for the transformation of hydrocarbons.<sup>1–4</sup> According to Parvulescu, *et al.*,<sup>5</sup> factors affecting the catalytic activity of SZ are their surface area and the sulfur content on the surface. Well prepared SZ catalysts can achieve surface areas around 100–120 m<sup>2</sup> g<sup>-1</sup>. Recently, Wolf and Risch<sup>6</sup> obtained SZ catalysts with high mesopore volume by prolonged reflux treatments. They found higher conversion in *n*-butane isomerization with this catalyst compared to results with a conventional catalyst with low mesopore volume. Hence, the preparation of SZ catalysts with high surface and high mesoporous volume is advantageous for *n*-butane isomerization. Thus it would be highly interesting to prepare SZ catalysts supported on mesoporous materials such as M41S with high surface area.<sup>7</sup> In this family, MCM-41 is an excellent support because of its uniform hexagonal array of mesopores and very high surface area (typically around 1000 m<sup>2</sup> g<sup>-1</sup> or higher).<sup>8–11</sup> A number of research groups have recently reported on the preparation of SZ on MCM-41,<sup>12</sup> SBA-15<sup>13</sup> and FSM-16<sup>14</sup> with various zirconium compounds as the precursors. However, the resulting catalysts were much inferior to the unsupported SZ owing to their lack of superacidity. They were, however, more suitable for medium strong and weak acid catalyzed reactions. Arata *et al.*<sup>15</sup> reported that zirconium

sulfate calcined at 725 °C shows strong acidity. Using zirconium sulfate as the precursor, SZ/MCM-41 was prepared in our previous paper.<sup>16</sup> However, the catalytic activities of SZ/MCM-41 for *n*-butane isomerization were very low. When Al was introduced into SZ/MCM-41, we found interesting strong acidity and good catalytic activities for *n*-butane isomerization. In this report, we continue our search for good promoters for SZ supported on MCM-41. With zirconium sulfate as the precursor, gallium-promoted SZ supported on pure siliceous MCM-41 was prepared by the direct impregnation method. The textural properties as well as acidities of the modified catalysts were characterized by X-ray powder diffraction (XRD), N<sub>2</sub> adsorption, and diffuse reflectance infrared fourier transform (DRIFT) spectroscopy. Their catalytic behaviors for *n*-butane isomerization in a flow system were studied. Very good improvements of catalytic activities were observed on the gallium-promoted SZ/MCM-41 catalysts. The influence of platinum addition was also considered.

## Results and discussion

For all the catalysts studied the ZrO<sub>2</sub> content was set at 50 wt%, which is close to the dispersion threshold of zirconia sulfate on MCM-41.<sup>16</sup> The samples were labeled according to their ingredients and the respective weight percent loading of

## Green Context

The search for highly active, stable and/or regenerable solid acids continues to be an important goal relevant to a range of processes. Sulfated zirconia has been proposed as a versatile highly acidic material with several possible applications. This article discusses the preparation of a form of sulfated zirconia on a high surface area support, and indicates that gallium in small amounts has a very beneficial effect in an important reaction type. *DJM*

gallium. For example, a promoted sulfated zirconia catalyst with 1.7% Ga is denoted as SZG(1.7)/MCM-41.

The structural characteristics of the SZG/MCM-41 catalysts with pore structure was confirmed by XRD. The strongest peak was at  $2\theta$  ca.  $2.3^\circ$  corresponding to the (100) reflection, characteristic of ordered porous structure in MCM-41 materials. The catalysts gave a set of broad, weak reflections between  $2\theta = 10$  and  $70^\circ$  that can be indexed as reflections from the tetragonal  $\text{ZrO}_2$  phase. BET analyses in Table 1 show that in comparison with those of the parent MCM-41, the surface area and pore volume over the modified MCM-41 was substantially decreased. The pore diameter of the modified samples was also decreased. These results suggest the presence of sulfated zirconia inside the pore channels of MCM-41. The sulfur contents of the modified MCM-41 are also listed in Table 1. The sulfur contents of SZG/MCM-41 catalysts are much higher than that of SZ/MCM-41. DRIFT spectra of adsorbed pyridine on SZ/MCM-41 samples before and after promotion with gallium were recorded. Under our experimental conditions, the pyridine adsorption bands for both sets of samples appeared only at 1607, 1490 and 1445  $\text{cm}^{-1}$ , with no band at 1540  $\text{cm}^{-1}$ . These data showed that Lewis acidity was dominant in both samples.

The isomerization reaction of butane was carried out at 250  $^\circ\text{C}$ . The material obtained by decomposition of  $\text{Zr}(\text{SO}_4)_2 \cdot 4\text{H}_2\text{O}$  was also tested. Decomposition of  $\text{Zr}(\text{SO}_4)_2 \cdot 4\text{H}_2\text{O}$  was performed by calcination at 680  $^\circ\text{C}$  for 3 h and the resultant sample is denoted Z680. The conversion of *n*-butane isomerization for Z680, SZ/MCM-41 and SZG(1.7)/MCM-41 catalysts is given in Table 2. SZ/MCM-41 has a similar activity to Z680. However, great improvements were observed in catalytic activities over SZG(1.7)/MCM-41. The initial catalytic activity of SZG(1.7)/MCM-41 was improved up to 43%. The selectivity to isobutene was also improved up to around 88%. Fig. 1 showed the effect of various amounts of Ga incorporated in SZ/MCM-41 catalysts on *n*-butane isomerization at 250  $^\circ\text{C}$ . The *n*-butane conversion increased with the Ga content up to 1.7 wt%, and then decreased as the Ga content was further increased.

**Table 1** Textural and physical properties of the parent MCM-41 and modified MCM-41 catalysts

Sample	$S_{\text{BET}}/\text{m}^2 \text{g}^{-1}$	Pore volume/ $\text{cm}^3 \text{g}^{-1}$	Pore diameter/nm	$\text{SO}_3$ content (wt%)
MCM-41	1010	1.10	2.86	—
SZ/MCM-41	442	0.31	2.15	2.3
SZG(0.57)/MCM-41	438	0.32	2.23	3.2
SZG(1.70)/MCM-41	480	0.36	2.26	3.6
SZG(2.84)/MCM-41	357	0.27	2.24	4.1

**Table 2** *n*-Butane conversion and product selectivity at 250  $^\circ\text{C}$  over Z680, SZ/MCM-41 and SZG/MCM-41 catalysts

Catalyst	Time/min	Conversion (%)	Selectivity (%)			
			$\text{C}_3$	<i>i</i> - $\text{C}_4$	<i>i</i> - $\text{C}_5$	<i>n</i> - $\text{C}_5$
Z680	5	4.26	9.86	81.1	4.93	1.81
	60	3.67	10.9	76.2	6.81	3.11
	360	—	—	—	—	—
SZ/MCM-41	5	5.17	9.16	80.8	4.02	1.49
	60	4.72	10	79	4.91	1.53
	360	—	—	—	—	—
SZG(1.7)/MCM-41	5	43.85	5.47	87.5	3.92	1.44
	60	29.10	5.26	89.4	2.71	1.03
	360	20.44	4.62	89.8	2.6	1.02

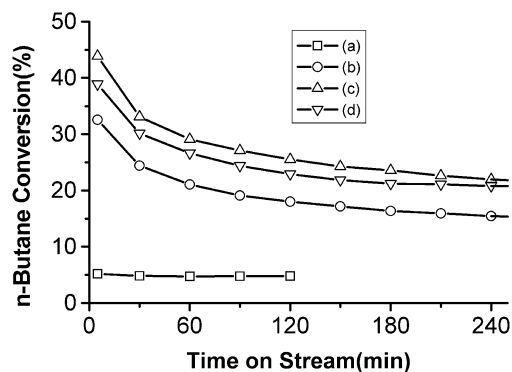


**Fig. 1** Catalytic activity of catalysts ( $\text{ZrO}_2$  content 50 wt%) calcined at 680  $^\circ\text{C}$  with the following Ga loadings: (a) 0.0 wt%, (b) 0.57 wt%, (c) 1.7 wt%, (d) 2.84 wt%.

Although, the activity of each SZG/MCM-41 sample decreased in the initial stage, the steady activity values of these SZG/MCM-41 samples were still higher than that of the SZ/MCM-41 catalyst.

For comparison, the results of other previous studies<sup>17,18</sup> are also listed in Table 2. We found much a higher initial activity in butane isomerization at 250  $^\circ\text{C}$  with time on stream with our SZG/MCM-41 catalyst compared to results with bulk SZ, SZ/ $\gamma$ - $\text{Al}_2\text{O}_3$ , SZ/ $\text{SiO}_2$  and Al-promoted SZ/MCM-41 (denoted SZA/MCM-41) catalysts. The initial activity of SZG(1.7)/MCM-41 is three times that of bulk SZ. In comparison with bulk SZ, SZ/ $\gamma$ - $\text{Al}_2\text{O}_3$  and SZ/ $\text{SiO}_2$  catalysts, great improvements were observed in both initial activities and steady activities of SZG/MCM-41. Previously, it was reported that aluminium is a good promoter for the SZ-catalyzed butane isomerization.<sup>17,18</sup> We observe from Table 3 that gallium is an even better promoter than aluminium under comparable conditions.

**Table 3** *n*-Butane isomerization activities of various catalysts at 250  $^\circ\text{C}$

Catalyst	Time/min	Activity/ $\text{mmol g}^{-1} \text{h}^{-1}$	Reference
SZG(0.57)/MCM-41	5	2.91	This study
	360	1.32	
SZG(1.7)/MCM-41	5	3.92	17
	360	1.825	
SZG(2.84)/MCM-41	5	3.47	18
	360	1.875	
60%SZ/ $\gamma$ - $\text{Al}_2\text{O}_3$	2	2.24	17
	360	1.425	
SZA/MCM-41	5	2.46	18
	360	1.6	
90%SZ/ $\text{SiO}_2$	2	0.46	17
	360	0.10	
SZ	2	1.125	17
	360	0.55	

The calcination temperature used for the preparation of SZG/MCM-41 catalysts has a significant effect on the catalytic activities for *n*-butane isomerization. Fig. 2 shows the depend-

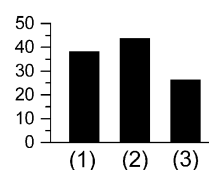


**Fig. 2** Effect of calcination temperature on butane conversion at time-on-stream of 5 min over the catalyst SZG(1.7)/MCM-41 at 250  $^\circ\text{C}$  ( $\text{ZrO}_2$ :50 wt%, Ga: 1.7 wt%): (1) 630  $^\circ\text{C}$ , (2) 680  $^\circ\text{C}$ , (3) 720  $^\circ\text{C}$ .

ence of butane conversion on calcination temperature. The initial conversion was above 43% on the catalyst calcined at 680 °C while catalysts calcined at 630 and 720 °C have low activities. When the catalyst was calcined at 720 °C, the initial conversion decreased to 26.5%.

The variation of the conversion vs. time on stream for SZG(1.7)/MCM-41 at several reaction temperatures are given in Fig. 3 from which it is observed that higher reaction temperatures gave higher initial activity. When the reaction was run at 220 °C, though the initial activity was lower, the activity became more stable with time on stream. When the reaction was run at 250 °C, the initial conversion ( $t = 5$  min) of around 44% fell to approximately 20% after 6 h on stream. After a fast initial deactivation, the isomerization activity declined at a lower rate. Though fast initial deactivation was observed, the catalyst could be completely recovered. The regeneration property of the catalyst is shown in Fig. 4. The catalyst after reaction on stream for 6 h can be regenerated by heating in dry air at 450 °C for 3 h. The regenerated catalyst has almost the same activity as the fresh catalyst. Possible deactivation of the SZ solid superacid catalyst is due to the loss of sulfur or to coking on the catalyst surface. From our experimental result it seems that coking may be the predominant factor.

The conversion vs. time curves obtained over the Pt-impregnated SZG/MCM-41 and SZG/MCM-41 catalysts are shown in Fig. 5. For the Pt-impregnated catalyst, a steady regime was attained. The conversion at 5 min was slightly lower than for the Pt-free form, whereas the steady conversion and selectivity to isobutane were enhanced. The steady conversion was improved up to around 28%.

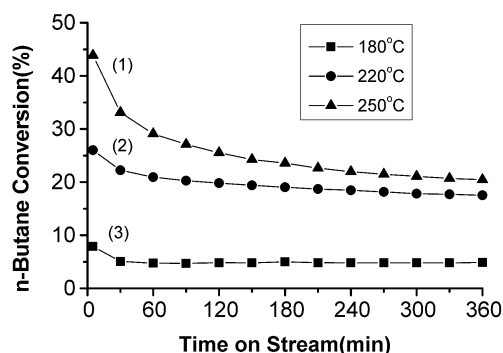


**Fig. 3** Influence of reaction temperature on conversion over the catalyst SZG(1.7)/MCM-41 ( $\text{ZrO}_2$ :50 wt%; Ga: 1.7 wt%): (1) 250 °C, (2) 220 °C, (3) 180 °C.

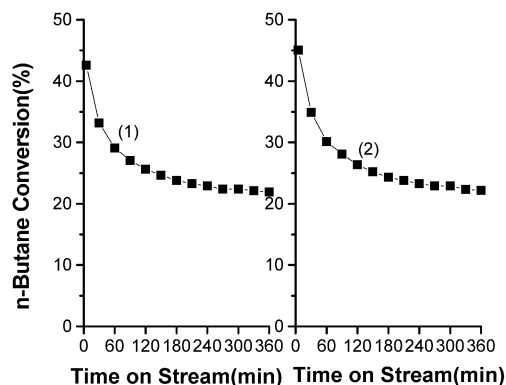


**Fig. 4** Regeneration of the catalyst SZG(1.7)/MCM-41 ( $\text{ZrO}_2$ :50 wt%; Ga:1.7 wt%): (1) fresh catalyst, (2) regenerated catalyst. Regeneration conditions: heating in dry air at 450 °C for 3 h.

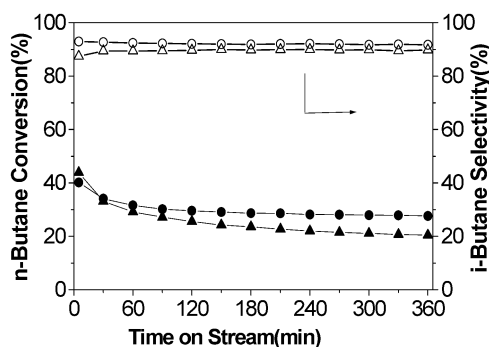


**Fig. 5** Catalytic activity of catalysts for the Pt-free and Pt-impregnated SZG/MCM-41 ( $\text{ZrO}_2$ :50 wt%; Ga:1.7 wt%) at 250 °C: (●,○) Pt-impregnated SZG/MCM-41 (Pt:0.5 wt%), (▲,△) SZG/MCM-41.

In summary, the Ga-promoted SZ/MCM-41 catalyst is a new kind of solid acid catalyst with substantial mesoporous volume. An environmentally friendly catalyst, unlike liquid superacid catalysts, such as  $\text{HF} + \text{SbF}_5$  and  $\text{HCl} + \text{AlCl}_3$ , it has a high catalytic activity for *n*-butane isomerization and can be completely regenerated.

## Experimental

As-synthesized pure siliceous MCM-41 was synthesized using the delayed neutralization process reported by Lin *et al.*<sup>19</sup> The gel was crystallized in static conditions at 100 °C for 5 days. Then the solid product was filtered off, washed with deionized water, and dried in air. The as-synthesized mesoporous material was impregnated with a desired amount of  $\text{Zr}(\text{SO}_4)_2$  in methanol and stirred at room temperature for about 10 h. The resulting sample was dried at 80 °C. Finally, it was calcined at 680 °C for 3 h in air. Ga-promoted samples were prepared in the same way with the desired amount of zirconium sulfate and gallium sulfate. The Pt-impregnated SZG/MCM-41 catalyst was prepared by impregnating  $\text{H}_2\text{PtCl}_6$  solution with SZG/MCM-41. The concentration of the solution was adjusted in order to obtain 0.5% Pt on the final catalyst. After impregnation, the sample was held for 4 h at room temperature. Then it was dried at 110 °C overnight and calcined in the reactor at 450 °C in an air stream for 3 h. Before reaction, the catalyst was reduced in a  $\text{H}_2$  stream for 1 h at 250 °C.

XRD measurements were carried out on a Bruker D8 Advance instrument with  $\text{Cu-K}\alpha$  radiation at 40 kV and 30 mA. BET surface areas of the samples were acquired on a Micromeritics ASAP 2010 automatic adsorption instrument using  $\text{N}_2$  as the adsorbent. DRIFT spectra of the adsorbed pyridine were recorded using a BOMEM MB155 FT-IR/Raman spectrometer. The sample was pre-heated at 300 °C for 3 h under  $10^{-6}$  mbar vacuum before pyridine vapor was introduced at room temperature, followed by evacuation at 400 °C for 1 h. Sulfur content in the catalysts was detected by a chemical method. The sulfate was converted into  $\text{BaSO}_4$  and determined by gravimetric method.

The isomerization of *n*-butane to isobutene was performed in a fixed-bed continuous flow reactor operated at atmospheric pressure. The catalyst samples were pelletized and sized to 20–60 mesh. Approximately 0.6 g of the catalyst was loaded into the reactor and then pretreated in flowing dry air ( $20 \text{ ml min}^{-1}$ ) at 450 °C for 3 h. The reactor temperature was then lowered to the reaction temperature of 250 °C or other desired temperature. After thermal equilibrium was established, the reaction was started by feeding an *n*-butane– $\text{H}_2$  mixture (1:10



v/v) at an *n*-butane weight hourly space velocity (WHSV) of 0.52 h<sup>-1</sup> through the catalyst. An on-line gas chromatograph equipped with FID was used to analyze the reaction products.

## Acknowledgments

We acknowledge the support of the Educational Department of Jiangsu Province project (00KJB530001 to C.-L. C.) and Key Laboratory of Chemical Engineering and Technology of Jiangsu Province.

## References

- 1 M. Hino, S. Kobayashi and K. Arata, *J. Am. Chem. Soc.*, 1979, **101**, 6439.
- 2 M. Hino and K. Arata, *J. Chem. Soc., Chem. Commun.*, 1979, 1148.
- 3 A. Corma, *Chem. Rev.*, 1995, **95**, 559.
- 4 X. Song and A. Sayari, *Catal. Rev.-Sci. Eng.*, 1996, **38**, 329.
- 5 V. Parvulescu, S. Cman, V. I. Parvulescu, P. Grange and G. Poncelet, *J. Catal.*, 1998, **180**, 66.
- 6 E. E. Wolf and M. A. Risch, *Appl. Catal. A.*, 1998, **172**, L1.
- 7 C. T. Kresge, M. E. Leonowicz, W. J. Roth, J. C. Vartuli and J. S. Beck, *Nature*, 1992, **359**, 710.
- 8 A. Corma, A. Martinez, V. Martinez-Soria and J. B. Monton, *J. Catal.*, 1995, **153**, 25.
- 9 A. Corma, A. Martinez and V. Martinez-Soria, *J. Catal.*, 1997, **169**, 480.
- 10 T. Ookoshi and M. Onaka, *Chem. Commun.*, 1998, 2399.
- 11 T. Blasco, A. Corma, A. Martinez and P. Martinea-Escolano, *J. Catal.*, 1998, **177**, 306.
- 12 Q. H. Xia, K. Hidajat and S. Kawi, *Chem. Commun.*, 2000, 2229.
- 13 T. Lei, W. M. Hua, Y. Tang, Y. H. Yue and Z. Gao, *J. Mol. Catal. A.*, 2001, **170**, 195.
- 14 H. Matsushashi, M. Tanaka, H. Nakamura and K. Arata, *Appl. Catal. A.*, 2001, **208**, 1.
- 15 K. Arata, M. Hino and N. Yamagata, *Bull. Chem. Soc. Jpn.*, 1990, **63**, 244.
- 16 C. L. Chen, T. Li, S. Cheng, H. P. Lin, C. J. Bhongale and C. Y. Mou, *Microporous Mesoporous Mater.*, 2001, **50**, 201.
- 17 T. Lei, J. S. Xu, Y. Tang, W. M. Hua and Z. Gao, *Appl. Catal. A.*, 2000, **192**, 181.
- 18 C. L. Chen, S. Cheng, H. P. Lin, S. T. Wong and C. Y. Mou, *Appl. Catal. A.*, 2001, **215**, 21.
- 19 H. P. Lin, S. Cheng and C. Y. Mou, *Microporous Mater.*, 1997, **10**, 111.



# A greener approach to cotton dyeings. Part 2: application of 1:2 metal complex acid dyes†

Richard S. Blackburn and Stephen M. Burkinshaw

Specialty Chemical Group, School of Textiles & Design, University of Leeds, UK.  
E-mail: r.s.blackburn@leeds.ac.uk

Received 21st February 2002

First published as an Advance Article on the web 14th May 2002

Further attempts were made to find a more environmentally friendly method of dyeing cotton as an alternative to standard reactive dyeing processes that require high levels of water, salt and alkali and produce high levels of effluent contamination. Pre-treatment with a polymeric cationic quaternary ammonium compound enabled dyeing of the fibre with 1:2 (M:L) metal complex acid dyes without salt at neutral/slightly acidic pH values. In comparison with standard reactive dyeing processes, both the time taken for the dyeing process to be completed and the volume of water required could be dramatically reduced. The dyeings secured using the pre-treatment method displayed high colour strength values, good to very good wash fastness and excellent light fastness.

## Introduction

The first paper in this series<sup>1</sup> discussed attempts made to find a more environmentally friendly method of dyeing cotton as an alternative to standard reactive dyeing processes that require high levels of water, salt and alkali and produce high levels of effluent contamination. By employing a pre-treatment method, salt and alkali could be completely eliminated from the dyeing process and, in comparison with standard reactive dyeing processes, the time taken for the dyeing process to be completed could be significantly reduced and the volume of water required could be halved.

The work in this paper concerns another green method of dyeing cotton without the need for salt or alkali and using considerably less water. Currently, the *Jarofast* system<sup>2</sup> is used to achieve the popular 'washed out' look of modern cellulosic garments. In this process 100% cotton is pre-treated with *Jarofix 391*, a cationic agent, then subsequently dyed with *Jarasol* dyes, which are water-soluble, anionic, C. I. Solubilised Sulphur dyes containing thiosulfonic acid (Buntë salt;  $-\text{SSO}_3^-$ ) groups. Dye-fibre substantivity arises primarily from ionic interactions between the anionic dyes and the cationic pre-treated substrate, negating the need for electrolyte in the dyebath. However, this system has several disadvantages associated with it, namely that it has a limited number of dyes (15) that can be used in the system, it confers generally poor wash fastness and gives low light fastness ratings.

It was thought that it would be possible to develop a *Jarofast*-type dyeing system with improved light and wash fastness that could be applied to cotton. In this context it was decided to pre-treat cotton fabrics with a cationic polymer, which has substantivity for cellulose.

Following this pre-treatment, 1:2 (M:L) metal complex acid dyes were to be applied as they furnish a full range of shades and display very high light fastness and good wash fastness on polyamide substrates such as wool, nylon and silk.<sup>3–5</sup> They are not currently supplied for application to cotton due to a lack of substantivity for the fibre,<sup>3</sup> but it was thought that the use of a

*Jarofast*-type system would enable their application to cotton without the need for salt, alkali or a wash-off procedure.

## Experimental

### General structure of pre-treatment agent

It was postulated that incorporation of cationic sites within a polymer, which could then be applied to cotton, could enable dyeing with metal complex acid dyes to be carried out in a more efficient manner at neutral/slightly acidic pH values without salt or alkali.

The pre-treatment agent employed is a developmental polymer and as such specific details of its structure cannot be disclosed. In general, it has a plurality of cationic centres and is made by polymerisation of monomers containing cationic centres. Desirably the cationic centres are quaternary ammonium groups. Generally, the most effective polymers have a degree of cationicity that is at least one cationic, particularly quaternary ammonium, centre per 500 g mol<sup>-1</sup>, with desirably at least 1 cationic centre per 5 monomer residues in the polymer. The polymer has a molecular weight in the region of 10000–30000 g mol<sup>-1</sup>. The cationic pre-treatment agent used in this study is a polymer of 4-vinylpyridine quaternised with chloroethane at a concentration to give 50% quaternisation of

## Green Context

**The dyeing industry is a large consumer of chemicals and a very large producer of waste, typically as aqueous waste which is very difficult to deal with. This article is another step forward in trying to reduce the environmental impact of this industry. It is demonstrated that pre-treatment of cotton with cationic polymer enables dyeing that has acceptable wash fastness and avoids salt and alkali, and consumes less water. Processing times are also shorter. Overall this represents a significantly greener alternative to standard reactive dyeing processes for cotton.** JHC

† Part 1 is ref. 1.

the pyridine residues leaving 50% unquaternised as free pyridine rings attached to the polymer (Fig. 1). The polymer has a molecular mass in the region of  $16000 \text{ g mol}^{-1}$ .

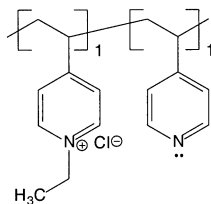


Fig. 1 Poly(4-vinyl-N-ethylpyridine) quaternised polymer.

### Operation of the pre-treatment system in dyeing with 1:2 metal complex acid dyes

The pre-treatment agent is highly substantive to cellulosic fibre, in the case of poly(4-vinylpyridine) quaternary ammonium compounds this is through a combination of ion–ion forces, strong hydrogen bonding and van der Waals forces. Adsorption of the pre-treatment agent onto cotton arises through ion–ion interactions operating between the cationic groups in the agent and the anionic carboxylic acid groups in the substrate,<sup>6,7</sup> which owing to their relatively low  $pK_a$  values will be ionised at the pH values of application (pH 6–7).

Strong H-bonding would be expected to contribute to agent–fibre attraction through so-called Yoshida forces<sup>8</sup> operating between the electron deficient hydrogen atom of the hydroxyl groups in the fibre and the  $\pi$ -electron system of the unquaternised pyridine rings in the pre-treatment agent. In addition, further ion–dipole interaction may be expected between the positively charged nitrogen atom of the pyridinium rings and the lone pair electrons on the oxygen atom of the cellulosic hydroxyl groups (Fig. 2).

Once the agent has been adsorbed onto the cotton, 1:2 metal complex acid dyes are introduced. The anionic dye molecules are attracted to the cationic sites in the polymer through ionic association and the extended  $\pi$ -electron systems of both dye and pre-treatment agent have high levels of interaction and association. This enables adsorption of the dye without the need

for adding salt at neutral or slightly acidic pH. The mechanism of how the pre-treatment agent works is shown schematically in Scheme 1.

### Materials

The 1:2 metal complex acid dyes used in the study and their Colour Index generic names are shown in Table 1. Crompton & Knowles, France generously supplied samples of each of the dyes. Commercially available 1:2 metal complex acid dyes are supplied as unsulfonated (*Neutrilan K*), monosulfonated (*Neutrilan S*) and disulfonated (*Neutrilan M*) types. The structure of C. I. Acid Violet 90 is given in Fig. 3 and the structure of C. I. Acid Blue 193 is given in Fig. 4.<sup>9</sup> The manufacturers do not disclose the detailed structures of the other seven dyes used, but in general they are complexes of two monoazo dye residues coordinated in an octahedral arrangement around a central  $\text{Cr}^{\text{III}}$  atom. The dyes are unsulfonated, monosulfonated or disulfonated as a result of the number of sulfonic acid groups on the whole complex and the complexes may be either symmetric, where the two dye residues are the same, or asymmetric, where the two dye residues are the different. By definition, monosulfonated 1:2 metal complex acid dyes are asymmetric.

Bleached, scoured, fluorescent brightener free, woven cotton ( $150 \text{ g m}^{-2}$ ) was supplied by Whaley's, Bradford, UK. Uniqema supplied the pre-treatment agent. All other chemicals were of general laboratory grade.

### Dyeing by pre-treatment method

Cotton samples were pre-treated and dyed in sealed stainless steel dye pots of  $300 \text{ cm}^3$  capacity, housed in a laboratory-scale *Roaches Pyrotec S* dyeing machine. At the end of dyeing the samples were removed and dried in the open air. The method used for each of the dyes shown in Table 1 is displayed graphically in Fig. 5. The pH of application was in the range pH 6–7, this being achieved without any adjustment through addition of the pre-treatment agent alone to the water of application. For comparison purposes, untreated cotton samples were dyed under the same conditions.

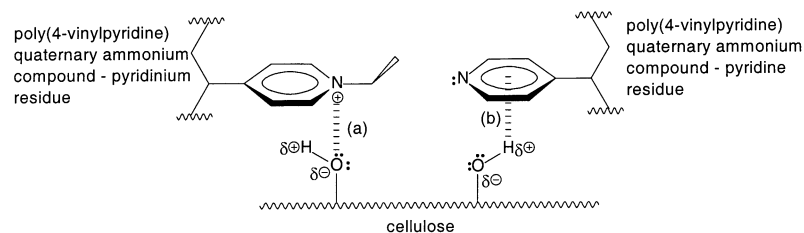
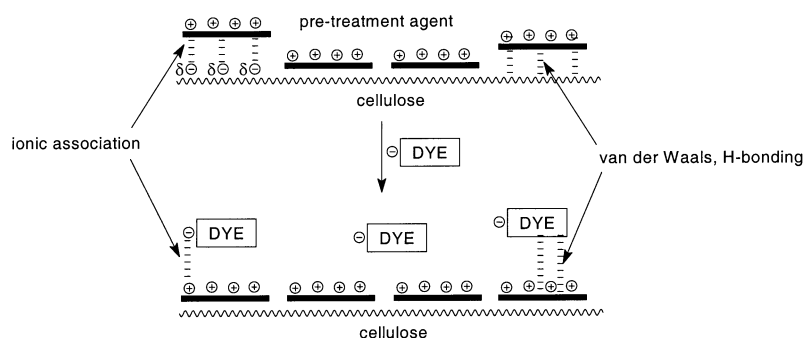


Fig. 2 (a) Ion–dipole interactions between cellulose hydroxy groups and pyridinium residues of the pre-treatment polymer and (b) Yoshida H-bonding between cellulose hydroxy groups and pyridine residues in the pre-treatment polymer.



Scheme 1 Mechanism of pre-treatment of cotton and dyeing with 1:2 metal complex acid dyes.

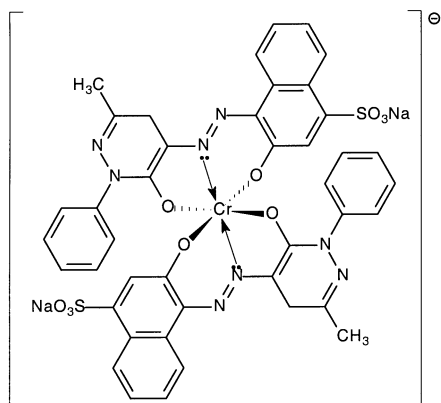


Fig. 3 C. I. Acid Violet 90.

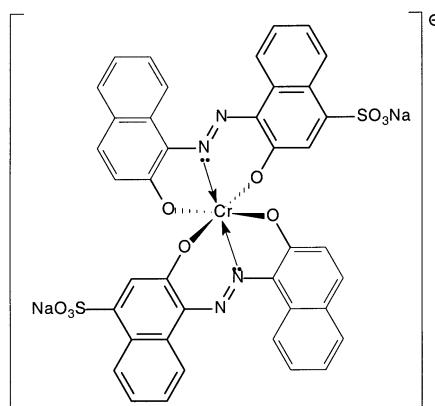


Fig. 4 C. I. Acid Blue 193.

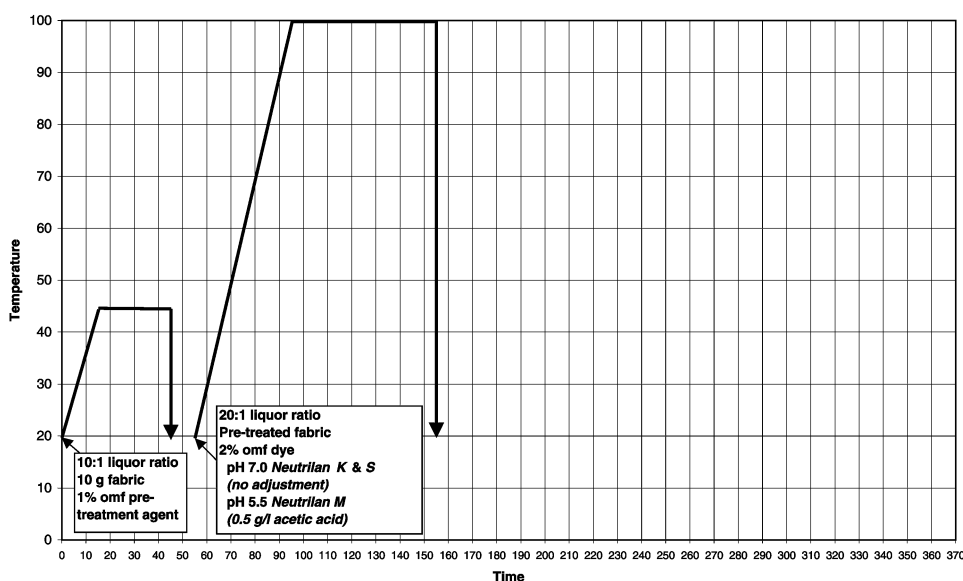


Fig. 5 Method of pre-treatment and application of reactive dyes to cotton.

### Wash fastness testing

Samples were subjected to the ISO 105:C06/A2 wash test (40 °C) using SDC (Society of Dyers & Colourists) multifibre fabric as adjacent.<sup>10</sup> After washing the samples were visually assessed using grey scales according to the ISO 105:A02 and ISO 105:A03 test protocols<sup>10</sup> to determine the degree of washdown and cross staining, respectively. The grey scale ranges from 5 for no shade change (or no stain on the adjacent fibres) down to 1 for a severe shade change (or staining), with half points in between.

### Light fastness testing

Samples were subjected to the ISO 105:B02 light fastness test (xenon arc, artificial light) using SDC blue wool standards 1 to 8 as reference.<sup>10</sup> The blue wool scale ranges from 8 for excellent light fastness down to 1 for very poor light fastness.

### Colour measurement

The samples were measured using a *Match-Rite*<sup>TM</sup> colour spectrophotometer attached to a personal computer. From the reflectance values at the  $\lambda_{\max}$  of the dyeings ( $R$ ), the colour strength ( $K/S$ ) of the sample was calculated using the Kubelka–Munk equation (eqn. (1)).<sup>11</sup>

$$K/S = (1 - R)^2/2R \quad (1)$$

Table 1 1:2 metal complex acid dyes used

Commercial name	C. I. Generic name
<i>Neutrilan Yellow K-3R</i>	C. I. Acid Yellow 137
<i>Neutrilan Bordeaux K-RL</i>	C. I. Acid Red 182
<i>Neutrilan Black K-BL</i>	C. I. Acid Black 107
<i>Neutrilan Orange S-R</i>	C. I. Acid Orange 144
<i>Neutrilan Rubine S-2R</i>	None ascribed
<i>Neutrilan Navy S-B</i>	C. I. Acid Blue 284
<i>Neutrilan Yellow M-3R</i>	C. I. Acid Brown 384
<i>Neutrilan Bordeaux M-B</i>	C. I. Acid Violet 90
<i>Neutrilan Navy M-BR</i>	C. I. Acid Blue 193

## Results and discussion

### Colorimetric analysis of dyed samples

Table 2 shows the colour strength ( $K/S$ ) values obtained for untreated and pre-treated cotton samples dyed with 1:2 metal complex acid dyes. It is evident that dyeings with high  $K/S$  values, up to 18 units, could be secured on cotton that had



**Table 2** K/S values for 1:2 metal complex acid dyes applied to pre-treated (PT) and untreated cotton

Dye	% omf	Untreated/PT	K/S
<i>Neutrilan Yellow K-3R</i>	2	Untreated	2.1
	2	PT	14.4
<i>Neutrilan Bordeaux K-RL</i>	2	Untreated	1.8
	2	PT	18.0
<i>Neutrilan Black K-BL</i>	2	Untreated	2.3
	2	PT	15.8
<i>Neutrilan Orange S-R</i>	2	Untreated	1.5
	2	PT	12.3
<i>Neutrilan Rubine S-2R</i>	2	Untreated	1.7
	2	PT	17.3
<i>Neutrilan Navy S-B</i>	2	Untreated	1.9
	2	PT	16.1
<i>Neutrilan Yellow M-3R</i>	2	Untreated	0.8
	2	PT	15.7
<i>Neutrilan Bordeaux M-B</i>	2	Untreated	1.4
	2	PT	16.3
<i>Neutrilan Navy M-BR</i>	2	Untreated	1.7
	2	PT	13.8

previously been treated with the cationic polymer. In contrast, cotton samples that had not received any pre-treatment prior to dyeing displayed very low *K/S* values. It could be surmised that the pre-treatment agent rendered the fabric substantive to the 1:2 metal complex acid dye molecules. The *K/S* values secured with the pre-treatment system are generally higher than those observed for standard reactive dyeing processes dyed at 2% omf (on mass of fibre) depth of shade (4–11 units). In addition, the 1:2 metal complex acid dyes used enable dyeing of cotton in shades that normally require a high concentration and/or a mixture of reactive dyes to achieve.

### Wash fastness assessment

Table 3 shows the wash fastness grey scale ratings for the dyes on the pre-treated cotton. It can be seen that, in general, the wash fastness ratings are good to very good, usually above grey scale 4, which is certainly superior to the wash fastness results secured with the *Jarofast* system and equal, if not superior, to the wash fastness ratings on polyamide fabric such as wool and Nylon-6,6 under normal dyeing processes.

It was observed that in the context of the staining of adjacent Nylon-6,6, the three dye types clearly differed in that fastness of the 2% omf dyeings decreased in the order:

unsulfonated < monosulfonated < disulfonated

However, in terms of the change in shade that occurred during washing, the opposite was observed, in that the fastness of the 2% omf dyeings increased in the order:

unsulfonated > monosulfonated > disulfonated

**Table 3** Wash fastness grey scale ratings of pre-treated 1:2 metal complex acid dyeings on cotton following ISO 105:C06/A2 wash test

Dye	S	D	C	N	P	A	W
<i>Neutrilan Yellow K-3R</i>	5	5	5	4/5	5	5	5
<i>Neutrilan Bordeaux K-RL</i>	5	5	5	4	5	5	5
<i>Neutrilan Black K-BL</i>	4/5	5	5	4	5	5	5
<i>Neutrilan Orange S-R</i>	4/5	5	5	4/5	5	5	5
<i>Neutrilan Rubine S-2R</i>	4	5	5	4/5	5	5	5
<i>Neutrilan Navy S-B</i>	4/5	5	5	4/5	5	5	5
<i>Neutrilan Yellow M-3R</i>	4	5	5	5	5	5	5
<i>Neutrilan Bordeaux M-B</i>	4	5	5	5	5	5	5
<i>Neutrilan Navy M-BR</i>	4	5	5	5	5	5	5

S, shade change; staining to D diacetate; C, cotton; N, nylon; P, polyester; A, acrylic; W, wool.

These observations can be explained in terms of the differing water-solubility (or hydrophobicity) of the three types of dye insofar as, the unsulfonated (*Neutrilan K*) dyes displayed smallest shade change because of their lower aqueous solubility (and thus greater hydrophobicity), whilst the disulfonated (*Neutrilan M*) dyes exhibited the greatest shade change because of their greater aqueous solubility. In contrast, the hydrophobicity of the unsulfonated dyes was responsible for their high staining of the relatively hydrophobic Nylon-6,6 fibre, whilst the high aqueous solubility of the hydrophilic disulfonated dyes was responsible for them having imparted little staining to adjacent Nylon-6,6 material. This is in agreement with the authors' findings in previous work carried out on the wash fastness of 1:2 metal complex acid dyes on Nylon-6,6 fibre.<sup>12</sup>

### Light fastness assessment

Table 4 shows the light fastness values for the 1:2 metal complex acid dyes on the pre-treated fabric; it was observed that the light fastness values secured were excellent, as is typical of 1:2 metal complex acid dyes on polyamide. This would suggest that the pre-treatment has no significant detrimental effect upon the light fastness of the dyes that can occur with other pre-treatment or after-treatment systems. Also, importantly, the light fastness values are in excess of those observed typically for standard reactive dyeings on cotton (typically 4–5).

**Table 4** Light fastness ratings of pre-treated 1:2 metal complex acid dyeings on cotton following ISO 105:B02 test

Dye	Light fastness rating
<i>Neutrilan Yellow K-3R</i>	7
<i>Neutrilan Bordeaux K-RL</i>	6
<i>Neutrilan Black K-BL</i>	7
<i>Neutrilan Orange S-R</i>	6
<i>Neutrilan Rubine S-2R</i>	6
<i>Neutrilan Navy S-B</i>	6
<i>Neutrilan Yellow M-3R</i>	6
<i>Neutrilan Bordeaux M-B</i>	6
<i>Neutrilan Navy M-BR</i>	7

### Comparison of the different dyeing processes

A summary of the differences between the pre-treatment system discussed here and the dyeing processes used in the previous paper<sup>1</sup> is given in Table 5. It was observed that the pre-treatment method vastly reduced the total time of the dyeing operation in comparison with standard reactive dyeing processes and even reduced time in comparison with the previously detailed pre-treatment system.

The amount of water used is calculated using eqn. (2) by a summation of the water used in each separate process; where the liquor ratio (LR) is given as a ratio of liquor to fibre, e.g. a 25:1 liquor ratio is 25 l of water per kg of fibre used.

$$\text{volume water used (l/kg fibre)} = \text{LR (dyeing)} + \text{LR (pretreatment)} + \text{LR (washoff 1)} + \text{LR (washoff 2)} + \dots \quad (2)$$

Each of the standard reactive dyeing processes used over 100 l of water per kg of fabric dyed, with most of the water consumed in wash-off processes, however, the pre-treatment method (Fig. 4) consumed less than half the volume, with only 30 l of water per kg of fabric used.

A high amount of salt (up to 1.6 kg per kg of fabric dyed) and alkali (0.5 kg Na<sub>2</sub>CO<sub>3</sub> per kg of fabric) is consumed in the standard reactive dyeing processes, but by employing the pre-

**Table 5** Comparison of different systems

Procedure	Time/min	Water (l/kg fabric)	NaCl (g/kg fabric)	Na <sub>2</sub> SO <sub>4</sub> (g/kg fabric)	Na <sub>2</sub> CO <sub>3</sub> (g/kg fabric)	Other chemicals (g/kg fabric)
<i>Remazol RR</i> standard reactive dyeing	355	145	0	1250	500	Acetic acid (60), detergent (20)
<i>Procion H-EXL</i> standard reactive dyeing	365	105	1625	0	500	Detergent (20)
<i>Cibacron F</i> standard reactive dyeing	295	125	0	1500	500	Acetic acid (60), detergent (20)
Pre-treatment (Part 1) (reactive dyes) <sup>1</sup>	195	50	0	0	0	Pre-treatment agent (10), phosphate buffer (120), detergent (20)
Pre-treatment (this work) (metal complex acid dyes)	155	30	0	0	0	Pre-treatment agent (10), acetic acid (10)

treatment method both salt and alkali were completely eliminated from the dyeing process.

Considering the other chemicals used in the dyeing processes, the pre-treatment agent was applied in relatively low concentration and it is suggested that it would have high exhaustion values, hence, its presence in the effluent would be expected to be in extremely low concentrations. It would be expected that the agent would not be removed during laundering due to the high affinity for cellulose. In addition, the agent is polymeric and as such poses minimal environmental impact. Although there is no definitive toxicological analysis at present for the agent, preliminary testing suggests that the agent is non-toxic. The cost to dyers of the pre-treatment agent is expected to be between £2.50 and £3.50 per kilogram, which is regarded as minimal when considering the potential cost savings.

With certain dyes it was possible to achieve complete exhaustion of the dyebath. For those that did not exhaust fully, the possibility exists for recycling as the dyebath contained only dye and water at the start of the dyeing cycle, thus the bath may be recharged with further dye and water to original levels and a new dyeing cycle commenced. The dyeing is a simple process requiring no costly and time-consuming wash-off procedures. Although there is concern over the use of metals in dyeing, the metal complex acid dyes used in this system contain the metal (typically chromium) as an integral part of the dye, which is not removed during processing and so is not released in any effluent.

## Conclusions

It has been demonstrated that the pre-treatment of cotton with cationic polymer enables the dyeing of uniform shades with high colour strength values, good to very good fastness to the ISO 105:C06/A2 wash test and excellent fastness to the ISO 105:B02 light fastness test.

Whilst it is accepted that the wash fastness of the dyeings secured is slightly inferior to those obtained with standard

reactive dyeing processes, the benefits of no salt, no alkali, considerably less water consumption, less processing time, minimal effluent, possibility of recycling dyebaths, deeper shades and higher light fastness values make this pre-treatment system a highly viable, greener alternative to standard reactive dyeing processes on cotton.

## Acknowledgements

The authors would like to thank Uniqema for their work in the development of the pre-treatment agent and the associated application methods, which are patent protected by Uniqema and The University of Leeds.

## References

- 1 R. S. Blackburn and S. M. Burkinshaw, *Green Chem.*, 2002, **4**, 47.
- 2 *Jarofast Cationic Dyeing Pattern Card*, James Robinson Ltd., Huddersfield, UK, 1993.
- 3 S. M. Burkinshaw, in *Wool Dyeing*, ed. D. M. Lewis, Society of Dyers and Colourists, Bradford, UK, 1992.
- 4 S. M. Burkinshaw, *Chemical Principles of Synthetic Fibre Dyeing*, Blackie Academic & Professional, London, UK, 1996.
- 5 D. M. Lewis, *The Dyeing of Wool with Pre-Metallised Acid Dyes*, IWS Publication, Ilkley, UK, 1992.
- 6 *Textile Chemistry*, ed. R. H. Peters, Elsevier, Amsterdam, 1975, **vol. III**.
- 7 T. P. Nevell, in *The Dyeing of Cellulosic Fibres*, ed. C. Preston, Dyers Co. Publications Trust, Bradford, UK, 1986.
- 8 Z. Yoshida, F. Osawa and R. Oda, *J. Phys. Chem.*, 1964, **68**, 2895.
- 9 *Colour Index International on CD-ROM*, Society of Dyers and Colourists, Bradford, UK, 1999.
- 10 *Standard Methods for the Determination of the Colour Fastness of Textiles and Leather*, Society of Dyers and Colourists, Bradford, UK, 5th edn., Amendment No. 1, 1992.
- 11 R. McDonald, *J. Soc. Dyers Colour.*, 1980, **96**, 486.
- 12 R. S. Blackburn and S. M. Burkinshaw, *J. Soc. Dyers Colour.*, 1998, **114**, 96.



# Knoevenagel condensation reactions in an ionic liquid†

Rajkumar V. Hangarge,<sup>a</sup> Dilip V. Jarikote<sup>b</sup> and Murlidhar S. Shingare\*<sup>a</sup>

<sup>a</sup> Department of Chemistry, Dr. Babasaheb Ambedkar Marathwada University, Aurangabad-431 004, India. E-mail: msshingare11@rediffmail.com

<sup>b</sup> OCT Division, National Chemical Laboratory, Pune-411 008, India

Received 20th December 2001

First published as an Advance Article on the web 20th May 2002

The condensation reaction of 4-oxo-(4*H*)-1-benzopyran-3-carbaldehydes and of aromatic aldehydes with 3-methyl-1-phenylpyrazolin-5-(4*H*)-one were carried out in an ionic liquid, ethylammonium nitrate, at room temperature in shorter times with higher yields of 78–92 and 70–75%, respectively, than found using conventional procedures.

## Introduction

The Knoevenagel condensation reaction between carbonyl compounds and active methylene compounds have largely been studied in heterogeneous media. These reactions are also facilitated by various catalysts.<sup>2</sup>

Because of their solvent properties, ionic liquids<sup>3,4</sup> are attracting increased attention. They afford significant environmental benefits and can contribute to green chemistry. As the introductions of cleaner technologies have become a major concern throughout industry and academia, the search for alternatives to the most damaging solvents has become a high priority. Solvents are at higher position in the list of damaging chemicals because of their requirement in large amounts and their volatility.

Publications to date show that replacing organic solvents by an ionic liquid can lead to remarkable improvements in well known procedures.<sup>3–5</sup>

The condensation reactions of 4-oxo-(4*H*)-1-benzopyran-3-carbaldehyde with compounds containing active methylene groups are well known.<sup>6–11</sup> These condensation reactions require acid or base catalysts with a prolonged heating period. The condensation reactions of 3-methyl-1-phenylpyrazolin-5-(4*H*)-one are also known; they require microwave irradiation<sup>12</sup> or prolonged heating<sup>13</sup> and the products are obtained in low yields (33–47%).

## Results and discussion

In continuation of work on 4-oxo-(4*H*)-1-benzopyran-3-carbaldehydes<sup>12,14</sup> and 3-methyl-1-phenylpyrazolin-5-(4*H*)-one,<sup>12</sup> we have developed a newer route for the condensation of various 3-formyl chromone and aromatic aldehydes with active methylene compounds such as 3-methyl-1-phenylpyrazolin-5-(4*H*)-one in an ionic liquid, ethylammonium nitrate, carried out at room temperature with constant stirring (Tables 1 and 2). The substrate, 4-oxo-(4*H*)-1-benzopyran-3-carbaldehyde has three active sites: the  $\alpha,\beta$  unsaturated carbonyl group *i.e.* the pyrone ring, a carbon–carbon double bond and a formyl group. Of these, the formyl group has the highest reactivity towards active methylene compounds. In this methodology, reactions were completed in a shorter time and with higher yields as compared to the reported methods. In addition, the conditions applied for the reactions are very mild. The condensed products are isolated

(a) by pouring the reaction mixture in cold water, which precipitates the solid product, filtering the obtained solid and recrystallizing from the appropriate solvent or (b) by extraction with diethyl ether, during which the ionic liquid separates and can be re-used. Products **3a** and **3b** are also isolated by distilling out the solvent under reduced pressure leaving the product in the reaction flask.

## Conclusions

The ionic liquid ethylammonium nitrate acts as an excellent solvent for Knoevenagel condensation reactions. In this reaction no additional catalyst is required for the condensation of 4-oxo-(4*H*)-1-benzopyran-3-carbaldehydes or aromatic aldehydes with 3-methyl-1-phenylpyrazolin-5-(4*H*)-one *i.e.* the ionic liquid acts as both solvent and catalyst. The liberated water during the reaction was adsorbed by the ionic liquid and hence the reactions proceed well. The condensation reactions were completed in very short time compared to reported methods. For 4-oxo-(4*H*)-1-benzopyran-3-carbaldehyde, which has three active sites, the reactions selectively occurred at the formyl group. All the reactions were carried out at room temperature with constant stirring *i.e.* using mild reaction conditions. Using this method the yields of the condensed products were high. (Tables 1 and 2).

## Experimental

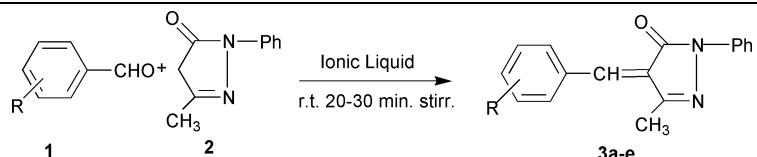
Melting points were measured in open capillaries in a paraffin-bath and are uncorrected. The reactions were monitored *via* TLC [silica, light petroleum–EtOAc (8:2)]. IR spectra were recorded as Nujol mulls on an FTIR instrument.<sup>1</sup>H NMR

## Green Context

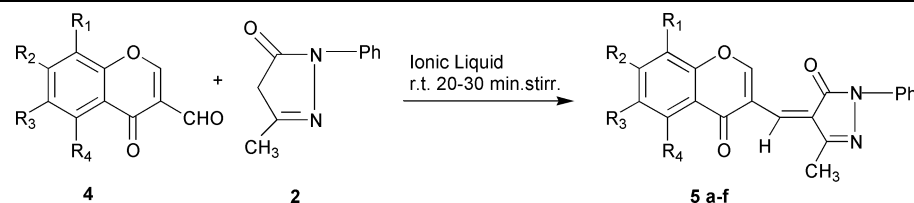
The Knoevenagel condensation reaction is a simple and effective method for forming carbon–carbon bonds. It has been widely studied in the context of green chemistry as a reaction that can be catalysed by solid bases, for example, but these systems generally require a solvent and a catalyst. Here we see how an ionic liquid can replace both the solvent and the catalyst, giving a simpler system—a good example of green chemistry reductions.

JHC

† See ref. 1.

**Table 1** Knoevenagel condensation reactions of aromatic aldehydes with 3-methyl-1-phenylpyrazolin-5-(4*H*)-one


Product	R	Solvent for crystallization	Yield (%)	Mp/°C
<b>3a</b>	<i>p</i> -Cl	Ethanol	70	108
<b>3b</b>	H	Ethanol	71	110
<b>3c</b>	<i>p</i> -NO <sub>2</sub>	Dioxane	71	172
<b>3d</b>	<i>p</i> -OMe	Dioxane	75	124
<b>3e</b>	<i>p</i> -Me	Dioxane	72	138

**Table 2** Knoevenagel condensation reactions of 4-oxo-(4*H*)-1-benzopyran-3-carbaldehydes with 3-methyl-1-phenylpyrazolin-5-(4*H*)-one


Product	R <sub>1</sub>	R <sub>2</sub>	R <sub>3</sub>	R <sub>4</sub>	Solvent for crystallization	Yield (%)	Mp/°C
<b>5a</b>	H	H	Cl	H	Dioxane	90	238
<b>5b</b>	Cl	H	H	H	Dioxane	88	218
<b>5c</b>	H	CH <sub>3</sub>	H	H	Dioxane	78	204
<b>5d</b>	H	H	CH <sub>3</sub>	H	Dioxane	80	240
<b>5e</b>	H	H	H	H	Dioxane	92	230
<b>5f</b>	H	H	Br	H	Dioxane	78	234

spectra were recorded at 300 MHz with CDCl<sub>3</sub> as solvent and TMS as an internal standard. Elemental analyses were consistent with the structures.

### Spectral data of principal compounds

**3d.** IR/cm<sup>-1</sup>: 3057(-C-H, Ar-H), 1788 (C=O, pyrazolinyl), 1687 (C=N, pyrazolinyl), 1580 (C=C), 1095 and 750 (C-O-C).

The <sup>1</sup>H NMR spectrum showed characteristic signals at δ 2.35 (s, 3H, -CH<sub>3</sub>), 3.89 (s, 3H, -OCH<sub>3</sub>), 6.98 (d, 2H, aromatic), 7.17 (t, 1H, aromatic), 7.32 (s, 1H, olefinic), 7.40 (t, 2H, aromatic), 7.95 (d, 2H, aromatic), 8.58 (d, 2H, aromatic).

Mass spectrum: *m/z* 293 (M + 1) and 292 (M<sup>+</sup>), 251, 224, 185, 168, 149, 137, 110, 91, 81, 71, 69, 57 (base peak), 55.

**5a.** The IR spectrum showed characteristic absorption bands (cm<sup>-1</sup>) at 3063 (-C-H, Ar-H), 1790 (C=O, pyrazolinyl), 1685 (C=N, pyrazolinyl), 1654 (C=O, chromone), 1460 (γ-pyrone), 750 (C-Cl).

The <sup>1</sup>H NMR spectrum showed characteristic signals at δ 2.4 (s, 3H, -CH<sub>3</sub>), 7.1–7.9 (m, 8H, aromatic and olefinic protons), 8.2 (d, 1H, *J* = 2.4 Hz, R<sub>4</sub> = H), 10.8 (s, 1H, C<sub>2</sub>-H of chromone moiety).

### Typical experimental procedure

A mixture of 4-oxo-(4*H*)-1-benzopyran-3-carbaldehyde or aromatic aldehyde (10 mmol) and active methylene compound 3-methyl-1-phenylpyrazolin-5-(4*H*)-one (10 mmol) in an ionic liquid; ethylammonium nitrate (20 mmol) were stirred at room

temperature for 20–30 min. The progress of the reaction was monitored by TLC. After completion of the reaction, the following three methods were used to isolate the products.

(a) **3a–e** and **5a–e**: The above stirred reaction mixture was poured into crushed ice, the solid separated out, filtered off, recrystallized from an appropriate solvent, and melting point recorded.

(b) **3a–e** and **5a–e**: diethyl ether was added to the reaction mixture, the organic layer separated, dried over sodium sulfate and the diethyl ether evaporated to obtain the solid product. The other layer consists of the ionic liquid.

(c) **3a** and **3b**: the solvent was distilled under reduced pressure to leave the product.

### Acknowledgements

R. V. H. is thankful to the CSIR, New Delhi, for the award of Senior Research Fellowship and also thankful to Mr Siddiqui and Dr B. M. Bhawal, OCT Division, National Chemical Laboratory, Pune for providing spectral data and reference work.

### References

- 1 P. Walden, *Bull. Acad. Imper. Sci.*, 1914, 1800; S. Sugden and H. Wilkins, *J. Chem. Soc.*, 1929, 1291.
- 2 S. Sebt, R. Nazih, R. Tahir and A. Saber, *Synth. Commun.*, 2001, **31**, 993.
- 3 T. Welton, *Chem. Rev.*, 1999, **99**, 2071 and references therein.
- 4 D. W. Morrison, D. C. Forbes and J. H. Davis, Jr., *Tetrahedron Lett.*, 2001, **42**, 6097.
- 5 M. Smietana and C. Mioskowski, *Org. Lett.*, 2001, **3**, 1037.



- 6 V. K. Polykov and R. G. Shevtsova, *Ukr. Khim. Zh.*, 1981, **47**, 85.
- 7 A. Treibs, R. William and D. Grimm, *Liebigs Ann. Chem.*, 1981, **3**, 306.
- 8 G. Hass, J. L. Stanton, A. Vonsprecher and W. Paul, *J. Heterocycl. Chem.*, 1981, **18**, 607.
- 9 A. P. Shkumat, Yu. P. Babich, N. S. Pivenko and V. K. Polyakov, *Zh. Obshch. Khim.*, 1989, **59**, 1116.
- 10 J. Prousek, *Collect. Czech. Chem. Commun.*, 1993, **58**, 3014.
- 11 G. V. S. Rama Sarma and V. M. Reddy, *Indian J. Heterocycl. Chem.*, 1993, **3**, 111.
- 12 B. K. Karale, V. P. Chavan, A. S. Mane, R. V. Hangarge, C. H. Gill and M. S. Shingare, *Synth. Commun.*, 2002, **32**, 497.
- 13 J. Sun, C-G. Yan and Y. Han, *Synth. Commun.*, 2001, **31**, 151 and refernces therein.
- 14 R. V. Hangarge, S. A. Sonwane, D. V. Jarikote and M. S. Shingare, *Green Chem.*, 2001, **3**, 310.



# A new catalyst for the synthesis of *N,N*-biphenylurea from aniline and dimethyl carbonate

N. Nagaraju\* and George Kuriakose

Department of Chemistry, St. Joseph's College Post Graduate Center, 46 Langford Road, Shanthi Nagar, Bangalore 560 027, India. E-mail: nagaraju@yahoo.com

Received 11th January 2002

First published as an Advance Article on the web 13th May 2002

An environmentally benign method for the synthesis of biphenylurea (BPU) in the presence of ecofriendly catalysts has been reported. Catalytic activity of various metal aluminophosphates, M-AlPO<sub>4</sub> (M = V, Fe, Co, Ni and Cu) and cobalt supported on hydrated Al<sub>2</sub>O<sub>3</sub>, SiO<sub>2</sub> and ZrO<sub>2</sub> has been investigated in the synthesis of BPU from aniline and dimethyl carbonate (DMC). All the catalysts used are amorphous. The catalytic activity studies have been carried out in the liquid phase under refluxing conditions. Formation of BPU is found to depend on the type of the catalyst, the molar ratio of aniline to DMC and the duration of the reaction. *N*-Methylaniline and methyl *N*-phenylcarbamate are formed as by-products of the reaction. Of all the catalysts used, Co-AlPO<sub>4</sub> has been found to yield the highest percentage of BPU whereas cobalt supported hydrated Al<sub>2</sub>O<sub>3</sub>, SiO<sub>2</sub> and ZrO<sub>2</sub> failed to give any BPU.

## Introduction

Biphenylurea (BPU) and its derivatives are important fine chemicals. They have found extensive useful applications as tranquilizers and antibiotic drugs, antioxidants in gasoline, corrosion inhibitors and herbicides.<sup>1</sup> Accordingly there have been numerous attempts to produce biphenylurea. However, the methods adopted to synthesize BPU involve either hazardous chemicals (SeO<sub>2</sub>) or expensive metal (Zr, Mo, Pt, Rh) or in some cases the reactant (phosgene) itself is highly toxic.<sup>2-4</sup> In this article we present the use of metal aluminophosphates as inexpensive and ecofriendly catalysts for the synthesis of biphenylurea *viz.*, alkylation of aniline using DMC. Dimethyl carbonate (DMC) which is used as one of the reactants in this work is produced by reacting phosgene with methanol. Enichem, however, have developed a non-phosgene DMC production route on an industrial scale based on one step oxycarbonylation of CH<sub>3</sub>OH.<sup>5,6</sup>

In the area of heterogeneous catalysis, alkylation of aniline has been extensively studied, as this reaction yields chemicals used as intermediates in dyes and pharmaceuticals. This reaction has been investigated using different alcohols<sup>7</sup> and dimethylcarbonate (DMC)<sup>8,9</sup> as the alkylating agents in the presence of various solid acids and bases as catalysts.<sup>10,11</sup> It is reported that in the presence of solid acid/base catalysts, alkylation of aniline using alcohol or DMC as alkylating agents, only C- and/or N-alkylated products are obtained. However, we have observed in our present investigation that BPU is formed as one of the major products in alkylation of aniline by DMC in the presence of amorphous metal aluminophosphate catalysts.

The aim of the present investigation was to measure the activity of various metal aluminophosphates and cobalt containing hydrated Al<sub>2</sub>O<sub>3</sub>, SiO<sub>2</sub> and ZrO<sub>2</sub> in alkylation of aniline by DMC to give BPU. The effect of variation of reaction parameters such as duration of the reaction, molar ratio of the reactants *etc.*, on the yield of BPU have also been investigated. In this paper we highlight the use of amorphous M-AlPO<sub>4</sub> (M = Fe, Co, Ni and Cu) as ecofriendly and inexpensive catalysts in the synthesis of BPU in the liquid phase from aniline and DMC.

## Experimental

### Preparation of the catalysts

**Preparation of AlPO<sub>4</sub> and M-AlPO<sub>4</sub>.** Aluminophosphate (AlPO<sub>4</sub>) and M-AlPO<sub>4</sub> (M = V, Fe, Co, Ni, Cu) were prepared by a precipitation method using aqueous ammonia (28%) as the precipitating agent as described in the literature.<sup>12</sup> The precipitate after washing with deionised water was initially dried overnight at 120 °C and finally calcined at 550 °C for 5 h.

**Preparation of catalysts containing Co on hydrated Al<sub>2</sub>O<sub>3</sub>, SiO<sub>2</sub> and ZrO<sub>2</sub>.** Al(OH)<sub>3</sub> gel was initially prepared by adding dropwise aqueous ammonia (28%) to a hot aqueous solution of aluminium nitrate containing 50 g of the salt per 500 cm<sup>3</sup> of the solvent. The precipitate was separated by filtration, washed free from the anions, dried at 120 °C in an air oven for 24 h, and calcined at 550 °C for 5 h to obtain hydrated Al<sub>2</sub>O<sub>3</sub>. Similarly, hydrated ZrO<sub>2</sub> was obtained starting from zirconium oxochloride using aqueous ammonia (28%)<sup>13</sup> as the precipitating agent. Hydrated SiO<sub>2</sub> was obtained starting from sodium silicate. Concentrated nitric acid was used as the precipitating agent.<sup>14</sup>

## Green Context

**Traditional syntheses of many important chemical intermediates suffer from the use of hazardous reagents and the simultaneous production of large volumes of waste. The synthesis of biphenylureas is a good example of this and can involve such undesirable chemicals as phosgene and selenium oxide. Clean synthesis is about simplified routes, non-hazardous chemicals and low waste production. Here we see a cleaner synthetic route to these useful ureas. Dimethyl carbonate and anilines are reacted together with solid M-AlPO<sub>4</sub> type catalysts. Under careful control of the reaction conditions, good selectivity to the desired ureas can be achieved.**

JHC

The hydrated metal oxides were separately mixed with cobalt acetate solution (5 ml per 10 g of the oxide) so as to have 5% Co in the oxide. The mixture was ground well using a pestle and mortar, dried overnight at 120 °C and calcined at 550 °C for 5 h.

### Characterization of catalysts

All catalysts were analyzed for their chemical composition. XRD patterns of these samples were recorded on a Philips PW1349/30 diffractometer. The total acidity of the samples was measured by the *n*-butylamine back titration method<sup>15–18</sup> and the surface area by the BET technique using NOVA-1000 Ver: 3.7 instrument.

### Catalytic activity studies

Catalytic activity studies were carried out at ambient pressure in the liquid phase under refluxing conditions. AlPO<sub>4</sub> and M-AlPO<sub>4</sub> were used as the catalysts in the reaction between aniline and DMC. The reaction parameters such as duration of reflux and aniline/DMC molar ratio were altered to check their effect on the product selectivity. In every case a blank parallel reaction was carried out in the absence of any catalyst. After a given period of time the reaction mixture was cooled and filtered, to separate the catalyst from it. The filtrate was analyzed by GC, using 10% Apeizonal + 10% KOH on Chromosorb W-AW, 2 m stainless steel column coupled with FID. The products were identified by comparing with standards. The solid product if any, was separated from the catalyst using hot ethanol. Purity of the solid product was checked by TLC and its melting point and further characterized by GC-mass, mass, <sup>1</sup>H NMR, <sup>13</sup>C NMR, IR and UV-Vis spectral analysis.

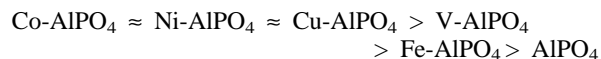
### Results and discussion

Surface acidity and the BET surface of all the catalyst samples are given in the Table 1. The surface area is found to be in agreement with the values reported in the literature for the corresponding samples so also the surface acidity values.

Analysis of the reaction mixture obtained by refluxing a solution (20 ml) of 1:5 mol/mol aniline/DMC for 2 h in the presence of 0.5 g of AlPO<sub>4</sub> or M-AlPO<sub>4</sub> indicated that no reaction occurred between aniline and DMC to yield either N- or C-alkylated products. However, when the reaction mixture was refluxed for 4 h, *N*-methylaniline (NMA) and methyl *N*-phenylcarbamate were selectively formed but to an extent of only around 3 and 18%, respectively. Further increase in the duration of the reaction to 6 and also to 8 h resulted no change in the nature and the percentage of the respective products.

Expecting a better conversion of aniline, a reaction mixture containing a higher concentration of aniline *i.e.*, a 1:1 mol/mol aniline–DMC solution, was refluxed for 4 h in the presence of the solid catalysts. The results were as expected but still the selectivity towards the nature of the products remained

unchanged (Table 2). The catalytic activity of various catalysts towards the formation of carbamate was found to be in the order:



These results prompted us to check the effect of further increase in the concentration of aniline and duration of the reaction on the percentage conversion of aniline and the nature of the products. For this purpose Co-AlPO<sub>4</sub> was selected as this catalyst showed highest activity in these experiments.

When a reaction mixture of 1:1 mol/mol aniline–DMC and the catalyst was refluxed for 6 h, very interestingly, needle like crystalline solid product appeared in the reaction mixture, in contrast to what has been reported. TLC analysis of this solid product and its sharp melting point indicated a high purity of the solid. Mass, <sup>1</sup>H NMR, <sup>13</sup>C NMR, IR and UV–Vis spectral analysis and a comparison with a standard revealed that the solid was *N,N*-biphenylurea, BPU (carbanilide). The results of further investigations carried out on Co-AlPO<sub>4</sub> using 2:1 aniline/DMC varying the duration of the reaction (2, 4, 6 and 8 h) were informative. With increasing the reaction time carbamate formation totally disappeared and that of *N,N'*-biphenylurea increased. This indicates that the carbamate is the reaction intermediate in the formation of carbanilide.

Finally, the catalytic activity of all the other M-AlPO<sub>4</sub> catalysts was investigated for the formation of carbanilide. The reactions were carried out using 1:1 and 2:1 mol/mol aniline–DMC solutions keeping the reaction time constant as 4 h. The results are presented in Table 3. It is noticed that when 1:1 solution was used all the catalysts were found to give NMA and carbamate. However 2:1 solutions led to only NMA and carbamate in the presence of AlPO<sub>4</sub> and V-AlPO<sub>4</sub> catalysts but other M-AlPO<sub>4</sub> (M = Fe, Co, Ni and Cu) did not lead to any carbamate but only carbanilide in the product mixture. Thus, M-AlPO<sub>4</sub> catalysts are found to be active as well as selective for the synthesis of biphenylurea in liquid phase alkylation of aniline by DMC.

The catalytic activity of cobalt aluminophosphates was compared with cobalt supported on hydrated Al<sub>2</sub>O<sub>3</sub>, SiO<sub>2</sub> and ZrO<sub>2</sub>. It was observed in the latter cases that only *N*-methylaniline was formed to a considerable extent and carbamate was obtained as only a minor product. However, none of the catalysts showed any activity towards formation of BPU (Table

**Table 2** Aniline conversion and the distribution of products formed in liquid phase alkylation of aniline with DMC over metal aluminophosphates (reaction time 4 h and 1:1 mol/mol aniline–DMC)

Catalysts	Aniline conversion (%)	Product yield (%)	
		NMA	Carbamate
AlPO <sub>4</sub>	10	2	8
V-AlPO <sub>4</sub>	37	8	29
Fe-AlPO <sub>4</sub>	24	8	16
Co-AlPO <sub>4</sub>	48	13	35
Ni-AlPO <sub>4</sub>	45	10	35
Cu-AlPO <sub>4</sub>	38	4	34

**Table 1** Surface acidity (total) and BET surface area of catalysts

Catalyst	Total surface acidity mmol/g	BET surface area/m <sup>2</sup> g <sup>-1</sup>	Catalyst	Total surface acidity mmol/g <sup>-1</sup>	BET surface area/m <sup>2</sup> g <sup>-1</sup>
AlPO <sub>4</sub>	0.41	172.0	Al <sub>2</sub> O <sub>3</sub>	0.37	201
V-AlPO <sub>4</sub>	0.39	160.3	Co-Al <sub>2</sub> O <sub>3</sub>	0.42	190
Fe-AlPO <sub>4</sub>	0.38	161.0	SiO <sub>2</sub>	0.53	105
Co-AlPO <sub>4</sub>	0.46	159.0	Co-SiO <sub>2</sub>	0.58	115
Ni-AlPO <sub>4</sub>	0.32	171.0	ZrO <sub>2</sub>	0.62	98
Cu-AlPO <sub>4</sub>	0.34	168.0	Co-ZrO <sub>2</sub>	0.59	98

**Table 3** Product distribution in the reaction between aniline and DMC in the presence of M-AlPO<sub>4</sub> catalysts (M = V, Fe, Co, Ni and Cu; reaction time 4 h)

Catalyst	Aniline:DMC molar ratio	Aniline conversion (%)	NMA (%)	Carbamate (%)	Carbanilide (%)
AlPO <sub>4</sub>	1:1	10	2	8	—
	2:1	29	13.5	15	—
V-AlPO <sub>4</sub>	1:1	37	8	29	—
	2:1	38	17	30	—
Fe-AlPO <sub>4</sub>	1:1	25	8	16	—
	2:1	77	22	—	54.5
Co-AlPO <sub>4</sub>	1:1	48.5	13	35	—
	2:1	92	24	—	68
Ni-AlPO <sub>4</sub>	1:1	46	10	36	—
	2:1	83	23	—	59.5
Cu-AlPO <sub>4</sub>	1:1	43	9	35	—
	2:1	75	24	—	50.5

**Table 4** Activity of oxides and cobalt containing hydrated metal oxides in the reaction between aniline and DMC (reaction time 4 h)

Catalyst	Aniline:DMC	Aniline conversion (%)	NMA (%)	Carbamate (%)	BPU (%)
Al <sub>2</sub> O <sub>3</sub>	1:1	7	3	4	—
	2:1	28	14	14	—
Co-Al <sub>2</sub> O <sub>3</sub>	1:1	11	4	7	—
	2:1	49	29	20	—
SiO <sub>2</sub>	1:1	—	—	—	—
	2:1	4	4	—	—
Co-SiO <sub>2</sub>	1:1	12	11	1	—
	2:1	14	12	2	—
ZrO <sub>2</sub>	1:1	—	—	—	—
	2:1	4	4	—	—
Co-ZrO <sub>2</sub>	1:1	—	—	—	—
	2:1	8	8	—	—

4). Preliminary investigations on the reaction of substituted anilines (toluidines and chloroaniline) and DMC (1:1 and 2:1) in the presence of Co-AlPO<sub>4</sub> did not give any C- or N-alkylated anilines or substituted BPU.

The results indicate that there is no correlation between the surface acidity of the solid catalysts used and their catalytic activity towards BPU formation. This indicates that it may not be the strong acidity or basicity of the solids used as catalysts that is the only factor that determines their activity in the formation of BPU. A more detailed explanation based on the surface properties of M-AlPO<sub>4</sub> including acid–base and redox behavior awaits further investigation. It can however be stated that M-AlPO<sub>4</sub> catalysts may be used for the synthesis of *N,N*-biphenylurea under very mild conditions in place of environmentally hazardous and expensive catalysts. The present study is the first of its kind with respect to the use of M-AlPO<sub>4</sub> catalysts for BPU synthesis.

## Conclusion

In the presence of amorphous M-AlPO<sub>4</sub> (M = V, Fe, Co, Ni and Cu) as catalysts, aniline and dimethyl carbonate (DMC) react under refluxing conditions to yield *N*-methylaniline, methyl *N*-phenylcarbamate and *N,N*-biphenylurea (BPU). The nature of the products depends not only on the type of the catalyst used but also on the duration of the reaction and the aniline:DMC molar ratio. At higher concentration of aniline *i.e.*, 2:1 mol/mol aniline–DMC, the conversion to BPU is very good. Of all the catalysts used Co-AlPO<sub>4</sub> led to the highest yield of BPU. A comparison of the catalytic activity of M-AlPO<sub>4</sub> with cobalt containing hydrated Al<sub>2</sub>O<sub>3</sub>, SiO<sub>2</sub> and ZrO<sub>2</sub> revealed that the latter samples are inactive in the formation of BPU. No correlation between the surface acidity of the catalyst and their catalytic activity in the formation of BPU was observed.

## Acknowledgements

The authors are grateful to the Department of Science and Technology (DST), New Delhi, India, for the financial support and I.I.Sc, Bangalore, India, for providing library facilities.

## References

- T. P. Vishnyakova, I. A. Golubeva and E. V. Glebova, *Russ. Chem. Rev.*, 1985, **54**, 249.
- H. S. Kim, Y. J. Kim, H. Lee, S. D. Lee and C. S. Chin, *J. Catal.*, 1999, **184**, 526.
- B. M. Reddy and V. R. Reddy, *Synth. Commun.*, 1999, **29**, 2789.
- S. A. R. Mulla, C. V. Rode, A. A. Kelkar and S. P. Gupte, *J. Mol. Catal. A: Chemical*, 1997, **122**, 103.
- F. Rivetti, *Acad. Sci. Paris Ser. IIC: Chem.*, 2000, **497**, 3.
- Y. Ono, *Appl. Catal. A: General*, 1997, **155**, 133.
- S. Narayanan and K. Deshpande, *Appl. Catal. A: General*, 2000, **199**, 1.
- Y. Ono, *Catal. Today*, 1997, **35**, 15.
- Z. Hautu and Y. Ono, *J. Mol. Catal.*, 1994, **91**, 399.
- F. M. Baustista, *Appl. Catal. A: General*, 1998, **166**, 39.
- F. M. Baustista, *J. Catal.*, 1997, **172**, 103.
- K. M. Parida, T. Mishra and B. S. Rao, *Catalysis Modern Trends*, ed. N. M. Gupta and D. K. Chakraborty, Narosa Publishing House, New Delhi, India, 1995, p. 139.
- L. M. Kustov, V. B. Kalansky, F. Figueras and D. Tichit, *J. Catal.*, 1994, **150**, 143.
- A. B. Stiles, in *Catalyst Supports and Supported Catalysts—Theoretical and Applied Concepts*, ed. A. B. Stiles, Butterworth Publishers, Oxford, UK, 1987, p. 58.
- H. A. Benesi, *J. Phys. Chem.*, 1957, **61**, 970.
- C. J. Walling, *J. Am. Chem. Soc.*, 1950, **72**, 1164.
- H. A. Benesi, *J. Am. Chem. Soc.*, 1956, **78**, 5490.
- Solid Acids and Bases—Their Catalytic Properties*, Academic Press, London, 1970.





# Ionic liquids as green solvents for the asymmetric synthesis of cyanohydrins catalysed by VO(salen) complexes†

Carlos Baleizão,<sup>ab</sup> Bárbara Gigante,<sup>a</sup> Hermenegildo Garcia<sup>b</sup> and Avelino Corma<sup>b</sup>

<sup>a</sup> INETI- Departamento de Tecnologia das Industrias Químicas, Estrada do Paço do Lumiar, 22, 1649-038 Lisbon, Portugal

<sup>b</sup> Instituto de Tecnología Química/CSIC-Av. de los Naranjos, s/n, 46022, Valencia, Spain.  
E-mail: acorma@itq.upv.es

Received 11th February 2002

First published as an Advance Article on the web 15th May 2002

It has been found that the ionic liquid 1-butyl-3-methylimidazolium hexafluorophosphate is a good substitute solvent for CH<sub>2</sub>Cl<sub>2</sub> to conduct the enantioselective cyanosilylation of aldehydes to their silylated cyanohydrins, using trimethylsilyl cyanide as reagent and a Schiff base vanadyl complex as catalyst. The mass balances (>90%), conversions (>80%) and enantiomeric excess (88% < ee < 90%) were high and comparable to those achieved in CH<sub>2</sub>Cl<sub>2</sub>. The ionic liquid containing the catalyst can be reused at least four times without losing activity.

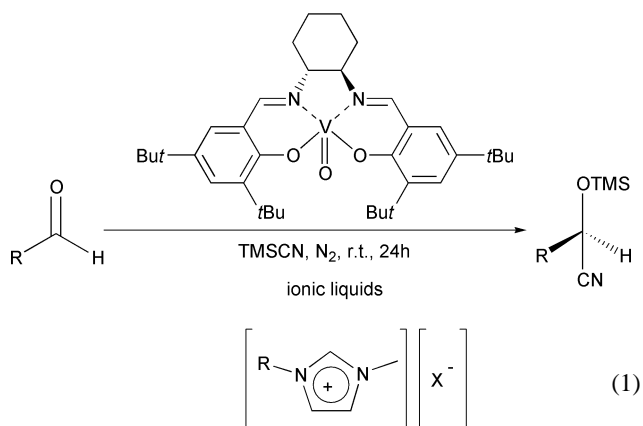
## Introduction

It is very well known that the medium, and specifically the solvent, plays a dramatic influence on the outcome of a chemical reaction. In recent years there has been an increasing interest in exploiting the potential of ionic liquids as reaction media aimed to develop green chemistry, avoiding the use of volatile organic solvents<sup>1</sup> and allowing reuse of the catalyst.<sup>2</sup> Ionic liquids being aprotic solvents combine a relative high polarity estimated between acetonitrile and methanol<sup>3</sup> with a broad capacity to dissolve organic compounds. In two pioneering reports, it was been shown that ionic liquids of the *N,N'*-dialkylimidazolium type can be good solvents to perform enantioselective catalytic reactions such as alkene epoxidations<sup>4</sup> and asymmetric ring opening of epoxides.<sup>5</sup> As a follow up of these studies, herein we report our study on the asymmetric synthesis of cyanohydrins catalysed by a chiral vanadyl Schiff base.

The reaction under study is shown in eqn. (1) and uses trimethylsilyl cyanide (TMSCN) as the nucleophilic reagent. Enantiomerically pure mandelonitrile is currently produced in multi-hundred ton scale, being one of the highest-production volume compounds in asymmetric catalysis. This reaction is therefore very important from the synthetic and commercial point of view<sup>6</sup> and has recently been studied in dichloromethane,<sup>7</sup> a chlorinated solvent that is clearly unsatisfactory due to environmental concerns. In addition, the high cost of the chiral catalyst and the need of reuse require of a more suitable reaction medium. Based on the precedents reporting the use of Mn and Cr Schiff base complexes as catalysts in ionic liquids for other enantioselective reactions, we anticipate that they could also be advantageous for the asymmetric synthesis of cyanohydrins.<sup>8</sup>

## Results and discussion

In a first stage, we used benzaldehyde as the substrate and selected four different imidazolium melts as solvents in which the alkyl substituent as well as the counter anion were varied.



1. [emim][PF<sub>6</sub>]. R=CH<sub>2</sub>CH<sub>3</sub>, X=PF<sub>6</sub>
2. [bmim][PF<sub>6</sub>]. R=CH<sub>2</sub>CH<sub>2</sub>CH<sub>2</sub>CH<sub>3</sub>, X=PF<sub>6</sub>
3. [bmim][Cl]. R=CH<sub>2</sub>CH<sub>2</sub>CH<sub>2</sub>CH<sub>3</sub>, X=Cl
4. [bmim][BF<sub>4</sub>]. R=CH<sub>2</sub>CH<sub>2</sub>CH<sub>2</sub>CH<sub>3</sub>, X=BF<sub>4</sub>

The results obtained as well the reaction conditions are indicated in Table 1. For the sake of comparison we have also included one result (entry 1) in dichloromethane under comparable experimental conditions. The conversion and enantiomeric excess (ee) obtained by us in CH<sub>2</sub>Cl<sub>2</sub> agrees relatively well with the original results reported in the literature (100% conversion and 94% ee).<sup>7a</sup> Comparing entries 2–5 of the Table 1, it can be seen that hexafluorophosphate is much more convenient than chloride or tetrafluoroborate as counter anion. Related precedents in which the nature of counter anion also plays an important role in the results achieved for a catalytic

## Green Context

The use of ionic liquids as involatile solvents for organic chemistry is a major area of green chemistry research. In this article, an asymmetric synthesis using an ionic liquid–catalyst system is described. The conversions, enantiomeric excess and mass balances are all high. Of particular note is the demonstration of good reusability of the catalyst–solvent system.

JHC

† Dedicated to Prof. W. Adam on the occasion of his 65th birthday.

**Table 1** Enantioselective synthesis of the benzaldehyde cyanohydrin catalyzed by chiral vanadyl salen complex using different ionic liquids as solvents.<sup>a</sup>

Entry	Solvent	Viscosity <sup>b/</sup> cP	Conversion <sup>c</sup> (%)	Ee <sup>d</sup> (%)	Mass balance <sup>e</sup> (%)
1	CH <sub>2</sub> Cl <sub>2</sub> <sup>f</sup>	—	90	90	—
2	[emim]PF <sub>6</sub>	—	85	89	95
3	[bmim]PF <sub>6</sub>	312	83	85	93
4	[bmim]Cl <sup>g</sup>	Solid	40	35	70
5	[bmim]BF <sub>4</sub>	154	63	5	90

<sup>a</sup> All reactions were run for 24 h in an N<sub>2</sub> atmosphere: benzaldehyde (1.64 mmol), TMSCN (1.1 eq.), catalyst (1 mol%) and ionic liquid (1 ml). <sup>b</sup> See ref. 10. <sup>c</sup> Determined in a GC column (TRB5, 30 m, 0.25 mm). <sup>d</sup> Determined in a chiral GC column (Chiraldex  $\gamma$ -TA, 30 m, 0.25 mm). <sup>e</sup> Determined using nitrobenzene as external standard. <sup>f</sup> *t* = 3 h, CH<sub>2</sub>Cl<sub>2</sub> (1.9 ml). <sup>g</sup> Temperature = 75 °C.

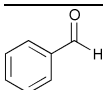
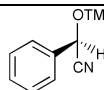
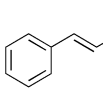
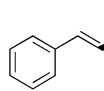
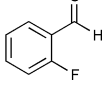
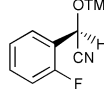
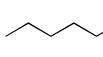
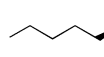
reaction in ionic liquids can be found in the literature.<sup>5</sup> Although not fully understood, the influence of the counter anion can be due, at least in part, to the difference in viscosity of the ionic liquids. Preliminary work from our laboratory has shown that the ee values achieved in this reaction are very sensitive to the solvent.<sup>9</sup> On the other hand, the performance of [bmim][PF<sub>6</sub>] and [emim][PF<sub>6</sub>] are very similar, although the latter shows consistently higher conversion and enantioselectivity than the butyl analogue [bmim]. Subsequent studies were, therefore, carried out in [emim]PF<sub>6</sub>.

With these results we extended our study to other aldehydes, namely cinnamaldehyde, 2-fluorobenzaldehyde and hexanal. The results obtained (see Table 2) show, for all the compounds under study, high conversions and good recoveries but, importantly, excellent enantioselectivities.

When dealing with reactions in ionic liquids one important point that requires attention is the mass balance of the recovered material after the reaction. Surprisingly no data concerning the mass balance have been reported in the precedents describing the use of ionic liquids in enantioselective reactions. In fact the main advantage of the use of ionic liquid is that once the reaction is complete the product should be recoverable by simple liquid–liquid extraction using a solvent immiscible with the ionic liquid. The success of this approach depends on the recovery of the reaction products while the catalyst remains in the ionic liquid.

In our hands using nitrobenzene as external standard the mass balances of the recovered material after extraction of the

**Table 2** Enantioselective synthesis of different cyanohydrins catalyzed by a chiral vanadyl salen complex using [emim]PF<sub>6</sub> as solvent.<sup>a</sup>

Aldehyde	Cyanohydrin	Conv. <sup>b</sup> (%)	Ee <sup>c</sup> (%)	Mass balance <sup>d</sup> (%)
		85	89	95
		76	98	87
		81	86	84
		97	83	94

<sup>a</sup> All reactions were run for 24 h in an N<sub>2</sub> atmosphere: aldehyde (1.64 mmol), TMSCN (1.1 eq.), catalyst (1 mol%) and [emim]PF<sub>6</sub> (1 ml). <sup>b</sup> Determined in a GC column (TRB5, 30 m, 0.25 mm). <sup>c</sup> Determined in a chiral GC column (Chiraldex  $\gamma$ -TA, 30 m, 0.25 mm). <sup>d</sup> Determined using nitrobenzene as external standard.

**Table 3** Recycling of the [emim]PF<sub>6</sub> and vanadyl salen complex in synthesis of the benzaldehyde cyanohydrin<sup>a</sup>

Run	Conversion <sup>b</sup> (%)	Ee <sup>c</sup> (%)	Mass balance <sup>d</sup> (%)
1	85	89	95
2	79	88	96
3	89	90	99
4	80	88	93
5	83	89	95

<sup>a</sup> All reactions were run for 24 h in an N<sub>2</sub> atmosphere: benzaldehyde (1.64 mmol), TMSCN (1.1 eq.), catalyst (1 mol %) and [emim]PF<sub>6</sub> (1 ml). <sup>b</sup> Determined in a GC column (TRB5, 30 m, 0.25 mm). <sup>c</sup> Determined in a chiral GC column (Chiraldex  $\gamma$ -TA, 30 m, 0.25 mm). <sup>d</sup> Determined using nitrobenzene as external standard.

reaction mixture in ionic liquids with hexane were excellent (see Tables 1 and 2) except for the case of [bmim][Cl], for which lower values were obtained. It is also observed that, when the reaction is complete and the products extracted, the ionic liquid [emim][PF<sub>6</sub>] containing the chiral catalyst could be reused four times without significant variations in the conversion, mass balance and enantioselectivity (see Table 3). Control experiments have shown that vanadyl salen complex is almost totally insoluble in hexane and highly soluble in ionic liquids.

In conclusion, we have found, as an alternative to dichloromethane, that the ionic liquid [emim][PF<sub>6</sub>] is a very convenient reaction medium for the enantioselective formation of cyanohydrins. The enantiomeric excesses achieved are very high and comparable to those obtained in CH<sub>2</sub>Cl<sub>2</sub>. The products can be recovered by extraction with hexane and the ionic liquid reused several times. Our communication constitutes another example of the advantages of ionic liquids in enantioselective catalysis.

## Experimental

The ionic liquid [emim]PF<sub>6</sub> was prepared according to the procedures reported in the literature.<sup>11</sup> The ionic liquids [bmim]PF<sub>6</sub> and [bmim]Cl were purchased from Solvent Innovation. The ionic liquid [bmim]BF<sub>4</sub> was synthesized from [bmim]Cl and NH<sub>4</sub>BF<sub>4</sub> in dry acetonitrile at 60 °C for 20 h under N<sub>2</sub>.

Before starting the reaction the ionic liquids (1 ml) were dried by heating at 50 °C under reduced pressure for 12 h (0.1 Torr). The vanadyl salen complex (10 mg) was added and the liquid stirred at room temperature for 15 min until dissolution of the solid was complete. The vanadyl salen complex was prepared using vanadyl sulfate and (*R,R*)-(–)-*N,N'*-bis(3,5-di-*tert*-butylsalicylidene)-1,2-cyclohexanediamine<sup>12</sup> in ethanol–water (1:1) following the reported procedure.<sup>13</sup> Aldehyde (1.64 mmol) and TMSCN (1.1 eq.) were added to the ionic liquid containing dissolved catalyst and the mixture stirred at room temperature under N<sub>2</sub> for 24 h. After this time the ionic melt was extracted with hexane (2 × 10 ml). To determine the mass balance, a given amount of ionic liquid was taken, weighed and dissolved with dichloromethane. To this solution nitrobenzene (5  $\mu$ l) was added as external standard and the solution injected in a GC (TRB5, capillary column). The enantiomeric excess was determined in a chiral GC column (Chiraldex  $\gamma$ -TA, 30 m, 0.25 mm). By analogy with the literature,<sup>7</sup> all products have an excess of the (*S*)-enantiomer of the cyanohydrin derivative.

## Acknowledgements

Financial support by the Spanish DGES (MAT2000-1768-CO2-01) is gratefully acknowledged. C. B. thanks the

Fundação para a Ciência e Tecnologia, Portugal, for scholarship (PRAXIS XXI/BD/21375/99).

## References

- (a) K. R. Seddon, *J. Chem. Tech. Biotechnol.*, 1997, **68**, 351; (b) P. Wasserscheid and W. Keim, *Angew. Chem., Int. Ed.*, 2000, **39**, 3772.
- (a) F. Liu, M. B. Abrams, T. Baker and W. Tumas, *Chem. Commun.*, 2001, 433; (b) A. E. Visser, R. P. Swatloski, W. M. Reichert, R. Mayton, S. Sheff, A. Wierzbicki, J. H. Davis and R. D. Rogers, *Chem. Commun.*, 2001, 135; (c) J. G. Huddleston, H. D. Willauer, R. P. Swatloski, A. E. Visser and R. D. Rogers, *Chem. Commun.*, 1998, 1765.
- S. N. V. K. Aki, J. F. Brennecke and A. Samanta, *Chem. Commun.*, 2001, 413.
- C. E. Song and E. J. Roh, *Chem. Commun.*, 2000, 837.
- C. E. Song, C. R. Oh, E. J. Roh and D. J. Choo, *Chem. Commun.*, 2000, 1743.
- (a) M. Freemantle, *Chem. Eng. News*, 2000, **78** (May 15) 37; (b) *Encyclopedia of Chemical Technology*, ed. M. H. Grant, John Wiley & Sons, New York, 1992, p. 821; (c) H. Gröger, E. Capan, A. Barthuber and K. D. Vorlop, *Org. Lett.*, 2001, **3**, 1969.
- (a) Y. N. Belekou, M. North and T. Parsons, *Org. Lett.*, 2000, **2**, 1617; (b) Y. N. Belekou, B. Green, N. S. Ikonnikov, M. North, T. Parsons and V. I. Tararov, *Tetrahedron*, 2001, **57**, 771.
- (a) R. J. H. Gregory, *Chem. Rev.*, 1999, **99**, 3649; (b) C. J. Peterson, R. Tsao, A. L. Eggler and J. R. Coats, *Molecules*, 2000, **5**, 648.
- C. Baleizao, B. Gigante, H. Garcia and A. Corma., to be published.
- J. G. Huddleston, A. E. Visser, W. M. Reichert, H. D. Willauer, G. A. Broker and R. D. Rogers, *Green Chem.*, 2001, **3**, 156.
- J. S. Wilkes and M. J. Zaworotko, *J. Chem. Soc., Chem. Commun.*, 1992, 965.
- W. Zhang and E. N. Jacobsen, *J. Org. Chem.*, 1991, **56**, 2296.
- K. Nakajima, K. Kojima, M. Kojima and J. Fujita, *Bull. Chem. Soc. Jpn.*, 1990, **63**, 2620.



# The nitration of arenes in perfluorocarbon solvents

Michael R. Crampton,<sup>\*a</sup> Emma L. Cropper,<sup>a</sup> Linda M. Gibbons<sup>a</sup> and Ross W. Millar<sup>b</sup>

<sup>a</sup> Chemistry Department, Durham University, Durham, UK DH1 3LE.

E-mail: m.r.crampton@durham.ac.uk

<sup>b</sup> QinetiQ Ltd, Fort Halstead, Sevenoaks, Kent, UK TN14 7BP

Received 17th January 2002

First published as an Advance Article on the web 21st May 2002

Perfluorocarbons have been used effectively as solvents and bulking agents in the reactions of toluene, benzene, phenol, benzyl chloride and chlorobenzene with nitric acid or dinitrogen pentoxide to yield highly nitrated products. Reactions are carried out in a single stage, at lower temperatures, and producing smaller amounts of waste acid than in traditional processes.

## Introduction

Nitration is one of the key processes in synthetic chemistry and is widely used industrially.<sup>1,2</sup> Despite the recent use of solid supports, including zeolites<sup>3–5</sup> and claycop,<sup>6</sup> particularly for the regiospecific nitration of aromatic compounds, and the effective use of dinitrogen pentoxide as a nitrating agent,<sup>7</sup> the most commonly used medium is still nitric acid in sulfuric acid (mixed acid). This system is used in the polynitration of toluene, benzene and phenol to produce energetic materials.

A major environmental problem with the use of mixed acid is the disposal of the spent materials. Here we report on the effective use of perfluorocarbons as bulking agents to reduce the quantity of waste products. Compounds, including perfluoromethylcyclohexane **1**, perfluorodecalin **2**, perfluoro-perhydrophenanthrene **3** and perfluoroethers **4**, are now commercially available. They are not ozone depleters and are chemically inert and immiscible with most organic solvents and aqueous media. This inertness has led to their previous use as solvent replacements or bulking agents<sup>8,9</sup> for reactions including halogen exchange<sup>10</sup> and transesterification.<sup>11</sup> In the nitrations we describe the solvents may be recycled without decomposition or measurable decrease in volume so that there is minimal loss to the gas phase.

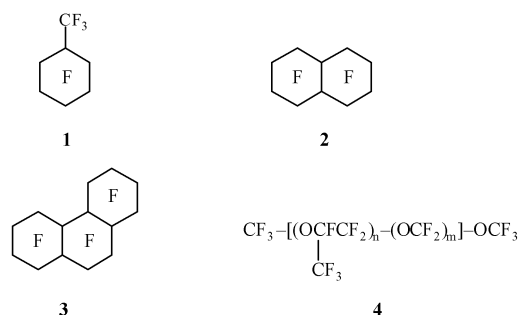




**Table 1**  $^1\text{H}$  NMR Shifts<sup>a</sup> in  $[\text{D}_6\text{DMSO}]$  of reaction products

	H2	H3	H4	H5	H6	$\text{CH}_3/\text{CH}_2\text{Cl}$
2,4-Dinitrotoluene	—	8.72	—	8.45	7.80	2.63
2,6-Dinitrotoluene	—	8.22	7.70	8.22	—	2.44
2,4,6-Trinitrotoluene	—	9.01	—	9.01	—	2.54
1,3-Dinitrobenzene	8.82	—	8.65	7.96	8.65	—
1,2-Dinitrobenzene	—	8.22	7.95	7.95	8.22	—
1,4-Dinitrobenzene	8.44	8.44	—	8.44	8.44	—
1,3,5-Trinitrobenzene	9.15	—	9.15	—	9.15	—
4-Nitrophenol	6.92	8.11	—	8.11	6.92	—
2,4-Dinitrophenol	—	8.71	—	8.37	7.28	—
2,6-Dinitrophenol	—	8.22	7.17	8.22	—	—
2,4,6-Trinitrophenol	—	8.58	—	8.58	—	—
2,4-Dinitrobenzyl chloride	—	8.77	—	8.59	8.08	5.14
2,6-Dinitrobenzyl chloride	—	8.33	7.90	8.33	—	4.95
2,4-Dinitrochlorobenzene	—	8.85	—	8.44	8.02	—
2,6-Dinitrochlorobenzene	—	8.34	7.83	8.34	—	—

<sup>a</sup> The expected spin-couplings were observed,  $J_{ortho} = 8.1\text{--}9.0$  Hz,  $J_{meta} = 2.5\text{--}3.0$  Hz.

times) which is immiscible with the perfluorocarbons. After neutralisation with potassium hydrogen carbonate and filtration, solvent removal yielded the product.

Our aim was to produce multiple nitrations while minimising the amounts of waste products for disposal.

### Nitration of toluene

Measurement of the UV absorbance at 260 nm allowed the solubility of toluene in perfluorocarbons to be determined. Values found for saturated solutions at 25 °C were **1**, 0.39 mol dm<sup>-3</sup>; **2**, 0.29 mol dm<sup>-3</sup>; **3**, 0.11 mol dm<sup>-3</sup>; **4**, 0.18 mol dm<sup>-3</sup>. Nitrated derivatives have considerably lower solubilities, e.g. in **3**: 4-nitrotoluene, 0.012 mol dm<sup>-3</sup>; 2,4-dinitrotoluene, 4.5 × 10<sup>-4</sup> mol dm<sup>-3</sup>.

In systems **A** and **B** reaction is likely to occur at the interface between toluene in the perfluorocarbon, and the nitrating agent in the upper layer. The results summarised in Table 2 show that where dinitrotoluenes are isolated the ratio of the 2,4-isomer to the 2,6-isomer is generally *ca.* 4:1 which is typical for nitronium ion nitrations.<sup>1,14</sup> However the use of **4** does appear to enhance the proportion of 2,4-isomer isolated.

Using nitric acid alone allows the ready conversion of toluene to dinitrotoluenes but no significant conversion to 2,4,6-trinitrotoluene (TNT) was observed even in the presence of excess acid

or using Nafion-H as an activator. However the use of mixed acid, system **B**, results in virtually complete conversion of toluene to TNT, with perfluorocarbons **1** and **2** giving better results than **3** or **4**. Yields of isolated products were > 60%, and for **1** with 5 equivalents of nitric and sulfuric acids a yield of 85% of TNT was achieved at 70 °C after 6 h. This compares with the conventional process which involves stepwise nitrations, mono- to di- to tri-nitrotoluene, each involving excess nitric acid with sulfuric acid as solvent.<sup>15,16</sup> The final stage is carried out at 90–100 °C with a two to three-fold excess of nitric acid in oleum (15% free sulfur trioxide) as solvent. Reactions on solid supports, although environmentally more friendly, do not yield trinitro-derivatives.<sup>6</sup>

The reaction of toluene with dinitrogen pentoxide, system **C**, occurs in solution. The mechanism is likely to involve reaction with molecular N<sub>2</sub>O<sub>5</sub> probably with a cyclic transition state.<sup>12,17</sup> This is a less powerful nitrating system than system **B** although some TNT is formed after prolonged reaction with 5 equivalents of N<sub>2</sub>O<sub>5</sub>. Due to the decomposition of N<sub>2</sub>O<sub>5</sub> at higher temperatures reaction at 0 °C is more effective than at 25 °C.

### Nitration of benzene

Our efforts here were directed towards the formation of 1,3,5-trinitrobenzene (TNB) directly from benzene. The results

**Table 2** Summary of the reactions for nitration of toluene

PFC	Molar equivalents			Temp/°C	Time/h	Composition <sup>b</sup> (%)		
	HNO <sub>3</sub>	H <sub>2</sub> SO <sub>4</sub>	N <sub>2</sub> O <sub>5</sub>			2,4-DNT	2,6-DNT	TNT
<b>3</b>	8	—	—	75	2	80	20	0
<b>4</b>	5	—	—	70	6	95	5	0
<b>1</b>	10 <sup>a</sup>	—	—	70	6	75	25	0
<b>1</b>	5	5	—	70	2	67	8	25
					4	49	8	43
					6	3	0	97
<b>2</b>	5	5	—	80	2	30	0	70
					4	10	0	90
					6	3	0	97
<b>4</b>	5	5	—	70	2	71	12	17
					4	68	0	32
					6	68	0	32
<b>4</b>	10	10	—	70	2	3	0	97
					3	9	7	75
<b>3</b>	13	10	—	75	6	5	0	95
<b>2</b>	—	—	3	0	12	78	16	7
<b>2</b>	—	—	5	0	12	73	16	11
<b>2</b>	—	—	5	25	12	90	10	0

<sup>a</sup> Nafion-H membrane was added as a potential activator.<sup>13</sup> <sup>b</sup> Values given are ±3%.

**Table 3** Summary of reactions for the nitration of benzene

PFC	Molar equivalents				Temp/°C	Time/h	Composition <sup>b</sup> (%)			
	HNO <sub>3</sub>	H <sub>2</sub> SO <sub>4</sub>	H <sub>2</sub> S <sub>2</sub> O <sub>7</sub>	N <sub>2</sub> O <sub>5</sub>			1,2-DNB	1,3-DNB	1,4-DNB	TNB
2	10	5	—	—	70	12	10	87	3	0
2	10	—	10	—	70	20	8	89	2	1
2	20 <sup>a</sup>	—	20	—	70	12	4	92	4	0
2	—	—	—	5	25	6	12	85	3	0
2	10a	—	—	3	70	9	6	92	2	0

<sup>a</sup> Nafion-H beads used as a potential activator.<sup>13</sup> <sup>b</sup> Values given are ±3%.

in Table 3 show that although dinitration is readily achieved only insignificant conversion to TNB is possible in these systems which included nitric acid and oleum or nitric acid and N<sub>2</sub>O<sub>5</sub>. As previously observed<sup>18,19</sup> small proportions of 1,2- and 1,4-dinitrobenzene were formed in addition to the major 1,3-isomer.

### Nitration of phenol

System C with N<sub>2</sub>O<sub>5</sub> was used for the homogeneous nitration of phenol. Products were separated by extraction with water. Reaction with 3 equivalents of N<sub>2</sub>O<sub>5</sub> for 10 min in **2** yielded 4-nitrophenol (24%), 2,4-dinitrophenol (24%), 2,6-dinitrophenol (8%) and 2,4,6-trinitrophenol (44%). However when 7 equivalents of N<sub>2</sub>O<sub>5</sub> were used for 2 h at 25° in **4**, 2,4,6-trinitrophenol was isolated as the only product in 97% yield. This method provides a convenient, one-step conversion of phenol to its trinitro derivative, and is useful since the direct reaction of phenol with nitric acid results in decomposition through oxidation.<sup>20</sup>

### Nitration of benzyl chloride **8** and chlorobenzene **9**

The effectiveness of N<sub>2</sub>O<sub>5</sub> in perfluorocarbons was also observed in the nitrations of **8** and **9**.

Reaction of **8** dissolved in solvent **1** containing 2.5 equivalents of N<sub>2</sub>O<sub>5</sub> gave 2,4- and 2,6-dinitrobenzyl chlorides in an 80:20 ratio with 90% yield. In the same solvent reaction of **9** with 3 equivalents of N<sub>2</sub>O<sub>5</sub> gave 2,4- and 2,6-dichlorobenzenes in a 97:3 ratio and 90% yield. Repeat experiments showed the recycled solvent to be equally effective. However, trinitration could not be achieved using excess N<sub>2</sub>O<sub>5</sub>. Extraction gives an acidic solution, resulting from formation of nitric acid equivalent to the N<sub>2</sub>O<sub>5</sub> used, which must be neutralised. However the acid to be disposed of is much less than in conventional processes for the formation of dinitrobenzyl chlorides<sup>21,22</sup> or dinitrochlorobenzenes,<sup>23</sup> which use sulfuric acid (*ca.* 10 equivalents) or oleum as the solvent.

### Conclusions

The use of perfluorocarbons as solvents and bulking agents allows the conversion of toluene to 2,4,6-trinitrotoluene, TNT, in one stage and at lower temperatures and with less acid than in traditional processes. The optimum conditions were using **1** at 70 °C with five equivalents of nitric and sulfuric acids; this gave 97% conversion to TNT in 85% yield after six hours. The product separates on washing with water and the perfluorocarbon can be recycled. Conversion of benzene to dinitrobenzenes may be achieved using either nitric acid or dinitrogen pentoxide; however trinitration was not observed. Reaction of phenol with nitrogen pentoxide in **4** results in the formation of 2,4,6-trinitrophenol in 97% yield. N<sub>2</sub>O<sub>5</sub> in

perfluorocarbons may also be used in the dinitration of benzyl chloride and of chlorobenzene.

### Experimental

Aromatic substrates were the purest available commercial samples. Perfluorocarbons **1–3** were obtained from F2 Chemicals and perfluoroether HT-135, **4**, from the Montefluos Company. Nitric acid was prepared by distillation from 98% sulfuric acid and potassium nitrate. Dinitrogen pentoxide was prepared by ozonation of N<sub>2</sub>O<sub>4</sub> as described previously,<sup>24</sup> and was stored at –60 °C; solutions were prepared immediately before use. All other chemicals and solvents were the purest available commercial materials. UV absorption spectra were recorded on Perkin-Elmer Lambda 2, or Shimadzu 2101-PC spectrophotometers. <sup>1</sup>H NMR spectra were recorded on Varian VXR-200, VXR-300 or VXR-400 instruments using [D<sub>6</sub>]DMSO as solvent.

### Acknowledgements

This work was funded as part of the Corporate Research Portfolio of the Defence Evaluation and Research Agency.

### References

- 1 K. Schofield, *Aromatic Nitration*, Cambridge University Press, Cambridge, UK, 1980.
- 2 G. A. Olah, R. Malhotra and S. C. Narang, *Nitration: Methods and Mechanisms*, ed. H. Feuer, Organic Nitro Series, VCH, New York, 1989.
- 3 K. Smith, A. Musson and G. A. De Boos, *Chem. Commun.*, 1996, 469.
- 4 K. Smith, T. Gibbins, R. W. Millar and R. P. Claridge, *J. Chem. Soc., Perkin Trans. 1*, 2000, 2753.
- 5 R. P. Claridge, N. L. Lancaster, R. W. Millar, R. B. Moodie and J. P. B. Sandall, *J. Chem. Soc., Perkin Trans. 2*, 1999, 1815.
- 6 N. L. Lancaster, R. B. Moodie and J. P. B. Sandall, *J. Chem. Soc., Perkin Trans. 2*, 1997, 847.
- 7 R. W. Millar, M. E. Colclough, N. Desai, P. Golding, P. J. Honey, N. C. Paul, A. J. Sanderson and M. J. Stewart, *ACS Symp. Ser.*, 1995, **623**, 104.
- 8 F. Montanari, G. Pozzi and S. Quici, *Chim. Ind. (Milan)*, 1998, **80**, 469.
- 9 D. S. L. Slinn and S. W. Green, in *Preparation, Properties and Industrial Applications of Organofluorine Compounds*, ed. R.E. Banks, Ellis Horwood, Chichester, 1982.
- 10 R. D. Chambers and A. R. Edwards, *J. Chem. Soc., Perkin Trans. 1*, 1997, 3623.
- 11 D.-W. Zhu, *Synthesis*, 1993, 953.
- 12 M. R. Crampton, L. M. Gibbons and R. W. Millar, *J. Chem. Soc., Perkin Trans. 2*, 2001, 1662.
- 13 G. A. Olah, R. Malhotra and S. C. Narang, *J. Org. Chem.*, 1978, **43**, 4628.

- 14 C. L. Coon, W. G. Blucher and M. E. Hill, *J. Org. Chem.*, 1973, **38**, 4243.
- 15 W. Seidenfaden and D. Pawellek, in *Houben-Weyl's Die Methoden der Organische Chemie*, G. Thieme Verlag, Stuttgart, 4th edn., 1971, vol. 10, Part 1.
- 16 W. H. Dennis, D. H. Rosenblatt, W. G. Blucher and C. L. Coon, *J. Chem. Eng. Data*, 1975, **20**, 202.
- 17 V. Gold, E. D. Hughes, C. K. Ingold and G. H. Williams, *J. Chem. Soc.*, 1950, 2452.
- 18 A. F. Holleman, *Chem. Rev.*, 1925, **1**, 187.
- 19 R. Taylor, *Electrophilic Aromatic Substitution*, Wiley, Chichester, 1990.
- 20 F. H. Westheimer, E. Segel and R. Schramm, *J. Am. Chem. Soc.*, 1947, **69**, 773.
- 21 P. Friedlander and M. Cohn, *Ber. Dtsch. Chem. Ges.*, 1902, **35**, 1266.
- 22 G. Bachman, H. B. Hass and G. O. Platau, *J. Am. Chem. Soc.*, 1954, **76**, 3972.
- 23 H. H. Hodgson and D. P. Dodgson, *J. Chem. Soc.*, 1948, 1006.
- 24 R. W. Millar and S. P. Philbin, *Tetrahedron*, 1997, **53**, 4371.



# The first example of heterogeneous oxidation of secondary amines by tungstate-exchanged Mg-Al layered double hydroxides: a green protocol†

B. M. Choudary,\* B. Bharathi, Ch. Venkat Reddy and M. Lakshmi Kantam\*

Indian Institute of Chemical Technology, Hyderabad-500007, India.

E-mail: choudary@iict.ap.nic.in

Received 28th February 2002

First published as an Advance Article on the web 27th May 2002

Tungstate exchanged Mg-Al layered double hydroxides as a recyclable heterogenised catalyst along with H<sub>2</sub>O<sub>2</sub> as an oxidant for the oxidation of *sec*-amines to nitrones is developed for the first time. Reactions proceed at a fast rate in aqueous media in a single step at room temperature in good to excellent yields. The heterogenised catalyst showed higher activity (TOF) over their homogeneous analogues and other heterogeneous catalysts reported so far. The obtained catalysts were well characterised by various instrumental techniques such as FT-IR spectroscopy, thermal analysis (TGA and DTA), powder XRD and chemical analysis. The catalyst can be reused for six cycles with consistent activity and selectivity.

## Introduction

Oxidation of amines is of interest in view of metabolism of amines *in vivo*. Nitrones, which are prepared by oxidation of secondary amines, are highly valuable synthetic intermediates<sup>1</sup> and excellent spin trapping reagents.<sup>2</sup> In particular nitrones are excellent 1,3 dipoles<sup>3</sup> for the preparation of various nitrogen containing biologically active compounds such as antibiotics, alkaloids, aminosugars and  $\beta$ -lactams. The direct oxidation of secondary amines is highly preferable to the classical methods of preparation by condensation of carbonyl compounds with N-monosubstituted hydroxylamines and oxidation of N, N-disubstituted hydroxylamines<sup>4</sup> as the preparation of the starting hydroxylamines is generally very tedious. Consequently several oxidising systems such as R<sub>2</sub>CuO<sub>2</sub>,<sup>5</sup> Na<sub>2</sub>WO<sub>4</sub> + H<sub>2</sub>O<sub>2</sub>,<sup>6</sup> SeO<sub>2</sub>,<sup>7</sup> tetra-*n*-propylammonium perruthenate (TPAP) + *N*-methylmorpholine *N*-oxide (NMO),<sup>8</sup> and urea hydrogen peroxide (UHP-M, M = Mo, W),<sup>9</sup> methyltrioxorhenium (MTO) + H<sub>2</sub>O<sub>2</sub>,<sup>10,11</sup> flavin 4*a*-hydroperoxyflavin (4*a*-FIE-tOOH)<sup>12</sup> have been reported to provide nitrones under homogeneous conditions. Either stoichiometric or catalytic quantities are employed in these homogeneous oxidising systems to coax the oxidation of secondary amines to nitrones to completion. Homogeneous catalytic reactions are preferred over the reactions that use stoichiometric quantities, since the latter are not only relatively expensive, but they also generate copious amounts of heavy-metal waste. However, an ideal system for such reactions would involve the use of a solid catalyst conducted under heterogeneous conditions, which allows easy separation of the catalyst from the reaction mixture and adaptability in large-scale production to conform to the class of 'greener' technologies. Another issue that worries environmentalists is the use of undesirable organic solvents, methanol and chlorinated hydrocarbons in such homogeneous reactions discussed above. Heterogeneous catalysts *viz.* titanium silicates conceived and employed for the oxidation of secondary amines in an effort to reduce pollution, has the limited scope of utility only to smaller molecules. Moreover in this process organic solvents such as methanol were used to obtain higher yields.<sup>13</sup>

In continued search for cleaner ('greener') technologies, there is a definite need for catalytic oxidations that use dioxygen (O<sub>2</sub>) or hydrogen peroxide as the stoichiometric oxidant<sup>14</sup> in conjunction with water as a solvent. Aqueous hydrogen peroxide (30%) is an ideal oxidant in view of its high effective-oxygen content, and cleanliness producing only water as by-product, safety in storage and operation, and low cost of production and transportation.<sup>15</sup> Besides this, reactions performed in water are safer, cheaper, and more environmentally friendly so as to meet stringent environmental specifications. With an ever-increasing level of global competition and environmental consciousness, there is thus an incentive to find new and strategically important processes with higher atom utilisation preferably close to theoretical values to eventually minimise pollution levels using greener ingredients.

The layered double hydroxides (LDH)<sup>16</sup> which include hydrotalcites and hydrotalcite like compounds have recently received much attention in view of their potential usefulness as adsorbents, anion exchangers and most importantly as catalysts.<sup>17</sup> The hydrophilicity of LDHs makes any hosted oxidation catalyst water compatible so that reactions can be conducted using water as the solvent. Recently we reported the catalytic *N*-oxidation of tertiary amines by tungstate exchanged Mg-Al-LDH catalyst in quantitative yields at faster rates in aqueous

## Green Context

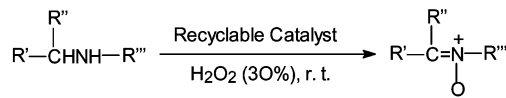
Like so many other oxidations, the oxidation of secondary amines provides highly valuable synthetic intermediates. Nitrones can be used to make important compounds including alkaloids, antibiotics, aminosugars and  $\beta$ -lactams. Unfortunately, and again like so many other oxidations, traditional methods present many environmental, toxicity and efficiency problems. Here we see the first reported example of the oxidation of secondary amines using a solid tungstate catalyst based on Mg-Al layered double hydroxides. The oxidant (hydrogen peroxide) and solvent (water) add to the environmental credentials of this new process. Indeed, remarkably, water proves to be the best solvent of several tested.

JHC

† IICT Communication No: 020213.



media.<sup>18</sup> In this article, we report an efficient and heterogeneous tungstate-exchanged layered double hydroxide (LDH-WO<sub>4</sub>) for the oxidation of secondary amines using H<sub>2</sub>O<sub>2</sub> as an oxidant in water with good to excellent yields (Scheme 1). The present catalyst has been shown to have good efficiency as reflected by its high turnover frequency (TOF) and retention of catalytic activity for several cycles. In addition, this is the first report on oxidation of secondary amines using an LDH-derived catalyst.



**Scheme 1** The oxidation of *sec*-amines to nitrones catalysed by tungstate-exchanged Mg-Al-LDH.

## Results and discussion

The structure of LDH consists of brucite [Mg(OH)<sub>2</sub>] type octahedral layers in which a part of the M(II) cations are isomorphously substituted by Al(III) cations. The excess positive charge of the octahedral layers resulting from this substitution is compensated by interstitial layers built of anions such as carbonates, nitrates, chlorides or cyanides as well as containing water of crystallization. Redox properties in hydroxalicates can be imparted and tuned according to the requirement. This can be done in different ways: one is by incorporating redox-active divalent or trivalent transition metal ions (or both). A second option is to vary the ratios of the redox metal ions chosen for the preparation of a specific catalyst. Yet another manner in which the redox property of the LDH is tuned or introduced is by incorporating transition metal oxides as anions to neutralise positive charge developed as a result of isomorphous substitution of Mg in the main framework of brucite as discussed above. These hydroxalcite like materials (LDHs) are thus represented by the general formula [M<sup>II</sup><sub>1-x</sub>M<sup>III</sup><sub>x</sub>·(OH)<sub>2</sub>]<sup>x+</sup>[(A<sup>y-</sup>)<sub>x/y</sub>·nH<sub>2</sub>O]<sup>x-</sup> where M<sup>II</sup> is a divalent cation such as Mg, Cu, Ni, Co, Mn, Fe, Zn; M<sup>III</sup> is a trivalent cation such as Al, Fe, Cr, V, Ru, Rh, Ga, In; A<sup>y-</sup> is an interlayer anion such as OH<sup>-</sup>, Cl<sup>-</sup>, CO<sub>3</sub><sup>2-</sup>, NO<sub>3</sub><sup>-</sup>, SO<sub>4</sub><sup>2-</sup> and the value of *x* is in the range of 0.1–0.33.

Small hexagonal LDH crystals with composition Mg<sub>1-x</sub>Al<sub>x</sub>(OH)<sub>2</sub>Cl<sub>x</sub>·zH<sub>2</sub>O were synthesized following existing procedures (here, *x* = 0.25). The anionic species tungstate, molybdate, vanadate and {PO<sub>4</sub>[WO(O<sub>2</sub>)<sub>4</sub>]}<sup>2-</sup> were exchanged on to LDH-Cl to give a series of LDH oxidation catalysts, LDH-WO<sub>4</sub> (cat 1) (Fig. 1),<sup>17e</sup> LDH-MoO<sub>4</sub> (cat 2) LDH-VO<sub>3</sub> (cat 3) and LDH-{PO<sub>4</sub>[WO(O<sub>2</sub>)<sub>4</sub>]} (cat 4),<sup>19</sup> respectively. All these

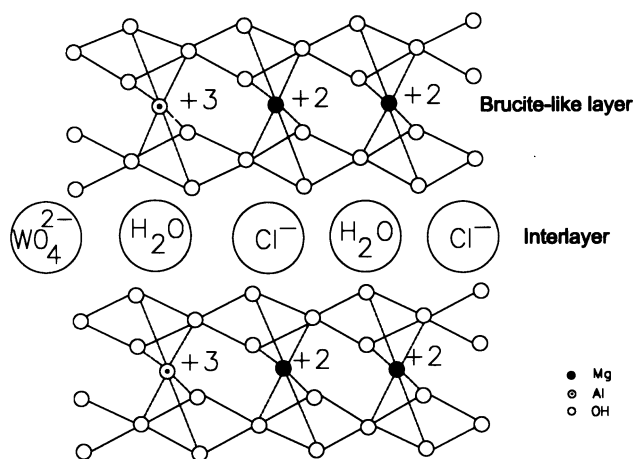


**Fig. 1** Schematic representation of LDH-WO<sub>4</sub>.

catalysts are fully characterized by XRD, TGA-DTA and chemical analysis.

## X-Ray powder diffraction

The X-ray diffraction patterns of the powdered samples were measured and LDH exchanged catalysts such as LDH-WO<sub>4</sub> (cat 1), LDH-MoO<sub>4</sub> (cat 2), LDH-VO<sub>3</sub> (cat 3) and LDH-{PO<sub>4</sub>[WO(O<sub>2</sub>)<sub>4</sub>]} show characteristic patterns of LDH (Fig. 2).<sup>20</sup> No new significant peaks in the XRD pattern corresponding to an insoluble Mg or Al salt to indicate the formation of new phases are observed. The X-ray powder diffraction patterns of the initial LDH materials and of the anion-exchanged LDH (cat 1–4) hardly differ in the range 2θ = 3–65°. The *d*<sub>003</sub> reflection corresponds to the interlamellar distance plus the thickness of mineral sheet (4.8 Å). In the case of the LDH chloride precursor (Fig. 2(e)) and cat 1–4, no change in the interlamellar distance is observed. These data clearly demonstrate that the anion is not intercalated but present at edge-on positions of the LDH in the solid catalyst.<sup>17e</sup>

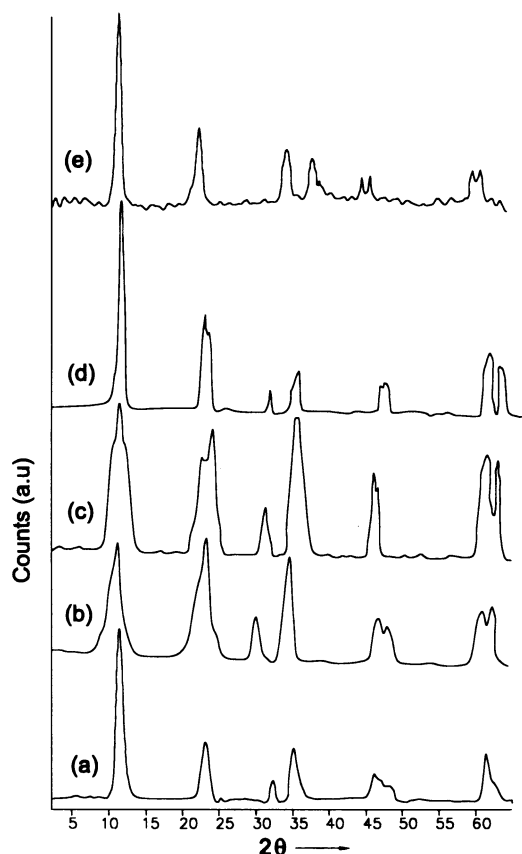


**Fig. 2** X-Ray powder-diffraction patterns of various anion-exchanged LDH catalysts and their precursor: (a) LDH-WO<sub>4</sub>, (b) LDH-MoO<sub>4</sub>, (c) LDH-VO<sub>3</sub>, (d) LDH-{PO<sub>4</sub>[WO(O<sub>2</sub>)<sub>4</sub>]}, (e) Mg-Al-Cl LDH.

## Thermal analysis

The results of thermogravimetric analysis and corresponding DTG profiles (Fig. 3) of solid catalysts (cat 1–4) and their precursor, Mg-Al-Cl LDH, are summarised in Table 1. The DTG shows two sets of endothermic peaks, a characteristic pattern of LDH structure. The first endotherm of DTG below 280 °C corresponds to the release of surface (physically absorbed) and interlayer water of the brucite. The second endotherm in the range 280–535 °C is attributed to structural

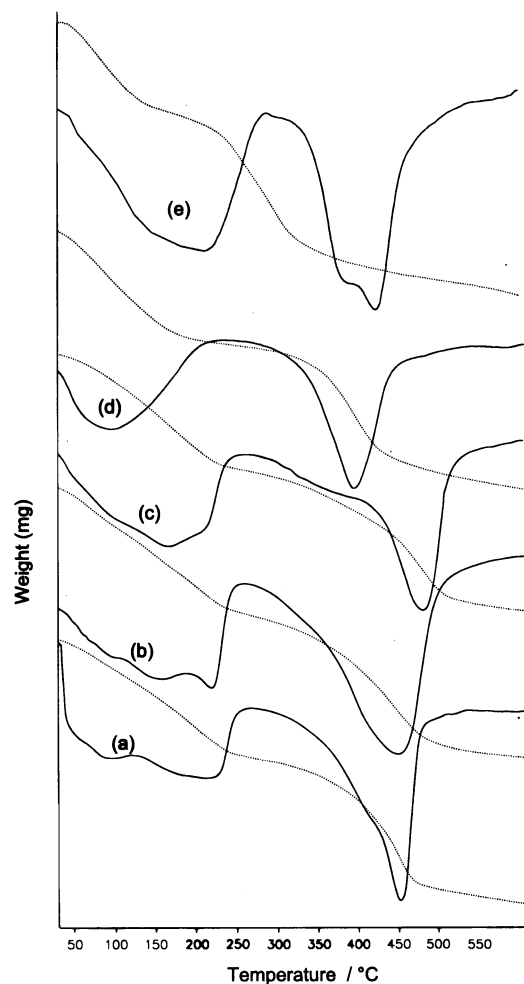


**Fig. 3** TG (dotted lines) and DTA (solid lines) of various anion-exchanged LDH catalysts and their precursor: (a) LDH- $\text{WO}_4$ , (b) LDH- $\text{MoO}_4$ , (c) LDH- $\text{VO}_3$ , (d) LDH- $\{\text{PO}_4[\text{WO}(\text{O}_2)_4]\}$ , (e) Mg-Al-Cl LDH.

dehydroxylation and decomposition of  $\text{Cl}^-$ . In general the weight loss above  $410^\circ\text{C}$  in the TG curves may be assigned to the elimination of unexchanged  $\text{Cl}^-$ .<sup>21</sup> These results clearly indicate that there is no structural disorder even after the ion-exchange.

### FT-IR Spectroscopy

The obtained solids (cat **1–4**) were studied by using FT-IR spectroscopy to probe structural modifications before (Mg-Al-Cl LDH) and after the anion-exchange process of the catalysts (Fig. 4). All the catalysts cat **1–4** showed broad absorption bands around  $3400\text{--}3600\text{ cm}^{-1}$  which are typical to that of OH hydroxy stretching vibrations of brucite, whereas for interlayer or physically adsorbed water the corresponding deformation mode of OH appeared around  $1630\text{ cm}^{-1}$  in all the samples

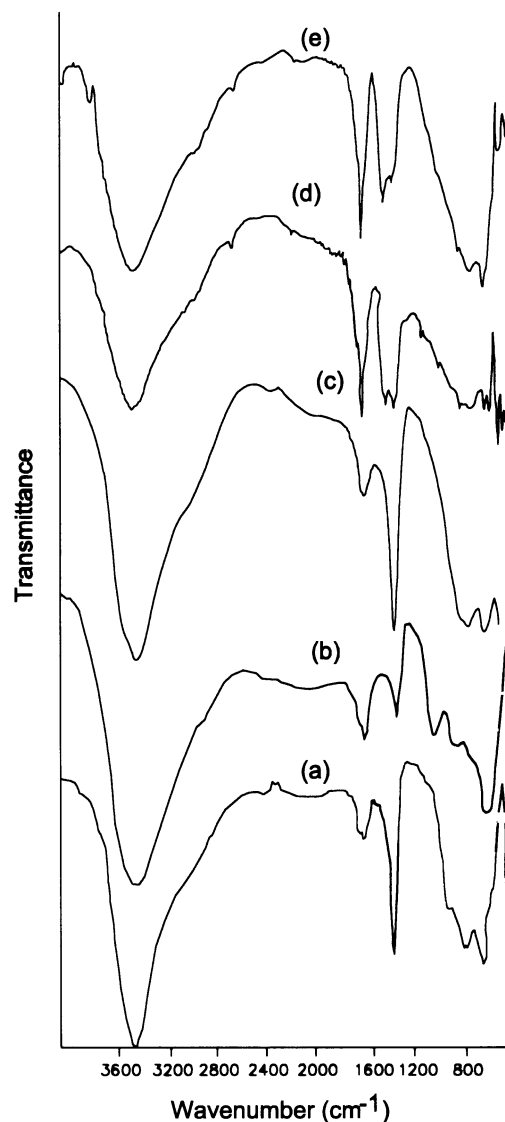


**Fig. 4** FT-IR spectra of various anion-exchanged LDH catalysts and their precursor: (a) LDH- $\text{VO}_3$ , (b) LDH- $\{\text{PO}_4[\text{WO}(\text{O}_2)_4]\}$ , (c) LDH- $\text{MoO}_4$ , (d) LDH- $\text{WO}_4$ , (e) Mg-Al-Cl LDH.

tested.<sup>22</sup> These FT-IR results also suggest that there is no structural disorder even after the ion-exchange.

### Chemical analysis

The chemical analysis of the catalysts showed the weight percentage of tungstate in cat **1** = 11.3 and cat **4** = 21, molybdate in cat **2** = 9.9, and vanadate in cat **3** = 7.8. The chemical analysis of precursor material, Mg-Al-Cl LDH showed a weight percentage of chloride = 11.2.

The exchanged LDH catalysts (cat **1–4**) and their homogeneous analogues were evaluated in the oxidation of dibutylamine using 3 molar equivalents  $\text{H}_2\text{O}_2$  per mole of the substrate

**Table 1** Thermogravimetric analyses of cat **1–4** and their precursor (Mg-Al-Cl LDH)

Sample no.	Catalyst	Step I/ $^\circ\text{C}$	Assignment	Wt%	Step II/ $^\circ\text{C}$	Assignment	Wt%
1	<b>1</b>	<280	$-\text{H}_2\text{O}$	15.35	280–535	$-\text{H}_2\text{O}$ , $\text{Cl}^-$	19.37
2	<b>2</b>	<280	$-\text{H}_2\text{O}$	18.85	280–535	$-\text{H}_2\text{O}$ , $\text{Cl}^-$	19.66
3	<b>3</b>	<280	$-\text{H}_2\text{O}$	15.04	280–535	$-\text{H}_2\text{O}$ , $\text{Cl}^-$	16.99
4	<b>4</b>	<280	$-\text{H}_2\text{O}$	14.40	280–535	$-\text{H}_2\text{O}$ , $\text{Cl}^-$	18.68
5	Mg-Al-Cl LDH	<280	$-\text{H}_2\text{O}$	21.20	280–535	$-\text{H}_2\text{O}$ , $\text{Cl}^-$	27.29

and water as solvent in order to identify the best catalyst in the oxidation of *sec*-amines to the corresponding N-oxides (Table 2). The order of the activity of LDH exchanged catalysts is: cat **1** > cat **2** > cat **4** > cat **3**. Essentially, there was no reaction with Mg-Al-Cl LDH, the precursor for the above catalysts (Table 2, entry 8). The heterogeneous catalysts displayed superior activity over their homogeneous counterparts. The efficacy of the catalyst is well established as is evident from the Table 2. LDH-WO<sub>4</sub> (cat **1**) exhibited the highest turnover frequency (TOF) of 21.7 h<sup>-1</sup> over the other exchanged LDH catalysts. Furthermore, the exchanged LDH oxidant catalysts showed 2–5 fold activity over their analogues homogeneous catalytic systems. Thus, LDH-WO<sub>4</sub> (cat **1**) is found to be the best catalyst among the various exchanged LDH catalysts and their homogeneous analogues for the oxidation of *sec*-amines. No reaction occurred without catalyst in the oxidation of dibutylamine (Table 2, entry 9). Aqueous H<sub>2</sub>O<sub>2</sub> is found to be the best oxidant among the oxidants, *tert*-butyl hydroperoxide (TBHP) and molecular oxygen, used in the oxidation of *sec*-amines. The oxidant TBHP gave very poor results, while the reaction employing molecular oxygen did not proceed. Thus H<sub>2</sub>O<sub>2</sub> is an ideal and environment-friendly oxidant, in terms of its price, availability and gives only water as by-product. The solvent effect was also studied in the oxidation of dibutylamine using LDH-WO<sub>4</sub> catalyst: the activity is found to be in the following order: H<sub>2</sub>O ≅ CH<sub>3</sub>OH > CHCl<sub>3</sub> > CH<sub>3</sub>CN > CH<sub>2</sub>Cl<sub>2</sub>. Thus water gave the best results among the solvents examined in the N-oxidation of secondary amines. The hydrophilic character of LDH, which render the catalyst water compatible is believed to promote the reaction with high yields. The high surface enrichment of secondary amines on LDH and ready formation of peroxide with LDH-WO<sub>4</sub> facilitates the higher throughput in the oxidation of secondary amines.

**Table 2** The N-oxidation of dibutylamine using various anion-exchanged LDH catalysts and their homogeneous analogues<sup>a</sup>

Sample no.	Catalyst	Time/h	Yield <sup>b</sup> (%)	TOF <sup>c</sup>
1	LDH-WO <sub>4</sub> (cat <b>1</b> )	1.0	96	21.8
2	LDH-MoO <sub>4</sub> (cat <b>2</b> )	3.5	90	4.2
3	LDH-VO <sub>3</sub> (cat <b>3</b> )	3.5	40	1.4
4	LDH-{PO <sub>4</sub> [WO(O <sub>2</sub> ) <sub>4</sub> ] (cat <b>4</b> )	3.5	40	7.6
5	Na <sub>2</sub> WO <sub>4</sub>	3.5	75	13.9
6	NaVO <sub>3</sub>	3.5	15	0.5
7	Na <sub>2</sub> MoO <sub>4</sub>	3.5	48	2.2
8	Mg-Al-Cl LDH	24	No reaction	—
9	None	24	No reaction	—

<sup>a</sup> All reactions were carried out using (2 mmol) of substrate with 200 mg of catalyst in 10 mL of water and 6.6 mL (6 mmol) of aqueous hydrogen peroxide (30% w/w). <sup>b</sup> Isolated yields. <sup>c</sup> TOF (turnover frequency) = mmol of product per mmol of catalyst per hour.

In an effort to understand the scope of the reaction, several other amines having different R groups attached to the secondary nitrogen atom were subjected for the oxidation using the LDH-WO<sub>4</sub>/H<sub>2</sub>O<sub>2</sub> system. (Table 3). The results are summarised in Table 2. Acyclic and cyclic amines were generally converted into the corresponding nitrones in good to excellent yields. The oxidation of dibenzyl amine **3a** afforded *N*-benzylidenebenzylamine *N*-oxide **3b**, a useful precursor for *N*-benzylhydroxylamines. Oxidation of diisopropylamine **4a** and dibutylamine **2a** provided *N*-(1-methylethylidene)isopropylamine *N*-oxide **4b** and *N*-butylidenebutylamine *N*-oxide **2b**, respectively, in 92–96% yield.

Furthermore the reusability was checked for several cycles with the best catalyst cat **1** which showed consistent activity and selectivity for six cycles as detailed in the Table 3, entry 2. Reaction did not proceed when the process was conducted with the filtrate obtained after the separation of the solid catalyst, which indicates the active ingredient is not leached out of the

**Table 3** Oxidation of *sec*-amines catalysed by LDH-WO<sub>4</sub> (cat **1**)<sup>a</sup>

Entry	Amine (a)	Nitronone (b)	t/h	Yield <sup>b</sup> (%)
1			3	96
2			3	97 (96) <sup>c</sup>
3			5	60
4			3	92
5			4	93
6			3	92
7			3	95

<sup>a</sup> Reaction conditions are as exemplified in Table 2 in footnote a. <sup>b</sup> Isolated yields and all the products are characterised using <sup>1</sup>H NMR, FT-IR and mass spectrometry. <sup>c</sup> Yield after 6th recycle.

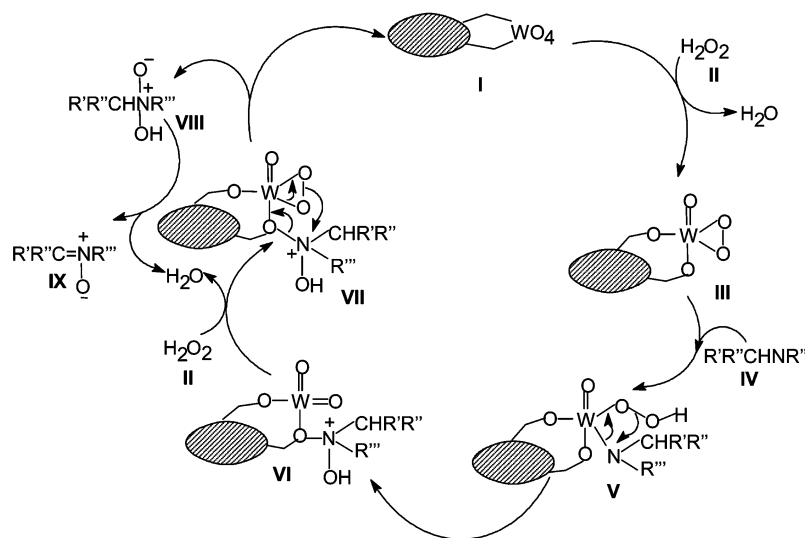
solid catalyst during the reaction. Thus, the catalyst is expected to be long-lived and stable for several cycles.

## Mechanism

The plausible catalytic cycle in the N-oxidation of *sec*-amines to nitrones as described in Scheme 2 involves the formation of a peroxotungstate (oxo-bridged complex) species **III** on interaction of tungstate LDH **I** with hydrogen peroxide **II**.<sup>17e</sup> A shift of λ<sub>max</sub> from 250 in LDH (**I**) to 325 nm (**III**) by UV-DRS spectroscopy confirms the formation of peroxotungstate species. These peroxy species will act as active species for the oxidation of secondary amines as described by Murahashi *et al.*, for the Na<sub>2</sub>WO<sub>4</sub> catalysed oxidation of secondary amines by hydrogen peroxide.<sup>6</sup> The secondary amine **IV** undergoes nucleophilic reaction with peroxotungstate **III** species derived from tungstate and hydrogen peroxide, to give hydroxylamine **VI** via intermediate **V**. Further oxidation of **VI** followed by dehydration gives nitrones **IX**, thus completing the catalytic cycle.

## Conclusion

In conclusion, the present study represents the sole example wherein a recyclable heterogenised tungstate-based Mg-Al LDH is used in catalytic amounts for the N-oxidation of secondary amines to nitrones in excellent yields. The attractive feature is the accomplishment of the reaction using water as a solvent to conform not only to present environmental specifications but also future restrictions. Other advantages include the use of environmentally benign H<sub>2</sub>O<sub>2</sub> as an oxidant, easy separation of the catalyst and high throughput, which makes the process highly attractive in comparison to the present process.



**Scheme 2** A plausible catalytic cycle for the N-oxidation of *sec*-amines to nitrones by tungstate-exchanged Mg-Al LDH.

## Experimental

Proton nuclear magnetic resonance ( $^1\text{H}$  NMR) spectra were recorded on a Gemini Varian at 200 MHz, as solutions in  $\text{CDCl}_3$  at 25 °C;  $\delta$  values were in ppm downfield from tetramethylsilane (TMS). Mass spectra were obtained at an ionization potential of 70 eV, scanned on a VG 70–70H (micro mass); only selected ions are reported here. IR spectra were recorded on a Nicolet 740 FT-IR spectrometer either as neat liquids or KBr pellets. Thin layer chromatography was performed on silica gel 60F<sub>254</sub> plates procured from E. Merck. ACME silica gel (60–120 mesh) was used for column chromatography. Starting materials and metal salts were purchased from Aldrich, Fluka and Lancaster or prepared by known methods. Solvents purchased from commercial sources were purified prior to use. Thermogravimetric (TG) and differential thermogravimetric (DT) analysis of thermal decomposition of catalysts were studied by means of a TG-DTA Mettler Toledo Star system using open aluminium crucibles with a sample weight of about 8–10 mg and nitrogen as purge gas at a linear heating rate of 10 K min<sup>-1</sup> for all measurements. X-Ray diffraction patterns were determined on a Siemens D-5000 powder X-ray diffractometer (diffraction geometry;  $\theta$ – $2\theta$ , in the range 5–65°), using a sealed Cu tube (2.2 kW). CHN analysis was performed on a Vario EL analyser.

### Preparation of catalysts

**Mg-Al-chloride LDH<sup>23</sup>**. Mg-Al-Cl LDH (3 : 1) was prepared as follows: a mixture of a solution of  $\text{AlCl}_3 \cdot 9\text{H}_2\text{O}$  (12.07 g, 0.25 mol l<sup>-1</sup>) and  $\text{MgCl}_2 \cdot 6\text{H}_2\text{O}$  (30.49 g, 0.75 mol l<sup>-1</sup>) in deionised and decarbonated water (200 mL) and an aqueous solution of sodium hydroxide (16 g, 2 mol l<sup>-1</sup>) in deionised and decarbonated water (200 mL) were added simultaneously dropwise from the respective burettes into a round bottomed flask. The pH of the reaction mixture was maintained constant (10.00–10.2) by the continuous addition of NaOH solution. The suspension thus obtained was stirred for 2 h under a nitrogen atmosphere. The solid product was isolated by filtration, washed thoroughly with deionised and decarbonated water, and dried at 70 °C for 15 h.

**Mg-Al-LDH tungstate (cat 1)<sup>17e</sup>**. To a solution of sodium tungstate (1.87 mM, 0.616 g) in water (100 mL) Mg-Al-Cl LDH (1.0 g) was added and stirred at 293 K for 24 h. The solid

catalyst was filtered off, washed with deionised and decarbonated water and lyophilized to dryness.

**Mg-Al-LDH molybdate (cat 2)**. To a solution of sodium molybdate (1.87 mM, 0.452 g) in water (100 mL) Mg-Al-Cl LDH (1.0 g) was added and stirred at 293 K for 24 h. The solid catalyst was filtered off, washed with deionised and decarbonated water and lyophilized to dryness.

**Mg-Al-LDH vanadate (cat 3)**. To a solution of sodium vanadate (1.87 mM, 0.228 g) in water (100 mL) Mg-Al-Cl LDH (1.0 g) was added and stirred at 293 K for 24 h. The solid catalyst was filtered off, washed with deionised and decarbonated water and lyophilized to dryness.

**Mg-Al-LDH-[ $\text{PO}_4\text{WO}(\text{O}_2)_4$ ] (cat 4)**. The preparation of  $(\text{NBu}^n)_3\{\text{PO}_4[\text{WO}(\text{O}_2)_2]_4\}$  was carried out according to the literature procedure.<sup>19</sup> To a solution of isolated  $(\text{NBu}^n)_3\{\text{PO}_4[\text{WO}(\text{O}_2)_2]_4\}$  (0.46 mmol) in acetone (3 ml) was added an aqueous solution of 30% (w/w)  $\text{H}_2\text{O}_2$  (1 ml) and Mg-Al-Cl LDH (1 g) and the mixture was stirred for 16 h at room temperature. The obtained material (cat 4) was treated consecutively with water–acetone (1 : 1) and acetone.

### General procedure for the oxidation of secondary amines

To the stirred solution of catalyst (200 mg, 0.088 mmol of  $\text{WO}_4^{2-}$ ) and *sec*-amine (2 mmol) in water (10 mL) was added an aqueous solution of 30% (w/w) hydrogen peroxide (6.6 mL, 6 mmol) in two to three portions at room temperature. The reaction was allowed to stir at room temperature. After completion of the reaction (followed by TLC), the catalyst was filtered off and a small amount of  $\text{MnO}_2$  was added to decompose the unreacted hydrogen peroxide. The treated reaction mixture was filtered to remove solid  $\text{MnO}_2$ , and the product was extracted with ethyl acetate, dried over  $\text{Na}_2\text{SO}_4$  and evaporated *in vacuo* to afford the corresponding amine oxide (nitron). Analytically pure compound was obtained after column chromatography (silica gel, hexane/ethyl acetate).

The products were characterised by  $^1\text{H}$  NMR, mass and IR spectroscopy and elemental analysis. These data for the N-oxidation of *sec*-amines are presented below in order of the products in Table 3.

**N-Ethylideneethylamine N-oxide (1b)<sup>13</sup>**. Starting from **1a** (0.207 mL, 2 mmol), **1b** was obtained. Yield 96% (0.167 g).  $^1\text{H}$



NMR (200 MHz, CDCl<sub>3</sub>):  $\delta$  0.95 (t, 3H,  $J = 5.2$  Hz), 1.5 (q, 3H,  $J = 5.2$  Hz), 3.4 (q, 2H,  $J = 4.7$ ), 6.5 (t, 1H,  $J = 4.7$  Hz); IR (neat) cm<sup>-1</sup>: 1596 (C=N), 1180 (NO); MS (EI, 70 eV),  $m/z$ : 87 (M<sup>+</sup>, 85), 72 (9), 70 (28), 59 (65), 55 (100). Anal. Calc. for C<sub>4</sub>H<sub>9</sub>NO: C, 55.17; H, 10.34; N, 16.09. Found: C, 55.16; H, 10.56; N, 16.23%.

**N-Butylidenebutylamine N-oxide (2b)**<sup>6</sup>. Starting from **2a** (0.33 mL, 2 mmol), **2b** was obtained. Yield 97% (0.277 g). <sup>1</sup>H NMR (200 MHz, CDCl<sub>3</sub>):  $\delta$  0.94 (t, 3H,  $J = 7.6$  Hz), 0.97 (t, 3H,  $J = 7.6$  Hz), 1.15–2.21 (m, 6H), 2.47 (m, 2H), 3.73 (t, 2H,  $J = 7.6$  Hz) 6.64 (t, 1H,  $J = 6.15$  Hz); IR (neat) cm<sup>-1</sup>: 2960, 2880, 1603 (C=N), 1477, 1425, 1383, 1190 (NO), 1120, 1065, 941; MS (EI, 70 eV),  $m/z$ : 143 (M<sup>+</sup>, 5), 128 (9), 100 (100), 84 (25), 72 (26), 57 (27), 41 (48). Anal. Calc. for C<sub>8</sub>H<sub>17</sub>NO: C, 67.13; H, 11.88; N, 9.79. Found: C, 67.08; H, 11.66; N, 9.83%.

**N-Benzylidenebenzylamine N-oxide (3b)**<sup>6</sup>. Starting from **3a** (0.384 mL, 2 mmol), **3b** was obtained. Yield 60% (0.253 g). <sup>1</sup>H NMR (200 MHz, CDCl<sub>3</sub>):  $\delta$  5.06 (s, 2H), 7.2–7.5 (m, 9H), 8.1–8.2 (m, 2H); IR (neat) cm<sup>-1</sup>: 3058, 1580 (C=N), 1561, 1496, 1457, 1350, 1320, 1209, 1152 (NO), 1076, 1025, 944, 920, 857, 821, 749, 711, 691; MS (EI, 70 eV),  $m/z$ : 213 (M<sup>2+</sup>, 2), 196 (5), 106 (36), 91 (100), 65 (12). Anal. Calc. for C<sub>14</sub>H<sub>13</sub>NO: C, 79.6; H, 6.16; N, 6.63. Found: C, 79.83; H, 6.36; N, 6.68%.

**N-(1-Methylethylidene)-1-methylethylamine N-oxide (4b)**<sup>6</sup>. Starting from **4a** (0.282 mL, 2 mmol), **4b** was obtained. Yield 92% (0.211 g). <sup>1</sup>H NMR (200 MHz, CDCl<sub>3</sub>):  $\delta$  1.38 (d, 6H,  $J = 6.4$  Hz), 2.15 (s, 6H), 4.48 (hept, 1H,  $J = 6.4$  Hz); IR (neat) cm<sup>-1</sup>: 2983, 1590 (C=N), 1480, 1455, 1398, 1190 (NO), 1134, 1050, 958, 763; MS (EI, 70 eV),  $m/z$ : 115 (M<sup>+</sup>, 36), 73 (77), 58 (59), 43 (100). Anal. Calc. for C<sub>6</sub>H<sub>13</sub>NO: C, 62.60; H, 11.30; N, 12.17. Found: C, 62.68; H, 11.16; N, 12.3%.

**N-(Phenylmethylene)phenylamine N-oxide (5b)**. Starting from **5a** (0.366 g, 2 mmol), **5b** was obtained. Yield 93% (0.366 g). <sup>1</sup>H NMR (200 MHz, CDCl<sub>3</sub>):  $\delta$  7.4–7.5 (m, 6H), 7.75–7.8 (m, 2H), 7.9 (s, 1H), 8.3–8.4 (m, 2H); IR (neat) cm<sup>-1</sup>: 2990, 1595 (C=N), 1559, 1550, 1495, 1451, 1350, 1150 (NO), 1077, 1028, 920, 752, 699; MS (EI, 70 eV),  $m/z$ : 197 (M<sup>+</sup>, 13), 105 (10), 91 (100), 77 (30), 64 (7), 51 (9). Anal. Calc. for C<sub>13</sub>H<sub>11</sub>NO: C, 79.18; H, 5.58; N, 7.10. Found: C, 79.22; H, 5.68; N, 7.23%.

**2,3,4,5-Tetrahydropyridine N-oxide (6b)**<sup>6</sup>. Starting from **6a** (0.196 mL, 2 mmol), **6b** was obtained. Yield 92% (0.182 g). <sup>1</sup>H NMR (200 MHz, CDCl<sub>3</sub>):  $\delta$  1.5–1.9 (m, 2H), 1.9–2.2 (m, 2H) 2.4–2.5 (m, 2H) 3.7–3.9 (m, 2H), 7.1–7.3 (m, 1H); IR (neat) cm<sup>-1</sup>: 2925, 2853, 1653, 1559 (C=N), 1453, 1375, 1190 (NO), 1165, 1100, 988, 926, 850, 795, 748; MS (EI, 70 eV),  $m/z$ : 99 (M<sup>+</sup>, 100), 84 (51), 69 (58), 55 (80). Anal. Calc. for C<sub>5</sub>H<sub>9</sub>NO: C, 60.60; H, 9.09; N, 14.14. Found: C, 60.59; H, 9.07; N, 14.32%.

**6-Methyl-2,3,4,5-tetrahydropyridine N-oxide (7b)**<sup>6</sup>. Starting from **7a** (0.235 mL, 2 mmol), **7b** was obtained. Yield 95%

(0.214 g). <sup>1</sup>H NMR (200 MHz, CDCl<sub>3</sub>):  $\delta$  1.64–1.88 (m, 2H), 1.94–2.0 (m, 2H) 2.12 (m, 3H), 2.45 (m, 2H), 3.81 (m, 2H); IR (neat) cm<sup>-1</sup>: 2928, 1616 (C=N), 1450, 1190 (NO), 1168, 968, 928, 865, 748; MS (EI, 70 eV),  $m/z$ : 113 (M<sup>+</sup>, 100), 83 (14), 55 (64), 41 (80). Anal. Calc. for C<sub>7</sub>H<sub>9</sub>SO<sub>2</sub>: C, 53.09; H, 9.73; S, 12.3. Found: C, 53.22; H, 9.64; N, 12.23%.

## Acknowledgments

B. B and Ch. V. R. thank the Council of Scientific and Industrial Research (CSIR), India, for providing research grants.

## References

- 1 K. B. G. Torssell, *Nitrile Oxides, Nitrones and Nitronates in Organic synthesis*, VCH Publishers, New York, 1988.
- 2 (a) C. A. Evans, *Aldrich. Chim. Acta*, 1979, **12**, 23; (b) E. G. Janzen, *Acc. Chem. Res.*, 1971, **4**, 31.
- 3 J. J. Tufariello, in *1,3-Dipolar cycloaddition Chemistry*, ed. A. Padwa, J. Wiley, New York, 1984, vol. 2, pp. 83 and 277.
- 4 (a) R. M. Coates and C. H. Cummins, *J. Org. Chem.*, 1986, **51**, 1983; (b) J. A. Robi and J. R. Hwu, *J. Org. Chem.*, 1985, **50**, 5913; (c) S. I. Murahashi, H. Mitsui, T. Watanabe and S. Zenki, *Tetrahedron Lett.*, 1983, **24**, 1049.
- 5 R. W. Murray and M. Singh, *J. Org. Chem.*, 1990, **55**, 2954.
- 6 S. I. Murahashi, H. Mitsui, T. Shiota, T. Tsuda and S. Watanabe, *J. Org. Chem.*, 1990, **55**, 1736.
- 7 S. I. Murahashi and T. Shiota, *Tetrahedron Lett.*, 1987, **28**, 2383.
- 8 A. Goti, F. D. Sarlo and M. Romani, *Tetrahedron Lett.*, 1994, **35**, 6571.
- 9 E. Marcantoni, M. Petrini and O. Polimanti, *Tetrahedron Lett.*, 1995, **36**, 3561.
- 10 R. W. Murray and K. Iyengar, *J. Org. Chem.*, 1996, **61**, 8099.
- 11 A. Goti and L. Nannelli, *Tetrahedron Lett.*, 1996, **37**, 6025.
- 12 (a) S. Ball and T. C. Bruice, *J. Am. Chem. Soc.*, 1980, **102**, 6498; (b) S. I. Murahashi, T. Oda and Y. Masui, *J. Am. Chem. Soc.*, 1989, **111**, 5002.
- 13 K. Joseph, A. Sudalai and T. Ravindranathan, *Synlett*, 1995, 1177.
- 14 K. Sato, M. Aoki and R. Noyori, *Science*, 1998, **281**, 1646–47.
- 15 G. T. Brink, I. W. C. E. Arends and R. A. Sheldon, *Science*, 2000, **287**, 1636.
- 16 F. Cavani, F. Trifiro and A. Vaccari, *Catal. Today*, 1991, **11**, 173.
- 17 (a) M. Lakshmi Kantam, B. M. Choudary, Ch. Venkat Reddy, K. K. Rao and F. Figueras, *Chem. Commun.*, 1998, 1033; (b) M. Lakshmi Kantam, B. M. Choudary, B. Kavitha, Ch. Venkat Reddy, K. K. Rao and F. Figueras, *Tetrahedron Lett.*, 1998, **39**, 3555; (c) B. M. Choudary, M. Lakshmi Kantam, B. Bharathi and Ch. Venkat Reddy, *Synlett*, 1998, 1203; (d) P. S. Kumbhar, J. S. Valente, J. Lopez and F. Figueras, *Chem. Commun.*, 1998, 535; (e) B. Sels, D. De vos, M. Buntinx, F. Pierard, A. K. Mesmaeker and P. A. Jacobs, *Nature*, 1999, **400**, 855; (f) B. M. Choudary, M. Lakshmi Kantam, Ateeq Rahman, Ch. Venkat Reddy and K. K. Rao, *Angew. Chem., Int. Ed.*, 2001, **40**, 763.
- 18 B. M. Choudary, B. Bharathi, Ch. Venkat Reddy and M. Lakshmi Kantam, *Chem. Commun.*, 2001, 1736.
- 19 D. Hoegaerts, B. F. Sels, D. E. Devos, F. Verpoort and P. A. Jacobs, *Catal. Today*, 2000, **60**, 209.
- 20 (a) S. Miyata, *Clays Clay Miner.*, 1983, **4**, 305; (b) P. K. Dutta and M. Puri, *J. Phys. Chem.*, 1989, **96**, 376.
- 21 S. Velu, V. Ram Kumar, A. Narayanan and C. S. Swamy, *J. Mater. Sci.*, 1997, **32**, 957.
- 22 Maria J. Hernandez-Moreno, Maria J. Ulibarri, J. L. Rendon and Carlos J. Serna, *Phys. Chem. Miner.*, 1985, **12**, 34–38.
- 23 S. Miyata, *Clays Clay Miner.*, 1975, **23**, 369.



# Rapid and selective retro-aldol condensation of glucose to glycolaldehyde in supercritical water

Mitsuru Sasaki,<sup>\*a</sup> Kohtaro Goto,<sup>b</sup> Kiyohiko Tajima,<sup>b</sup> Tadafumi Adschiri<sup>c</sup> and Kunio Arai<sup>c</sup>

<sup>a</sup> Genesis Research Institute, Inc, 4-1-35 Noritake-shinmachi, Nishi-ku, Nagoya 451-0051, Japan. E-mail: sasaki@arai.che.tohoku.ac.jp

<sup>b</sup> Noguchi Institute, 1-8-1 Yoga, Itabashi-ku, Tokyo 173-0003, Japan

<sup>c</sup> Department of Chemical Engineering, Tohoku University, Aza-Aoba 7, Aramaki, Aoba-ku, Sendai 980-8579, Japan

Received 20th March 2002

First published as an Advance Article on the web 23rd May 2002

Retro-aldol condensation of glucose occurred preferentially relative to dehydration and isomerization under low water density conditions in supercritical water, and glycolaldehyde was successfully produced in a rapid and selective manner without any catalyst.

Glycolaldehyde can be utilized as a raw material of glycolic acid that has recently been focused on as a source material for resin production. This chemical intermediate is produced by various synthetic methods from formaldehyde, allyl alcohol or ethylene glycol. Although the usual glycolaldehyde production techniques are useful as a quantitative manufacturing method, they must use petrochemicals, catalysts and microorganisms, which requires considerable waste treatment. Moreover, from the viewpoint of 'post petrochemistry', research has been directed towards alternative resources, cleaner solvents and non-catalytic reaction routes.

Biomass is an important energy resource that has been focused on as one of alternatives for petroleum. It is possible that carbon dioxide once discharged from biomass can be fixed in biomass again by photosynthesis with water and solar energy. Therefore, chemical synthesis processes using biomass resources have been realized as an environmentally benign technology. Cellulose is one of the major components of biomass and has been utilized in extensive fields such as pulp, paper, fiber, food and cosmetics. Glucose, which is a repeating unit of cellulose, can be also an important chemical intermediate for many synthetic polymers that have been manufactured in the present petrochemical industries.<sup>1</sup>

Supercritical water ( $T > 647.2$  K,  $P > 22.1$  MPa) shows some unique properties and has been considered as a reaction field for the decomposition of organics and for chemical synthesis.<sup>2,3</sup> Solvent properties such as density and dielectric constant can be varied by manipulating temperature and pressure. In our previous work, we clarified that chemical substances such as glucose and cellooligosaccharides can be rapidly and selectively recovered from cellulose in supercritical water.<sup>4</sup> From the study on the phase behaviour of the cellulose–water system, it was found that cellulose can dissolve in high-temperature and high-pressure water.<sup>5</sup> Our recent kinetic studies of glucose and cellobiose indicated that the main reactions of saccharides were hydrolysis, retro-aldol condensation, isomerization and dehydration, and that these reactions can be probably controlled by manipulating temperature and pressure in near-critical and supercritical water.<sup>6</sup> In this study, we aimed to evaluate effects of temperature and pressure on retro-aldol condensation of glucose and to explore an optimal reaction condition in which glycolaldehyde was selectively obtained through non-catalytic glucose decomposition experiments in subcritical and supercritical water.

Reactions of glucose were conducted using a continuous flow-type micro-reactor for high-temperature and high-pressure conditions. The reactor was made from 316 stainless steel tubing (1.59 mm O.D.; 0.50 mm I.D.). Prior to the experiment, distilled water was introduced in a system by a high-performance liquid chromatography (HPLC) pump (Nihon-Seimitsu Industries Co., Ltd., Model NP-AX-15) at a flow rate of  $14 \text{ g min}^{-1}$ , and subsequently pressurized using a back-pressure regulator (TESCOM, Model 26-1721-24) in the range 25–40 MPa. Then, the distilled water was heated with an electric furnace (Seiwa-Riko Co., Ltd., Model FTO-6), and mixed at the mixing point with a  $1.0 \text{ mol L}^{-1}$  glucose aqueous solution supplied from the other line at  $2 \text{ g min}^{-1}$  using a HPLC pump (GL Science Co., Ltd., Model PUS-3). The glucose solution was rapidly heated to the desired reaction temperature (623–723 K). The reactor was submerged into a metal-salt bath that was set at the reaction temperature in advance to keep the temperature uniform. The reaction time was ranged from 0.02 to 1.02 s by replacing the reactor tubing whose length is different in each experiment. At the reactor outlet, the reacted solution was quenched by a cooling jacket, and then collected in a sampling bottle for a fixed time after it was decompressed. Liquid products were identified by NMR, FAB-MS and HPLC-RI, and quantified with HPLC-RI/UV (wavelength of 210 nm in UV). Carbon recovery in the aqueous product solution in each experiment was examined by a total organic carbon analyser (Shimadzu Co., Ltd., Model TOC-5000A). In this study, the analytical error of the quantification of products was in the range 0.5–2.0%, and the carbon recovery ranged from 93 to 102% in all the experiments. Glucose conversion ( $X$ ), product yield ( $Y$ ) and selectivity ( $S$ ) were defined on the carbon basis.

## Green Context

The conversion of renewable resources into useful chemical building blocks is of great importance, as petrochemical resources become scarcer. Here, the conversion of glucose into glycolaldehyde using supercritical water is described. The system chosen allows the decomposition of glucose to a range of useful products, primarily via retro-aldol reaction to glycolaldehyde, a raw material which can be used in a variety of industrial processes and applications. *DJM*

The main products obtained in this experiment were erythrose, glycolaldehyde, fructose, glyceraldehyde, dihydroxyacetone, 1,6-anhydro- $\beta$ -D-glucose (1,6-AHG) and 5-hydroxymethyl-2-furfural (5-HMF), *cf.* the report of Kabylemela *et al.*<sup>7</sup> According to the proposed reaction pathways of glucose decomposition,<sup>8</sup> glucose can primarily be converted to erythrose plus glycolaldehyde, to fructose, and to 1,6-AHG or 5-HMF *via* retro-aldol condensation, isomerization and dehydration, respectively. Fig. 1 shows a typical variation of glucose decomposition products in supercritical water at 673 K and 40 MPa. The yield of erythrose was optimised at 0.1 s and decreased with time, whereas the yield of glycolaldehyde increased with increasing time and reached 48.8% at 0.76 s by retro-aldol condensation of the erythrose formed. Fructose was formed at the initial stage of glucose decomposition and then was converted to form glyceraldehyde, dihydroxyacetone and 5-HMF. Dehydration products such as 1,6-AHG and 5-HMF were also formed, although the product yields were low.

In order to explore an optimal reaction condition for glycolaldehyde production and to determine effect of temperature and pressure on glucose decomposition, we conducted experiments at 623–723 K, 25–40 MPa and 0.02–1.02 s, and results are summarized in Table 1. At 623 K, products of retro-aldol condensation of glucose were mainly obtained, but by-products from dehydration and isomerization of glucose also formed in relatively high yields. In supercritical water, the yield of glycolaldehyde became higher and the contributions of both dehydration and isomerization were lowered. This tendency became dramatic with a decrease in water density of the reaction atmosphere in supercritical water. A dramatic change of the product distribution will occur if supercritical water experiments under lower water density conditions than the conditions reported here are conducted. However, such experiments have not yet been conducted due to some limitations of the experimental setup (*e.g.* limited operating temperatures and pressures) preventing experiments at higher temperatures and lower pressures. It is hoped that such experiments can be conducted in the future.

From the experimental findings, we clarified the main reaction pathways of glucose under low water density conditions in supercritical water as shown in Scheme 1. Antal *et al.*<sup>3</sup> reported that dehydration preferentially took place under hydrothermal conditions in the absence of acid catalyst. Thus, it can be considered that dehydration scarcely takes place in supercritical water. Isomerization of glucose (1) to fructose (2) is also suppressed with a rise of temperature, and therefore, glyceraldehyde (7), dihydroxyacetone (8) and 5-HMF (6) did not form to a significant extent. By contrast, retro-aldol condensation of both glucose (1) and erythrose (4) to form glycolaldehyde (5) becomes dominant under low water density conditions in supercritical water.

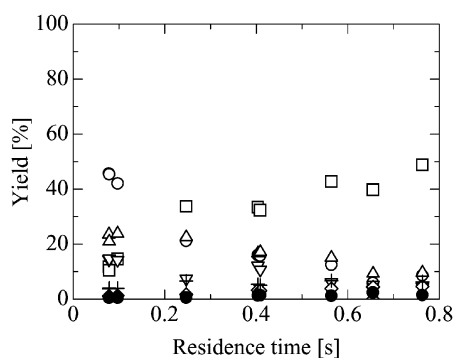


**Fig. 1** A typical variation of glucose decomposition products in supercritical water at 673 K and 40 MPa; glucose (○); erythrose (△); glycolaldehyde (□); fructose (▽); dihydroxyacetone (◇); glyceraldehyde (+); 5-hydroxymethyl-2-furfural (5-HMF) (●); 1,6-anhydro- $\beta$ -D-glucose (1,6-AHG) (×).

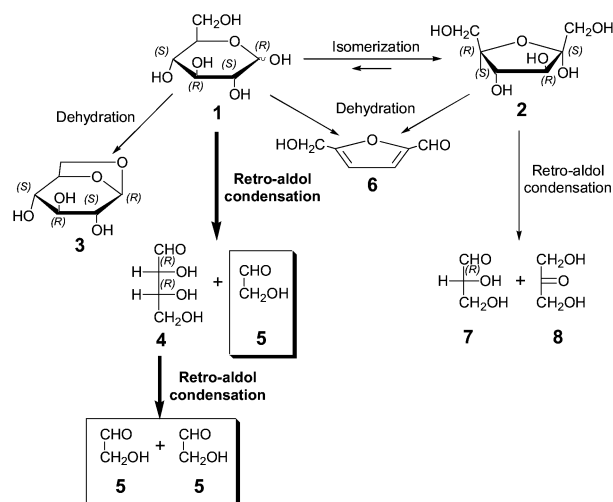
**Table 1** Effect of temperature and pressure on the product distribution of glucose decomposition in subcritical and supercritical water at 623–723 K and 25–40 MPa

T/K	P/MPa	$\rho_w/g\text{ cm}^{-3}$	t/s	X [C%]	Y [C%] (S [C%])				
					RA <sup>a</sup>		Iso <sup>a</sup>		DH <sup>a</sup>
					5	4	2, 7, 8	3	6
623	40	0.67	1.02	50.8	11.1	16.5	15.4	6.3	3.3
					(21.9)	(32.5)	(30.3)	(12.4)	(6.5)
	25	0.63	0.92	45.1	11.8	10.1	16.4	5.2	2.3
					(26.2)	(22.4)	(36.4)	(11.5)	(5.1)
673	40	0.52	0.76	91.4	48.8	9.6	15.3	tr.	1.5
					(53.4)	(10.5)	(16.7)	(—)	(1.6)
	25	0.17	0.24	87.0	48.0	18.3	16.5	tr.	0.3
					(55.2)	(21.0)	(19.0)	(—)	(0.3)
723	40	0.27	0.34	98.9	59.2	3.4	4.6	tr.	0.5
					(59.9)	(3.4)	(4.7)	(—)	(0.5)
	35	0.20	0.25	99.4	63.8	4.5	5.4	tr.	0.5
					(64.2)	(4.5)	(5.4)	(—)	(0.5)

<sup>a</sup> RA: Retro-aldol condensation; Iso: isomerization; DH: dehydration.

The reason why this reaction to form glycolaldehyde is undergone selectively under low water density conditions in supercritical water can be explained as follows. In supercritical water, the contribution of retro-aldol condensation to glucose decomposition increased and that of both isomerization and dehydration decreased as the water density of the supercritical atmosphere was lowered. It is well known that retro-aldol condensation of a saccharide occurs *via* formation of intramolecular hydrogen bond linkages. For a low water density reaction atmosphere, the formation of intramolecular hydrogen bond linkages of the saccharide becomes easier than that of intermolecular hydrogen bond linkages between water and saccharide. As a result, glycolaldehyde is selectively obtained by lowering the water density in supercritical water. Also, from equilibrium considerations, retro-aldol condensation leads to two aldehyde molecules from one saccharide molecule, and a lower hydration energy of the product, thus at higher water densities retro-aldol condensation is suppressed.

In summary, glycolaldehyde was obtained in a relative high selectivity *via* retro-aldol condensation of glucose in supercritical water (maximum selectivity = 64.2% at 723 K, 35 MPa and 0.25 s) without any catalyst. This finding suggests an effective and environmentally benign technique that can produce glycolaldehyde from cellulosic biomass resource with



**Scheme 1** Reaction pathways for glycolaldehyde production on glucose decomposition under low water density conditions in supercritical water: 1 glucose, 2 fructose, 3 1,6-AHG, 4 erythrose, 5 glycolaldehyde, 6 5-HMF, 7 glyceraldehyde, 8 dihydroxyacetone.

supercritical water as a reaction medium. Additionally, supercritical water can provide an unique atmosphere for chemical synthesis from biomass resources.

The authors gratefully acknowledge support by a Grand-in-Aid for Scientific Research on Priority Area 'Mechanism of hydrolysis in supercritical water' (#11450295) from the Ministry of Education, Culture, Sports, Science and Technology.

## References

- 1 H. Danner and R. Braun, *Chem. Soc. Rev.*, 1999, **28**, 395; K. Tajima, *Biosci. Bioind.*, 1998, **56**(10), 23.
- 2 P. E. Savage, *Chem. Rev.*, 1999, **99**, 603; J. An, L. Bagnell, T. Cablewski, C. R. Strauss and R. W. Trainor, *J. Org. Chem.*, 1997, **62**, 2505; A. R. Katritzky, S. M. Allin and M. Siskin, *Acc. Chem. Res.*, 1996, **29**, 399; Y. Tsujino, C. Wakai, N. Matsubayashi and M. Nakahara, *Chem. Lett.*, 1989, 287; Y. Ikushima, K. Hatakeda, O. Sato, T. Yokoyama and M. Arai, *J. Am. Chem. Soc.*, 2000, **122**, 1908; H. Ito, J. Nishiyama, T. Adschiri and K. Arai, *Kobunshi Ronbunshu*, 2001, **58**(12), 679.
- 3 M. J. Antal, M. Carlsson, X. Xu and D. G. M. Anderson, *Ind. Eng. Chem. Res.*, 1998, **37**, 3820; M. J. Antal and W. S.-L. Mok, *Carbohydr. Res.*, 1990, **199**, 91.
- 4 T. Adschiri, R. M. Malaluan, S. Hirose and K. Arai, *J. Chem. Eng. Jpn.*, 1993, **26**(6), 676; M. Sasaki, B. M. Kabyemela, R. M. Malaluan, S. Hirose, N. Takeda, T. Adschiri and K. Arai, *J. Supercrit. Fluids*, 1998, **13**, 261.
- 5 M. Sasaki, Z. Fang, Y. Fukushima, T. Adschiri and K. Arai, *Ind. Eng. Chem. Res.*, 2000, **39**(8), 2883.
- 6 B. M. Kabyemela, M. Takigawa, T. Adschiri and K. Arai, *Ind. Eng. Chem. Res.*, 1997, **37**(2), 357; B. M. Kabyemela, T. Adschiri, K. Arai and H. Ozeki, *Ind. Eng. Chem. Res.*, 1997, **36**(12), 2025.
- 7 B. M. Kabyemela, T. Adschiri and K. Arai, *Ind. Eng. Chem. Res.*, 1999, **38**(8), 2888.
- 8 K. Goto, K. Tajima, M. Sasaki, T. Adschiri and K. Arai, *Kobunshi Ronbunshu*, 2001, **58**(12), 685.





# A toxicity decrease on soil microbiota by applying the pesticide picloram anchored onto silica gel

Alexandre G. S. Prado and Claudio Airoidi\*

*Instituto de Química, Universidade Estadual de Campinas, Caixa Postal 6154, 13083-970 Campinas, São Paulo, Brasil. E-mail: airoidi@iqm.unicamp.br*

Received 11th March 2002

First published as an Advance Article on the web 28th May 2002

A route for picloram (4-amino-3,5,6-trichloropicolinic acid) immobilisation onto silica gel was established after reacting at the first stage, the precursor silylating agent 3-chloropropyltrimethoxysilane with the support. The pesticide was covalently anchored to available chloro groups of the precursor, giving 1.11 mmol g<sup>-1</sup> of picloram per gram of silica. IR, <sup>13</sup>C and <sup>29</sup>Si NMR spectra are in agreement with the proposed reaction between nitrogen of the chloride group of the previously anchored silica. The immobilisation of pesticide picloram onto a silica gel surface results in a decrease in its toxicity to soil microbial activity, compared to free pesticide added to soil.

## Introduction

The herbicide 4-amino-3,5,6-trichloropicolinic acid (picloram) is commonly used in Brazilian agriculture, mainly in sugar cane plantations. In a typical commercial formulation it is mainly associated with 2,4-dichlorophenoxyacetic acid (2,4-D). Picloram was applied during the Vietnam War, as the so-called 'Agent White', before being extensively used in agricultural crops to eliminate weeds. Its high persistence in water and in soil, more than for the majority of other man-made pesticides used in agriculture, is also a particular property.<sup>1,2</sup>

Nowadays, herbicides, insecticides, fertilisers and fungicides are incrementally used in normal agriculture in order to increase food production.<sup>3</sup> However, the abuse of pesticides in agriculture is a matter of environmental concern because these chemicals are recognised as a source of potential adverse impact.<sup>4-6</sup> Thus, high amounts them are often applied to crops, in doses greater than required, and cause losses associated with runoff and leaching processes.<sup>3</sup> To avoid losses a new proposal was established through the immobilisation of traditional pesticides onto a silica gel surface.<sup>7,8</sup> As a consequence, lesser amounts should be required for agricultural purposes. Furthermore, the immobilisation of the pesticides reduces their toxic effects on soil microflora, as previously observed.<sup>7</sup>

From the environmental point of view, this feature related to modified compounds in order to obtain controlled release properties, is very important to minimise the application of the xenobiotics in aquatic and soil environments, a procedure which surely causes a decrease of the toxic effects in a given ecosystem.<sup>9</sup> Moreover, the decrease of the generation of the undesirable products and the production of less toxic compounds are relevant goals of green chemistry.<sup>10</sup>

The greatest interest devoted to modified silica gel studies has focused on direct application as supports in high performance liquid chromatography,<sup>11</sup> inorganic compound separations,<sup>12</sup> ion-exchange,<sup>13</sup> preconcentration of inorganic compounds<sup>14</sup> and pesticides preconcentration,<sup>15</sup> as well as being chemical sensors and finding use in catalysis.<sup>16</sup> On the other hand, up to now, such innovative technology has not been investigated to produce new agrochemical with controlled release properties. Pesticide compounds with controlled release prospectus have been investigated,<sup>17,18</sup> but the immobilisation of pesticides onto silica gel to obtain a designed surface that could modify pesticide properties has not yet been explored.

Taking into account that pesticides are integral components of modern agriculture, their immobilisation onto a silica gel surface is an important feature to be investigated. In such cases, the synthesised surface can be applied in smaller amounts than in traditional doses. As a result, the mobility of pesticide to rivers and underground waters is decreased.

## Experimental

### Chemicals

The pesticide 4-amino-3,5,6-trichloropicolinic acid (picloram) (Sigma) and the silylating agent 3-chloropropyltrimethoxysilane (CPTS) (Aldrich) were used without purification. Silica gel (Merck) with a particle size of 70–230 mesh and with mean diameter pore size of 60 Å was activated by heating for 10 h at 423 K in a stream of dry nitrogen. After this activation the silica was immediately used. A specific area of 387.1 ± 21.9 m<sup>2</sup> g<sup>-1</sup> was determined by the BET method.<sup>8</sup>

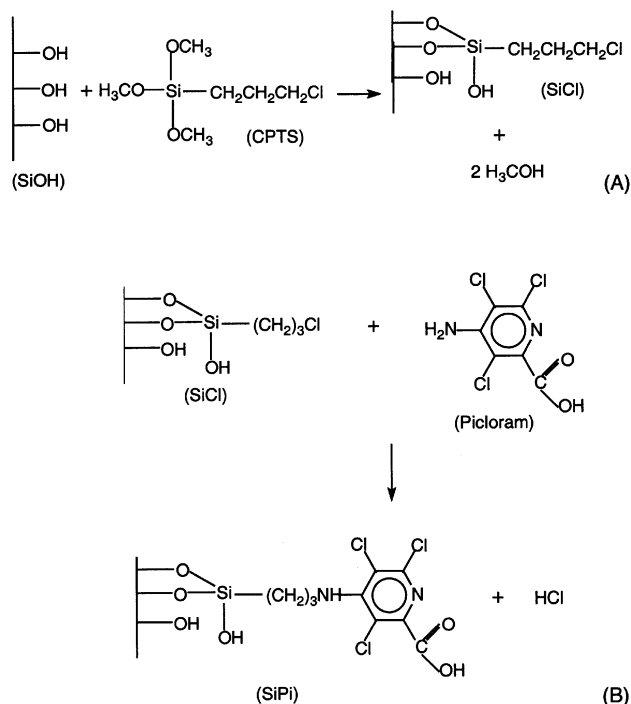
### Organofunctionalisation

The immobilisation of the pesticide picloram is summarised in Scheme 1. Activated silica gel (45.0 g) suspended in 100.0 cm<sup>3</sup> of dry xylene was refluxed with mechanical stirring for 1 h under dry nitrogen.<sup>7,8</sup> To this suspension 15.0 cm<sup>3</sup> of 3-chloro-

## Green Context

**Controlled release pesticides may be helpful in the balance between beneficial effects of increased crop yield and the potential for environmental damage in cases of over-dosage. Encapsulation is one approach which has been investigated for both pesticides and pharmaceuticals, but this article describes a simpler methodology, which may prove beneficial in agriculture. Attachment of a relatively persistent pesticide (picloram) to silica gel results in a material with lower toxicity than the free agent, due to a slower release into the soil. Such behaviour indicates some promise for an extension into controlled release pesticides, using a benign host.**

*DJM*



**Scheme 1** Diagrammatic representation of the reaction between silica (SiOH) and CPTS (A), and the subsequent immobilisation of picloram onto the SiCl surface (B).

propyltrimethoxysilane (CPTS) was added dropwise and the mixture was kept in reflux for another 72 h.<sup>7,8</sup> The solid was filtered off and washed with water and ethanol. This precursor immobilised surface, denoted SiCl, was dried in vacuum at room temperature.

### Immobilisation of picloram

A sample of 5.0 g of SiCl was suspended in 100 cm<sup>3</sup> of dry xylene and refluxed with mechanical stirring with 5.25 g of picloram for 72 h under dry nitrogen. The resulting solid containing the immobilised pesticide, denoted SiPi, was filtered off and washed with water and ethanol to eliminate the excess of picloram. This final anchored surface was dried in vacuum at room temperature for several hours.

### Characterisation

The degree of CPTS functionalisation on silica gel and the corresponding amount of anchored picloram were based on carbon and nitrogen content determined through elemental analysis on a PE-2400 elemental analyser. The IR spectra were measured on KBr pellets on a MB-Bomem FTIR spectrophotometer.<sup>7,8</sup>

NMR spectra of the solid samples were obtained on an AC 300/P Bruker spectrometer at room temperature. For each run, approximately 1.0 g of each modified silica was compacted into a 7 mm zirconium oxide rotor. The measurements were obtained at frequencies of 75.47 and 59.61 MHz, for carbon and silicon, respectively, with a magic-angle spinning speed of 4 Hz. In order to increase the signal to noise ratio of the solid-state spectra, the CP/MAS technique was used.<sup>7,8</sup> The <sup>29</sup>Si and <sup>13</sup>C CP/MAS spectra were obtained with pulse repetitions of 1 and 3 s and contact times of 1 and 5 ms, respectively.<sup>7,8</sup>

### Toxicity studies

The toxicity effects caused by picloram and SiPi applications in red Latosol soil, collected and characterised as before,<sup>4-6</sup> were

followed by evolution of the thermal effect generated by microbial activity, detected by a heat-flow LKB 2277 microcalorimeter. Such thermal effect data were obtained by using 5.0 cm<sup>3</sup> stainless steel ampoules charged with 1.50 g of soil plus 0.80 cm<sup>3</sup> of solution, containing 6.0 mg of glucose plus 6.0 mg of ammonium sulfate at 298.15 ± 0.02 K,<sup>2,4,6</sup> in the absence of the pesticide and in presence of 2.50 μg g<sup>-1</sup> of active agent for picloram and SiPi, respectively. The thermal effect output directly associated with nutrient degradation was recorded as a function of time. The final value was calculated by comparing the integrated area of the power-time curve for each experimental determination.<sup>2,4,6</sup>

## Results

### Elemental analysis

Determinations of the amounts of CPTS and picloram immobilised onto silica gel surface were based on elemental analysis, as shown in Table 1. The anchored SiCl surface indicated the presence of 1.24 ± 0.06 mmol of the CPTS per gram of the silica, which confirmed that the organic molecule is covalently bonded on this surface. Based also on the elemental analysis, the final compound, SiPi, contained 1.11 ± 0.02 mmol of the pendant molecule per gram of the silica gel. These data confirmed the occurrence of an excellent level of immobilisation of pesticide picloram onto the SiCl surface, resulting in a yield of 89.5% of this pesticide anchored onto surface.

**Table 1** Elemental carbon and nitrogen analysis (%) for SiCl and SiPi silicas and the correspondent immobilised amounts (*Q*) for CPTS and picloram onto silica surfaces.

Compound	C (%)	N (%)	<i>Q</i> /mmol g <sup>-1</sup>
SiCl	4.46 ± 0.21	—	1.24 ± 0.06
SiPi	11.99 ± 0.14	3.11 ± 0.11	1.11 ± 0.02

### IR experiments

The IR spectra for SiCl and SiPi surfaces were obtained in order to aid the characterisation of these silicas, the spectra of which are shown in Fig. 1, which present the ordinary Si silica gel bands such as: (i) the overlapped peaks within the range 3600–3200 cm<sup>-1</sup>, attributed to O–H stretching of silanol groups and residual adsorbed water, (ii) siloxane stretching at 1100 cm<sup>-1</sup>, and (iii) Si–O stretching frequency at 900 cm<sup>-1</sup> assigned to silanol groups.

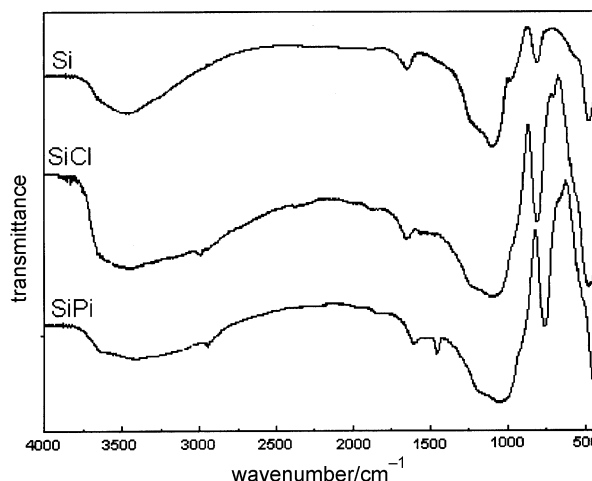


**Fig. 1** IR spectra of silica gel (Si) and functionalized silicas SiCl and SiPi.

The IR spectra of SiCl and SiPi displayed a low intensity peak at  $2950\text{ cm}^{-1}$  which corresponds to C–H stretching band of tetrahedral carbon, corroborating the attachment of the organic molecule onto the inorganic backbone surface. In the SiPi spectrum, an N–C aromatic carbon stretching frequency at  $1490\text{ cm}^{-1}$  was observed. This band also indicates the success of the reaction between picloram and the precursor SiCl surface which should occur through covalent bond formation between the picloram amine group and the chloride attached to the end of the organic chain in the SiCl structure of the compound, as represented in Scheme 1.

### Solid state NMR studies

Three well-formed peaks in  $^{13}\text{C}$  NMR spectra at 7.67; 22.5 and 44.9 ppm for SiCl and at 10.1, 28.1 and 49.5 ppm for SiPi immobilised surfaces (Fig. 2) are attributed to the precursor carbon atoms of the pendant groups C1, C2 and C3. Two broad peaks for SiPi at 100–145 ppm and at 150–190 ppm are attributed to carbon atoms C4, C5, C6 and C7 and to carbons C8 and C9, respectively. This sequence of peaks unmistakably confirmed the immobilisation of picloram onto the precursor SiCl surface.

$^{29}\text{Si}$  NMR spectra for both silicas presented a typical silica  $\text{SiO}_4$  ( $Q_4$ ) signal at  $-110\text{ ppm}$  and another signal corresponding to  $\text{O}_3\text{Si-OH}$  ( $Q_3$ ) at  $-100\text{ ppm}$ ,<sup>7,8</sup> as shown in Fig. 3. The appearance of organosilane signals at  $-65$  and  $-57\text{ ppm}$ , due to the presence of an organic group (R) bonded to the silica framework, are attributed to  $\text{O}_3\text{SiOR}$  ( $T_4$ ) and  $(\text{OH})_2\text{OSiOR}$  ( $T_2$ ) species, respectively, for both silicas, and are characteristic for fully cross-linked organosilane species, demonstrating the incorporation of the functional groups within the framework of the silica gel.<sup>19–21</sup>

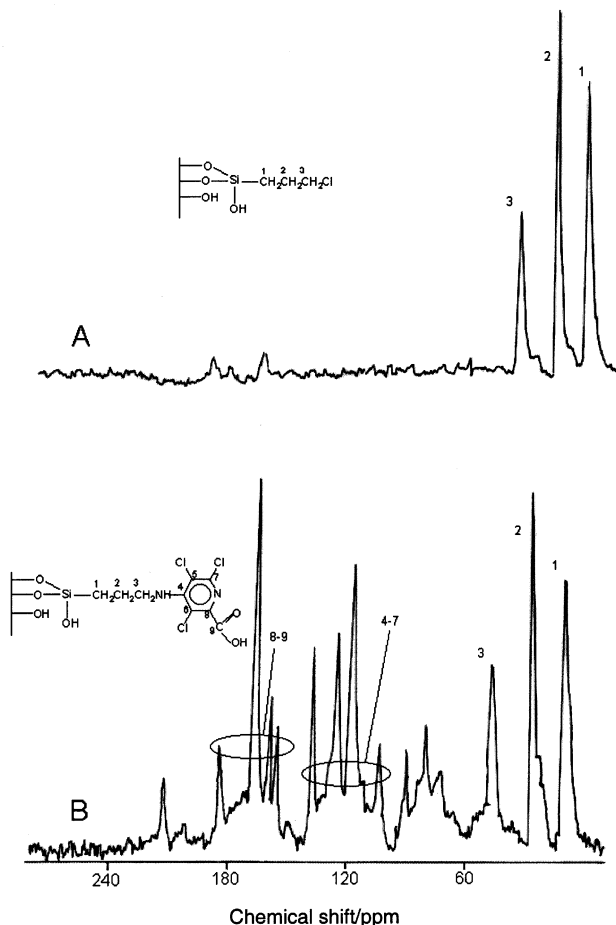


Fig. 2  $^{13}\text{C}$  NMR spectra of SiCl (A) and SiPi (B) anchored silicas.

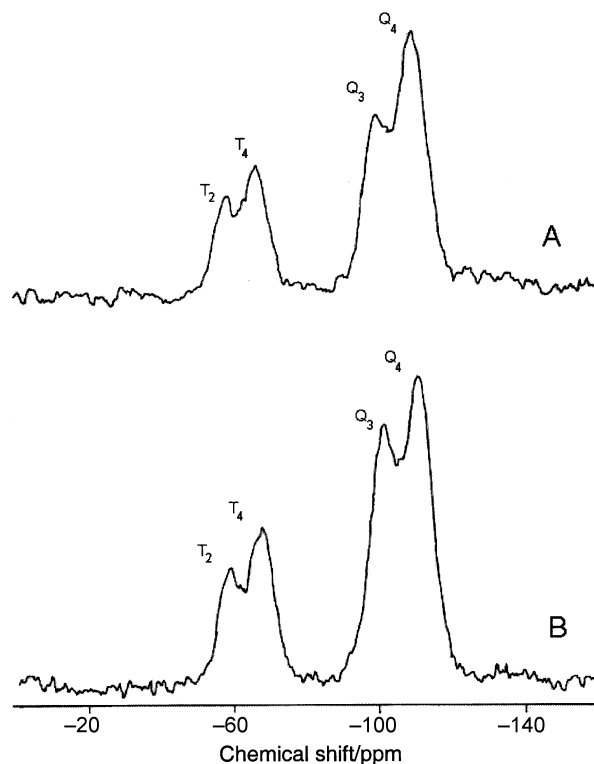


Fig. 3  $^{29}\text{Si}$  NMR spectra of SiCl (A) and SiPi (B) immobilised silicas.

### Toxicity studies

The microorganism metabolic activity in the soil involves an exothermic effect originating from degradation of nutrients (catabolism) and an endothermic effect caused by microbial growth (anabolism).<sup>5,6</sup> Thus, the thermal effect output and respiration rate are distinguishable features, and detectable through the microcalorimetric technique, which is a useful tool to follow the microbiological activity in soil.<sup>22–25</sup>

Stimulation through nutrients, composed of glucose, ammonium sulfate and water in any system results in a clear response, as shown in Fig. 4. These nutrients have the properties of changing the metabolism, presented in curve A, which was drastically affected by addition of free picloram, as illustrated in curve B. The application of SiPi also decreased the stimulus level of the soil microbial activity, shown in curve C. The application of  $2.50\text{ }\mu\text{g g}^{-1}$  of picloram presented a decrease of 67.1% of typical soil microbial activity, however, by using the same active amount of picloram in the SiPi immobilised compound, only a decrease of 24.8% in the activity was

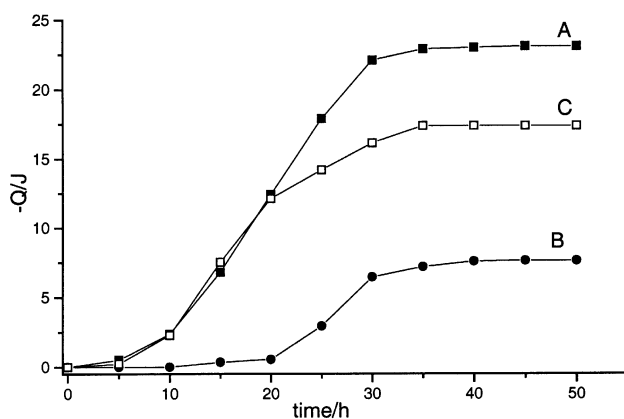


Fig. 4 Thermal effect,  $Q$ , generated by soil microbial activity as a function of time without pesticides (A) and with doses of  $2.50\text{ }\mu\text{g g}^{-1}$  of active compound for picloram (B) and for SiPi (C).

detected. These data also showed that the original soil microbial activity started after 10 h and that the presence of SiPi did not affect the start time of metabolism without xenobiotics. However, the presence of  $2.50 \mu\text{g g}^{-1}$  of free picloram led to a delay in the soil microbial activity to 20 h.

The immobilised picloram showed a much lower toxic effect to microbial activity than the free picloram pesticide (*cf.* curves B and C in Fig. 4). On the other hand, when the agent is anchored there is minimisation of leaching and runoff. Thus, these results suggest that immobilisation of this pesticide should be explored in order to develop a new agrochemical with low toxicity and possible controlled release properties.

## Conclusion

This investigation clearly demonstrated successful immobilisation of the pesticide picloram onto pre-functionalized silica gel. This route established an efficient method for anchoring this pesticide. The silica gel surface anchored pesticide shows a new way to develop agrochemicals with lower toxicity, due to the fact these preliminary studies show a significant decrease in toxicity of this commercial pesticide, after its immobilisation onto a silica gel surface.

## Acknowledgements

The authors are indebted to FAPESP for financial support and a fellowship to A. G. S. P. and to CNPq for a fellowship to C. A.

## References

- 1 D. J. Oakes and J. K. Pollak, *Toxicology*, 1999, **136**, 41.
- 2 A. G. S. Prado and C. Airoidi, *J. Environ. Monit.*, 2001, **3**, 394.
- 3 E. R. Kenawy and D. C. Sherrington, *Eur. Polym. J.*, 1992, **8**, 841.
- 4 A. G. S. Prado and C. Airoidi, *Pest Manag. Sci.*, 2001, **57**, 640.
- 5 A. G. S. Prado and C. Airoidi, *Thermochim. Acta*, 2001, **371**, 169.
- 6 A. G. S. Prado and C. Airoidi, *Thermochim. Acta*, 2000, **349**, 17.
- 7 A. G. S. Prado and C. Airoidi, *Pest Manag. Sci.*, 2000, **56**, 419.
- 8 A. G. S. Prado and C. Airoidi, *J. Colloid Interface Sci.*, 2001, **236**, 161.
- 9 A. Akelah, *Mater. Sci. Eng. C*, 1996, **4**, 83.
- 10 P. Tundo, P. Anastas, D. S. Black, J. Breen, T. Collins, S. Memoli, J. Miyamoto, M. Polyakoff and W. Tumas, *Pure Appl. Chem.*, 2000, **72**, 1207.
- 11 C. R. Silva, I. C. S. F. Jardim and C. Airoidi, *J. Chromatogr. A*, 2001, **913**, 65.
- 12 A. G. S. Prado, L. N. H. Arakaki and C. Airoidi, *J. Chem. Soc., Dalton Trans.*, 2001, 2206.
- 13 P. M. Padilha, L. A. D. Gomes, C. C. F. Padilha, J. C. Moreira and N. L. Dias, *Anal. Lett.*, 1999, **32**, 1807.
- 14 A. G. S. Prado and C. Airoidi, *Anal. Chim. Acta*, 2001, **432**, 201.
- 15 A. G. S. Prado and C. Airoidi, *Fresenius' J. Anal. Chem.*, 2001, **371**, 2208.
- 16 E. B. Mubofu, J. H. Clark and D. J. Macquarrie, *Green Chem.*, 2001, **3**, 23.
- 17 F. N. Kok, M. Y. Arika, O. Genar, K. Abak and V. Hasira, *Pestic. Sci.*, 1999, **55**, 1194.
- 18 A. Ferraz, J. A. Souza, F. T. Silva, A. R. Goncalves, R. E. Bruns, A. R. Cotrim and R. M. Wilkins, *J. Agr. Food. Chem.*, 1997, **45**, 1001.
- 19 L. Mercier and T. J. Pinnavaia, *Chem. Mater.*, 2000, **12**, 188.
- 20 K. D. Behringer and J. Blumel, *J. Liq. Chromatogr. Rel. Technol.*, 1996, **19**, 2753.
- 21 C. Merckle and J. Blumel, *Chem. Mater.*, 2001, **13**, 3617.
- 22 I. Barja and L. Nunez, *Soil Biol. Biochem.*, 1999, **31**, 441.
- 23 B. P. Albers, F. Beese and A. Hartmann, *Biol. Fert. Soils*, 1995, **19**, 203.
- 24 K. Drong and I. Lamprecht, *Pure Appl. Chem.*, 1993, **65**, 1967.
- 25 R. B. Kemp and I. Lamprecht, *Thermochim. Acta*, 2000, **348**, 1.